

N O T I C E

THIS DOCUMENT HAS BEEN REPRODUCED FROM
MICROFICHE. ALTHOUGH IT IS RECOGNIZED THAT
CERTAIN PORTIONS ARE ILLEGIBLE, IT IS BEING RELEASED
IN THE INTEREST OF MAKING AVAILABLE AS MUCH
INFORMATION AS POSSIBLE

E82-10363

CTR-169012

**DEVELOPMENT OF VISIBLE/INFRARED/
MICROWAVE AGRICULTURE CLASSIFICATION
AND BIOMASS ESTIMATION ALGORITHMS**

"Made available under NASA sponsorship
in the interest of early and wide dis-
semination of Earth Resources Survey
Program information and without liability
for any use made thereof."

by

**Wesley D. Rosenthal
Marshall J. McFarland
Sidney W. Theis
Cheryl L. Jones**

February 1982

Supported by:

**National Aeronautics and Space Administration
Goddard Space Flight Center
Beltsville, Maryland
Contract NSG-5134**



**TEXAS A&M UNIVERSITY
REMOTE SENSING CENTER
COLLEGE STATION, TEXAS**



(E82-10363) DEVELOPMENT OF
VISIBLE/INFRARED/MICROWAVE AGRICULTURE
CLASSIFICATION AND BIOMASS ESTIMATION
ALGORITHMS Final Report (Texas A&M Univ.)
221 p HC A10/MF A01

N82-26761

Unclas
00363

CSCL 02C G3/43

**DEVELOPMENT OF VISIBLE/INFRARED/MICROWAVE AGRICULTURE
CLASSIFICATION AND BIOMASS ESTIMATION ALGORITHMS**

By

Wesley D. Rosenthal
Marshall J. McFarland
Sidney W. Theis
Cheryl L. Jones

Remote Sensing Center
Texas Engineering Experiment Station
Texas A&M University System
College Station, Texas 77843

February 1982

Supported by:

National Aeronautics and Space Administration
Goddard Space Flight Center
Beltsville, Maryland

Contract NSG-5134

TABLE OF CONTENTS

	Page
LIST OF FIGURES	iv
LIST OF TABLES.	xi
PREFACExii
ABSTRACT.xiii
INTRODUCTION.	1
Objectives and Research	7
REVIEW OF LITERATURE.	9
Spectral Theory.	9
Classification Models.	22
Biomass Models	24
Literature Overview.	28
DATA COLLECTION	29
Guymon Aircraft and Ground Data.	29
Dalhart Aircraft and Ground Data	40
Scatterometer Processing	51
NS001/M ² S Processing	53
Passive Microwave Processing	54
ANALYSIS.	55
Techniques	55
RESULTS	58
Guymon Crop Condition.	58
Dalhart Biomass and Crop Yield	58
Problem 1.	60
Problem 2.	81
Problem 3.	86
Problem 4.125

SUMMARY AND CONCLUSIONS140
Problem 1140
Problem 2141
Problem 3141
Problem 4143
Overview144
REFERENCES147
APPENDIX A DATA QUALITY, CALIBRATION AND OMISSIONS.152
APPENDIX B DALHART DATA SET.172
APPENDIX C GUYMON DATA SET183

LIST OF FIGURES

Figure	Page
1	Reflectance of 2 and 8 stacked mature cotton leaves. Standard deviation between observed and calculated points is about 1%. From Allen <u>et al.</u> , 1970. 16
2	Averaged normalized differences (IR-red/IR+red) values plotted against soybean wet biomass. From Tucker <u>et al.</u> , 1979 17
3	Diagram illustrating the principle of the perpendicular vegetation index (PVI) model. A perpendicular from candidate plant coordinates (Rp5, Rp7) intersects the soil background line at coordinates (Rg5, Rg7). A PVI=0 indicates soil, and a PVI>0 indicates vegetation. From Richardson and Wiegand, 1977. 27
4a	Area map of Guymon showing the relative locations of each field map 30
4b	Legend for the Guymon, Oklahoma fields maps 31
4c	Locations of the sample fields at Guymon, East end, Lines 1 and 2. 32
4d	Locations of the sample fields at Guymon, South end, Lines 3 and 4. 33
4e	Locations of the sample fields at Guymon, West end, Lines 1 and 2. 34
4f	Area map of Clayton showing the relative location of the field map 35
4g	Legend for the Clayton, New Mexico field maps 36
4h	Location of the sample fields at Clayton. 37
5	Sampling pattern for fields at Guymon and Dalhart. Points 1, 2, 7 and 8 were moved outside the circle for rectangular fields 41
6	Soil moisture sampling depths at Dalhart and Guymon. The 15-30 and 30-45 cm core samples were also taken in addition to the above. Samples were collected from 5-9 cm and 9-15 cm at Guymon and 5-15 cm at Dalhart. 42

7a	Area map of Dalhart showing the relative locations of each field map	43
7b	Legend for the Dalhart, Texas field maps.	44
7c	Locations of the sample fields at Dalhart, East end, Lines 1 and 2	45
7d	Locations of the sample fields at Dalhart, Lines 1 and 2	46
7e	Locations of the sample fields at Dalhart, West end, Lines 1 and 2	47
8	Scatterometer data processing procedure	52
9	Spectra for millet and corn fields at Dalhart. [H = C band horizontal (MFMR), V = C band vertical pole (MFMR), L = L band horizontal (MFMR), H = like pole 40° look angle (SCATTS), V = cross pole 40° look angle (SCATTS), A = 0-2 cm soil moisture (SM), B = 2-5 cm soil moisture (SM)].	61
10	Spectra for bare soil, pasture and wheat stubble at Dalhart. [H = C band horizontal (MFMR), V = C band vertical pole (MFMR), L = L band horizontal (MFMR), H = like pole 40° look angle (SCATTS), V = cross pole 40° look angle (SCATTS), A = 0-2 cm soil moisture (SM), B = 2-5 cm soil moisture (SM)]	62
11	Spectra comparing vegetated and non-vegetated fields at Dalhart. [H = C band horizontal (MFMR), V = C band vertical pole (MFMR), L = L band horizontal (MFMR), H = like pole 40° look angle (SCATTS), V = cross pole 40° look angle (SCATTS), A = 0-2 cm soil moisture (SM), B = 2-5 cm soil moisture (SM)].	63
12	An infrared aerial photo (scale 1:45,000) of stressed corn fields (fields 1 and 2) at Dalhart. The healthy areas are dark shaded and the stressed areas are light shaded.	66
13	Spectra comparing healthy and stressed corn at Dalhart. No microwave comparisons could be made.	67
14	Spectra comparing alfalfa, sorghum, and bare soil fields at Guymon. [H = C band horizontal (MFMR), V = C band vertical pole (MFMR), L = L band horizontal (MFMR), H = like pole 40° look angle (SCATTS), V = cross pole 40° look angle (SCATTS), A = 0-2 cm soil moisture (SM), B = 2-5 cm soil moisture (SM)]	68

15	Spectra comparing sorghum fields with rows perpendicular and parallel to the flight line. [H = C band horizontal (MFMR), V = C band vertical pole (MFMR), L = L band horizontal (MFMR), H = like pole 40° look angle (SCATTS), V = cross pole 40° look angle (SCATTS), A = 0-2 cm soil moisture (SM), B = 2-5 cm soil moisture (SM)]	70
16	Spectra comparing wet bare soil, and a dry sorghum field at Guymon. [H = C band horizontal (MFMR), V = C band vertical pole (MFMR), L = L band horizontal (MFMR), H = like pole 40° look angle (SCATTS), V = cross pole 40° look angle (SCATTS), A = 0-2 cm soil moisture (SM), B = 2-5 cm soil moisture (SM)]	71
17	Spectra comparing corn and sorghum at Clayton. No passive microwave or visible/infrared data was available. [H = like pole 40° look angle (SCATTS), V = cross pole 40° look angle (SCATTS)]	72
18	Spectra comparing corn and sorghum at Clayton. No passive microwave or visible/infrared data was available. [H = like pole 40° look angle (SCATTS), V = cross pole 40° look angle (SCATTS)]	73
19	Line plots (σ^0 vs time) for all like polarized scatterometer data at 10° and 40° off nadir	79
20	Line plots (σ^0 vs time) for all cross polarized scatterometer data at 10° and 40° off nadir	80
21	Dendrogram (tree-classification) model using NS001 bands 2, 3, and 4, C, L and P band cross pole Dalhart data (accuracy 78%).	83
22	Dendrogram (tree-classification) model using NS001 bands C, L and P band cross pole Dalhart data (accuracy 80%)	84
23	Dendrogram (tree-classification) modeling using M ² S bands 4, 7, 8 and 9, C and L band cross pole Guymon data (accuracy 70%).	85
24	Dendrogram (tree-classification) model using all NS001 bands Dalhart (accuracy 78%).	87
25	Dendrogram (tree-classification) model using M ² S bands 4, 7, 8 and 9 data at Guymon (65% accuracy)	88

26	The relationship between total biomass (g/m^2), and TVI and PVI at Dalhart.	96
27	The relationship between final crop yield (Kg/Ha), and TVI and PVI at Dalhart.	98
28	Field radiance reflectance values of NS001 bands 1 and 2 versus band 3 at Dalhart in 10^{-4} watts $\text{cm}^{-2} \text{ster}^{-1}$	99
29	Field radiance reflectance values of NS001 bands 4 and 5 versus band 3 at Dalhart in 10^{-4} watts $\text{cm}^{-2} \text{ster}^{-1}$100
30	Field radiance reflectance values of NS001 bands 6 and 7 versus band 3 at Dalhart in 10^{-4} watts $\text{cm}^{-2} \text{ster}^{-1}$101
31	Field radiance reflectance values of NS001 bands 1 and 2 versus band 4 at Dalhart in 10^{-4} watts $\text{cm}^{-2} \text{ster}^{-1}$102
32	Field radiance reflectance values of NS001 bands 3 and 5 versus band 4 at Dalhart in 10^{-4} watts $\text{cm}^{-2} \text{ster}^{-1}$103
33	Field radiance reflectance values of NS001 bands 6 and 7 versus band 4 at Dalhart in 10^{-4} watts $\text{cm}^{-2} \text{ster}^{-1}$104
34	Field radiance reflectance values of NS001 bands 1 and 2 versus band 5 at Dalhart in 10^{-4} watts $\text{cm}^{-2} \text{ster}^{-1}$105
35	Field radiance reflectance values of NS001 bands 3 and 4 versus band 5 at Dalhart in 10^{-4} watts $\text{cm}^{-2} \text{ster}^{-1}$106
36	Field radiance reflectance values of NS001 bands 6 and 7 versus band 5 at Dalhart in 10^{-4} watts $\text{cm}^{-2} \text{ster}^{-1}$107
37	The relationship between total (wet) biomass (g/m^2) and PVI64 at Dalhart.108
38	The relationship between PVI64, and PVI and TVI at Dalhart.110

39	A photo indicating different PVI64 levels within a stressed corn field (1 and 2) at Dalhart111
40	A photo indicating different PVI64 levels within a sorghum field (V2) at Dalhart.112
41	A photo indicating different PVI64 levels within alfalfa fields (V11, V12, V13) at Dalhart.113
42	The relationship between L band cross pole σ^0 and look angle for a corn field (field 9) and bare field (field 15)114
43	The relationship between L band cross pole σ^0 and look angle for a millet field (field 3) under different soil moisture conditions.115
44	The L band cross pole σ^0 response as a function of look angle for the same sorghum field (field 1X) from two different directions, the flight line parallel and perpendicular to the tillage direction.117
45	The relationship between total biomass and the scatterometer vegetation index, SVI. (4.75 HV 40° look angle - 4.75 HV 5° look angle) ($R^2 = 0.88$)119
46	The relationship between SVI (db), and TVI and PVI at Dalhart.120
47	The relationship between SVI (db), and TVI and PVI at Guymon121
48	The relationship between SVI (db), and 0-2 cm soil moisture (%) for selected fields at Guymon and Dalhart122
49	The relationship between soil moisture corrected SVI (db) and TVI and PVI at Dalhart123
50	The relationship between the soil moisture corrected SVI (db), and TVI and PVI at Guymon.124
51	The red/near-infrared relationship for fields at Guymon and Dalhart.127
52	The K band like pole σ^0 response as a function of look angle for bare soil (field 22), sorghum (field V2 and V6), and corn (field 2) at Dalhart128

53	The C band cross pole σ^0 response as a function of look angle for bare soil (field 22), sorghum (field V2 and V6), and corn (field 2) at Dalhart129
54	The L band cross pole σ^0 response as a function of look angle for bare soil (field 22), sorghum (field V2 and V6), and corn (field 2) at Dalhart131
55	The P band cross pole σ^0 response as a function of look angle for bare soil (field 22), sorghum (field V2 and V6), and corn (field 2) at Dalhart132
56	The K band like pole σ^0 response as a function of look angle for bare soil (field 14), alfalfa (field 4), emerging sorghum (field 15) and headed sorghum (field 1X).133
57	The C band cross pole σ^0 response as a function of look angle for bare soil (field 14), alfalfa (field 4), emerging sorghum (field 15) and headed sorghum (field 1X).134
58	The L band cross pole σ^0 response as a function of look angle for bare soil (field 14), alfalfa (field 4), emerging sorghum (field 15) and headed sorghum (field 1X).135
59	The P band cross pole σ^0 response as a function of look angle for bare soil (field 14), alfalfa (field 4), emerging sorghum (field 15) and headed sorghum (field 1X).136
60	The relationship between total biomass at Dalhart and the modified scatterometer vegetation index, SVIM [(C band cross pole 40° - C band cross pole 5°) + (P band cross pole 40° - P band cross pole 5°)] .	.138
61	The relationship between the modified SVI (SIVM) and TVI and PVI at Guymon139
A1	Field 1X (sorghum) P band like and cross pole response with rows perpendicular to the flight line . .	.160
A2a	Scatterometer response from the P band like pole system over field 25 (sorghum) with rows perpendicular to the flight line.161
A2b	Scatterometer response from the P band cross pole system over field 25 (sorghum) with rows perpendicular to the flight line.162

Figure

Page

A3 Scatterometer response (C and L like and cross pole) from field 25 at Dalhart on 8/16/80164

A4 Scatterometer response (K band like pole) from field 19 at Dalhart on 8/16/80 and field 14 at Guymon on 8/5/78. Soil moisture conditions were approximately 90% of field capacity165

A5 Scatterometer response (C band like and cross pole) from field 19 at Dalhart on 8/16/80 and field 14 at Guymon on 8/5/78. Soil moisture conditions were approximately 90% of field capacity166

A6 Scatterometer response (L band like and cross pole) from field 19 at Dalhart on 8/16/80 and field 14 at Guymon on 8/5/78. Soil moisture conditions were approximately 90% of field capacity167

A7 Scatterometer response (P band like and cross pole) from field 19 at Dalhart on 8/16/80 and field 14 at Guymon on 8/5/78. Soil moisture conditions were approximately 90% of field capacity168

LIST OF TABLES

Table		Page
1	Operating sensors for the Guymon, Oklahoma study.	39
2	Operating sensors for the Dalhart, Texas study.	50
3	Dalhart biomass and crop yield.	59
4	Results of Duncan's Multiple Range Test for Dalhart active microwave data	75
5	Results of Duncan's Multiple Range Test for Guymon active microwave data.	77
6	Dalhart discriminant analysis results using (a) all NS001 channels and (b) all NS001 channels plus K band like pole and L band cross pole (40° look angle) data from August 14 and 18 as a train- ing classifier. The results are from August 16 testing of the model.	90
7	Dalhart discriminant analysis using (a) NS001 channels 2, 3 and 4 and (b) NS001 channels 2, 3, and 4 and K band like pole and L band cross pole data. Contingency table results from the model tested on August 16 spectral data	91
8	Discriminant analysis of Guymon visible/infrared data using August 2 and 17 data as the training classifier. Results from classification of August 5, 8, 11, and 14 data	92
9	Dalhart stepwise classification regression equations using (a) all NS001 band (Ch) data and (b) all NS001 data plus scatterometer data (40° look angle) [Crop Type: 10 = corn, 8 = sorghum, 6 = weeds, 4 = bare soil and weeds, 3 = pasture, 2 = wheat stubble, 1 = bare soil]	94
10	Guymon stepwise classification regression equations using (a) only visible/infrared data and (b) scat- terometer (40° look angle) and visible/infrared data [Crop Type: 8 = sorghum, 4 = alfalfa, 0 = bare soil]. . .	95
A1	Equations used to convert raw NS001/M ² S digital counts (DC) to radiance values, R, (10 ⁻⁴ watts cm ⁻² ster ⁻¹) for Guymon (a) and Dalhart (b).	153

Table		Page
A2	Questionable scatterometer data for Dalhart156
A3	Questionable scatterometer data for Guymon.157
A4	Guymon and Dalhart questionable MFMR data170

PREFACE

The final report of Project RSC-3458, "Measurement of Soil Moisture Trends with Airborne Scatterometers" is divided into three volumes. The first volume deals primarily with the work completed by Dr. Sidney Theis relating multispectral (visible through microwave) information to soil moisture trends in bare and vegetated fields. The second volume deals primarily with the work of Dr. Wesley Rosenthal in relating the same multispectral data sets to agricultural crop classification and biomass estimation. The third volume by Ms. Cheryl Jones, details field work, aircraft schedules, data processing and calibrations, and the final data sets.

ABSTRACT

Due to inadequate crop acreage and biomass estimates using satellite and aircraft visible and infrared data, a study was conducted to (1) develop and test agricultural crop classification models using two or more spectral regions (visible through microwave), and (2) estimate biomass by including microwave with visible and infrared data. The study was conducted at two locations; Guymon, Oklahoma in 1978, and Dalhart, Texas in 1980. Aircraft multispectral data collected during the study included visible and infrared data (multiband data from 0.5 μm - 12 μm), passive microwave data [C band (6 cm) vertical and horizontal polarizations, and L band (20 cm) horizontal polarization] and active microwave data [K band (2 cm), C band (6 cm), L band (20 cm), and P band (75 cm) like and cross polarizations]. Ground truth data from each field consisted of soil moisture at both sites and biomass at Dalhart. The study was divided into four problems: (1) are differences in individual band responses related to crop type differences? (2) what is the most accurate multifrequency crop classifying dendrogram (tree classifier) at both locations? (3) what is the utility of microwave data alone or in combination with other spectral bands for classifying crops and estimating total biomass? and (4) is the multifrequency tree-classification model variability dependent on phenological or biomass differences? Results indicated that inclusion of C, L, and P band active microwave data from look angles greater than 35° from nadir with visible and infrared data improved crop discrimination and biomass estimates compared to results using only visible and infrared data. The active microwave frequencies were

sensitive to different biomass levels. K and C band were sensitive to differences at low biomass levels, while P band was sensitive to differences at high biomass levels. In addition, two indices, one using only active microwave data and the other using data from the middle and near infrared bands, were well correlated to total biomass. Results from the study implied that inclusion of active microwave sensors with visible and infrared sensors on future satellites could aid in crop discrimination and biomass estimation.

INTRODUCTION

With world population increasing to a point where food supplies will become scarce, the need to improve global agricultural information systems becomes critically important. Such emphasis is needed to avert potential world disasters of starvation and malnutrition due to inadequate food supplies. The delicate imbalance is demonstrated by the fact that since 1948 the amount of exported grain from developed countries to developing countries has risen dramatically. As a result, the less developed countries are more dependent on surplus production in a few developed countries (Wortman, 1976). A recent World Food and Nutrition Study (National Academy of Sciences, 1977) emphasized the need for improved systems by recommending high priority research on

1. information needs of producers,
2. crop monitoring systems,
3. international data bases for land and nutrition, and
4. a total information system.

Perhaps the major priority is developing crop monitoring systems. This world-wide need was emphasized when the United States lost millions of dollars by selling wheat to the Soviet Union, who later sold the wheat at much higher prices. An adequate crop monitoring system would possibly have averted the deal. The benefits of improved agricultural monitoring systems used for predicting food production would include

1. commodity prices would be more stable,
2. governments will be able to plan foreign policy, and

3. storage, transportation and processing facilities will be more efficiently used.

The first benefit would prevent rapid and drastic seasonal commodity price fluctuations due to large and small supplies. Second, the United States government, with an estimate of foreign production, would be able to deal according to the foreign government's true needs. This would prevent events such as the U. S./Soviet Union wheat deal of 1974. Third, more efficient use of transport and storage facilities would help achieve the first two benefits.

The major problem of monitoring production systems within foreign countries is the inadequate source of data on acreages and climate variables. Several countries do not presently have any means for estimating acreage or production within the country. Other countries have production monitoring systems which are highly inaccurate. Acreage and yield estimates by the government are often inaccurate. In addition, several countries do not permit other countries to use the production information. Consequently, a universal technique is needed soon.

One technique developed within the past twenty years uses remotely sensed data--sensors aboard satellites or aircraft--to estimate production. From remotely-sensed data much information can be obtained with a minimum of ground sampling (Bauer, 1975). Such information would drastically reduce the cost of monitoring agricultural systems. The technique is based primarily on the relationship of reflectance in the visible and infrared region of the electromagnetic spectrum to vegetation type, cover, and crop condition. Idealistically, each healthy species has a characteristic electromagnetic signa-

ture at a given growth stage. Any departure from the signature indicates physiological stress which could impact crop yield. However, the actual spectrum varies to an extent that crop and stress identification is impossible using available data. The variability of a crop spectrum due to stress is much larger than variability due to differences between crops. The vegetation spectrum also differs significantly from the non-vegetated spectrum. Consequently, based upon the difference within the spectrum, crop types have been discriminated to a good degree of accuracy. Also, based on the spectra, models have been developed which estimate biomass, leaf area index, or percent cover (Richardson and Wiegand, 1977; Rouse et al., 1973). Biomass estimates can then be correlated to final economic yield (Holliday, 1960a, b; Donald, 1963). As a result, visible/infrared satellite and aircraft data have been used in (1) estimating the percentage of area planted in a given crop, and (2) evaluating crop condition and biomass. The combination of the two gives a production estimate for the area (MacDonald, 1979). Consequently, through the use of satellite and aircraft data, agricultural classification and biomass estimation became important as a means of obtaining reasonable estimates of planted acreage and ultimately, yield. In addition, agricultural data can be collected by satellites and aircraft from isolated areas of the world where agricultural information had been difficult to obtain.

The major experiment during the 1970s which classified wheat and estimated wheat acreage using only visible and near infrared data from Landsat was the Large Area Crop Inventory Experiment (LACIE) (MacDonald, 1979). LACIE was developed primarily at the request of the

U. S. government to help monitor foreign production. The objective was to estimate foreign wheat production in several key countries, such as the Soviet Union and Argentina. Success of the program would prevent another U. S./Soviet Union grain trade incident. Results were well documented and the experiment was successful in some geographical areas (Heydorn et al., 1979a; Potter et al., 1979). From that experiment and other studies, many crops were discriminated from bare soil and water, but acreage estimates were still inaccurate as a result of similar spectral responses from other crops grown during the same time of year (Heydorn et al., 1979a). To improve estimates, ground ancillary data, such as crop growth stage or spectral data from different wavelength regions, are needed. With the proposed launch of the Thematic Mapper, with finer spatial resolution and different spectral bands than Landsat, land-use and vegetation classification will again be the primary objective of further research (National Research Council, 1976). The Thematic Mapper will have spatial resolution of 30 m x 30 m while Landsat has a resolution of 80 m x 80 m. The Thematic mapper will have spectral bands of (1) 0.45 to 0.52 μm , (2) 0.52 to 0.60 μm , (3) 0.63 to 0.69 μm , (4) 0.76 to 0.90 μm , (5) 1.00 to 1.30 μm ; (5) 1.55 to 1.75 μm and (7) 2.08 to 2.35 μm . Landsat has spectral bands of (1) 0.50 to 0.60 μm (2) 0.60 to 0.70 μm (3) 0.70 to 0.80 and (4) 0.80 to 1.1 μm .

Different supervised and unsupervised classification techniques emerged from LACIE. In the first method, "samples" of spectral data were compared to a "training" sample of known land use. If the two samples were similar, the sample was classified as the same land use or vegetation cover that was present in the training area. In this

technique, the analyst input the training information in a classifier algorithm (Bauer et al., 1977). In the unsupervised method, similar responses are grouped together into clusters and these clusters are then compared to actual species clusters (Cooley and Lohnes, 1971). From this technique a tree-classification diagram can be developed based on spectral differences between the clusters. Both techniques are widely used in analyzing visible/near infrared spectral data with supervised techniques being more widely used with satellite data.

The major problems in classifying agricultural crops with visible/infrared data have been the dependence for reliable data on clear weather and the variability of the classification estimate due to phenological or biomass differences. Billingsley et al. (1976) proposed to eliminate these problems by including data from additional bands, such as microwave data, which are independent of cloud cover. Spectral data from many countries are predominantly influenced by excessive cloud cover. In many countries, agricultural Landsat data were obtained only once during the growing season. Consequently, more frequent passes or additional bands were needed to improve satellite coverage. Also, with additional bands more accurate biomass estimates may be possible. During the LACIE experiment it was also found that climate data, primarily precipitation, was necessary before good estimates of yield could be obtained. In the LACIE study, precipitation was used to estimate the soil moisture available to the crop. The microwave sensors have been recognized as a possible source of moisture estimates. In addition to this purpose they could also be used to aid in discriminating crops.

Sensors can detect from two modes of radiation--active and passive. Active sensors refer to sensing reflected surface radiation which originated from a known man-made energy source. Passive sensors refer to detection of natural surface emitted and reflected radiation. In this case, the surface is the source of radiation. Considerable effort has been made to take advantage of polarization effects in active sensors while little has been done in polarization effects in passive systems. Both have significant polarization differences; however, passive microwave systems have too coarse spatial resolution to be used effectively in crop discrimination. Microwave data can be either active or passive. Active microwave responses are expressed as σ^0 , the scattering coefficient, while passive microwave responses are expressed as brightness temperature. In contrast to the microwave data, visible studies are primarily passive systems. Active visible/infrared data have been analyzed, but are too complicated to be widely used.

Active microwave responses are primarily dependent on two surface characteristics--surface roughness and soil moisture. Consequently, crops having different roughnesses or morphologies would respond differently in different radar bands (Simonett et al., 1967). Higher frequencies and the consequent shorter wavelength should be more sensitive than lower frequencies to the roughness characteristics of vegetation. Different microwave frequencies should also have different capabilities of penetrating crop canopies and different sensitivity to soil moisture. Active microwave responses in the 8-18 GHz range at high incidence angles of HH (horizontally polarized transmit and received) and VV (vertically polarized transmit and received) have

been related to vegetative characteristics (Ulaby et al., 1975). High emissivity in the passive microwave have also been related to vegetative biomass (Sibley, 1973; Peake et al., 1966; Newton, 1977).

In spite of the extensive research in the active microwave region, few studies have related combinations of visible, infrared, and microwave data to vegetation characteristics (Brakke et al., 1981; Ulaby et al., 1981). Consequently, it is felt that a classification and biomass estimation study using visible, near infrared, far or thermal infrared, and microwave data collected over an agricultural area may produce a multifrequency system that will provide improved estimates of crop acreage and crop conditions.

Objectives and Research

The purpose of this study was to (1) develop and test an agricultural classification model using two or more spectral regions (visible through microwave), and (2) estimate biomass by including microwave with visible and infrared data. The hypothesis was that microwave data can improve classification and biomass estimation accuracy over present classification and estimation techniques that use visible and infrared data.

The study was divided into four problems which were intended to answer the previously mentioned goals. The first two deal primarily with crop classification and the last two with biomass and crop classification:

1. Are differences in individual spectral band responses related to crop type differences and what is the relationship of each individual multispectral band response to crop type?

2. What is the most accurate multifrequency dendrogram (tree-classification diagram) of agricultural crops in the Dalhart, Texas and Guymon, Oklahoma areas?
3. What is the utility of microwave data alone or in combination with other spectral bands for classifying agricultural crops and estimating biomass?
4. Is the multifrequency crop tree-classification model influenced by phenological or biomass differences and can the model be adjusted to apply for all biophases?

Data used in this study were collected from the Guymon, Oklahoma area in 1978 and the Dalhart, Texas area in 1980. Aircraft data were collected using the NASA C-130 aircraft with its full complement of sensors and crew from the Johnson Space Center in Houston, Texas. Ground measurements were collected and processed with extensive support from graduate students and technical personnel from both Texas A&M University and the University of California at Santa Barbara. Further discussion of the collection and processing of these data will be found in a following section.

A valid hypothesis implies that more accurate production estimates are possible by including microwave with visible and infrared data. Microwave data could add another dimension--vegetative roughness--to the analysis of visible and infrared data which are highly correlated to the amount of biomass. In addition, the independence of microwave data to weather conditions allows analysis of many other areas of the world which were difficult to monitor using visible and infrared data.

REVIEW OF LITERATURE

Classification and biomass models are based on spectral response differences between and within crop types in given wavelength regions. Consequently, to better understand classification models, an understanding of the spectral response at all wavelengths is required.

Spectral Theory

The reflection of electromagnetic radiation from a given surface as given by equations 1 and 2 is described by Janza (1975):

$$R_v = \frac{-(\epsilon_2 \cos \theta_i) + \sqrt{\epsilon_2 - \sin^2 \theta_i}}{(\epsilon_2 \cos \theta_i) + \sqrt{\epsilon_2 - \sin^2 \theta_i}} \quad (1)$$

and

$$R_h = \frac{(\cos \theta_i) - \sqrt{\epsilon_2 - \sin^2 \theta_i}}{(\cos \theta_i) + \sqrt{\epsilon_2 - \sin^2 \theta_i}} \quad (2)$$

where R_v and R_h are the reflection coefficients for vertical and horizontal polarizations, respectively; ϵ_2 is the dielectric constant of the reflecting medium, and θ_i is the incidence angle of the plane wave source. Consequently, the dielectric constant plays an important role in determining reflectance at all wavelengths. The dielectric constant varies with wavelength, moisture content, and temperature. For example, variations of the dielectric with wavelength are demonstrated by water--the dielectric at high microwave frequencies is 81,

and in the visible, 1.77 (Janza, 1975). Also, the relationship between wavelength and roughness affects reflectance. If surface roughness is greater than one-eighth of the wavelength, the reflectance is diffuse; otherwise, reflectance is primarily specular. This explains why some surfaces look rough at one frequency and smooth in another. Equations 1 and 2 apply for conditions involving an external source.

In the visible and near-infrared spectral regions, solar radiation is the primary source for reflected radiation at the earth surface. In this spectral region, different materials possess different reflective properties. These spectral differences can be analyzed and used in discriminating many materials on earth. Given that solar radiation is relatively constant at a given zenith angle--assuming constant atmospheric absorption and transmission--reflectance is analyzed through radiance. Radiance (L) can be defined as radiant flux per unit of projected source area in a specified direction (Janza, 1975). Radiance is calculated for a wavelength channel, $\lambda_2-\lambda_1$, by

$$L = \frac{1}{\pi} \int_{\lambda_1}^{\lambda_2} \left[E(\lambda)R(\lambda)(T_B(\lambda)T_z(\lambda)p(T)\sin B + \rho'_B(\lambda)) \right] d\lambda \quad (3)$$

where $E(\lambda)$ is the specular solar irradiance at the top of the atmosphere at normal incidence, $R(\lambda)$ the spectral response function of the wavelength channel, $T_B(\lambda)$ the monochromatic one-way transmissivity of the atmosphere at elevation angle B, $T_z(\lambda)$ the monochromatic transmissivity of the atmosphere in the zenith direction for solar radia-

tion reflected by the surface to the nadir-viewing sensor, $p(\lambda)$ the reflectance of the surface, and $p'_B(\lambda)$ the atmospheric reflectances as dependent on solar elevation, B .

Microwave emissions can be measured in two modes--active (surface reflection of energy from a source) or passive (emitted from the surface). This is in contrast with visible and infrared data which is generally sensed in a passive mode. Active visible research has been conducted using lidar, but measurements are quite complicated. The active microwave (radar) responses from many surfaces have been extensively analyzed primarily due to the application of active systems by the military; however, passive microwave research has been less developed due to limitations in spectral resolution or antenna size. Since active and passive microwave data are two different sensing modes, the responses are expressed differently--radar returns are expressed in σ^0 and passive microwave returns are expressed as brightness temperature.

The microwave region has more complex relationships which define reflected radiation. With active microwave systems, surface characteristics have been analyzed by comparing the power returned to a radar receiver with the transmitted power as calculated from the radar equation

$$W_r = \frac{W_t G_t}{4\pi R^2} \sigma \frac{1}{4\pi R^2} A \quad (4)$$

where W_r is the received power, W_t the transmitted power, G_t the gain of the transmitting antenna in the direction of the target, R the distance between the antenna and target, σ the radar cross section,

and A_r the effective area of the receiving antenna aperture (Janza, 1975). Most applications involve targets which are larger than a resolution cell of radar. Consequently, it is more convenient to consider the average return power over an irradiated area. The average differential cross-section is known as the scattering coefficient, σ^0 . The above equation implies that radar returns from a target depend upon the strength of the transmitted energy and the reflecting capability of the target. The target roughness and dielectric characteristics produce varying proportions of the return described by the backscatter. In addition to determining the return power, scattering properties of targets can also depolarize the return causing cross-polarized (HV or VH) radar data to be useful in geological and agricultural applications. Such depolarization leaves the cross-polarized data sensitive to dielectric properties.

The effect of roughness and the dielectric constant on active and passive microwave returns differ. The roughness effect dominates the active microwave returns, while the dielectric influence dominates the passive microwave return. The effects also depend on look angle. At high look angles, roughness becomes even more predominant.

According to Planck's equation, emitted radiation from the earth surface peaks in the thermal infrared region. Total emitted surface radiation is described by the Stephan-Boltzmann Law (Planck's Equation applied over all wavelengths):

$$R = \epsilon_s \sigma T^4 \quad (5)$$

where R is emitted radiation, ϵ_s is the emissivity of the surface, σ is the Stephan-Boltzmann constant ($5.7 \times 10^{-8} \text{ Wm}^{-2} \text{ K}^{-4}$), and

T is the absolute temperature. Most natural objects have emissivities between 0.8 and 1.0 in the thermal region. This will be different in the microwave region. Several factors, such as topography and weather, have made it difficult to classify crops using thermal infrared data. Thermal data, however, have often been used to evaluate soil moisture conditions.

Emissions in the passive microwave region are much smaller than thermal infrared emission. Emitted responses are based upon Rayleigh-Jean's approximation to Plank's equation (Wolfe and Zissis, 1978)

$$R_b = \frac{2kT}{\lambda^2} \quad (6)$$

where R_b is radiation (brightness) from a blackbody, T the absolute temperature, k Plank's constant and λ the wavelength. The emitted radiation in the microwave region is often expressed as brightness temperature. It can be expressed as a function of ground and atmospheric emissivity (ϵ_g and ϵ_a), ground reflectance (p_g), and sky, ground, and atmospheric (clouds, water vapor, particulates) temperatures (T_s, T_g, T_a):

$$T_b = p_g T_s + \epsilon_g T_g + \epsilon_a T_a + p_g T_a \quad (7)$$

Effects of the atmosphere are often negligible, especially with cloudless sky. Consequently, T_a is often neglected giving

$$T_b = \epsilon_g T_g + (1 - \epsilon_g) T_s \quad (8)$$

Since T_s and $(1 - \epsilon_g)$ are both small, the reflection term, $(1 - \epsilon_g) T_s$, is often omitted leaving only

$$T_b \approx \epsilon_g T_g \quad (9)$$

The variation in ground emissivity, ϵ_g provides much information on dielectric constant and roughness. Since healthy crops contain over 50% water and appear rough in certain microwave wavelengths, ground emissivity will vary under different vegetation conditions (Peake, 1966; Sibley, 1973).

Given the spectral theory, which is applicable at all wavelengths, one must turn to the factors which primarily influence spectral responses of agricultural crops. To simplify the description, the electromagnetic spectrum will be divided into the visible/infrared and the microwave regions.

Visible/Infrared Responses

Water and chlorophyll are the most important substances which influence vegetation and soil reflectance in the visible/infrared. At high solar elevation angles, water strongly absorbs solar radiation in both the visible and infrared. Consequently, visible and infrared reflectance from a soil would often decrease under high moisture conditions. The moisture effect is highly dependent on conditions within the top thin layer of the surface being observed. No subsurface moisture can be directly determined using wavelengths shorter than one centimeter (Davis et al., 1965).

Leaves, however, have a completely different spectrum. Due to Fresnel reflectance at air/water interfaces within the leaves, near

and middle infrared radiation is strongly reflected (Figure 1) (Gates, 1980). Figure 2 demonstrates that the relationship between biomass and reflectance is dependent upon crop type and maturity (Tucker et al., 1979, Park and Deering, 1981). Reflectance increases rapidly with total biomass in the near- and middle-infrared region until a saturated reflectance is reached. At that point reflectance becomes insensitive to increases in biomass. Then at a point near maturity, the reflectance in this region begins to decrease with biomass. Consequently for corn and soybeans, crops with a near-complete canopy cover, reflectance is insensitive to total biomass increases for a given period of time. Other techniques are needed to quantify biomass estimates in this region. Reflectance is also a function of the chlorophyll content. Chlorophyll absorbs radiation in the red and blue regions, and has a slight reflectance in the green and high reflectance in the near infrared. Studies by Hoffer and Johannsen (1969) indicated changes in chlorophyll content allowed other carotenoids and xanthophylls to become evident, thus affecting primarily the visible/infrared reflectance. Since infrared reflectance is strongly dependent on the air/water interface and chlorophyll content, any environmental effect which changes the area of air/water interface or the number of leaves will influence the reflectance. Consequently, disease and stress (moisture, nutrient, etc.) drastically decrease infrared reflectance. In spite of these effects, differences between the visible and near infrared data have been the basis for classifying vegetation and estimating biomass. The main premise is that at a given phenological period for a crop, spectral characteristics in the

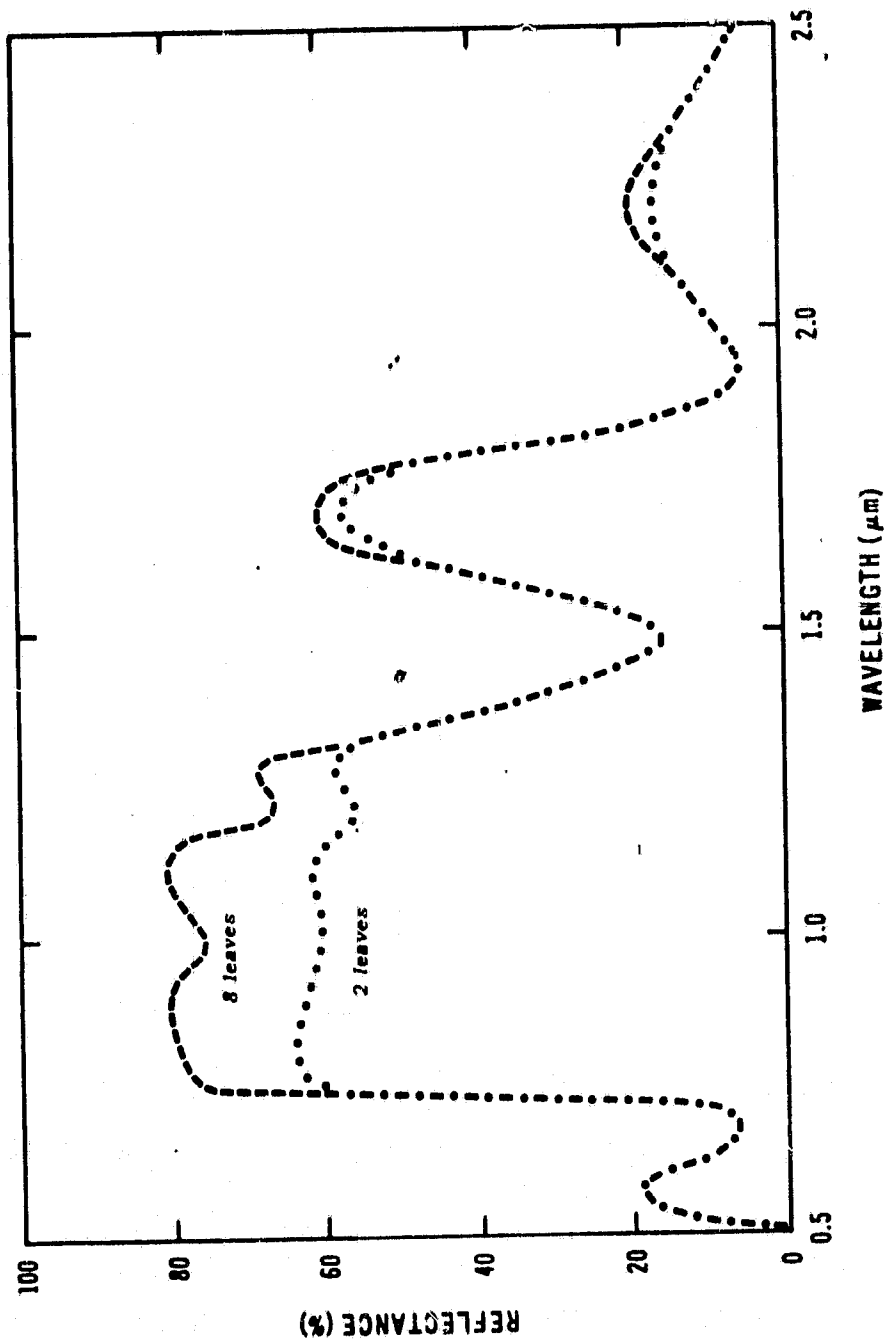


FIG. 1 Reflectance of 2 and 8 stacked mature cotton leaves. Standard deviation between observed and calculated points is about 1%. From Allen et al., 1970.

ORIGINAL PAGE IS
OF POOR QUALITY

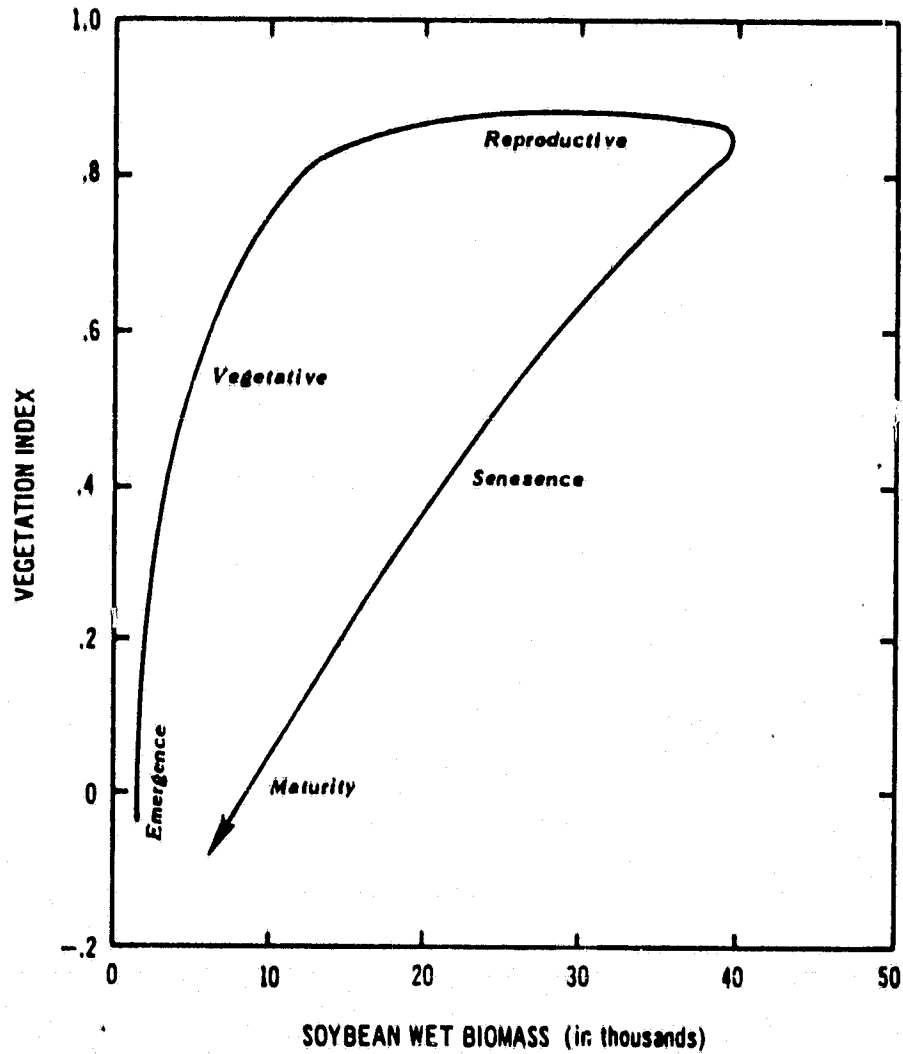


FIG. 2. Averaged normalized difference (IR-red/IR + red) values plotted against soybean wet biomass. From Tucker *et al.*, 1979.

crop allow for crop discrimination--assuming that spectral differences within the crop attributed to stress or disease are less than the differences between crops. Also, if two crops have the same phenology and spectral characteristics, they will not be spectrally separable. Given difference in chlorophyll content and leaf succulence between plant species, classification and biomass estimation models have been developed. The detection is consequently based on visible/infrared differences between crop types. Different biomass models will be discussed later.

Integrating the soil and vegetation reflectance has been a problem. Many have tried to model canopy (integrated) reflectance (Kubelka and Munk, 1931; Chance and LeMaster, 1977; Richardson et al., 1975). Chance and LeMaster (1977) used the Suits model to estimate reflected and non-reflected radiation from a boundary layer. However, the model showed little agreement with wheat reflectance data as a function of solar angle. Richardson et al. (1975) used the Kubelka-Munk and a regression model, using biophysical parameters for extracting plant, soil, and shadow reflectance components of cropped fields. The model did correlate well to actual scene reflectance.

Microwave Responses

Three factors primarily affect reflectance and emission from agricultural surfaces in the microwave region--surface roughness, soil moisture, and vegetation. To fully understand the return from an agricultural scene, one must account for each factor. Each factor will be discussed in greater detail.

Roughness - As mentioned before, for active microwave systems σ^0 is governed by the geometric properties of the surface. Beckman (1966) found the backscatter to be related to the variance and mean slope of the surface. Ulaby et al. (1978) found σ^0 variations attributable to soil roughness decrease with look angle out to 10° from nadir, which is the least sensitive to roughness. Fenner et al. (1981) and Ulaby and Bare (1979) found row direction was very important in the radar return. Rows perpendicular to the emitted beam have much higher returns compared to rows parallel to the emitted beam. At certain look angles and frequencies the surface roughness effect may dominate the terms that are due to changes in the dielectric constant brought about by changes in soil moisture.

Wang et al. (1980) noted that tilled row direction is also a major factor in passive microwave emission, especially when the antenna is directed off nadir to the ground. The difference between vertical and horizontal polarized returns in passive microwave returns can be related to the soil surface roughness (Newton 1977, Choudhury et al., 1979). The effect appears to decrease at look angles larger than 35 degrees off nadir. The roughness effect is also dependent on the relative height of the roughness in relation to the wavelength of the sensor.

Soil moisture - The effect of the dielectric constant on the active microwave response is demonstrated by changes in soil moisture. In the high frequency microwave regions, soil has a dielectric constant of 3, and water, 81. Consequently, any significant change in soil moisture should be detectable. The relationship has been studied

in great detail using active systems. Laboratory experiments by Lundien (1971) showed L band (21 cm wavelength) data should be more sensitive to soil moisture differences than K band (1.55 cm wavelength) due to differences in the dielectric constant of water at the two frequencies. However, Ulaby et al. (1978) found C band active microwave data to be most sensitive to soil moisture differences in the surface two centimeters. The severe effect of roughness that is inherent in active microwave returns was minimum in Ulaby's experiment which was carried out over tillage common to Kansas using C band at 10° off nadir.

Field experiments by Newton (1977) and analysis of satellite data by McFarland (1976) had shown L band passive microwave data was sensitive to soil moisture changes within approximately the surface 5 cm layer. Other similar work had been done in using active and passive microwave data. An excellent review of studies concerning soil moisture estimates using microwave systems was given by Schmugge (1978).

Vegetation - The effect of vegetation on the active microwave return has been studied since the mid-1960s. Early work concentrated on analyzing effects in the K band (1-2 cm) region (Simonett et al., 1967, Ellermeier et al., 1969). The studies indicated radar was a potential tool for discriminating crops. The response is based on both moisture and roughness. As a crop matures, the crop moisture increases to the time that the crop begins to senesce and then decreases. At look angles of greater than 40° from nadir, σ^0 is strongly correlated to plant water content in corn and wheat (Ulaby and Bush, 1976a and 1976b). Consequently, biomass could be estimated

for the growing period. Also, crops have different morphologies which can be applied to crop discrimination. However, other factors may influence the scatterometer return. De Loor et al. (1974) found σ^0 to vary as much as 4 to 5 db under different wind speeds. Brakke et al. (1981), however, found no influence of wind speed on σ^0 over wheat and sorghum in the K band region. Ulaby et al. (1975) found that crops can be discriminated with multifrequency vertically polarized data (between 8 to 18 GHz (2.5-3.5 cm)). Look angles at 30° to 65° from nadir removed the soil moisture effects leaving only the vegetative effects. Comparisons between like- and cross-polarized active microwave data (1.25 GHz--25 cm) also provided valuable information on vegetation. Classification accuracies improved from 65% to 71% by including cross with like-polarized data (Ulaby et al., 1980).

Comparisons of different polarizations of passive microwave data also indicated crop morphological differences (Kirdyashev et al., 1979). Relationships between biomass, height, plant moisture content and brightness temperature at multiple frequencies were found. Such parameters can be related to crop type differences. The passive microwave data, however, are less practical for crop discrimination due to the poor resolution associated with aircraft and spacecraft passive systems.

To summarize, active microwave data at look angles greater than 30° from nadir appear to be related to vegetative characteristics which can imply crop type differences. Active microwave systems are more sensitive to roughness, while passive systems are more sensitive to soil moisture. Multifrequency passive microwave data also have been related to similar vegetative characteristics but are less

sensitive to roughness and vegetation, and have less acceptable resolution capabilities than the active systems. The sensitivity to all three factors is dependent on wavelength (frequency) as well as polarization and look angle for both active and passive systems.

Classification Models

Supervised Models

From the previously mentioned visible and near-infrared relationships of vegetation, several classification models have been developed. Heydorn et al. (1979b) gave a general description of several supervised and unsupervised techniques which emerged from studies with LACIE.

Supervised classification techniques became one of the key classification techniques. The methods required information on the classes--means, standard deviations, or vectors of data. This information was termed the training classifier. Using various comparison techniques, sampled data were compared to the training classifier and placed into the proper class. To separate classes, discriminant functions as determined from class statistics were calculated. Any sample which fell on either side of the function was placed into one of the classes (Swain and Davis, 1979). Several of the widely used supervised techniques were maximum likelihood per point, maximum likelihood per homogeneous group, ECHO--Extraction and Classification of Homogeneous Objects--minimum distance to the class means, and standard deviations to calculate the probability of including the sample in a given class. The only difference between the ECHO classifier and the maxi-

imum likelihood classifier was the sample; ECHO uses a homogeneous group of sample points, while the maximum likelihood per point method analyzes only one sample point at a time. In the minimum distance classifier, a Euclidean distance was calculated between the data vector at one point and the mean vector. If the distance was less than a given threshold, the point was placed into the given class. The layered classifier differed from the maximum likelihood per point classifier in that multiple decisions, rather than one decision were made at each point. This allowed for different subsets of channels to be used. Bauer et al. (1977) found no significant difference in accuracy using each of these techniques. However, the minimum distance classifier had the lowest computer cost.

Unsupervised Models

Unsupervised classification, or clustering, models require no information on classes. The techniques grouped similar spectral averages. The most widely used technique involved the minimum distance between observations (Johnson, 1967). Another similarity criterion technique involved minimizing variance or the sum of squares. Other techniques were described by Orloci (1978) and Hartigan (1974). Such techniques had been used in combination with other supervised techniques to classify agricultural scenes and estimate areal coverage from Landsat data (Heydorn et al., 1979a). A major part of the classifier was the "tree structure" which defined decision points as determined by variable differences between spectral classes involved.

Classification accuracies using these techniques had varied from one location to another. The areas having the lowest accuracy had

"confusion" crops growing in the same area--crops which have the same spectra at a given period. Accuracies ranged from 60% to over 90% in some areas.

In the microwave region, success in classifying vegetation has been equally as accurate. Simonett et al. (1967) was one of the first to classify an agricultural scene using like- and cross-polarized data. Ulaby et al. (1980) also classified correctly 71% of an area using like- and cross-polarized microwave data. Other work was done by Morain and Simonett (1967), Schwarz and Caspell (1968), Waite and MacDonald (1971), and Ulaby et al. (1975). Blanchard et al. (1979) classified pasture, timber and bare soil with reasonable accuracy using airborne scatterometer data. Land use was correctly determined in greater than 80% of the cases by analyzing the differences in the 10° and 35° look angle σ° values for like-polarized data, differences in the like- and cross-polarized data at 10° look angle, and the cross polarized data at 10° look angle. Few studies, however, have combined active and passive microwave data with visible and near-infrared data. Ulaby et al. (1981) analyzed scatterometer and Landsat data collected over an agricultural area in 1978. Classification accuracy increased 10% by including scatterometer data with Landsat data. Further work needs to be done relating vegetation type to visible, infrared, and passive and active microwave data.

Biomass Models

Visible/Infrared Region

Because infrared leaf reflectance is strongly influenced by the number of leaves, which in turn is related to plant biomass, many

models have been developed using a combination of visible/infrared reflectance data. Only a few significant models are mentioned here.

The transformed vegetation index (TVI) has been used primarily as an estimator of rangeland biomass (Rouse et al., 1973; Deering et al., 1975). The model was expressed as

$$TVI = \sqrt{\frac{MSS7 - MSS5}{MSS7 + MSS5}} + 0.5 \quad (10)$$

where MSS7 and 5 are radiances from Landsat bands 7 (0.8-1.1 μm) and 5 (0.6-0.7 μm), respectively. The ratio was used as a normalizing term to remove temporal index variations, such as illumination differences due to aerosols and solar angle, and 0.5 was added to keep the term under the square root from going negative. A modification of the index involved replacing band 6 (0.7-0.8 μm) data for band 7. The modified index was TVI6. Both were well correlated to green biomass.

Kauth and Thomas (1976) developed transformation matrices which converted Landsat data for cultivated agricultural areas to data which enhanced greenness, brightness, and yellowness. By comparing transformed data from temporal scenes, the progression of phenology followed the shape of a "tasseled cap." Converting the matrices to index

$$GVI = -0.290 \text{ MSS4} - 0.562 \text{ MSS5} + 0.600 \text{ MSS6} + 0.491 \text{ MSS7} \quad (11)$$

and the brightness index was

$$SBI = 0.433 \text{ MSS4} + 0.632 \text{ MSS5} + 0.586 \text{ MSS6} + 0.264 \text{ MSS7} \quad (12)$$

where MSS4, 5, 6 and 7 refer to Landsat bands 4, 5, 6 and 7 digital counts. GVI had been found to be highly correlated to leaf area index (Richardson and Wiegand, 1977).

Another vegetation index model used to estimate biomass is the perpendicular vegetation index (PVI), developed by Richardson and Wiegand (1977). PVI was calculated by the equation

$$PVI = \sqrt{(R_{gg5} - R_{p5})^2 + (R_{gg7} - R_{p7})^2} \quad (13)$$

where R_p is the reflectance for a candidate vegetation point for Landsat bands MSS5 and MSS7 and R_{gg} is the reflectance of soil background corresponding to the same candidate vegetation point. Figure 3 describes the principle of the perpendicular vegetation index. Simply, PVI is the perpendicular distance from a given radiance in bands 5 and 7 to the soil background line. It was demonstrated by Richardson and Wiegand (1977) that PVI6 and TVI6 (where Landsat band 6 is used instead of band 7) are both highly correlated to leaf area index.

Microwave Models

Work is just beginning in relating microwave data to vegetation characteristics. Brakke et al. (1981) related corn, wheat, and sorghum characteristics, such as plant moisture content, crop height, and leaf area index, to microwave, visible and near-infrared data. The authors determined dry matter was highly correlated with σ^0 at look angles of 70° off nadir. Jackson et al. (1981) compared biomass estimates to changes in the slope of regression lines relating soil moisture and normalized passive microwave brightness temperature. As biomass increased, the sensitivity of normalized brightness temperature related to soil moisture decreased.

ORIGINAL PAGE IS
OF POOR QUALITY

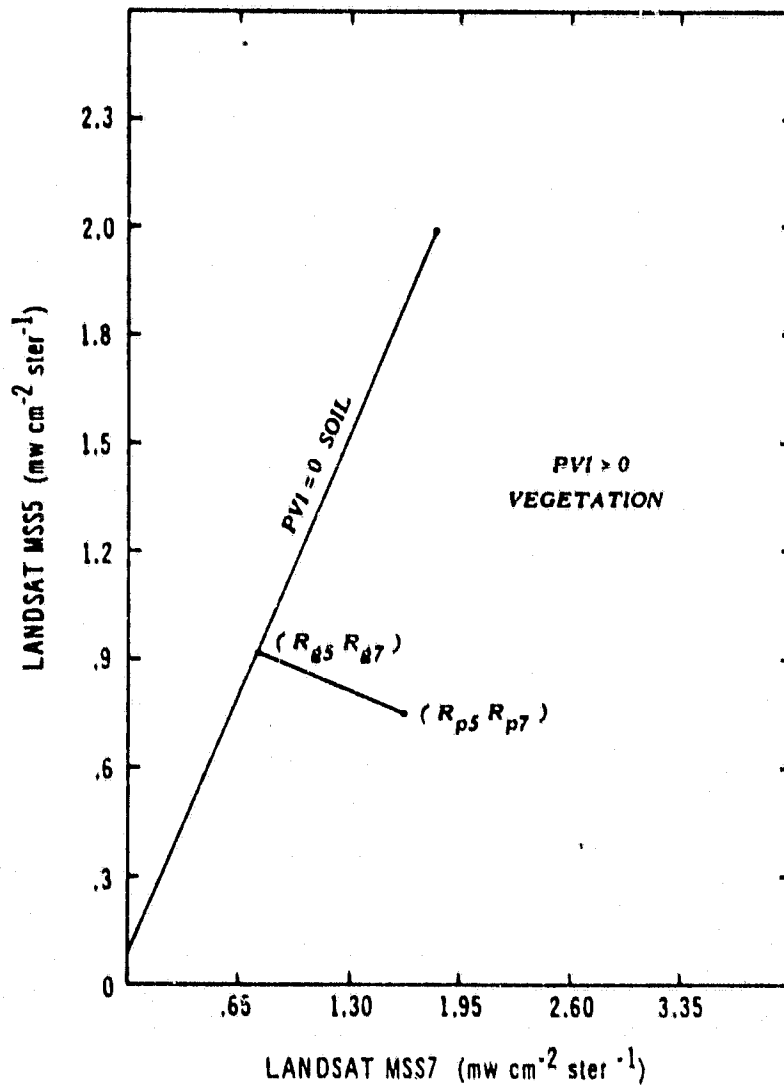


FIG. 3. Diagram illustrating the principle of the perpendicular vegetation index (PVI) model. A perpendicular from candidate plant coordinates (R_{p5} , R_{p7}) intersects the soil background line at coordinates (R_{g5} , R_{g7}). A $PVI=0$ indicates soil, and a $PVI>0$ indicates vegetation. From Richardson and Wiegand (1977).

Literature Overview

From the research reported, it is evident that simultaneous data using visible, infrared, and microwave bands have rarely been collected. More data sets of visible, infrared, and microwave data are needed to compare against vegetation type and characteristics, such as biomass. According to theory, microwave frequencies should be sensitive to different vegetation characteristics (primarily geometric and dielectric properties) than characteristics seen by visible and infrared data. As a result, classification accuracies and biomass estimates should improve by including microwave (active or passive) bands with visible and infrared.

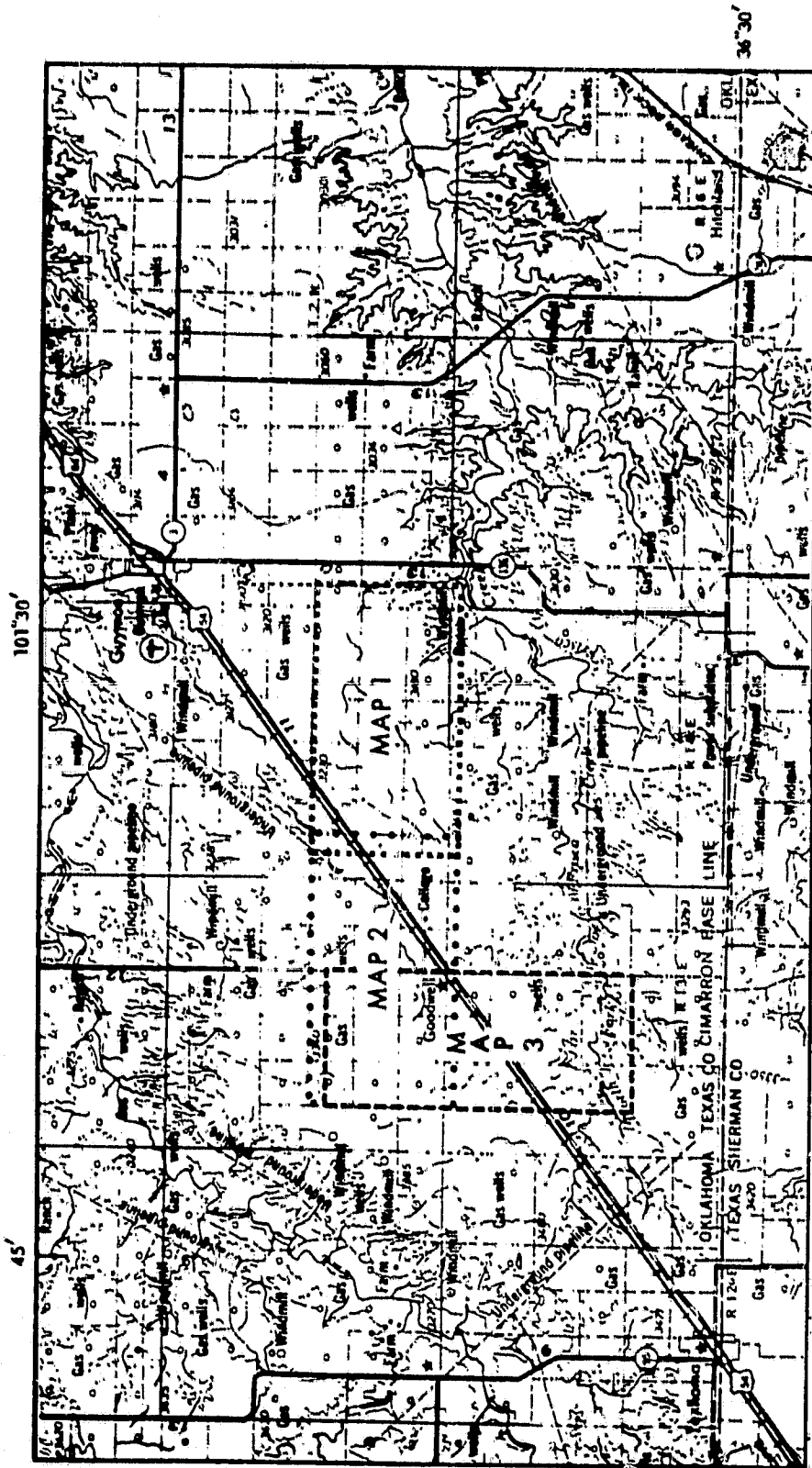
DATA COLLECTION

Aircraft data were collected near Guymon, Oklahoma in August, 1978, and near Dalhart, Texas in August 1980. Data collection and processing will be described for each site.

Guymon Aircraft and Ground Data

In August, 1978, aircraft and ground data were collected in commercial agricultural fields located from 3 to 20 km southwest of Guymon, Oklahoma and near Clayton, New Mexico (Figures 4a through 4h). Vegetative cover in the area included bare soil, corn, sorghum, and alfalfa. Soil type was generally a silty clay (averaging 35% clay, 35% silt, and 30% sand) with many areas having a caliche (CaCO_3) layer near the surface. Different tillage practices allowed spectral data from sorghum and bare fields having rows perpendicular and parallel to the flight line to be analyzed. Aircraft and ground data were collected in fields along four flight lines covering 38.4 km² area (1.6 x 24 km).

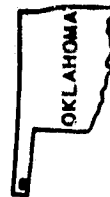
Aircraft data collected by the NASA C-130 on August 2, 5, 8, 11, 14, and 17 consisted of (1) seven scatterometer frequencies and polarizations, (2) three passive microwave frequencies and polarizations, (3) five visible/near-infrared/thermal channels, (4) Barnes PRT-5 radiometer thermal data, and (5) black and white aerial photography. The aircraft flew at least twice at 500 m over each flight line on each flight day. Also, on August 5, the C-130 collected only scatterometer data over fields near Clayton, New Mexico.



GUYMON AREA MAP INDEX TO FIELD MAPS

Approximate scale is 1:250,000

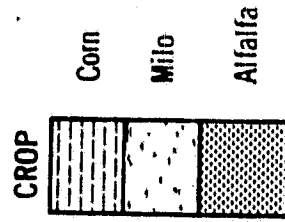
FIG. 4a Area map of Guymon showing the relative locations of each field map.





GUYMON, OKLAHOMA 1978

LEGEND FOR FIELD MAPS 1, 2 & 3



Consult field notes for row crop orientation to aircraft flight lines.

Prepared by the Texas A&M University Remote Sensing Center.
Base data compiled from USGS Topographic maps, R.S.C. team
field notes and NASA contracted aerial photography collected
August 2-17, 1978.

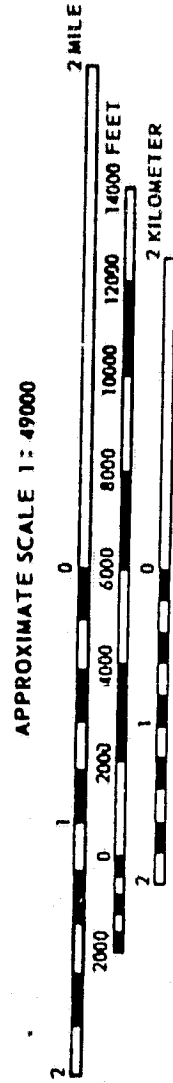


FIG. 4b Legend for the Guymon, Oklahoma field maps.

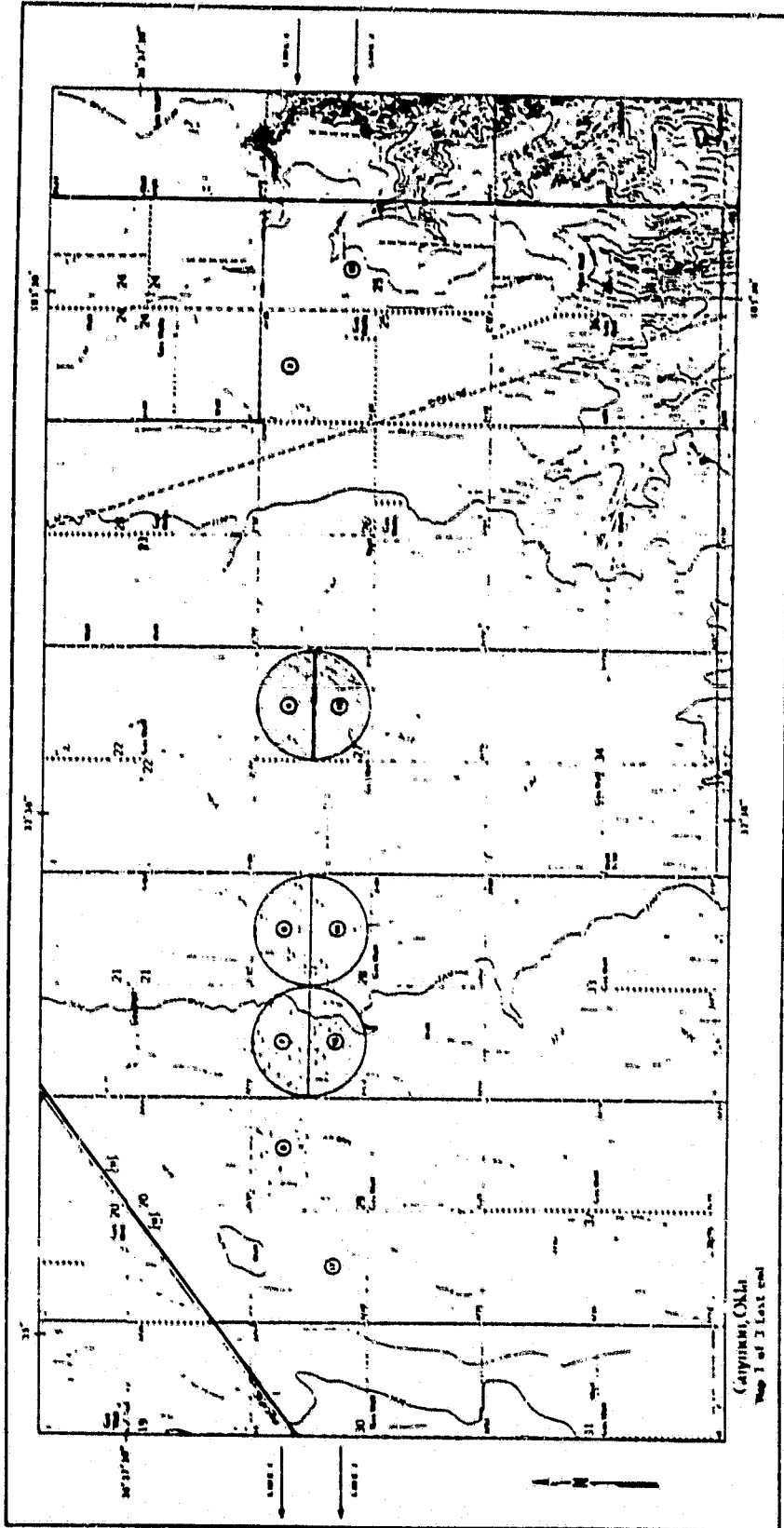


FIG. 4c Locations of sample fields at Guymon, East end, Lines 1 and 2.

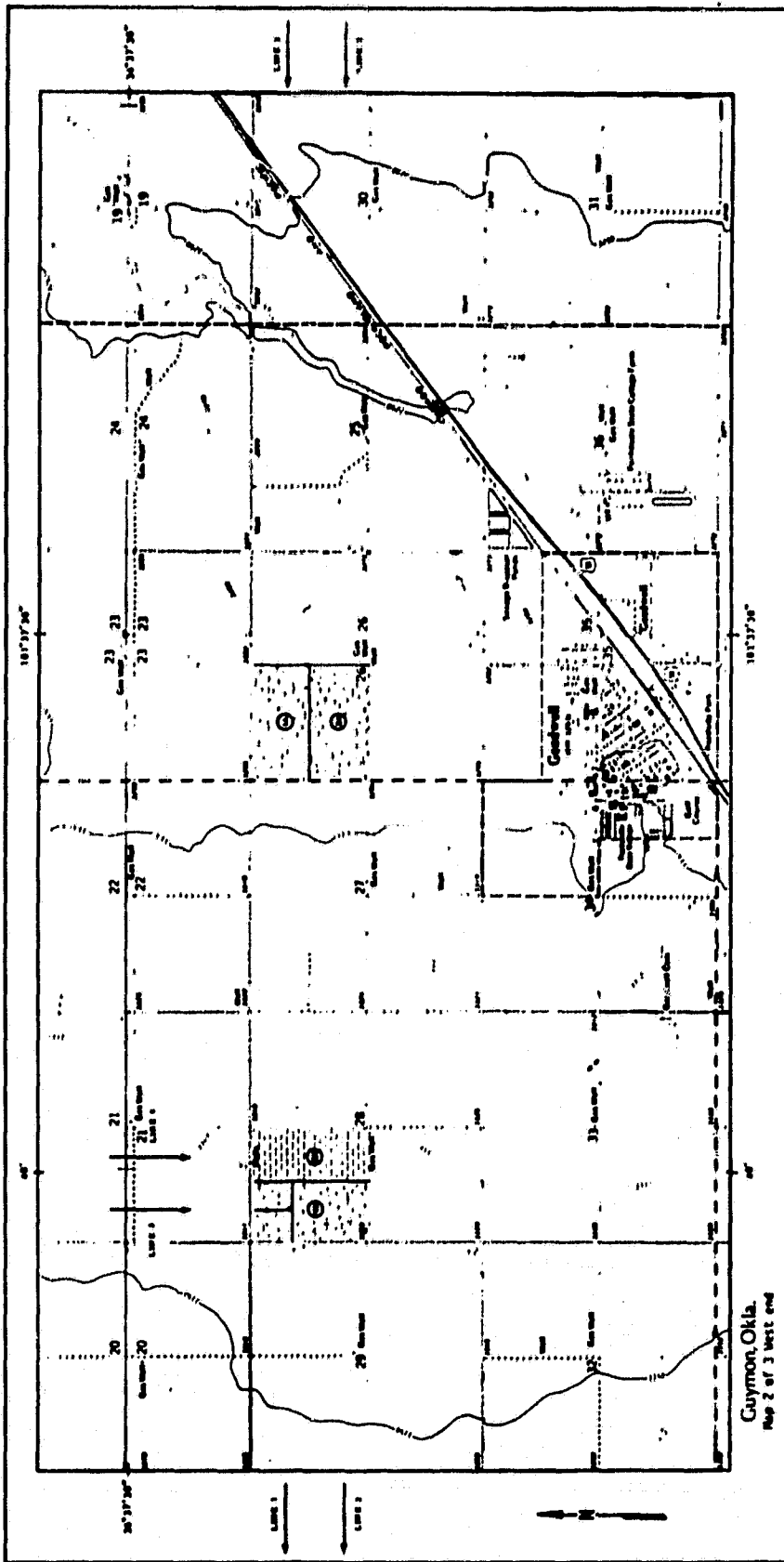


FIG. 4d Locations of sample fields at Guymon, West end, Lines 1 and 2.

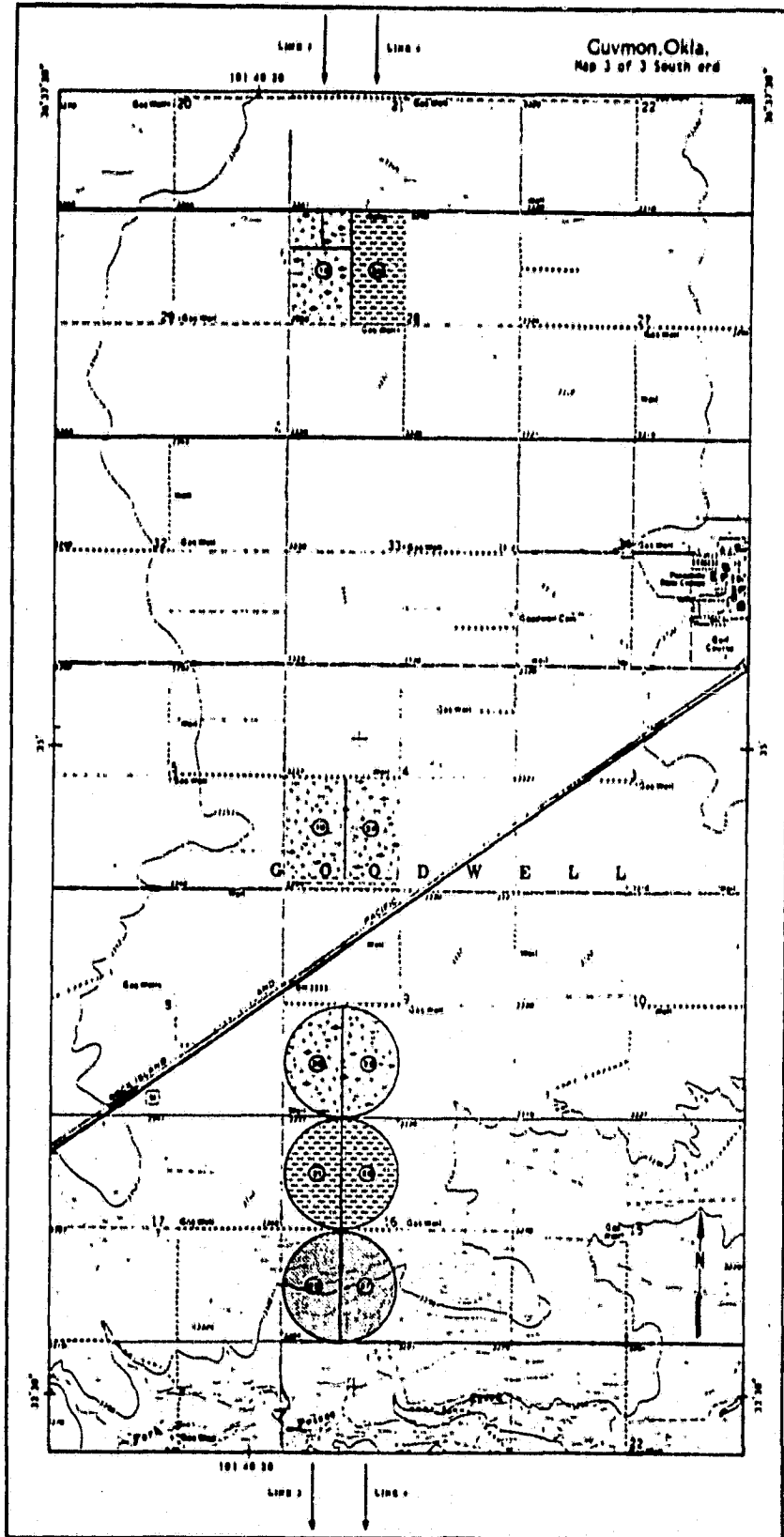
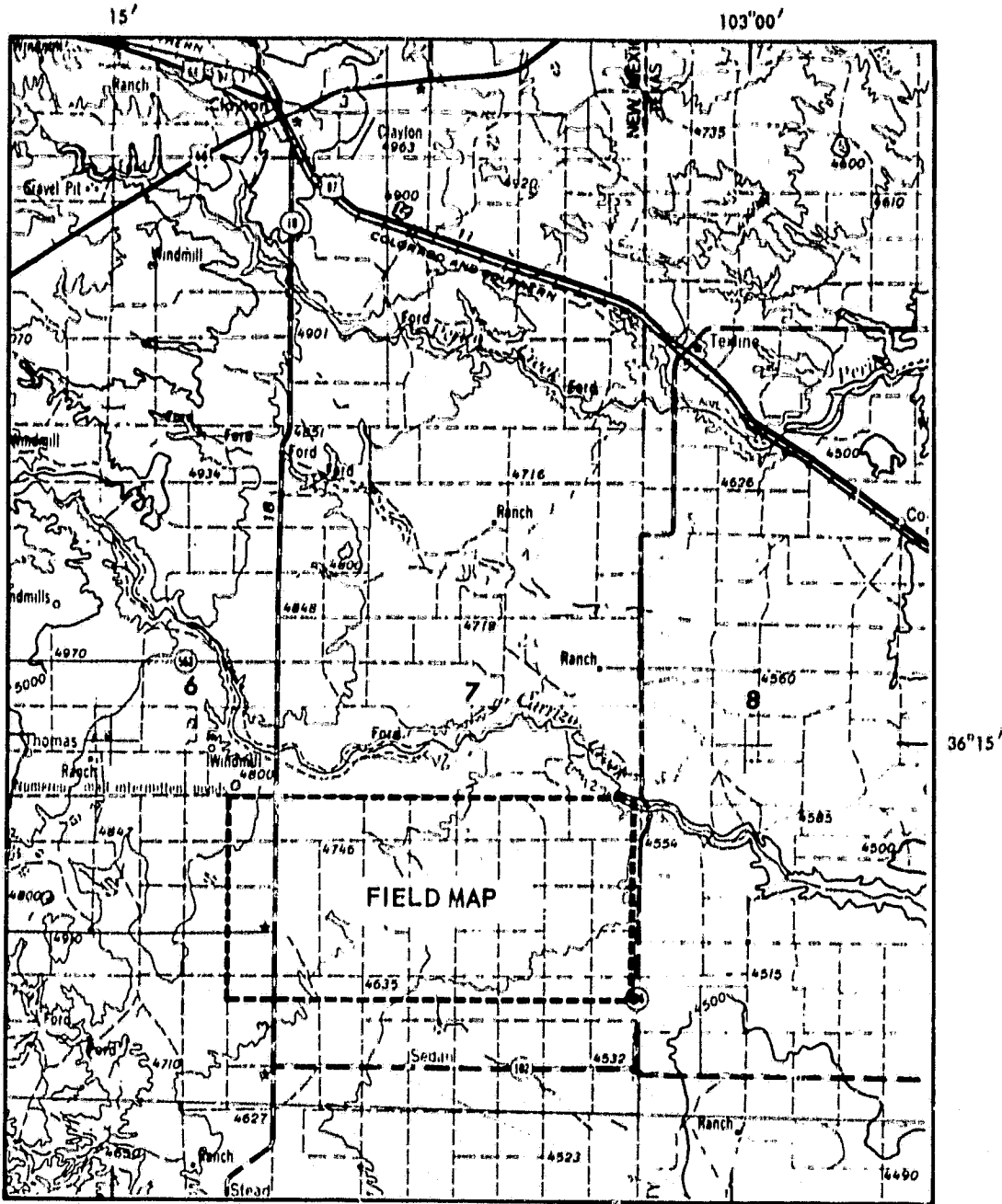


FIG. 4e Locations of sample fields at Guymon, South end, Lines 3 and 4.

ORIGINAL PAGE
OF POOR QUALITY

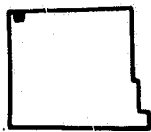


CLAYTON AREA MAP

Approximate scale is 1:250,000

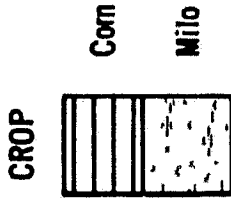


FIG. 4f Area map of Clayton showing the relative location of the field map.



CLAYTON, NEW MEXICO 1978

LEGEND FOR FIELD MAP



Sample fields in Clayton had no ground truth measurements.

Prepared by the Texas A&M University Remote Sensing Center.
Base data compiled from USGS topographic maps, R.S.C. team
field notes and visicorder data from a NASA aircraft flight on
August 5, 1978.

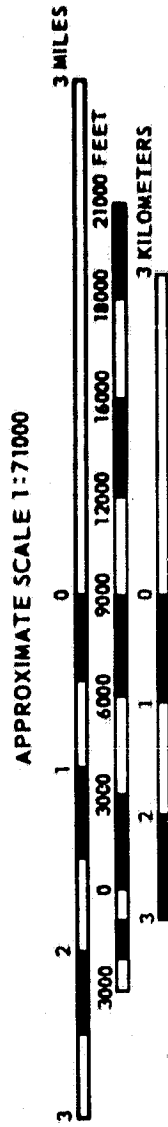


FIG. 4g Legend for the Clayton, New Mexico field maps.

ORIGINAL FACE IS
OF POOR QUALITY

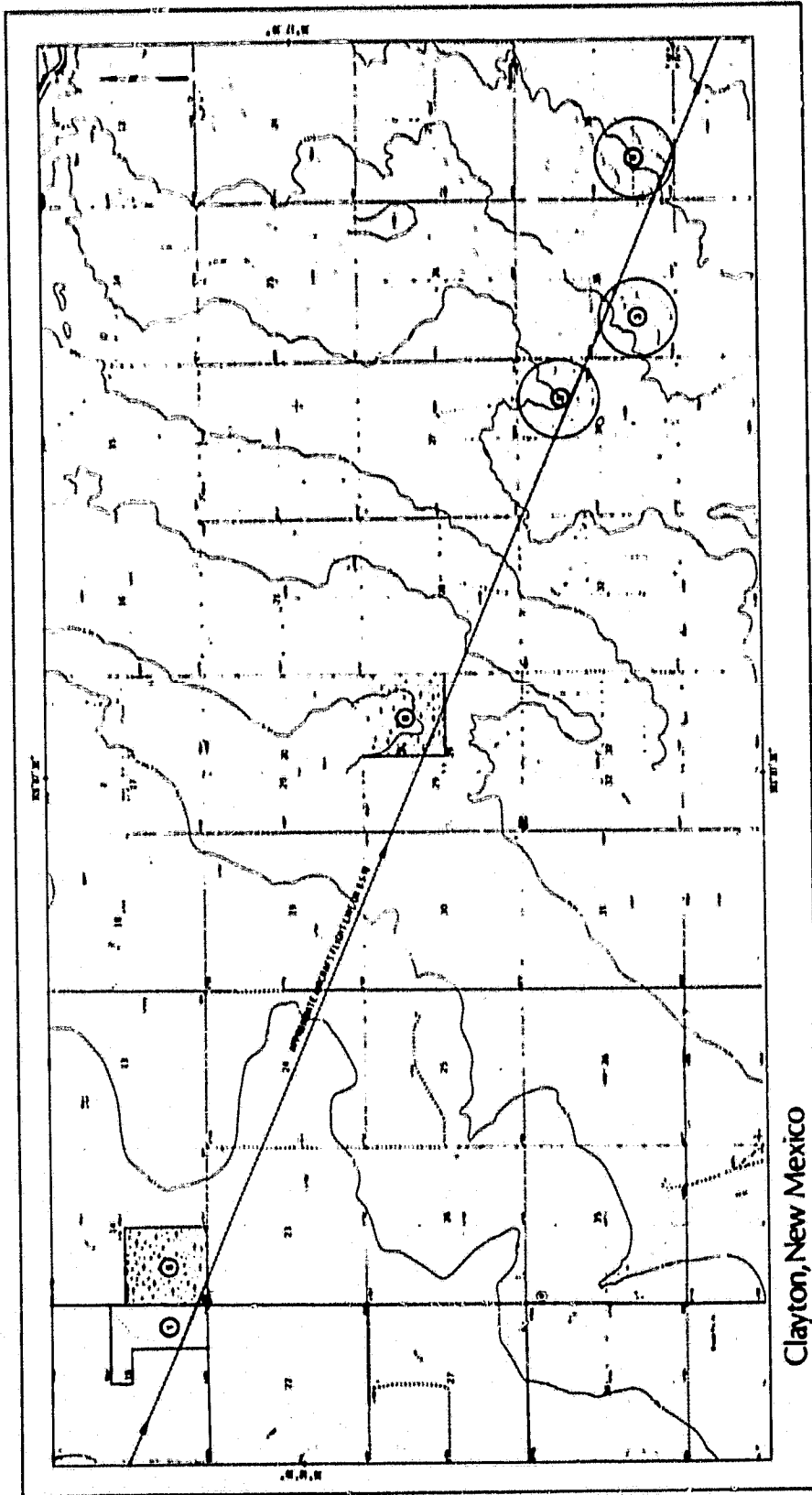


FIG. 4h Locations of the sample fields at Clayton.

The scatterometer frequencies and polarizations included (1) 13.3 GHz VV (K band) vertically polarized transmitted and received), (2) 4.75 GHz HH (C band horizontally polarized transmitted and received), (3) 4.75 GHz HV (horizontally polarized transmitted and vertically polarized received), (4) 1.6 GHz HH (L band), (5) 1.6 GHz HV, (6) 0.4 GHz HH (P band), and (7) 0.4 GHz HV. These frequencies will be referred to as K band, C band, L band or P band throughout the remainder of this report. The polarizations will be referred to as like pole or cross pole instead of HH or HV, respectively. Data from eight look angles from nadir were processed for each frequency: 5°, 10°, 15°, 20°, 25°, 35°, 40°, 45°.

Passive microwave data were collected in 1.6 GHz (L band) horizontal polarization, and 4.75 GHz (C band) vertical and horizontal polarizations. These data will be referred to as L band horizontal, C band vertical and C band horizontal, respectively.

Five channels from the modular multispectral scanner (M²S) were available: (1) channel 4: 0.548-0.583 μm , (2) channel 7: 0.662-0.701 μm , (3) channel 8: 0.703-0.747 μm , (4) channel 9: 0.770-0.863 μm , and (5) channel 11: 8.000-12.080 μm .

Barnes PRT-5 measurements were also included to calibrate the M²S thermal band (channel 8) and normalize the passive microwave brightness temperature.

The sensors were operating at different times throughout the study because the active microwave data would interfere with the passive microwave data. Windy conditions on August 14 also forced a third run over each flight line. Table 1 lists the operating sensors

TABLE 1. Operating Sensors for the Guymon, Oklahoma Study

Date	Line	Run	Operating Sensors
8/2/78	1-4	1	all scatterometer; M ² S; PRT-5; C-band
8/5/78			passive microwave; photos;
8/8/78			
8/11/78	1-4	2	K-band, C-band, P-band scatterometer; and
8/17/78			L-band passive microwave; PRT-5; photos
8/14/78	1-4	1	all scatterometer; M ² S; C-band passive microwave; PRT-5; photos
	1-4	2	K-band, C-band, P-band scatterometer; and L-band passive microwave; PRT-5; photos
	1-4	3	all scatterometer; M ² S; C-band passive microwave; PRT-5, photos

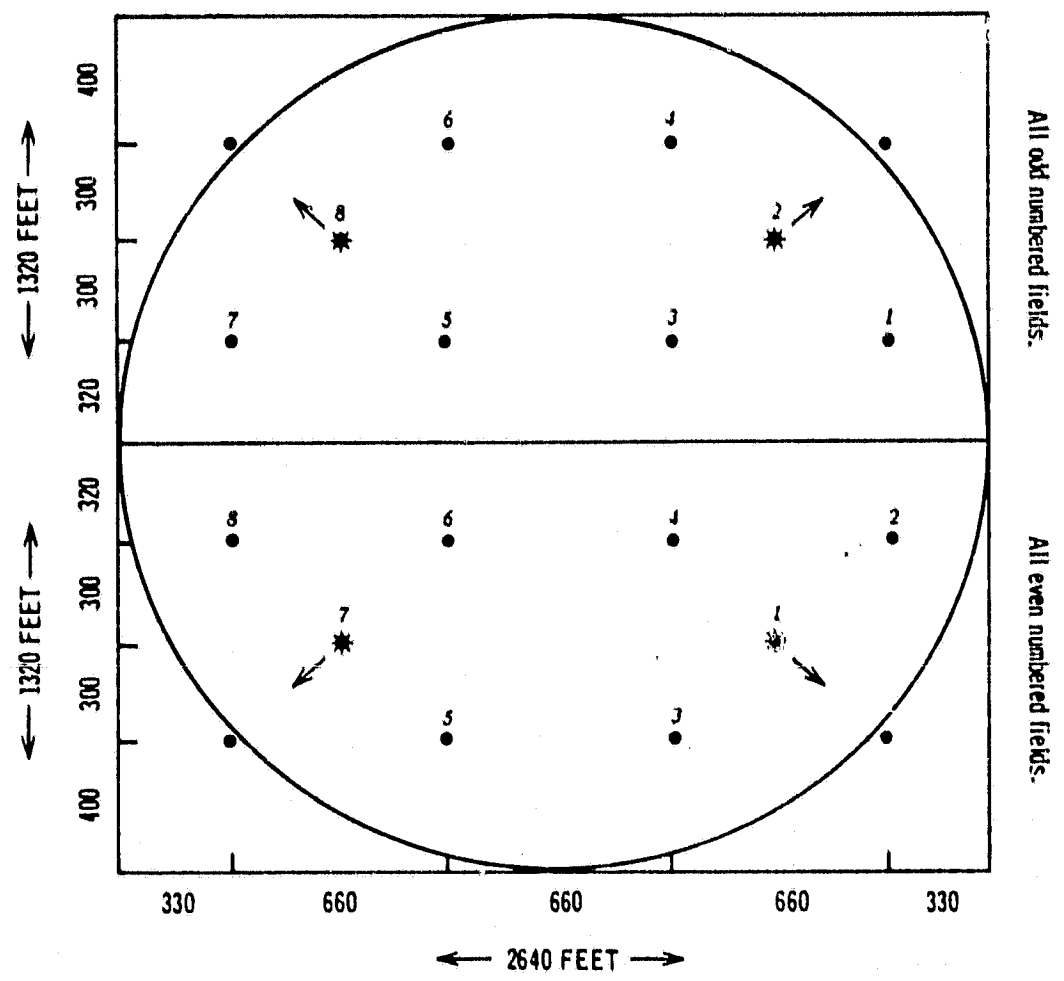
for each flight line and run. Field averages were determined for each sensor. Because of the uncertainty of the target and look angle, field averages were deleted from the data set when the NASA C-130 had excessive roll (greater than 3.5°) and/or drift (greater than 9°).

Soil moisture samples were collected at eight points approximately 200 m apart within each 32 hectare field (Figure 5). Samples collected at each site were 0-2 cm, 2-5 cm, 5-9 cm, 9-15 cm, 0-15 cm, 15-30 cm, and 30-45 cm (Figure 6). Field averages were calculated for each depth. Data included in calculating the average were from sites within the maximum sensor swath width. In the majority of the cases, data from all eight sample points were included. Approximately one-third of the fields were sampled on flight days. As a result, moisture averages for fields not sampled on flight days were interpolated from time series plots of measurements taken the day before or the day after flights. Field notes of tillage, center pivot location and wet/dry areas were also tabulated. No biomass information was collected at Guymon; however, photographs of crops at the time of the experiment were collected which provided a rough estimate of crop cover.

Dalhart Aircraft and Ground Data

During August, 1980, aircraft and ground data were collected in commercial agricultural fields 20 km northwest of Dalhart, Texas (Figures 7a through 7e). Figure 7a represents the general view of the area showing the relative locations of 7b, c and d. Figure 7e is the legend which describes the crop types. Crop types within the area included bare soil, pasture, corn, alfalfa and sorghum. The soil type

QUALITY OF POOR QUALITY



* These points were moved outside the pivot boundary for Fields 5 & 6.

FIG. 5 Sampling pattern for fields at Guymon and Dalhart. Points 1, 2, 7 and 8 were moved outside the circle for rectangular fields.

ORIGINAL PAGE IS
OF POOR QUALITY

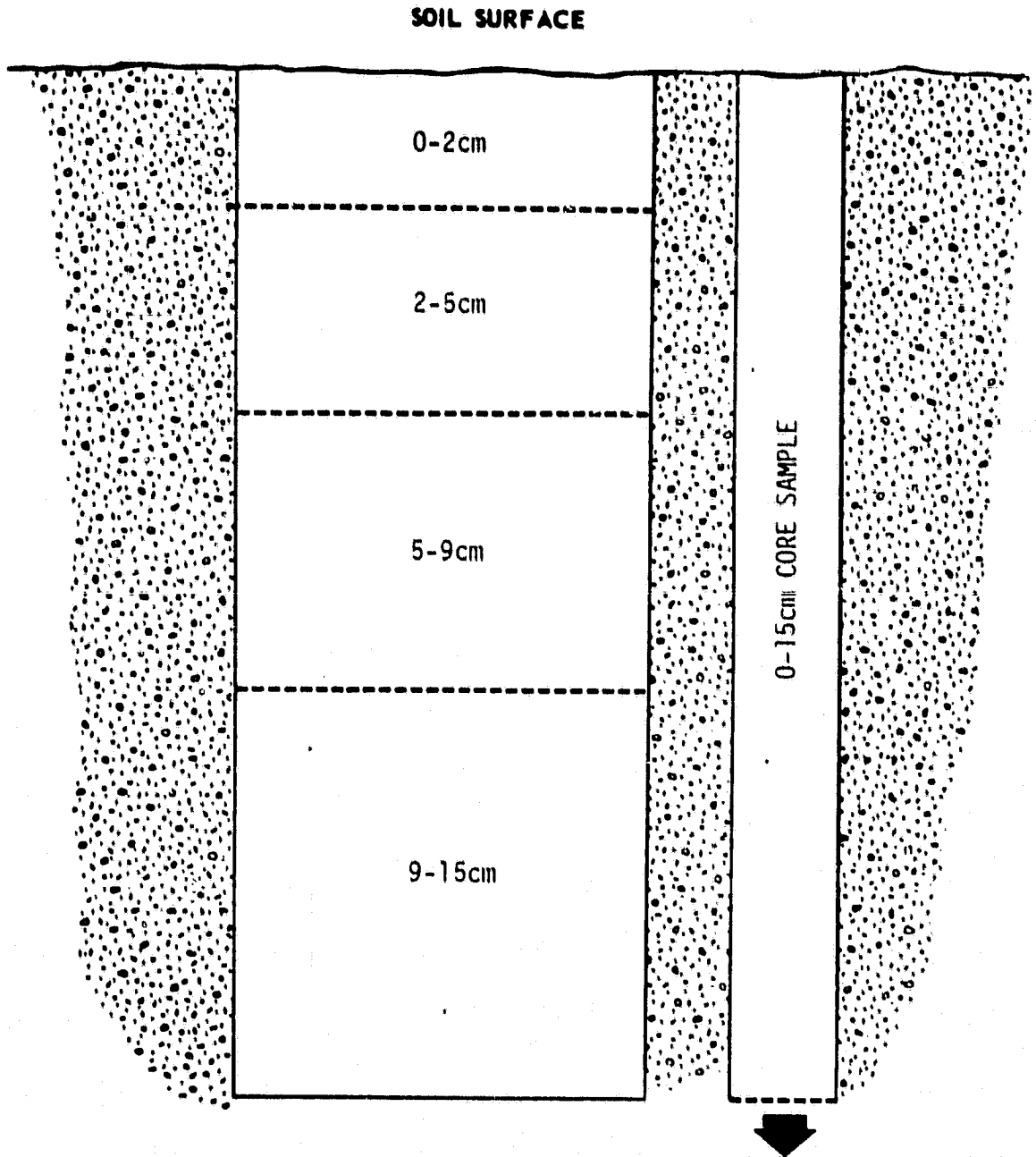
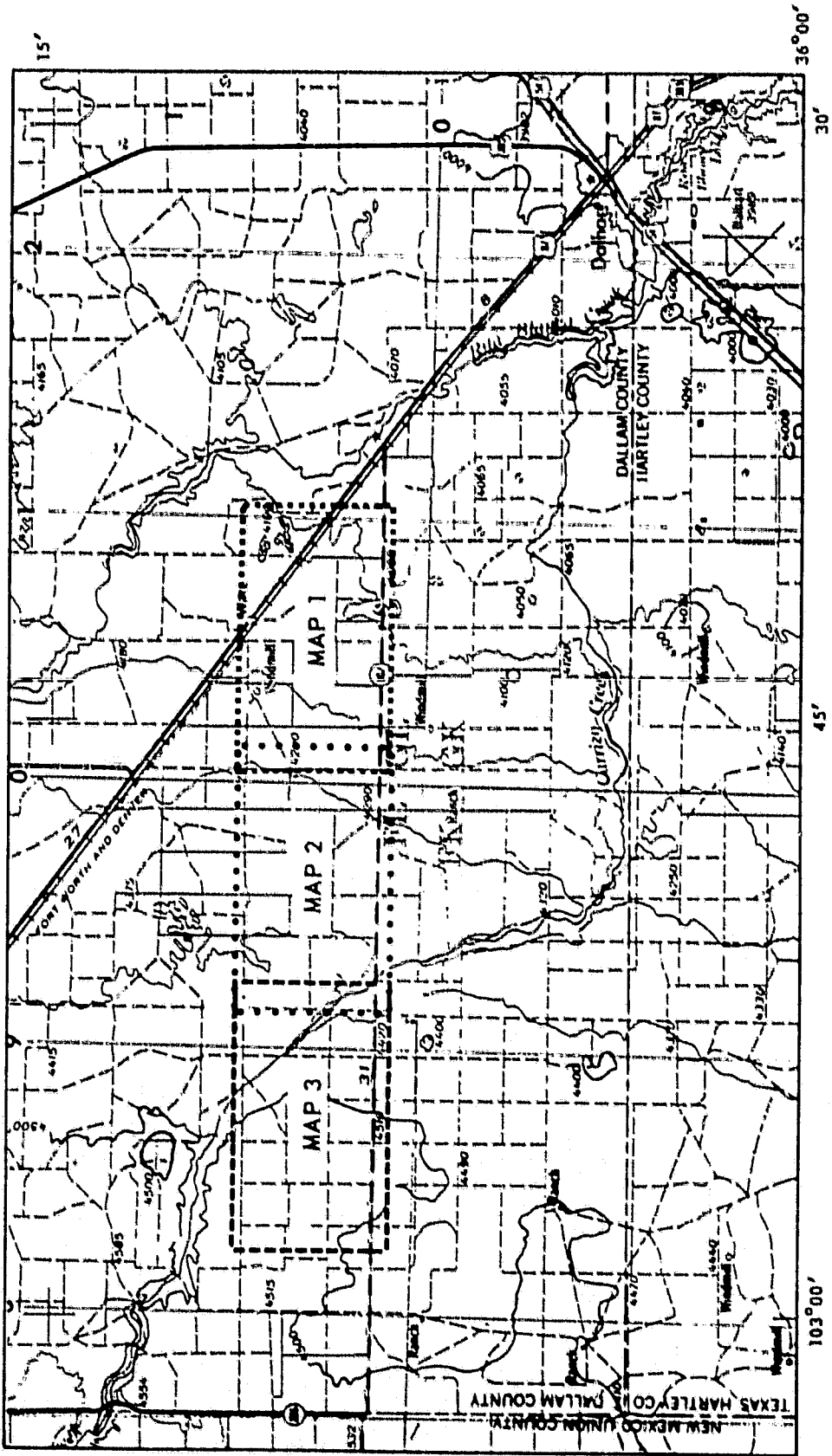


FIG. 6 Soil moisture sampling depths at Dalhart and Guymon. The 15-30 and 30-45 cm core samples were also taken in addition to the above. Samples were collected from 5-9 cm and 9-15 cm at Guymon and 5-15 cm at Dalhart.



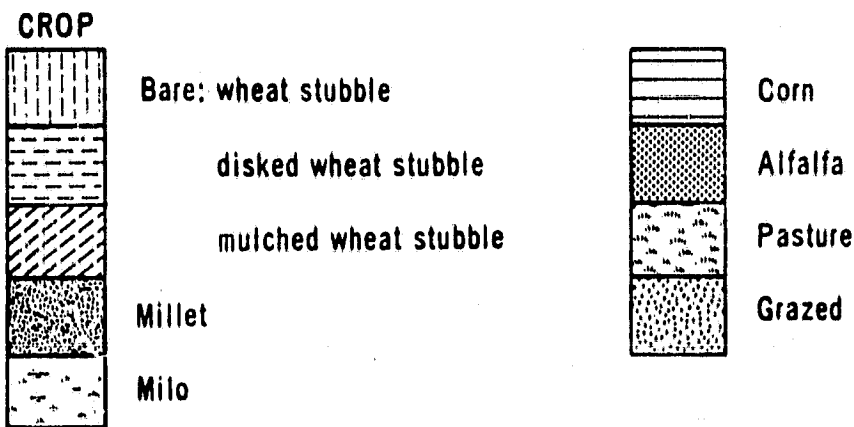
DALHART AREA MAP
INDEX TO FIELD MAPS
Approximate scale 1:250,000

FIG. 7a Area map of Dalhart showing the relative locations of each field map.



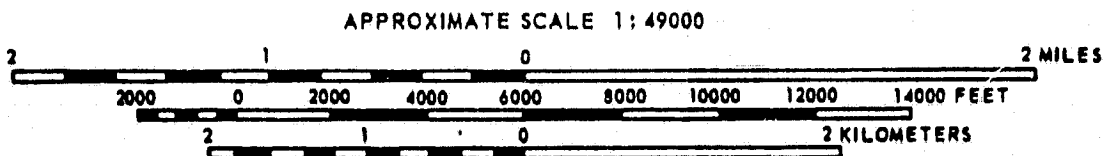
DALHART, TEXAS 1980

LEGEND FOR FIELD MAPS 1, 2 & 3



- Flight line markers
- ▲ Corner reflectors
- * Rain gauges
- Vegetation sample sites

Row direction was east-west for all sample fields with row crops.



Prepared by the Texas A&M University Remote Sensing Center. Base data compiled from USGS topographic maps, R.S.C. team field notes and NASA contracted aerial photography collected August 14-18, 1980.

FIG. 7b Legend for the Dalhart, Texas field maps.

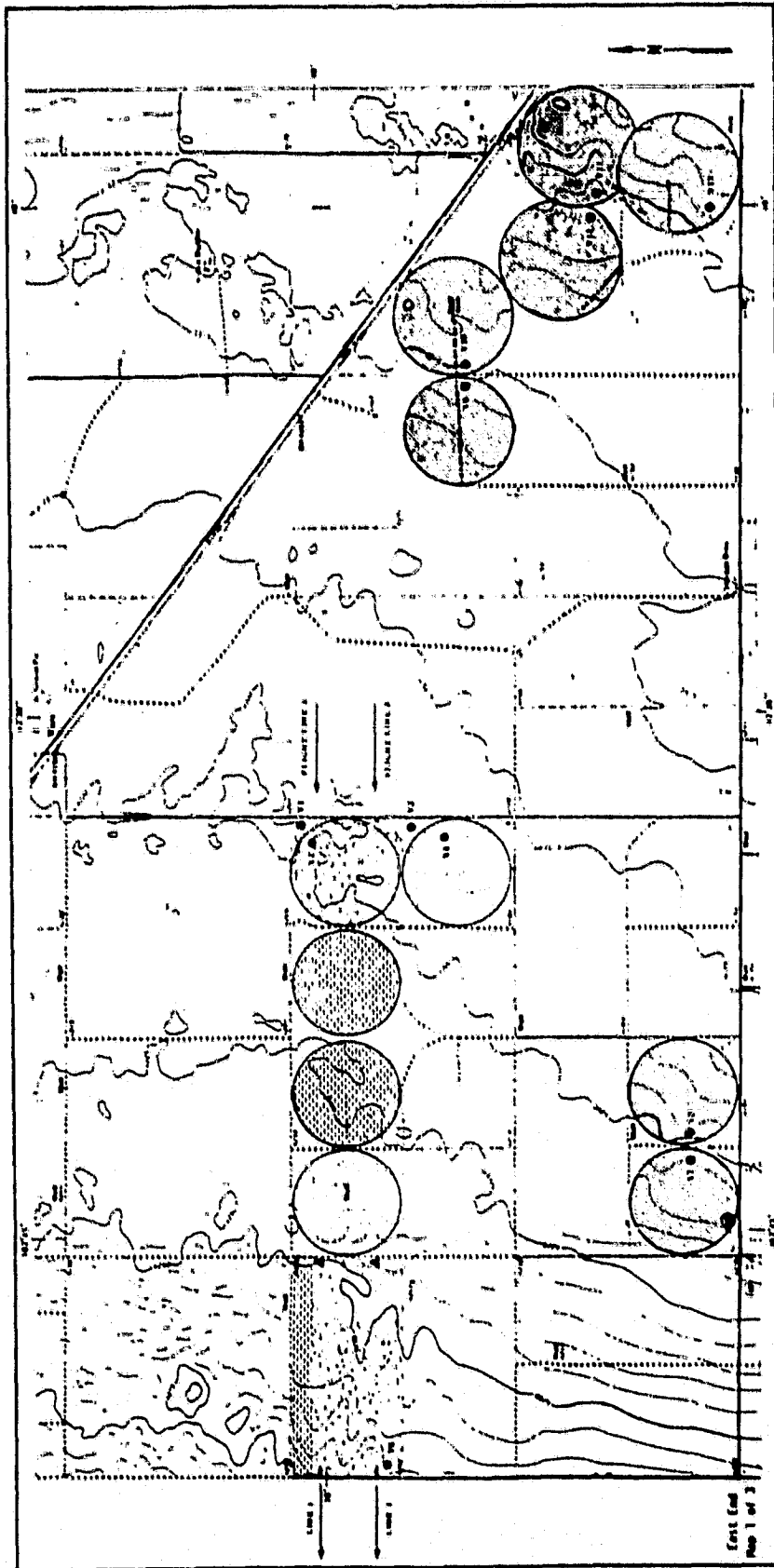


FIG. 7c Locations of sample fields at Dalhart, East end, Lines 1 and 2.

ORIGINAL PAGE
OF POOR QUALITY

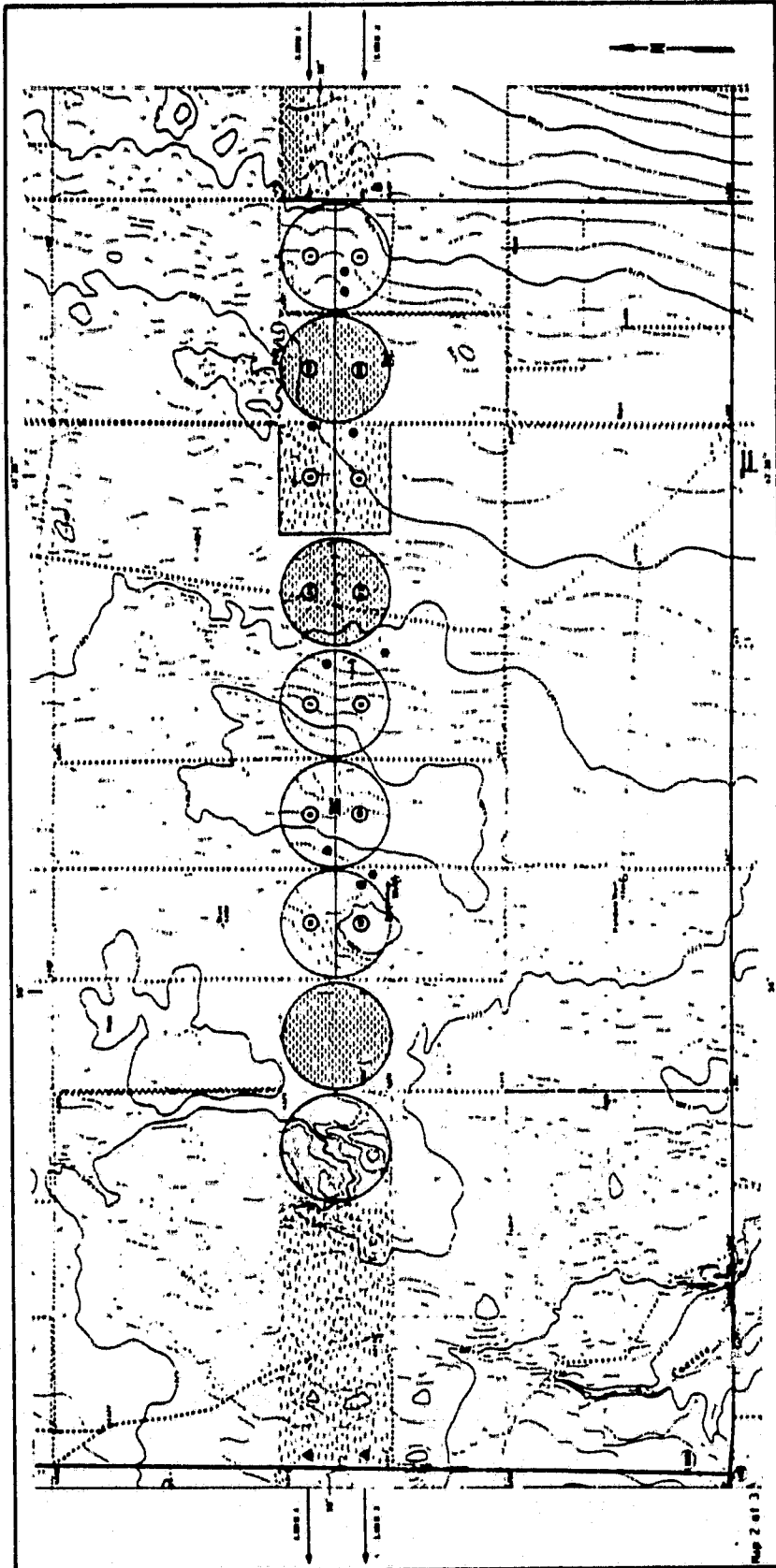


FIG. 7d Locations of the sample fields at Dalhart, Lines 1 and 2.

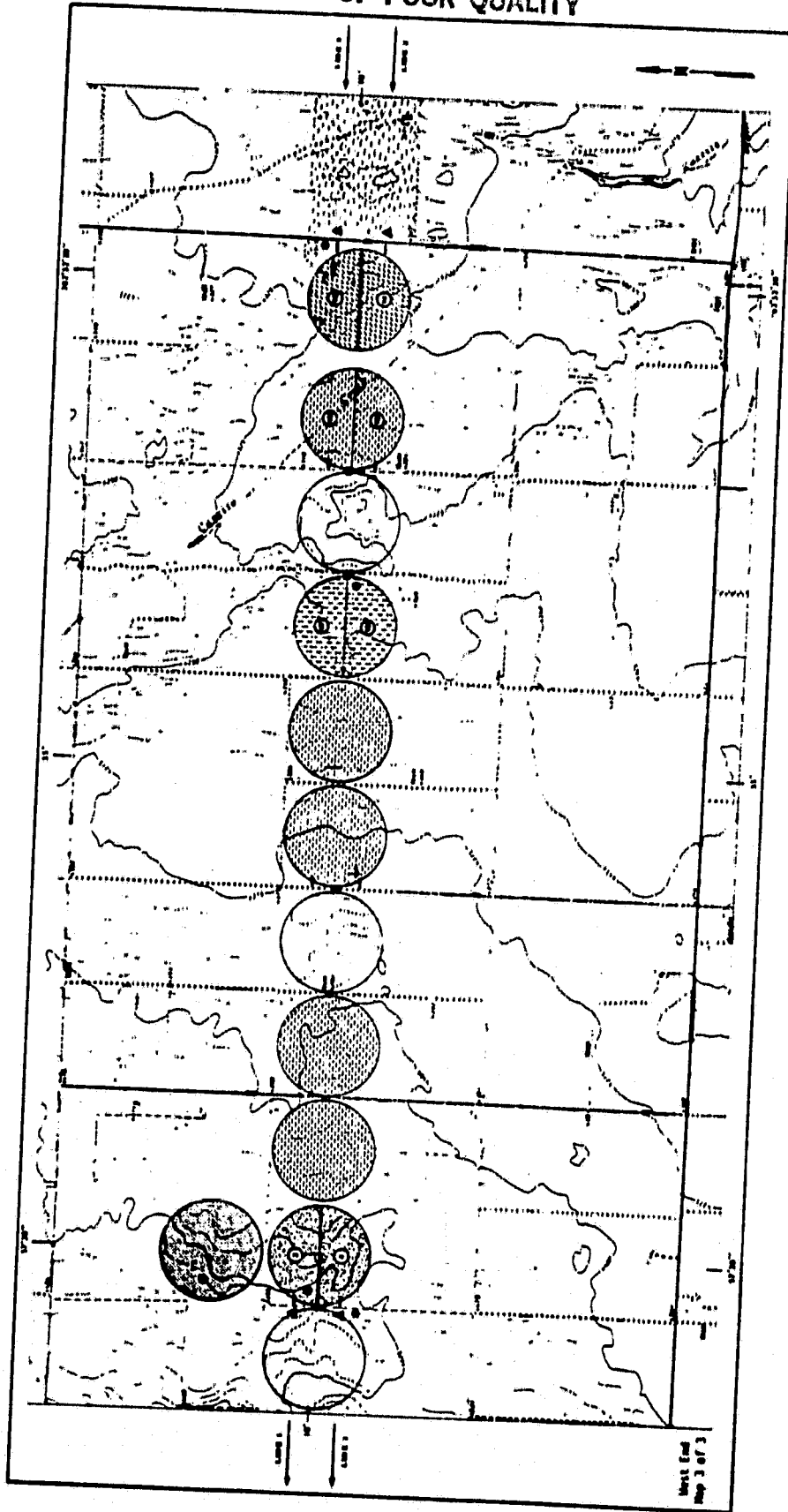


FIG. 7e Locations of sample fields at Dalhart, West end, Lines 1 and 2.

of the surface 30 cm was a sandy loam (75% sand, 10% silt and 15% clay). The commercial fields were located along two flight lines covering a 36 km² area (1.6 x 22.5 km).

Aircraft data, which were collected by the NASA C-130 on August 14, 16, and 18, consisted of (1) seven scatterometer frequencies and polarizations, (2) three passive microwave radiometer frequencies and polarizations, (3) eight visible, near- middle- and far-infrared bands, (4) Barnes PRT-5 radiometer thermal data, and (5) color infrared aerial photography. The aircraft flew twice at 500 m over each flight line and once at 1500 m over the general area.

The scatterometer frequencies and polarizations are the same as the scatterometer sensors at Dalhart. For each scatterometer, data were processed at the same look angles analyzed at Guymon: 5°, 10°, 15°, 20°, 25°, 35°, 40°, 45°.

The passive microwave radiometer frequencies and polarizations operating over Dalhart were the same channels operating over Guymon: L band horizontal and C-band horizontal and vertical polarizations. The L band passive microwave radiometer used at Dalhart was not the same instrument used at Guymon.

The eight channels of NS001 scanner data (simulated thematic mapper bands) included channel 1: 0.45-0.52 μm , channel 2: 0.52-0.60 μm , channel 3: 0.63-0.69 μm , channel 4: 0.76-0.90 μm , channel 5: 1.00-1.30 μm , channel 6: 1.55-1.75 μm , channel 7: 2.08-2.35 μm , and channel 8: 10.40-12.50 μm . The channels are similar to the proposed data channels of the thematic mapper aboard Landsat D. Channel 7 (M²S) matches well with channel 3 (NS001); channel 9 (M²S) matches

with channel 4 (NS001); and channel 11 (M²S) matches with channel 8 (NS001).

The sensors were operating at different times compared to the Guymon study. For example, at Dalhart all scatterometers were on during the first run, while at Guymon selected scatterometer sensors operated at all times. Table 2 lists the operating sensors for each flight line and run. Field averages were determined for each field. Again, field averages of the sensor data were deleted from the data set when the aircraft had excessive roll (greater than 3.5°) and/or drift (greater than 9°).

The ground data consisted only of soil moisture samples, biomass data, and photographs of crops. The soil moisture sampling scheme was similar to Guymon except for minor modification of the depth intervals and time of sampling. First, the 5-9 and 9-15 cm sampling depths were combined into a 5-15 sampling depth. Second, fields were sampled less intensively on each flight day. And finally, each field was sampled every other day, rather than every third day. Two flights were flown on the same day (8/16/80). The rest of the soil moisture sampling scheme was similar to the Guymon study.

Biomass samples were collected within each soil moisture sampling field along the flight lines in addition to several alfalfa and sorghum fields just south of the flight lines. The sampling locations are shown in Figure 7c, d and e. Samples were collected from a 1 m² area representative of biomass conditions in the field.

TABLE 2. Operating Sensors for the Dalhart, Texas Study

<u>Date</u>	<u>Line</u>	<u>Run</u>	<u>Operating Sensors</u>
8/14/80	11	1	scatterometers, NS001, PRT-5, color IR photos
	12	1	scatterometers, NS001, PRT-5, color IR photos
	11	2	passive microwave, NS001, PRT-5, color IR photos
	12	2	passive microwave, NS001, PRT-5, color IR photos
	13	1	NS001, PRT-5, and color IR photos
8/16/80 (2 flights) and 8/18/80	11	1	passive microwave, NS001, PRT-5, color IR photos
	12	1	passive microwave, NS001, PRT-5, color IR photos
	11	2	scatterometers, NS001, PRT-5, color IR photos
	12	2	scatterometers, NS001, PRT-5, color IR photos
	13	1	NS001, PRT-5, and color IR photos

Scatterometer Processing

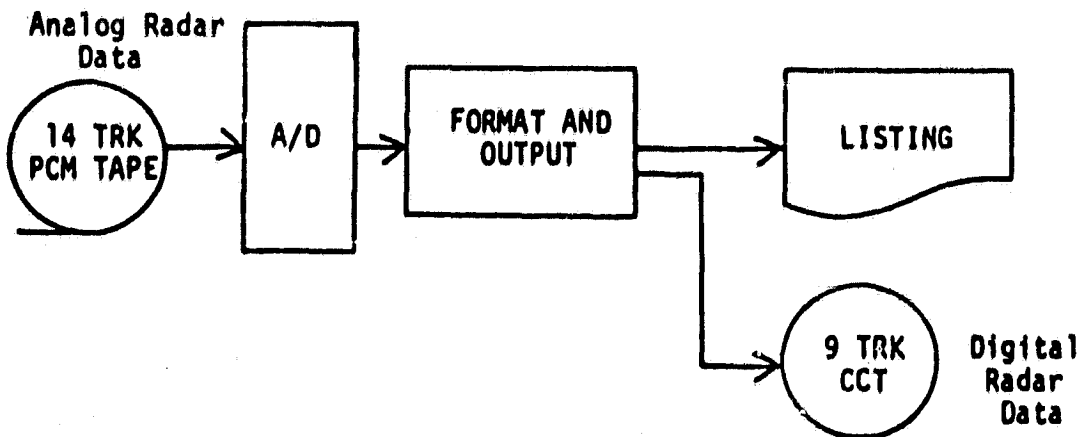
Scatterometer data were collected aboard the NASA C-130 in analog form on a 14-track tape. Copies of the tape were later sent to Texas A&M University/Remote Sensing Center for processing, which consisted of two phases (Figure 8). The initial processing converted the analog data to digital values and copied the digital data onto 9-track magnetic tapes. The second phase processed the digital data using software which calculated the scattering coefficient (σ^0) for each look angle at given time intervals. Data were processed so that a cell size roughly had a length of 25 m for K band, 38 m for C band, 50 m for L band, and 75 m for P band. The processing software was described by Claassen et al. (1979) and Clark and Newton (1979). Cross-over effects from the like-polarized data to the cross-polarized L band data were removed using a technique described by Blanchard and Theis (1981).

The cross-over effect is due to the inability to construct receivers which detect microwave energy in a single polarization. In actuality, a single polarized transmitter emits energy in one polarization when upon interacting with the surface is further modified and is received in two polarizations, thus influencing the cross- as well as the like-polarized data. Blanchard and Theis (1981) modeled the effect of the signal impurity on the cross-polarized data and effectively calculated a correction factor for the small look angles.

After processing scatterometer data, field start and stop times were determined for each frequency and polarization from line plots of

ORIGINAL PAGE IS
OF POOR QUALITY

PHASE I



PHASE II

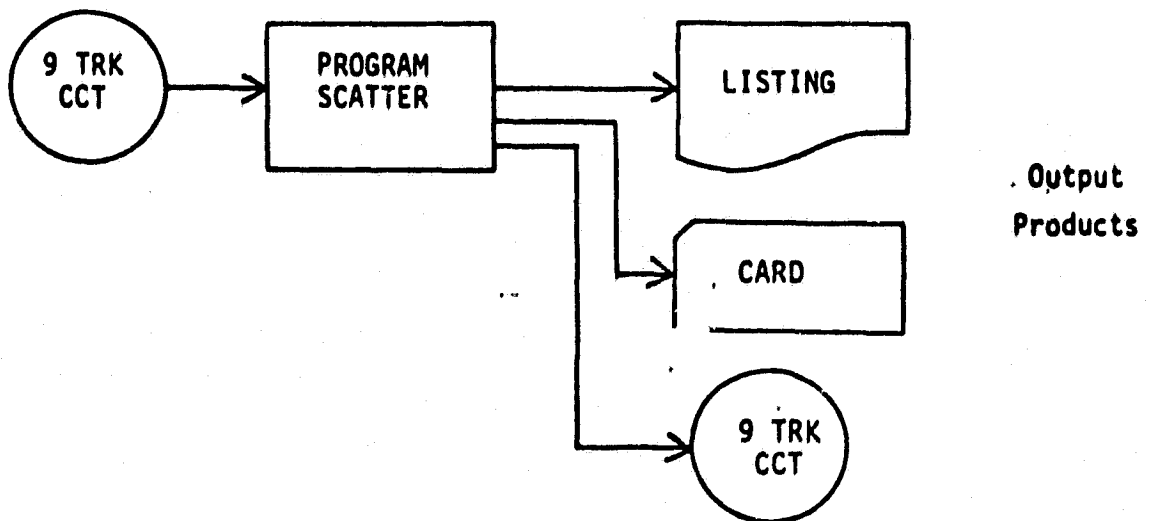


FIG. 8 Scatterometer data processing procedure.

σ^0 versus time, and aerial photographs. Times were adjusted by shifting the start/stop times at least 0.5 seconds toward the field center to insure full scatterometer coverage within the field. The final start and stop times defined the field boundary and were used in determining field averages for each frequency, polarization, and look angle. Time frames during excessive aircraft roll and drift (roll greater than 3.5° ; drift greater than 9°) were noted and data from affected look angles were deleted from further analysis.

No known technique or mechanism was available to calibrate all of the scatterometers. Consequently, any temporal variation in σ^0 was assumed to indicate either soil moisture, roughness, or vegetation changes.

NS001/M²S Processing

The data were processed onto 9-track tapes at NASA/Johnson Space Center. Included with the surface data were calibration data consisting of digital counts from looks at constant radiance targets within the sensor. The calibration data were then used to convert digital counts to radiance. To minimize processing costs, only data from the first runs were processed.

Since radiance is a function of the solar angle, a correction factor was needed before comparing crop radiance differences. All the Dalhart data were normalized to August 18--the day with the smallest solar zenith angle; Guymon data were adjusted to August 11 zenith angle conditions. The correction factor used was

$$R_c = \frac{R_i}{\cos \theta} \quad (14)$$

where R_i and R_c are the non-normalized and normalized radiance values, respectively, and θ is the solar zenith angle.

Passive Microwave Processing

The raw analog data collected aboard the aircraft were converted to digital uncorrected brightness temperatures at NASA/Goddard Space Flight Center (GSFC). Corrected brightness temperatures (T_B) were calculated from an equation developed at NASA/JSC (O'Neill, 1981):

$$T_B = \frac{1}{t} \left[T_u \left(\frac{L}{1-r^2} \right) - \frac{r^2(T_\sigma)(L)}{1-r^2} - T_L(L-1) - e T_R \right] \quad (15)$$

where t is the transmittance of the radome, e is the emissivity of the radome, T_u is the uncorrected brightness temperature based on raw digital counts, L is antenna cable loss factor, T_L is an antenna temperature factor, T_R is the radome temperature factor, r^2 is an internal parameter for each frequency, and T_σ is the self-emission of the receiver. For the Dalhart L band horizontal data, the radome terms are omitted since the sensor used on these flights was operating in the open rear door of the aircraft. The various constants used in the equation were determined from flights over homogeneous areas. Once brightness temperatures were calculated, line plots of T_B versus time were produced and field start and stop times were determined from the plots. The times defining field boundaries used for scatterometer data were also used in calculating fields averages for each frequency and polarization.

ANALYSIS

Techniques

Once field averages had been calculated for each sensor and soil moisture depth, the ground and aircraft data sets were merged. Each problem mentioned in the objectives and research subsection was analyzed.

In the first problem, the major task was to note sensor variables which responded well to differences in crop type. Analysis techniques included a Duncan's multiple range technique, and graphical analysis--spectrums and response changes as a function of time (Cooley and Lohnes, 1971). Both Dalhart and Guymon spectral data sets were analyzed. The results consisted of a list of sensor variables which are sensitive to crop type differences. From this set, linear combinations were developed which should enhance crop discrimination sensitivity.

The procedure to solve the second problem used unsupervised (based on a minimized distance criterion) classification techniques to discriminate crops. A hierarchical (tree) classification system was developed using separation criterion emerging from the unsupervised techniques. Individual spectral bands and combinations, such as TVI, PVI, and other visible/infrared and scatterometer combinations, were analyzed. The supervised classification technique was developed using August 2 and 17, 1978 and August 14 and 18, 1980, data. The model was then tested on August 5, 8, 11 and 14, 1978 and August 16, 1980 spectral data. The unsupervised classification technique used all

Guymon and Dalhart data sets. From the unsupervised technique, tree-classification models (dendrograms) were developed for the Guymon and Dalhart data sets. The dendrograms were constructed using the same separation criterion used in the unsupervised technique. For example, if the separation criterion between two clusters were σ^0 differences in the L band cross pole data, then this variable was used in the dendrogram model to separate groups. The dendrograms at both locations were compared and similarities noted, which may be applicable in developing a multifrequency dendrogram classification model.

The third problem was solved by developing linear step-wise regression, supervised and unsupervised crop classification and biomass estimation models to see if microwave data could improve classification and biomass estimation accuracy. Models using only visible/infrared data were compared to models which included visible/infrared and microwave data. Any microwave sensor or combination which was more strongly related to crop type differences or biomass estimation than other visible/infrared variables or combinations suggested an improvement over present techniques using only visible and infrared data. The linear step-wise models used spectral data from Guymon and Dalhart. The supervised and unsupervised classification models were developed and tested on the same spectral data set as mentioned for problem 2.

The fourth problem analyzed the variability of the classification and biomass estimation models developed in problems 2 and 3, and associated the variability with biomass differences (phenological differences) or soil moisture differences. The basic analysis technique was graphical analysis of σ^0 versus look angle and visible/

infrared responses due to different growth stages or different soil moisture regimes. The results gave an indication of the model utility under different phenological and moisture regimes. If the model output variability was too large, the model was adjusted to remove influencing effects. This physically involves reducing the component variances of soil moisture and roughness, leaving vegetation variance as the major component of the total variance. Care was taken not to remove variance created by different biophases or stress conditions.

The results from each problem were merged to give an overall view of classification improvements that are possible with combinations of visible, infrared and microwave data, and similar improvements that can be made in biomass estimation.

RESULTS

With the analysis divided into four problems, the results from each problem will be discussed separately. But preceding each problem, a discussion of biomass and final yield conditions is in order.

Guymon Crop Condition

A wide range of growing conditions was evident at Guymon. Irrigated sorghum fields ranged in height from 20 cm to 1 m, and in growth stage from just emerging (fields 7 and 8) to anthesis (field 1X). Two irrigated alfalfa fields (fields 22 and 27) were cut on August 17, the last measurement day. Alfalfa height ranged from 15 cm to 60 cm. One of the bare fields (field 2X) was tilled extensively on the last flight day where furrows were as deep as 30 cm. Two bare fields were irrigated during the experiment (fields 6 and 14). Most of the other vegetated fields were also irrigated.

Since no biomass or yield data were collected from Guymon, all biomass data were inferred using present visible/infrared combinations, such as PVI and TVI.

Dalhart Biomass and Crop Yield

The 1980 crop year proved to be a below normal year in crop biomass and yield due to extremely high temperatures and shortage of moisture during critical growth stages (Table 3). Corn fields were in the tasseling stage and the millet field was just beginning to enter the heading stage during the experiment period. With maximum air temperatures near 40° C, the yields were reduced as much as 50% compared to 1979 yields.

TABLE 3. Dalhart biomass and crop yield

Field	Crop Type	Wet Biomass (g/m ³)	Dry Biomass (g/m ³)	Yield (Kg/Ha)	Height (m)	Corn Popul. (plants/m)
1/2 (Healthy)	Corn	6915.1	1259.8	4287	2.1-2.4	6
1/2 (Stressed)	Corn	2005.7	411.1	0	1.8	6
3/4	Millet	797.5	120.6	1500	0.3	
5/6	Pasture	125.3	16.2	-	0.05	
7/8	Corn	7891.1	1340.6	5676	2.1-2.4	10
9/10	Corn	7665.3	1280.4	5499	2.1-2.4	7
11/12	Corn	5892.7	1148.6	9245	2.1-2.4	7
17/18(Wheat)	Stubble	365.2	340.5	-	0.3	
V1	Sorghum	642.0	139.8	-	0.9-1.2	
V2	Sorghum	1268.2	305.0	3500	0.9-1.2	
V3	Sorghum	2117.0	387.4	-	1.2	
V4	Sorghum	4804.3	844.2	-	2.1	
V5	Alfalfa	945.3	108.7	-	0.3-0.6	
V6	Sorghum	801.6	173.9	-	0.6-0.9	
V7	Alfalfa	218.2	62.8	-	0.15	
V8	Alfalfa	1202.7	128.3	-	0.9	
V9	Alfalfa	897.7	95.0	-	0.8	
V10	Alfalfa	524.7	54.1	-	0.6	
V11	Alfalfa	946.5	113.1	-	0.8	
V12	Alfalfa	556.0	66.7	-	0.6	
V13	Alfalfa	814.9	115.4	-	0.8	

The biomass samples were generally related to final crop yields-- higher biomass indicated higher yields. The exception was field 11/12 where corn yield was the highest, but biomass was third highest. The discrepancy is likely in the unrepresentative biomass sample.

Problem 1

The easiest method of graphical analysis of crop type differences was through spectral analysis. Returns from each spectral channel for each field were compared and differences attributed to soil moisture, roughness or vegetation. Several examples of spectra are given in Figures 9 through 11. The range of radiance for the visible and infrared region (bands 1-7) is 0 to 3.0 $\text{mw cm}^{-2} \text{steradian}^{-1}$; the temperature range for the thermal (band 8 or 5) and microwave brightness temperature (BT) is 220° to 325°K. The normalized brightness temperature (E) ranged from 0.70 to 1.0 and the scatterometer response (K band to P band) for like (H) and cross (V) pole data ranges from -60 to 0 db. The soil moisture field averages (SM) ranged from 0 to 25% by volume for each sampling depth (0-2 cm = A, 2-5 cm = B). The scatterometer 40° look angle was arbitrarily selected because of the strong relationship with vegetation as determined through other studies reported in the literature.

Examples of mature corn (field 2) and millet fields (field 3) with similar surface soil moisture conditions (approximately 9% by volume) are illustrated in Figure 9. The largest difference was in the C, L, and P band active microwave data--as large as 6 db in the L band cross pole data. Band 4 data also showed a difference of 0.3 $\text{mw cm}^{-2} \text{steradian}^{-1}$. No NS001 data was collected in the corn in bands

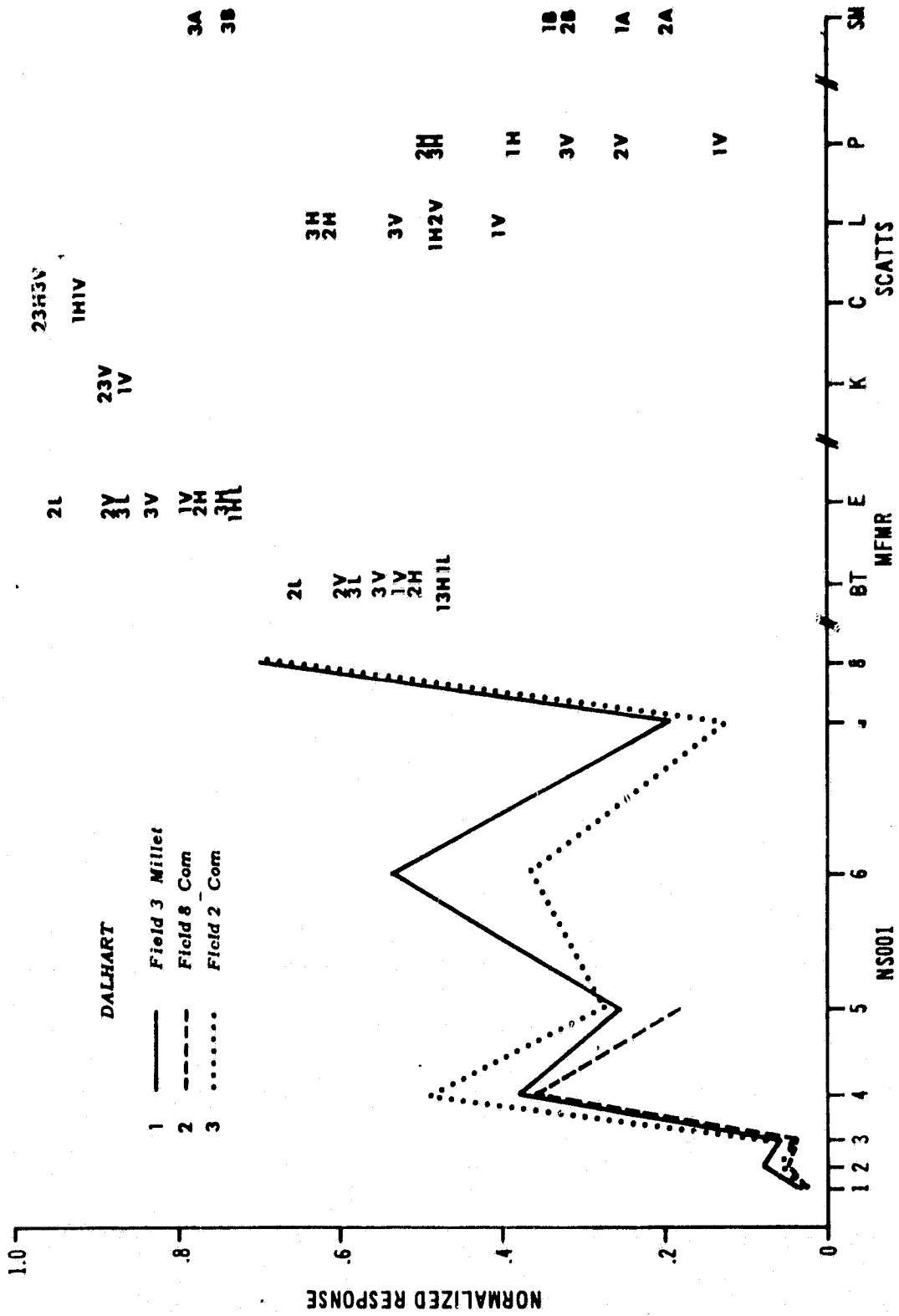


FIG. 9 Spectra for millet and corn fields at Dalhart. [H = C band horizontal (MFMR), V = C band vertical pole (MFMR), L - L band horizontal (MFMR), H - like pole 40° look angle (SCATTS), V = cross pole 40° look angle (SCATTS), A = 0-2 cm soil moisture (SM), B = 2-5 cm soil moisture (SM)].

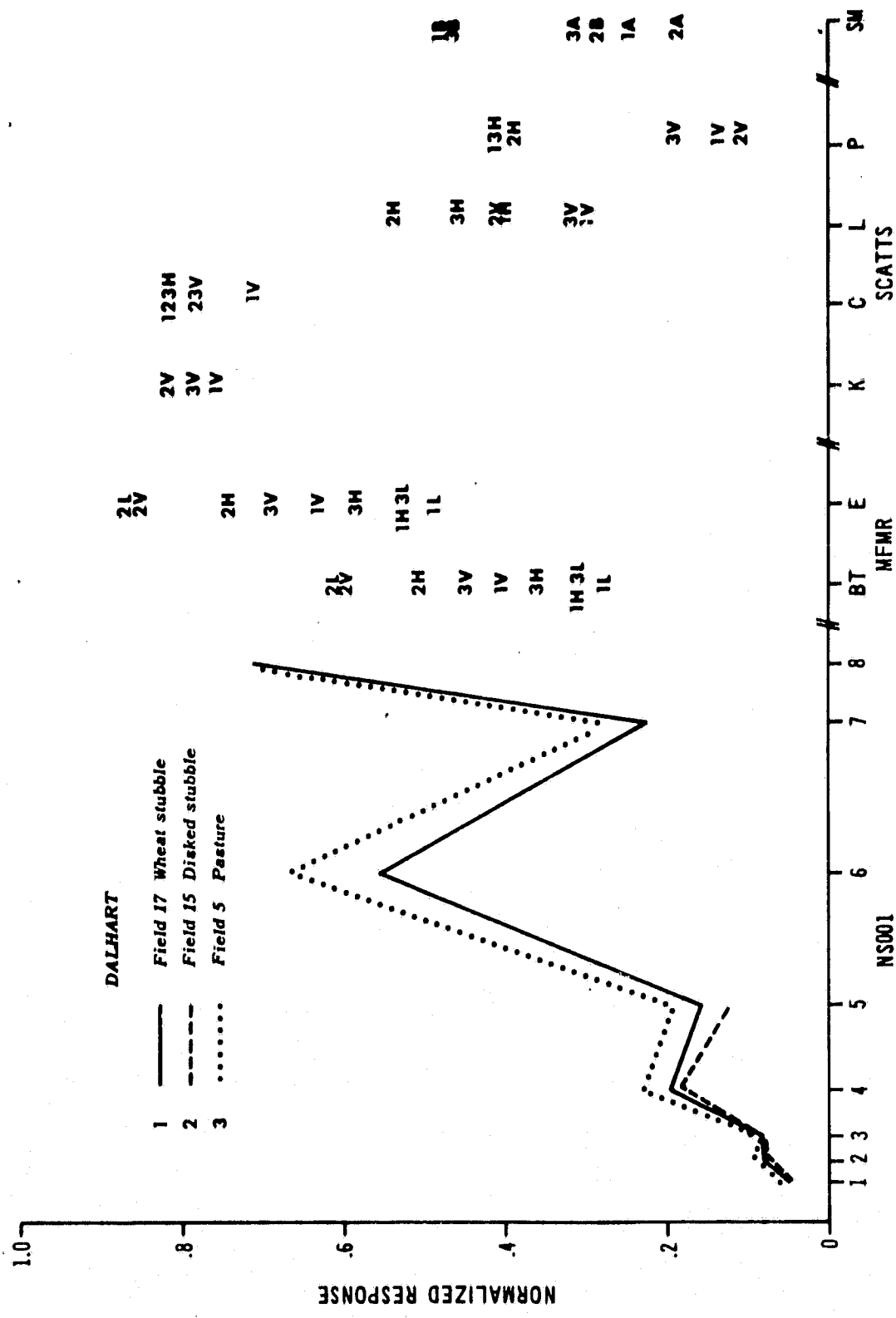


FIG. 10 Spectra for bare soil, pasture and wheat stubble at Dalhart. [H = C band horizontal (MFMR), V = C band vertical pole (MFMR), L - L band horizontal (MFMR), H = like pole 40° look angle (SCATTS), V - cross pole 40° look angle (SCATTS), A = 0-2 cm soil moisture (SM), B = 2-5 cm soil moisture (SM)].

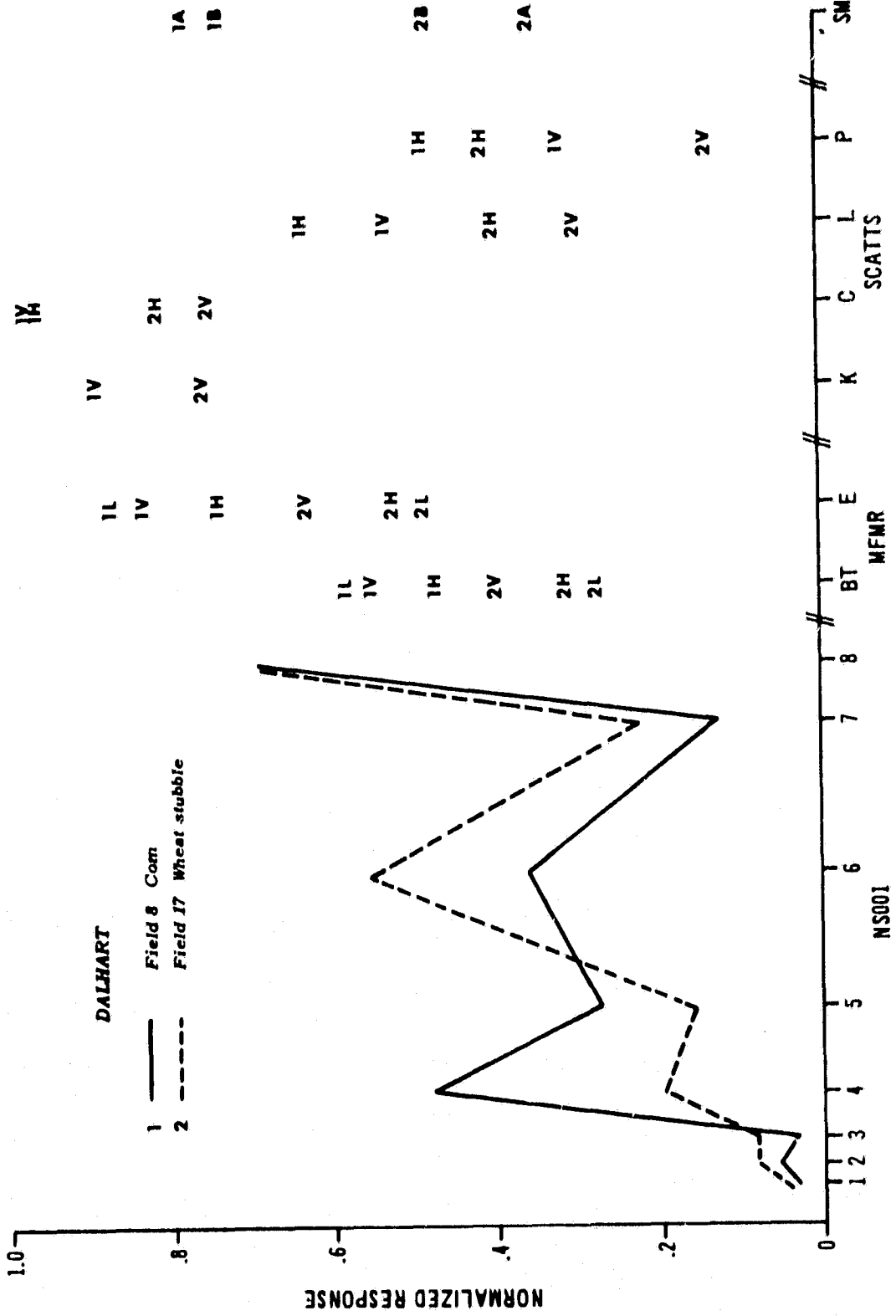


FIG. 11 Spectra comparing vegetated and non-vegetated fields as Dalhart. [H = C band horizontal (MFMR), V = C band vertical pole (MFMR), L - L band horizontal (MFMR), H - like pole 40° look angle (SCATTS), V = cross pole 40° look angle (SCATTS), A = 0-2 cm soil moisture (SM), B = 2-5 cm soil moisture (SM)].

6 and 7. Under wetter conditions in the corn (Field 8) the difference was enhanced in several frequencies and the maximum difference in return was 15 db in the P band cross pole data. The difference in the L band cross pole and bands 4 and 5 (NS001) remained the same. Consequently, the major variation in σ^0 at the 40° look angle in L band cross pole data appeared to be caused by vegetation. Responses from like-polarized microwave data were not very sensitive to the crop type differences.

Examples of bare soil, pasture, and wheat stubble having similar surface moisture are shown in Figure 10. Only minor differences occurred in the visible and infrared bands, especially in bands 4 and 6. Band 6 and 7 data were unavailable for field 15. Other bands which had differences were L band like and cross pole and C band cross pole scatterometer data. These differences are likely due to surface roughness differences between the fields. The wheat stubble and pasture fields were smoother than the other tilled bare fields. The smoother fields consequently acted as a spectral reflector giving a lower σ^0 at the 40° look angle.

Comparing the response differences between vegetated and non-vegetation fields, several spectral regions were significant (Figure 11). Obvious differences were in bands 4, 5, and 6 of the NS001 data. Possible combinations using these bands may prove to be helpful in discriminating vegetation from non-vegetation. In addition, all of the active microwave channels were able to distinguish vegetative differences to some degree of success. The most significant differences occurred in the C band and L band σ^0 values--as much as 12 db in the L band cross pole data.

An interesting anomaly demonstrating stressed and non-stressed conditions was evident in corn fields 1 and 2. Parts of the field were stressed as a result of a faulty irrigation system which did not apply adequate amounts of water in several areas through the growing season. A black and white aerial photo of the field is shown in Figure 12. Approximately 30-50% of the field was undergoing moisture stress. The stressed areas essentially had no grain yield; thus the total yield represented yield of the healthy areas. The visible/infrared spectra showed significant differences between healthy and unhealthy corn in several bands (Figure 13). The differences were especially significant ($0.3 \text{ mw cm}^{-2} \text{ ster}^{-1}$) in NS001 channels 4, 5, and 7, suggesting possible combinations using these bands may indicate biomass differences or stress conditions.

At Guymon, the crop types were different--alfalfa, sorghum, and bare soil. Examples of bare soil (field 10), mature sorghum (field 1X), and alfalfa (field 4) spectra having similar surface soil moisture conditions are shown in Figure 14. Reflectance in the visible and infrared differed significantly between vegetated and non-vegetated fields (as much as $6-10 \text{ mw cm}^{-2} \text{ ster}^{-1}$). Differences in the active microwave, especially L, C and P band were also indicative of crop types differences. For example, a difference of 9 db in the L and P band like pole data was common between sorghum and bare soil or sorghum and alfalfa. Part of the difference may be due to roughness variability in the soil surface. Also some microwave frequencies may be penetrating through the canopy and detecting tillage direction. The sorghum responses in field 1X figure 14 were from a field with rows perpendicular to the flight line. An example of a response from

ORIGINAL PAGE
BLACK AND WHITE PHOTOGRAPH

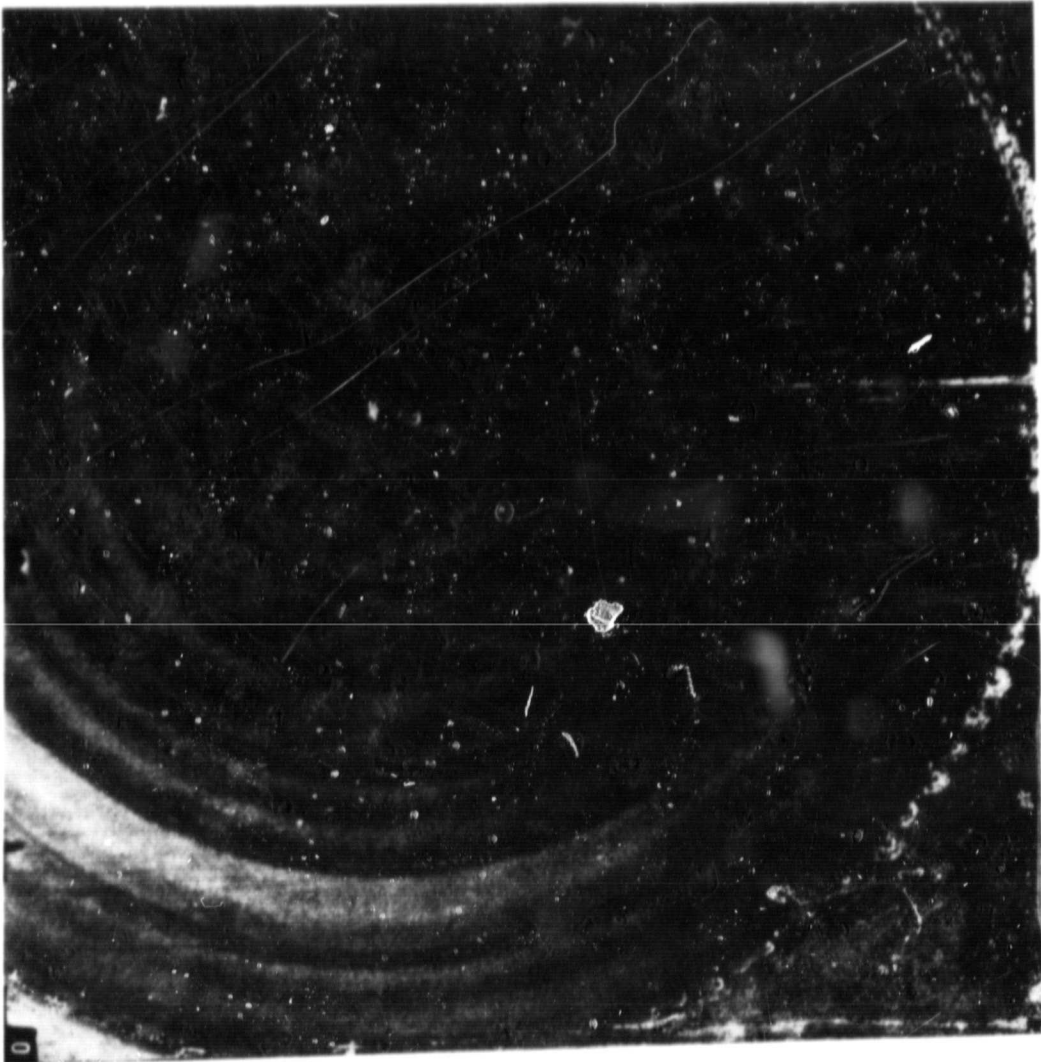


FIG. 12 An infrared aerial photo (scale 1:45,000) of stressed corn fields (fields 1 and 2) at Dalhart. The healthy are dark shaded and the stressed areas are light shaded.

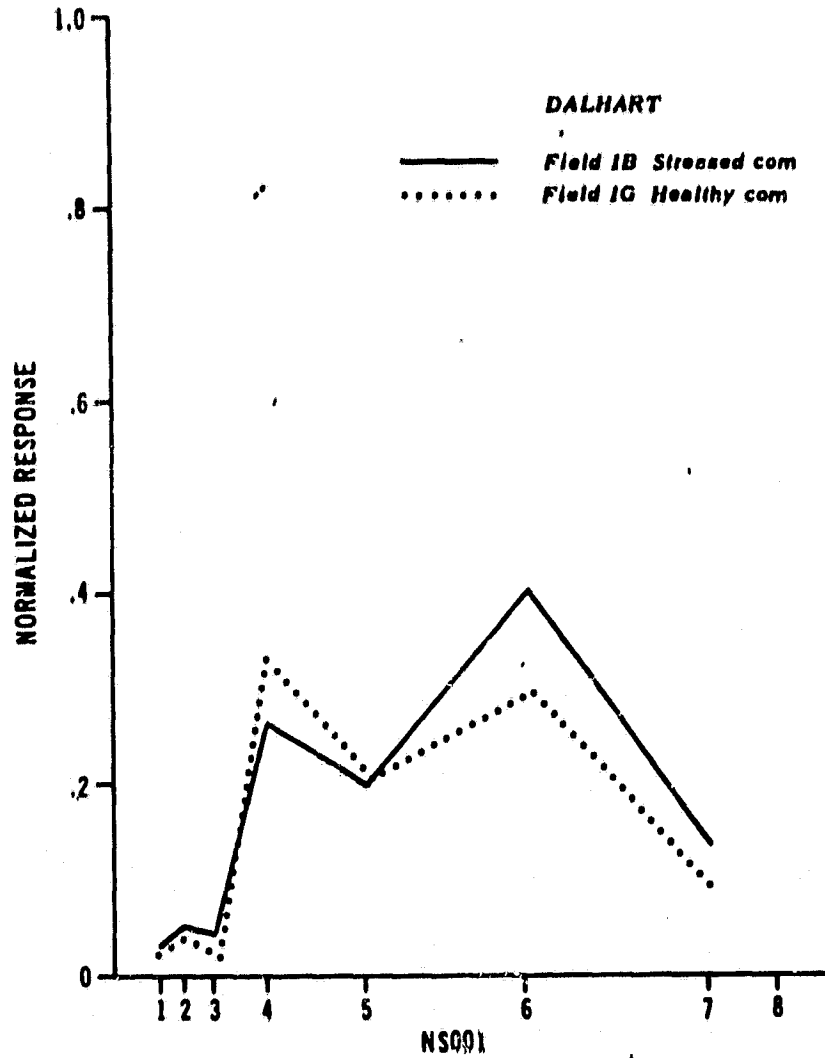


FIG. 13 Spectra comparing healthy and stressed corn at Dalhart. No microwave comparisons could be made.

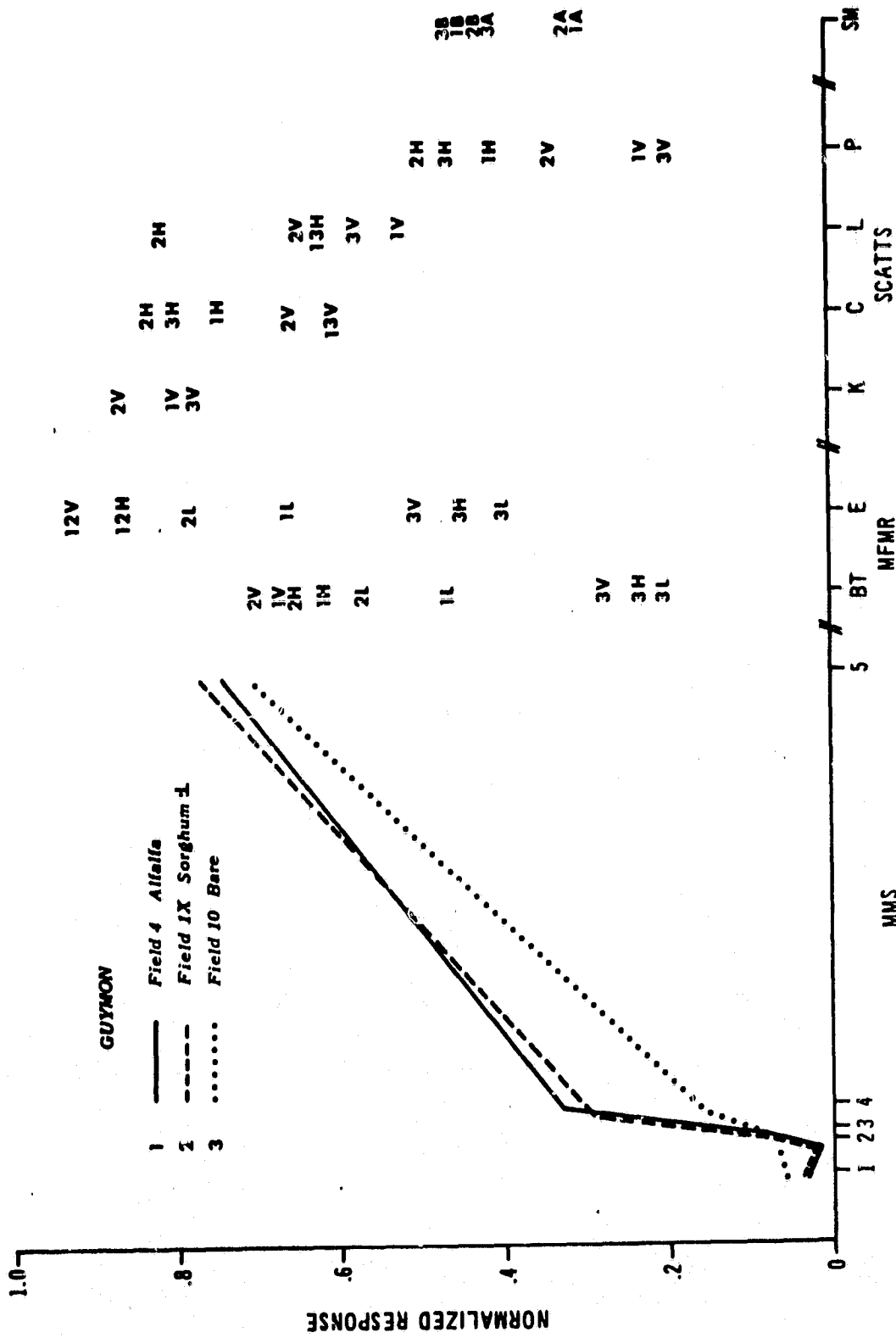


FIG. 14 Spectra comparing alfalfa, sorghum, and bare soil fields at Guymon. [H = C band horizontal (MFMR), V = C band vertical pole (MFMR), L = L band horizontal (MFMR), H = like pole 40° look angle (SCATTS), V = cross pole 40° look angle (SCATTS), A = 0-2 cm soil moisture (SM), B = 2-5 cm soil moisture (SM)].

a sorghum field with rows parallel to the flight line (field 2A) is given in Figure 15. The most significant differences were in the C band like pole and L band data--a 5db difference. The near infrared band indicated field 2A had less canopy cover. Wetter conditions also affected the return. For example, the spectra from a wet bare soil, field 14 (Figure 16) was similar to spectra for a dry sorghum field (field 2A), especially in the scatterometer like pole data. Consequently, responses which include roughness and soil moisture differences are masking the crop type differences.

Soil moisture differences were removed from the analysis of data from Clayton, New Mexico since the entire area had been saturated with a uniform rainfall on a large area of uniform soils. As a result of the rains, every field had approximately the same high soil moisture content, thus leaving only roughness and vegetation to affect the active microwave return. Assuming tillage practices were similar between crop types (corn and sorghum), the roughness effect is also minimized, leaving only vegetation effects. Analysis of the spectra from four corn (C1 through C4) and two sorghum fields, M1 and M2 (Figures 17 and 18) indicated that scatterometer L and P band like and cross pole data discriminated between corn and sorghum well. Corn tended to have higher returns in the L and P band data as compared to the returns from sorghum fields. Other frequencies had smaller or no response difference between corn and sorghum.

Statistical analysis of the Dalhart and Guymon data sets, using Duncan's Multiple Range Technique confirmed results noted in graphical analysis. The channels which discriminated the crops at Dalhart best were the K, C and L band active microwave data at look angles from 40°

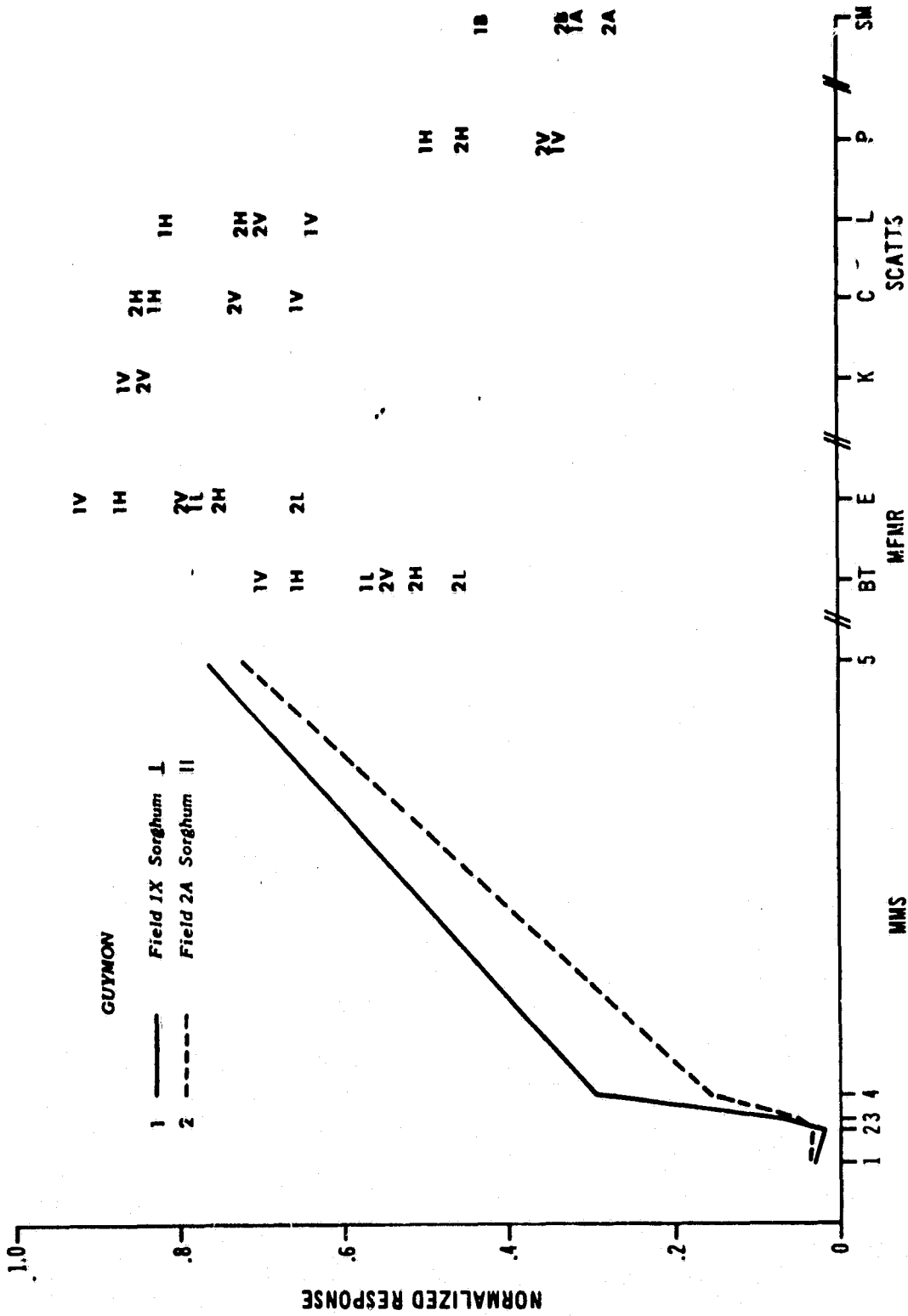


FIG. 15 Spectra comparing sorghum fields with rows perpendicular and parallel to the flight line. [H = C band horizontal (MFMR), V = C band vertical pole (MFMR), L = L band horizontal (MFMR), H = like pole 40° look angle (SCATTS), V = cross pole 40° look angle (SCATTS), A = 0-2 cm soil moisture (SM), B = 2-5 cm soil moisture (SM)].

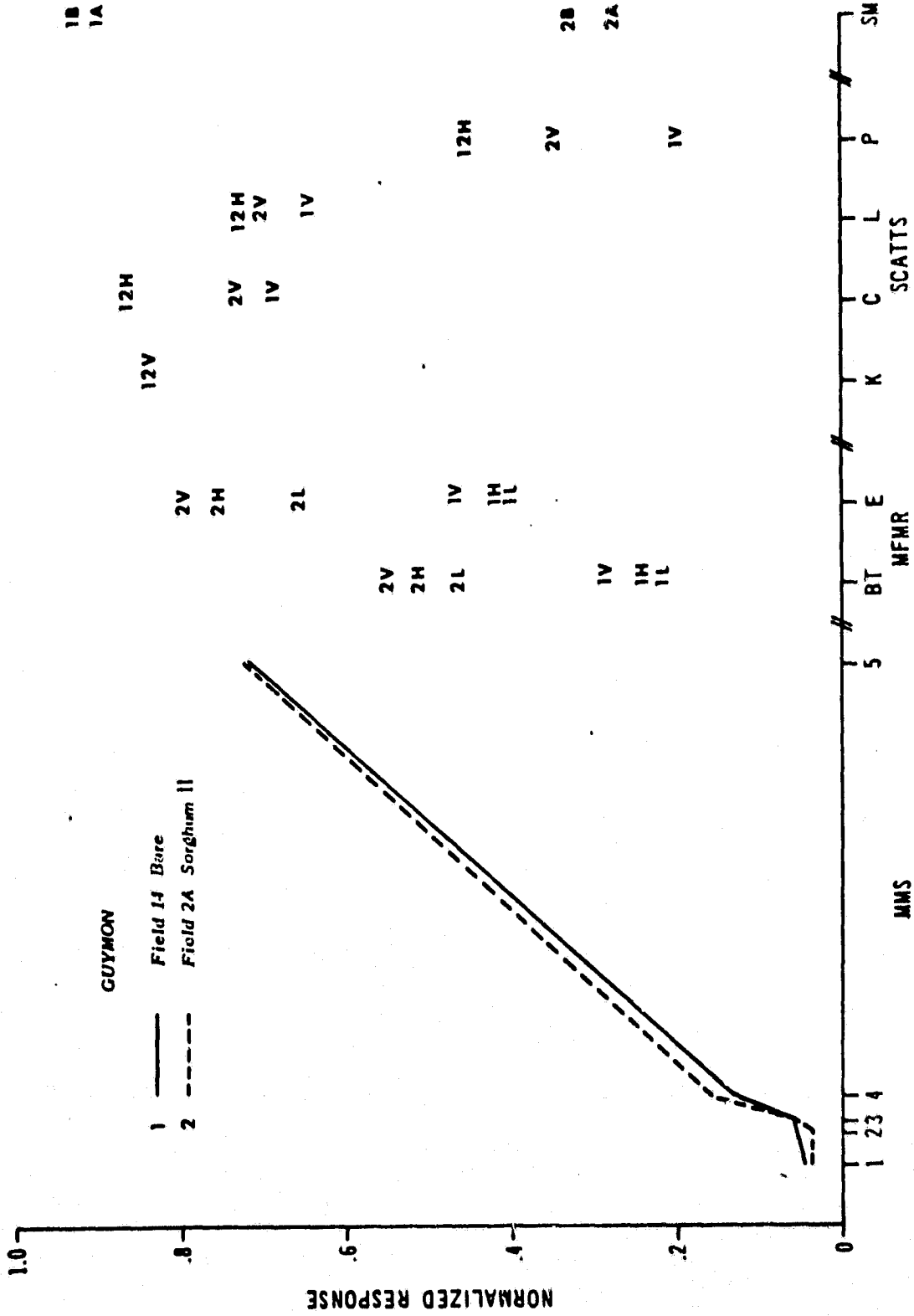


FIG. 16 Spectra comparing wet bare soil, and a dry sorghum field at Guymon. [H = C band horizontal (MFMR), V = C band vertical pole (MFMR), L = L band horizontal (MFMR), H = like pole 40° look angle (SCATTS), V = cross pole 40° look angle (SCATTS), A = 0-2 cm soil moisture (SM), B = 2-5 cm soil moisture (SM)].

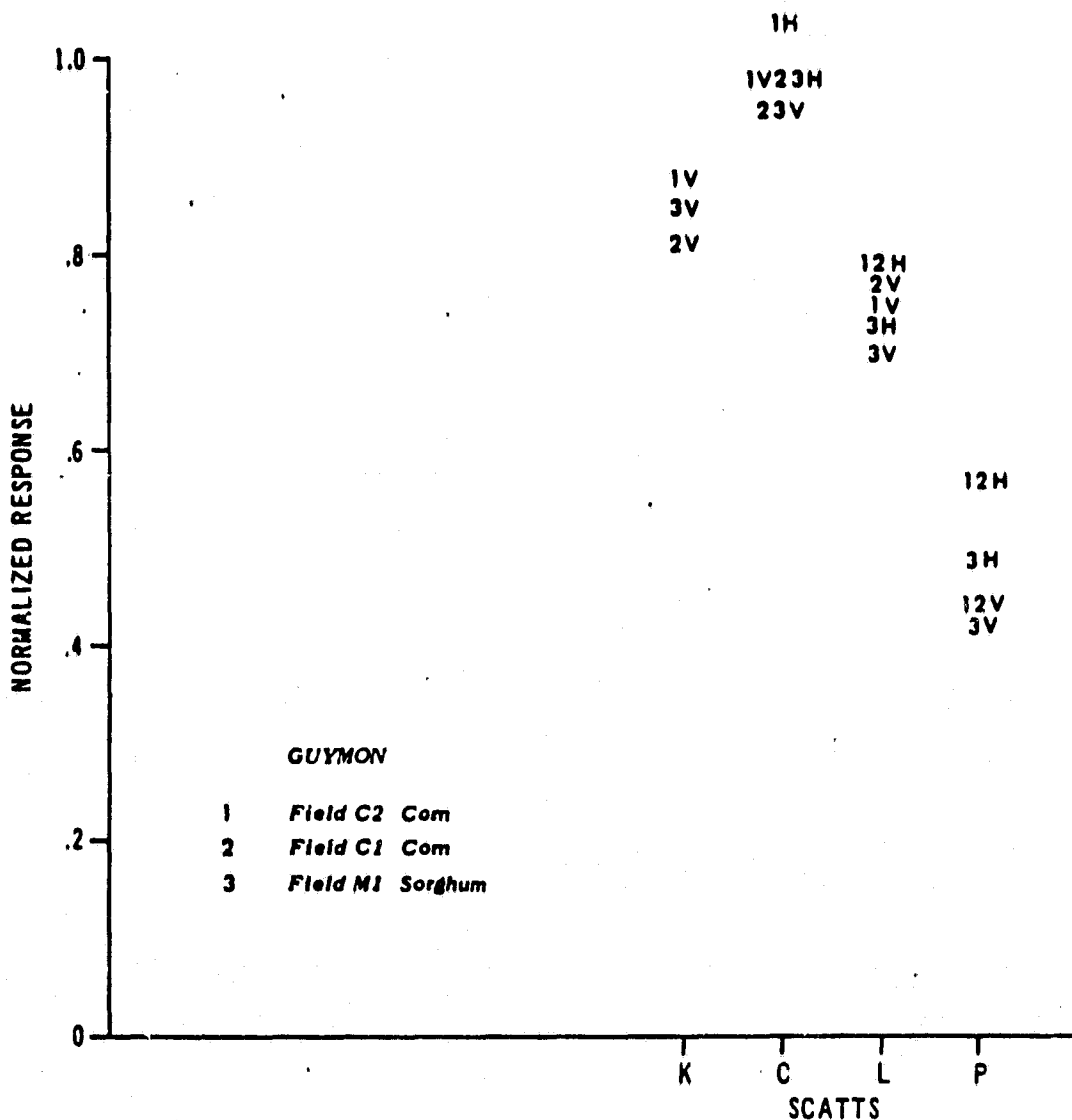


FIG. 17 Spectra comparing corn and sorghum at Clayton. No passive microwave or visible/infrared data was available. [H = like pole 40° look angle (SCATTS), V = cross pole 40° look angle (SCATTS)]

ORIGINAL PAGE IS
OF POOR QUALITY

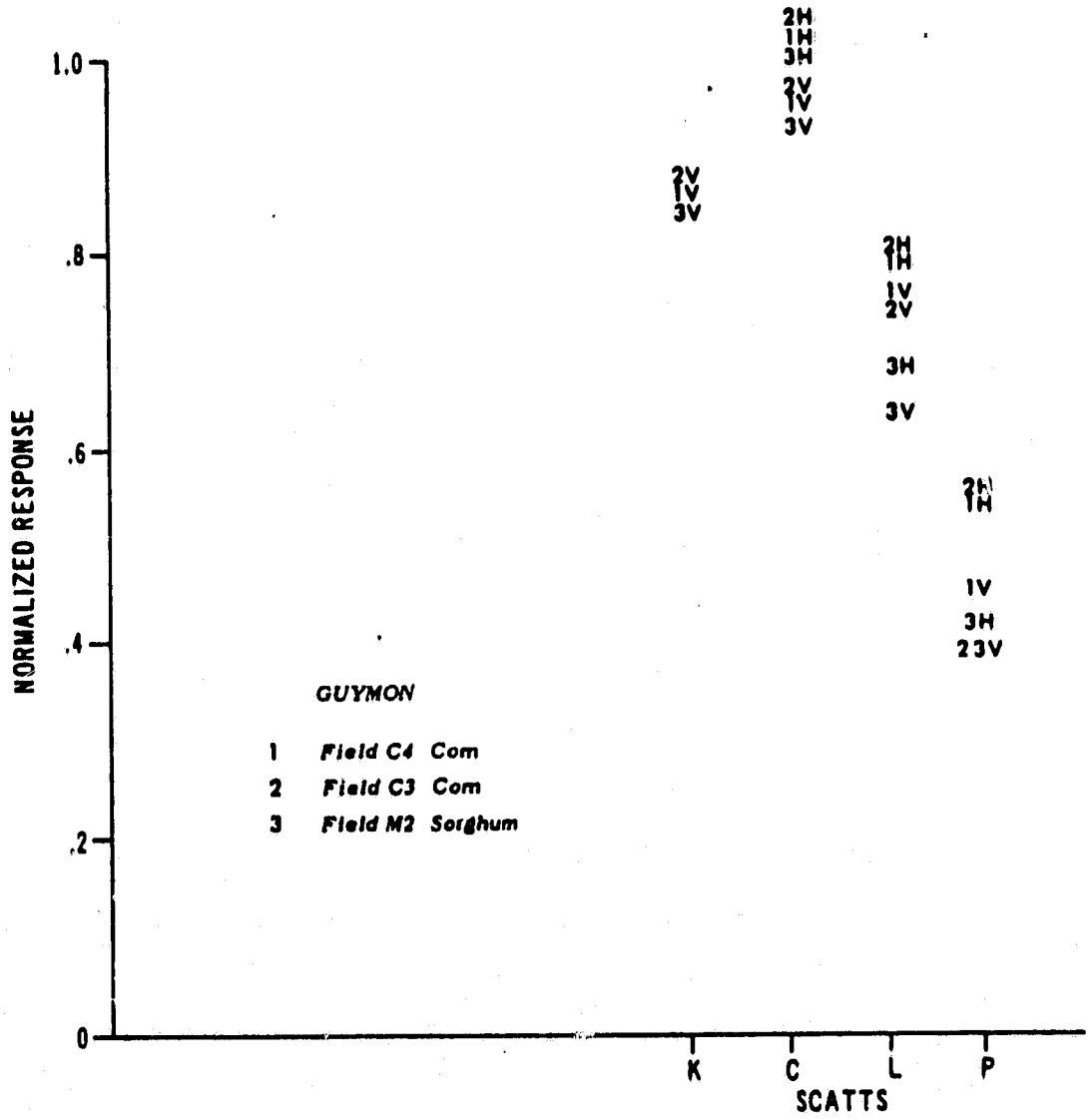


FIG. 18 Spectra comparing corn and sorghum at Clayton. No passive microwave or visible/infrared data was available. [H = like pole 40° look angle (SCATTS), V = cross pole 40° look angle (SCATTS)]

and 45° off nadir (Table 4). The visible and infrared bands were able to discriminate between vegetated and non-vegetated fields very well, but not differences within the vegetated fields. At Guymon, the same active microwave frequencies did the best job of discriminating crops (Table 5). Fields and crops with higher biomass had the higher response, while fields with little or no biomass had the lower response. However, roughness also played an important role as indicated by differences between sorghum fields having perpendicular and parallel rows. The roughness effect was reduced in the cross-polarized data, thus suggesting the L band cross pole and C band cross pole active microwave data as possibly the best microwave frequencies and polarizations to use.

Another means of demonstrating the effect of vegetation in the active microwave region was analyzing line plots of the data (σ° as a function of time). An example of three fields having roughly the same surface soil moisture is given in Figures 19 and 20. Data from a near (10°) and far (40°) look angle were plotted. The area covered fields V6, 1 and 19, on 8/16/80 at Dalhart, Texas. The crop types represented included sorghum (field V6), corn, (field 1) and bare soil (field 19). Crop type differences were enhanced at the far look angles, especially in the C, L and P band data. The responses from the near look angles tended to be fairly stable along the flight line, especially at the lower frequencies.

Summarizing, in addition to several visible/infrared channels, active microwave frequencies (C, L and P band) are sensitive to crop type differences between selected crop pairs. For instance, L band and P band discriminated between sorghum and corn, while C band did

TABLE 4. Results of Duncan's Multiple Range Test for Dalhart active microwave data

<u>40° look angle</u>			<u>45° look angle</u>		
<u>Crop</u>	<u>K band like pole</u>	<u>Mean</u>	<u>Crop</u>	<u>K band like pole</u>	<u>Mean</u>
Corn		-7.1 a*	Corn		-7.1 a
Millet		-9.1 b	Millet		-8.8 b
Weeds and Bare Soil		-10.9 c	Weeds and Bare Soil		-10.6 c
Bare Soil		-11.3 c	Bare Soil		-10.9 c
Pasture		-14.0 d	Pasture		-13.6 d
Wheat Stubble		-14.6 d	Wheat Stubble		-14.3 d

<u>I. band like pole</u>		<u>L band like pole</u>	
Corn	-22.4 a	Corn	-23.1 a
Weeds and Bare Soil	-29.8 a	Weeds and Bare Soil	-30.9 b
Millet	-30.6 b	Millet	-31.9 b
Bare Soil	-30.7 b	Bare Soil	-32.9 b
Pasture	-34.7 c	Pasture	-36.8 c
Wheat Stubble	-36.2 c	Wheat Stubble	-37.3 c

<u>L band cross pole</u>		<u>L band cross pole</u>	
Corn	-28.9 a	Corn	-28.6 a
Millet	-37.1 b	Millet	-37.2 b
Bare Soil	-39.5 c	Weeds and Bare Soil	-39.3 bc
Weeds and Bare Soil	-39.7 c	Bare Soil	-41.2 c
Wheat Stubble	-44.2 d	Pasture	-44.6 d
Pasture	-44.2 d	Wheat Stubble	-48.8 d

<u>C band like pole</u>		<u>C band like pole</u>	
Corn	-2.6 a	Corn	-4.1 a
Millet	-4.7 a b	Millet	-5.8 a b
Weeds and Bare Soil	-7.5 b c	Weeds and Bare Soil	-8.7 a b c
Bare Soil	-8.0 b c	Bare Soil	-10.1 b c
Pasture	-11.6 c	Pasture	-13.2 c d
Wheat Stubble	-12.9 c	Wheat Stubble	-15.4 d

TABLE 4. (Continued)

<u>40° Look Angle</u>		<u>45° Look Angle</u>	
<u>C band cross pole</u>		<u>C band cross pole</u>	
Corn	-5.6 a	Corn	-6.0 a
Millet	-11.4 b	Millet	-11.5 b
Weeds and Bare Soil	-14.4 b c	Weeds and Bare Soil	-14.0 b
Wheat Stubble	-17.6 b c	Bare Soil	-17.4 b
Bare Soil	-17.8 c	Wheat Stubble	-18.1 b
Pasture	-19.5 c	Pasture	-19.2 b
<u>P band like pole</u>		<u>P band like pole</u>	
	Mean		Mean
Corn	-28.7 a	Corn	-28.9 a
Weeds and Bare Soil	-35.1 b	Weeds and Bare Soil	-36.3 b
Wheat Stubble	-35.3 b	Wheat Stubble	-37.3 b
Millet	-36.2 b	Millet	-37.6 b
Bare Soil	-37.3 b	Bare Soil	-38.0 b
Pasture	-37.5 b	Pasture	-38.5 b
<u>P band cross pole</u>		<u>P band cross pole</u>	
Corn	-43.9 a	Corn	-43.9 a
Weeds and Bare Soil	-47.6	Weeds and Bare Soil	-52.9 b
Wheat Stubble	-52.7	Bare Soil	-54.2 b
Bare Soil	-52.8	Millet	-54.2 b
Millet	-52.9	Wheat Stubble	-54.8 b
Pasture	-54.9 c	Pasture	-55.1 b

*The treatment means followed by the same letter in each column are not significantly different at the 5% probability level of Duncan's Multiple Range Test.

TABLE 5. Results of Duncan's Multiple Range Test for Guymon active microwave data

<u>Crop</u>	<u>40° Look Angle</u>	<u>Mean</u>	<u>Crop</u>	<u>45° Look Angle</u>	<u>Mean</u>
<u>K band like pole</u>			<u>K band like pole</u>		
Sorghum(perp. rows)		-7.1 a	Sorghum (perp. rows)		-7.7 a
Sorghum(paral. rows)		-9.5 b	Sorghum (paral. rows)		-9.7 b
Bare Soil		-12.1 c	Bare Soil		-12.3 c
Alfalfa		-12.1 c	Alfalfa		-12.5 c
<u>L band like pole</u>			<u>L band like pole</u>		
Sorghum(perp. rows)		-9.3 a	Sorghum (perp. rows)		-11.9 a
Sorghum(paral. rows)		-18.1 b	Sorghum (paral. rows)		-19.2 b
Bare Soil		-18.2 b	Bare Soil		-21.1 b
Alfalfa		-20.5 b	Alfalfa		-21.9 b
<u>L band cross pole</u>			<u>L band cross pole</u>		
Sorghum(perp. rows)		-19.1 a	Sorghum (perp. rows)		-20.2 a
Sorghum(paral. rows)		-21.5 a	Sorghum (paral. rows)		-22.4 a
Bare Soil		-27.1 b	Alfalfa		-27.9 b
Alfalfa		-27.7 b	Bare Soil		-28.5 b
<u>C band like pole</u>			<u>C band like pole</u>		
Sorghum(perp. rows)		-8.2 a	Sorghum (perp. rows)		-10.3 a
Sorghum(paral. rows)		-12.5 b	Sorghum (paral. rows)		-13.7 b
Alfalfa		-14.2 b	Alfalfa		-15.4 b
Bare Soil		-15.2 b	Bare Soil		-16.3 b
<u>C band cross pole</u>			<u>C band cross pole</u>		
Sorghum(perp. rows)		-17.2 a	Sorghum (perp. rows)		-19.5 a
Sorghum(paral. rows)		-19.6 a b	Sorghum (paral. rows)		-22.0 a b
Alfalfa		-22.6 b	Alfalfa		-23.7 b
Bare Soil		-26.9 c	Bare Soil		-28.7 c
<u>P band like pole</u>			<u>P band like pole</u>		
Sorghum (perp. rows)		-27.8 a	Sorghum (perp. rows)		-23.7 a
Bare Soil		-31.4 b	Bare Soil		-30.3 b
Sorghum (paral. rows)		-31.5 b	Sorghum (paral. rows)		-32.0 b c
Alfalfa		-35.6 c	Alfalfa		-35.1 c

TABLE 5. (Continued)

<u>P band cross pole</u>		<u>P band cross pole</u>	
Sorghum (perp. rows)	-37.2 a	Sorghum (perp. rows)	-34.3 a
Sorghum (paral. rows)	-38.5 a	Sorghum (paral. rows)	-37.4 a
Alfalfa	-46.5 b	Bare Soil	-45.6 b
Bare Soil	-47.4 b	Alfalfa	-46.9 b

*The treatment means followed by the same letter in each column are not significantly different at the 5% probability level of Duncan's Multiple Range Test.

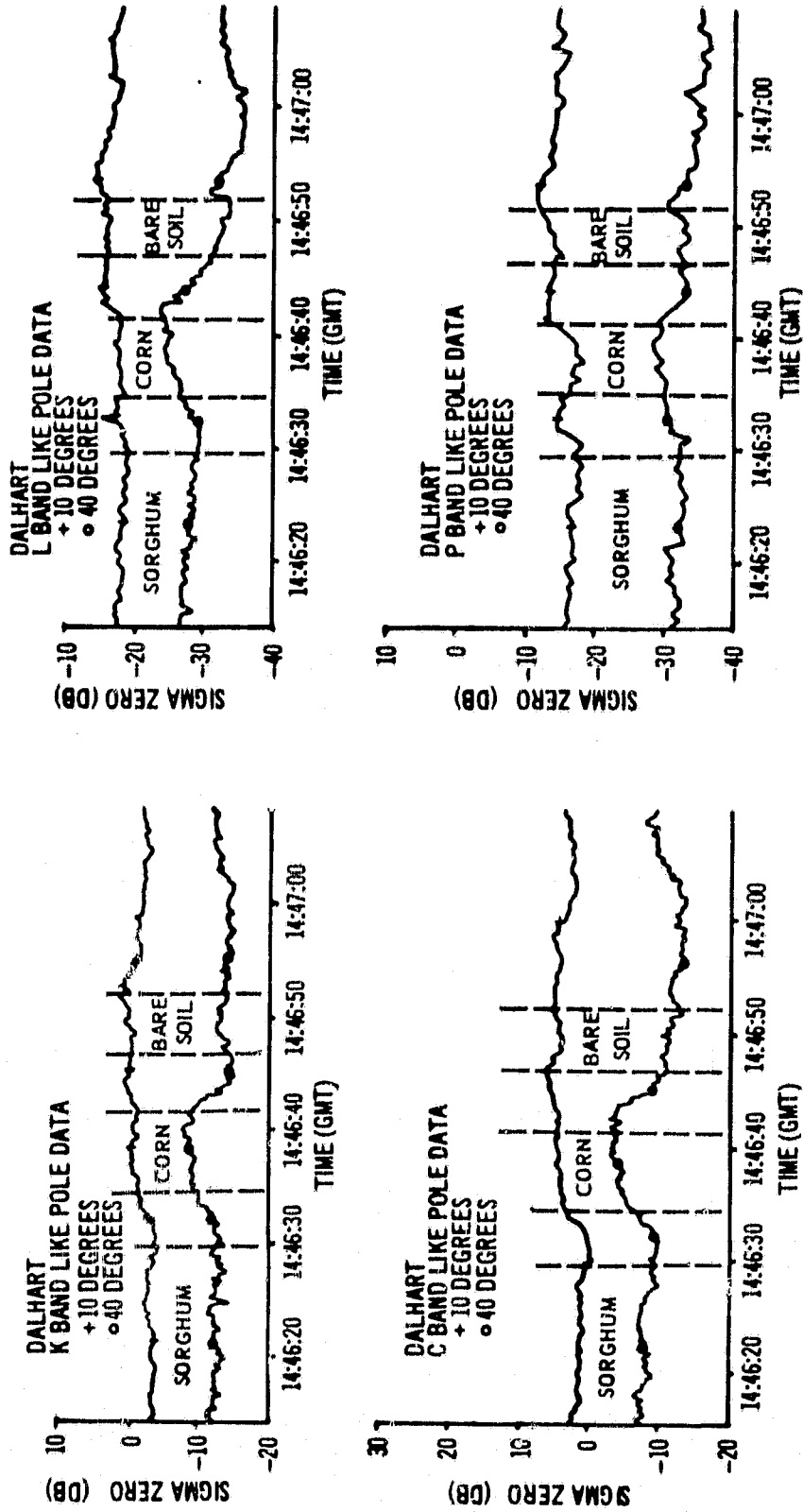


FIG. 19 Line plots (σ^0 vs time) for all like polarized scatterometer data at 10° and 40° off nadir.

ORIGINAL PAGE IS
OF POOR QUALITY

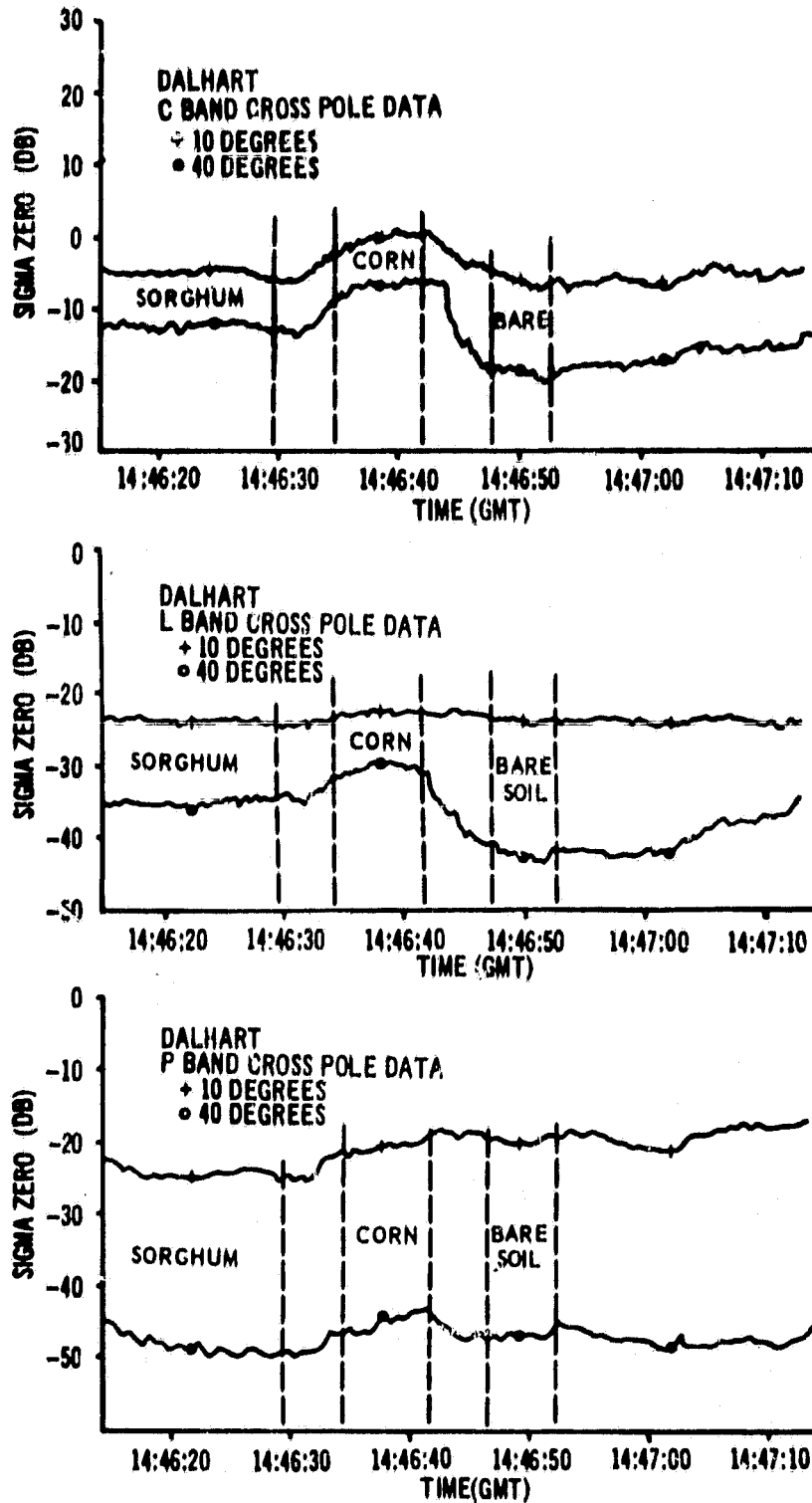


FIG. 20 Line plots (σ^0 vs time) for all cross polarized scatterometer data at 10° and 40° off nadir.

not. C band discriminated between bare soil and alfalfa while K, L and P bands did not discriminate between this pair. All bands discriminated between corn and bare soil. Soil moisture and roughness had an effect on the active microwave responses, but the vegetation effect generally predominated at the far look angles (greater than 35°).

Problem 2

To develop the proper combination for analyzing crop type differences in a tree-classification model, a hierarchical (unsupervised) clustering routine was used. The routine was based on a cluster criterion of a minimum Euclidean distance from the mean of the cluster. By going through the same classifying criteria used within the routine, individual channels or combinations which separated individual clusters were detected. By following this technique through several iterations, a dendrogram (tree-classification system) using visible, infrared, and microwave data was developed. Data from crop discriminating scatterometer frequencies and polarizations at 40° look angles were included with the visible/infrared data (omitting thermal) at Guymon and Dalhart. In addition, a dendrogram was developed from the Dalhart spectral data set using the scatterometer 40° look angle and only bands 2, 3, and 4 from the NS001 data. This analysis was done to allow unbiased comparisons of classification accuracy between the Dalhart and Guymon data sets. Active microwave data from the 40° look angle was used because the data from this look angle was most sensitive to crop type differences (results from the previous problem).

Results from the Dalhart dendrogram using the active microwave bands and NS001 bands 2, 3 and 4 indicated that C and L band cross pole data can classify reasonably well without visible and near infrared information (Figure 21). The largest error was separating wheat stubble and pasture from bare soil. Allowing these three groups to be classified the same, the overall accuracy was 78%. The first separation criterion used differences in the L band cross pole 40° look angle data to separate corn and sorghum, (class 1) from weeds, pasture, bare soil, and wheat stubble. The second criterion again used differences in the sum of L band and C band cross pole 40° look angle data to separate millet, corn and sorghum (class 2) from millet, pasture, wheat stubble and weeds. The third criterion used the same sum to separate pasture, wheat stubble and bare soil (class 3) from other weeds, pasture and bare soil. Then the last criterion used was C band cross pole data to separate pasture, wheat stubble and bare soil (class 5) from weeds and bare soil (class 4). The difference between the bare fields in class 4 and 5 was the class 4 bare fields included some weeds while class 5 bare fields did not. Consequently, responses in class 4 appear to be sensitive to low biomass levels.

Using all of the NS001 with active microwave data, the accuracy improved to 80% as more information was gathered in NS001 bands 3, 4, 5 and 6. The dendrogram was different in that most of the criterion used L and C band cross pole data (Figure 22).

In spite of the different crop types and visible/infrared bands, a similar dendrogram to the one using all NS001 data was developed at Guymon (Figure 23). The first criterion level used the same type of data as Dalhart--L band cross pole. These steps separated corn and

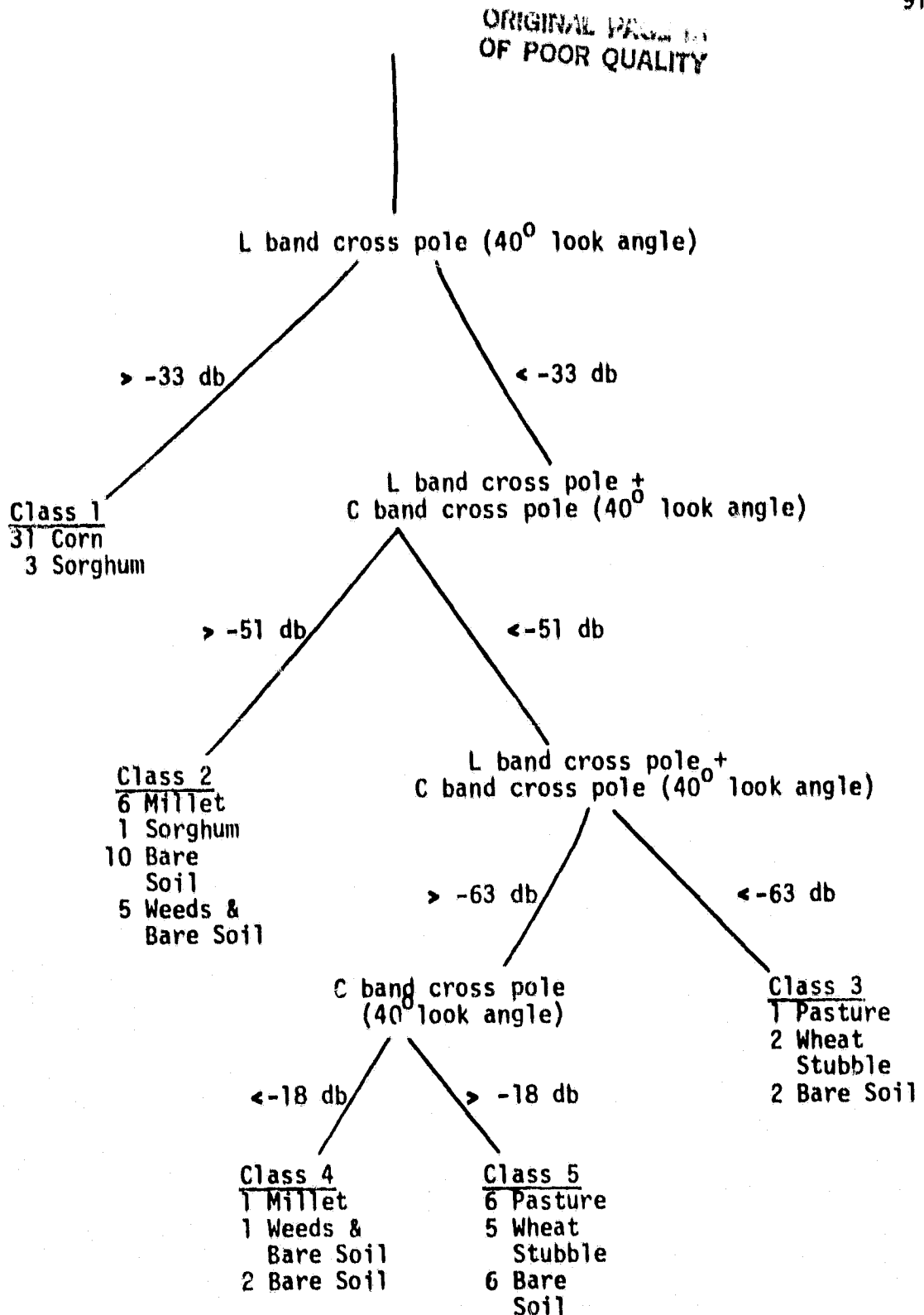


FIG. 21 Dendrogram (tree-classification) model using NS001 bands 2, 3, and 4, and C, L and P band cross pole Dalhart data (accuracy 78%).

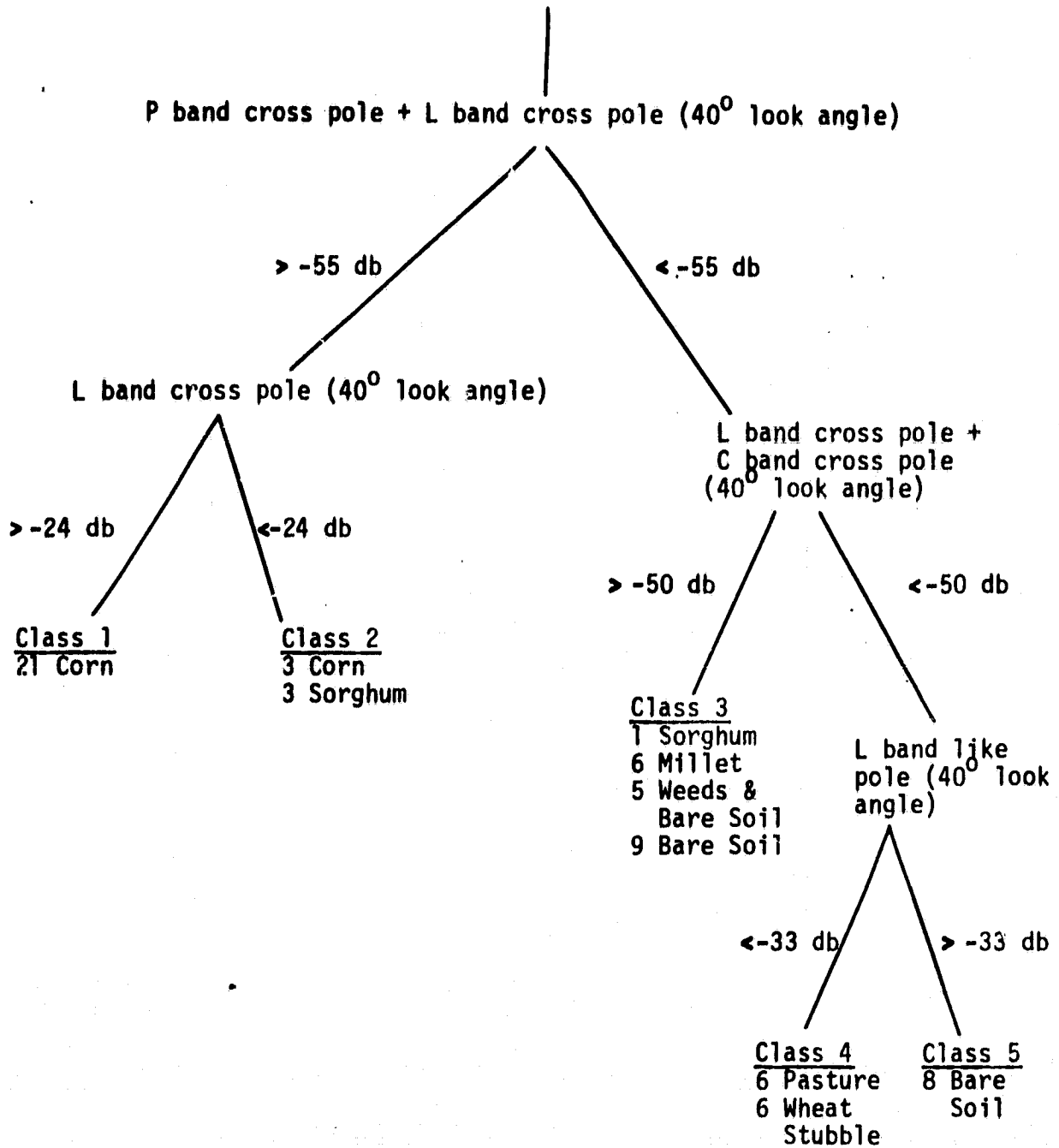


FIG. 22 Dendrogram (tree-classification) model using all NS001 bands C, L and P band cross pole Dalhart data (accuracy 80%).

ORIGINAL PAGE IS
OF POOR QUALITY

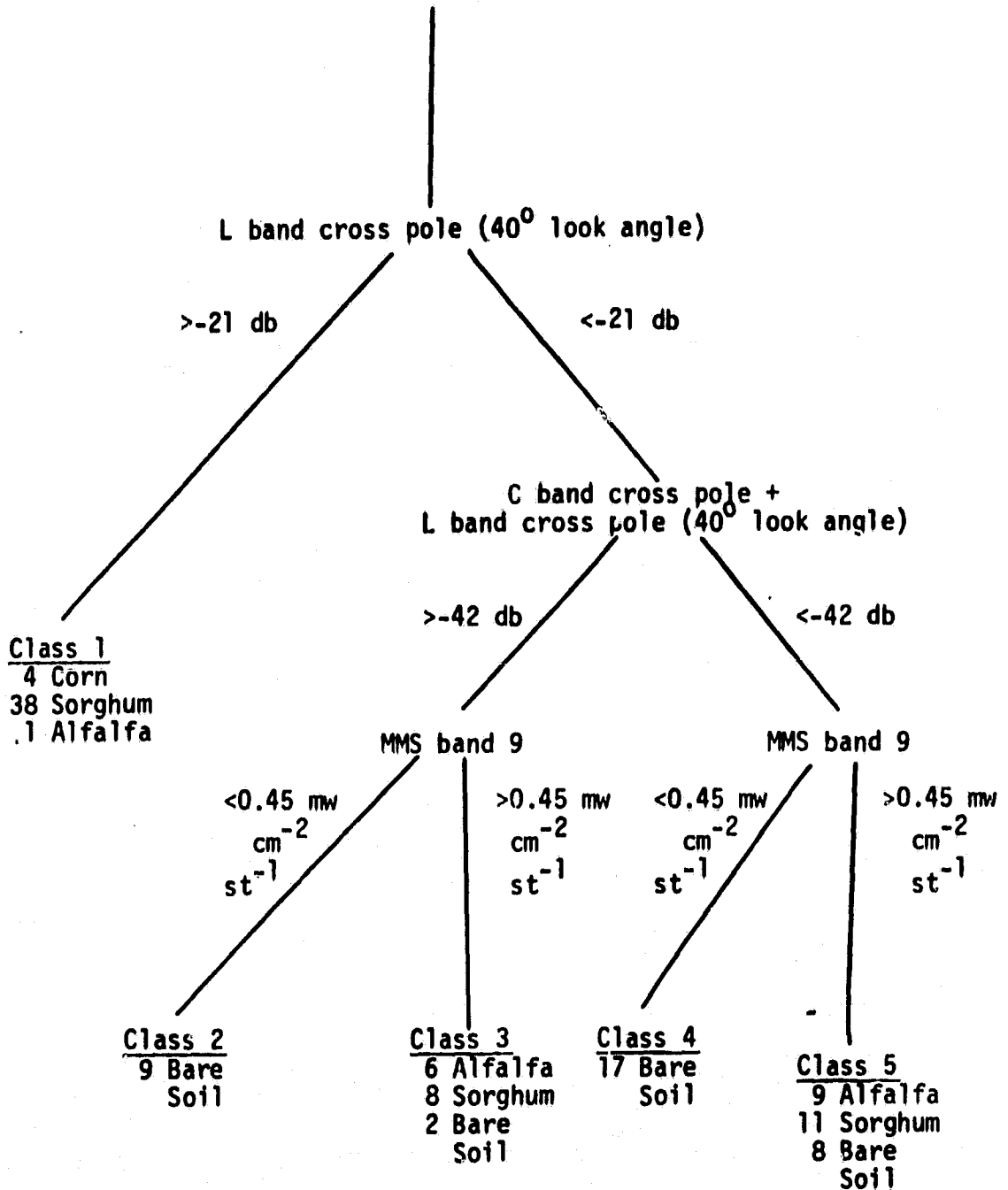


FIG. 23 Dendrogram (tree-classification) model using M²S bands 4, 7, 8 and 9, C and L band cross pole Guymon data (accuracy 70%).

sorghum from other crops. The next criterion used differences in the sum of C and L band cross pole data. The last two steps used M²S band 9 data to separate vegetation from bare soil. The overall accuracy of the model was 70%. One bare field, 10, was frequently classified with fields having vegetation. The reason for the misclassification was due to the presence of weeds within the field late in the experiment. The similarity between the two models is striking. Fields with high biomass were separated from other fields using microwave data and vegetation was separated from bare soil using visible and infrared data. The similarity will be discussed further in the next section.

A problem arose when data sets from both Guymon and Dalhart were combined. Due to the fact the visible and infrared regions did not match and no calibration of the scatterometer data was available, no dendrogram for the combined data set was developed.

Problem 3

This problem deals with both crop classification and biomass estimations. One technique used to determine the utility of microwave data in classification was to make a comparison between unsupervised classification result accuracies using visible, infrared and microwave data and accuracies using only visible and infrared data. As mentioned in the previous subsection, cluster analysis using microwave, visible, and infrared data had classification accuracies equal to or greater than 70%. Using only visible/infrared data, the classification accuracies decreased to 65% at Guymon and 78% at Dalhart. The tree-classification system using visible and infrared data at Dalhart and Guymon are given in Figures 24 and 25, respectively. The major

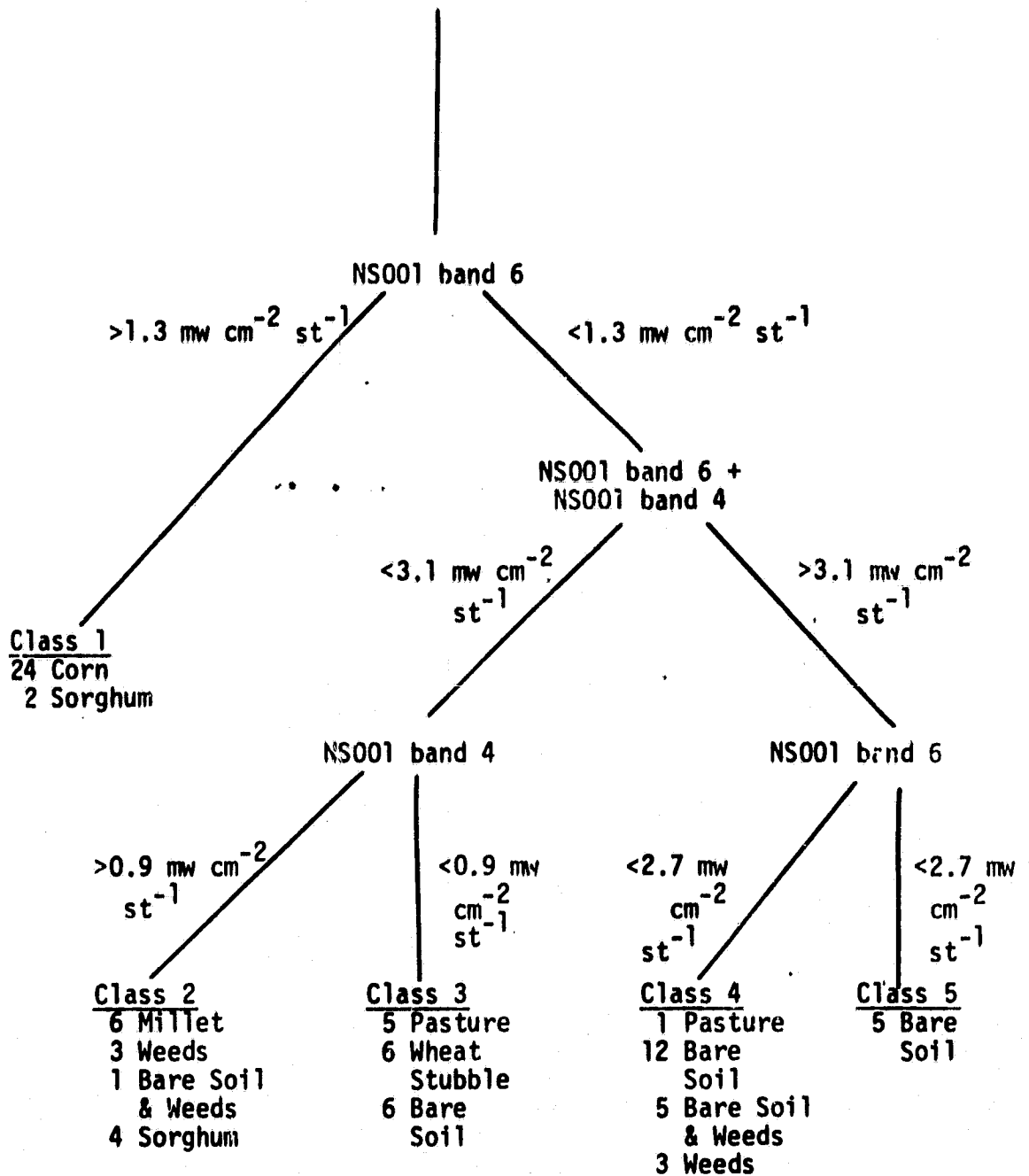


FIG. 24 Dendrogram (tree-classification) model using all NS001 data at Dalhart. (78% accuracy)

ORIGINAL PAGE IS
OF POOR QUALITY

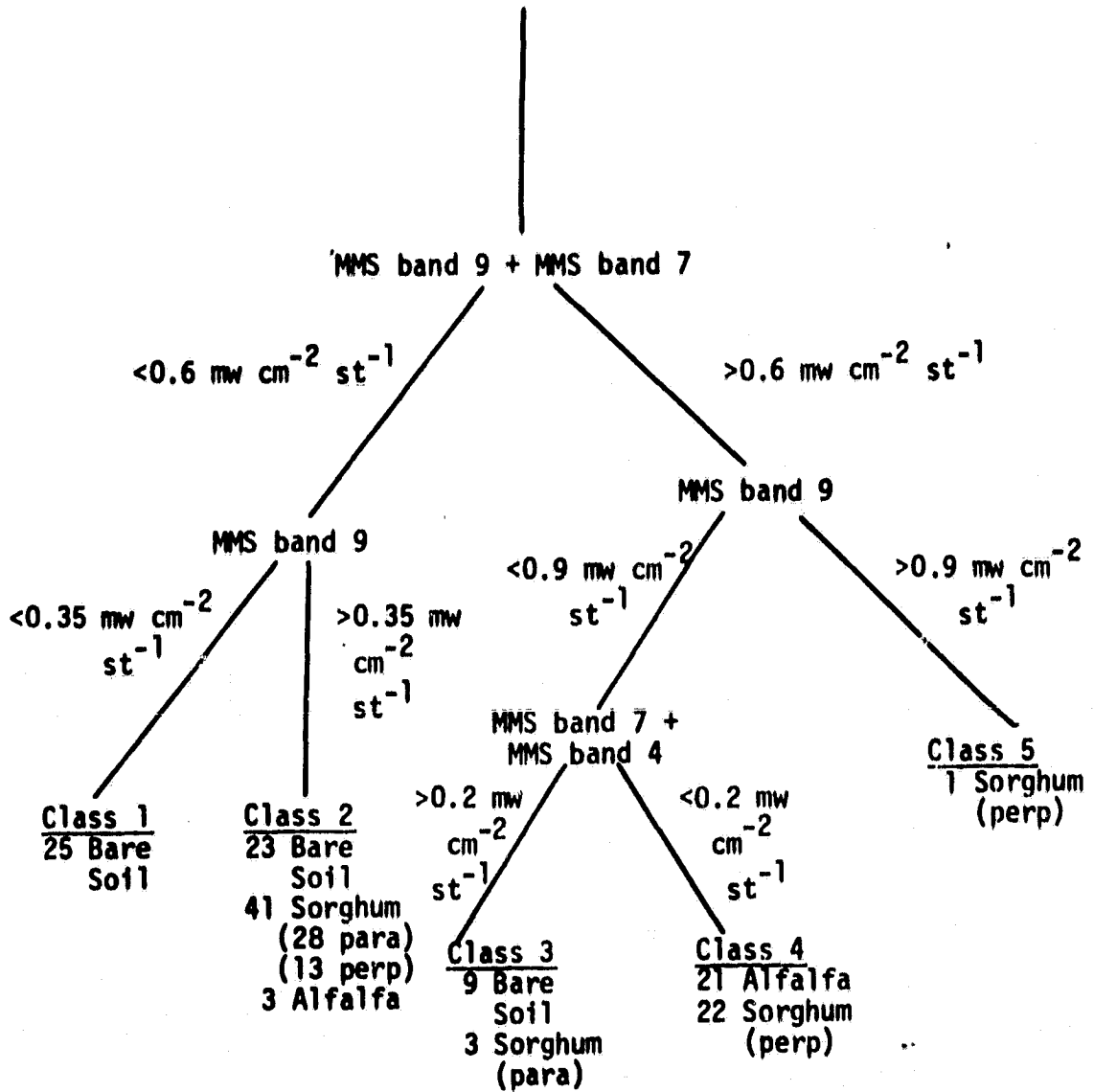


FIG. 25 Dendrogram (tree-classification) model using M²S band 4, 7, 8 and 9 data at Guymon (65% accuracy).

misclassification using visible and infrared data were high biomass fields being classified as one group. For instance, at Guymon twenty-one observations of alfalfa and twenty-two observations of sorghum fields at different biophases were classified into one group. Consequently, result comparisons from the unsupervised technique proved that inclusion of microwave data enhanced classification accuracy.

Supervised classification (discriminant analysis) results also indicated microwave data improved classification accuracy. The contingency table results from classifying fields on August 16 using only NS001 data from August 14 and 18 as the training classifier is given in Table 6a. The overall accuracy was 73%. By including K band like pole and L band cross pole data the accuracy increased to 92% (Table 6b). To make unbiased comparisons with the Guymon spectral data sets, NS001 bands 2, 3 and 4 were analyzed. Following the same techniques, the August 16 classifier accuracy was 81% (Table 7a). By including K and L band cross pole active microwave data, the accuracy improved only slightly to 84% (Table 7b). No known reason explained the discrepancy between results using all or parts of the NS001 data.

At Guymon, spectral data from August 2 and 17 were used as inputs into the training classifier, and the classifier was tested on August 5, 8, 11 and 14 spectral data. Using only M²S visible and infrared data, the classification accuracy was 88% (Table 8a). By including K band like pole and L band cross pole data the accuracy remained the same 88% (Table 8b). Consequently, supervised classification results using the Dalhart and Guymon spectral data sets indicated inclusion of microwave data with visible/infrared data maintained or improved

TABLE 6. Dalhart discriminant analysis results using (a) all NS001 channels and (b) all NS001 channels plus K band like pole and L band cross pole (40° look angle) data from August 14 and 18 as a training classifier. The results are from August 16 testing of the model.

(a)

		Number of Observations Classified into Crop Types:					
From Crop Types:	Corn	Bare Soil	Wheat Stubble	Weeds and Bare Soil	Pasture	Millet	Weeds
Corn	16	0	0	0	0	0	0
Bare Soil	0	16	0	0	0	0	0
Wheat Stubble	0	4	0	0	0	0	0
Weeds and Bare Soil	0	3	0	0	0	0	0
Pasture	0	4	0	0	0	0	0
Millet	0	0	0	0	0	4	0
Weeds	0	0	0	0	2	2	0

*Accuracy of 73%

(b)

		Number of Observations Classified into Crop Types:					
From Crop Types:	Corn	Bare Soil	Weeds and Bare Soil	Pasture	Millet	Wheat Stubble	Weeds
Corn	16	0	0	0	0	0	0
Bare Soil	0	11	0	0	0	0	0
Weeds and Bare Soil	0	4	0	0	0	0	0
Pasture	0	0	0	4	0	0	0
Millet	0	0	0	0	4	0	0
Wheat Stubble	0	0	0	0	0	4	0
Weeds	0	0	0	0	1	0	0

*Accuracy of 92%

TABLE 7. Daliart discriminant analysis using (a) NS001 channels 2, 3, and 4 and (b) NS001 channels 2, 3 and 4 and K band like pole and L band cross pole data. Contingency table results from the model tested on August 16 spectral data.

(a)

Number of Observations Classified into Crop Types:

From Crop Types:	Corn	Bare Soil	Weeds and Bare Soil	Pasture	Millet	Weeds	Wheat Stubble
Corn	16	0	0	0	0	0	0
Bare Soil	0	12	0	0	0	0	0
Weeds and Bare Soil	0	0	3	0	0	1	0
Pasture	0	0	0	3	0	1	0
Millet	0	0	0	0	0	4	0
Weeds	0	0	0	0	0	4	0
Wheat Stubble	0	4	0	0	0	0	0

*Accuracy of 81%

(a)

Number of Observations Classified into Crop Types:

From Crop Types:	Corn	Bare Soil	Weeds and Bare Soil	Pasture	Millet	Weeds	Wheat Stubble
Corn	15	0	0	0	1	0	0
Bare Soil	0	12	0	0	0	0	0
Weeds and Bare Soil	0	3	1	0	0	0	0
Pasture	0	0	0	4	0	0	0
Millet	0	0	0	0	4	0	0
Weeds	0	0	1	0	0	0	0
Wheat Stubble	0	4	0	2	0	0	0
Sorghum	3	1	0	0	0	0	0

*Accuracy of 84%

TABLE 8. Discriminant Analysis of Guymon visible/infrared data using August 2 and 17 data as the training classifier. Results from classification of August 5, 8, 11, and 14 data.

(a)

From Crop Types:	Number of Observations Classified into Crop Types:			
	Alfalfa	Bare	Paral. Sorghum	Perp. Sorghum
Alfalfa	12	0	3	1
Bare	0	32	4	1
Parallel Row Sorghum	1	1	18	1
Perpendicular Sorghum	1	0	2	21

*Accuracy is 88% (assuming parallel sorghum and perpendicular sorghum are one group)

(b)

From Crop Types:	Number of Observations Classified into Crop Types:			
	Alfalfa	Bare	Paral. Sorghum	Perp. Sorghum
Alfalfa	9	0	2	1
Bare	0	23	2	2
Parallel Row Sorghum	1	1	8	6
Perpendicular Row Sorghum	0	0	0	19

*Accuracy is 88% (assuming parallel sorghum and perpendicular sorghum are one group)

classification accuracy compared to using only visible and near infrared data.

Using step-wise regression techniques to determine the utility of microwave data, an increase in the coefficient of determination using microwave data is apparent (Tables 9 and 10). At Guymon and Dalhart, the C band active microwave data were especially sensitive to crop types differences.

Biomass estimation was the second portion of the problem and the results from the previous section have already indicated that combinations of red and near-infrared data may help in estimating biomass. Two such combinations described previously are the perpendicular vegetation index (PVI) and the transformed vegetation index (TVI).

In spite of the difference in the sensor wavelength regions, the soil regression lines for both Guymon and Dalhart data sets were quite similar. Consequently, it was felt PVI and TVI were reasonably comparable at Guymon and Dalhart. The equations used to calculate PVI at Guymon and Dalhart were

$$PVI = \sqrt{(RG5 - Z15)^2 + (RG7 - Z25)^2} \quad (16)$$

$$RG5 = (0.176 * Z15) + (0.381 * Z25) \quad (17)$$

$$RG7 = (0.381 * Z15) + (0.825 * Z25) \quad (18)$$

where Z15 is the scene radiance from band 9 at Guymon or band 3 at Dalhart, and Z25 is the scene radiance from band 8 at Guymon or band 5 at Dalhart. Both combinations were strongly related to total biomass at Dalhart (Figure 26) with PVI showing slightly greater sensitivity at higher biomass levels. Due to the higher sensitivity and strong relationship to biomass, PVI was used as the basic combination which

TABLE 9. Dalhart stepwise classification regression equations using (a) all NS001 band (Ch) data and (b) all NS001 data plus scatterometer data (40° look angle) [Crop Type: 10 = corn, 8 = sorghum, 6 = weeds, 4 = bare soil and weeds, 3 = pasture, 2 = wheat stubble, 1 = bare soil].

	<u>R²</u>
(a) Crop Type = $-(Ch3*1.99)+(Ch4*0.71)+3.03$	0.94
Crop Type = $(Cn2*1.78)-(Ch3*3.60)+(Ch4*0.60)+3.26$	0.95
Crop Type = $(Ch2*1.90)-(Ch3*3.66)+(Ch4*0.63)-(Ch5*0.07)+3.26$	0.95
Crop Type = $(Ch2*1.97)-(Ch3*3.69)+(Ch4*0.60)-(Ch6*0.05)+(Ch7*0.11)+3.31$	0.95
Crop Type = $-(Ch1*0.04)+(Ch2*1.87)-(Ch3*3.67)+(Ch4*0.60)-(Ch6*0.05)+(Ch7*0.12)+3.35$	0.95
(b) Crop Type = $(Ch7*1.08)+(Ch5*1.44)+3.38$	0.96
$-(Ch3*2.07)+(Ch4*0.65)+3.85$	0.95
$-(Ch3*1.25)+(Ch5*1.39)-(Ch7*0.60)+3.06$	0.97
Crop Type = $(Ch2*2.03)-(Ch3*3.90)+(Ch4*0.54)+3.83$	0.96
$(Ch2*1.84)-(Ch3*2.33)+(Ch5*1.19)-(Ch7*0.77)+3.33$	0.97
Crop Type = $-(Ch3*2.35)+(Ch4*0.63)-(L \text{ band cross pole} *0.13)+(C \text{ band like pole}*0.13)+0.88$	0.96
$-(Ch3*0.73)-(Ch4*0.56)+(Ch5*2.33)-(Ch7*0.96)$	0.98
Crop Type = $(Ch2*2.38)-(Ch3*4.34)+(Ch4*0.55)+(L \text{ band like pole}*0.15)-(L \text{ band cross pole}*0.15)+2.39$	0.96
$+(C \text{ band like pole}*0.13)+4.22$	
Crop Type = $(Ch2*1.73)-(Ch3*3.83)+(Ch4*0.55)+(L \text{ band like pole}*0.14)-(L \text{ band cross pole}*0.19)+(C \text{ band like pole}*0.07)$	0.98
$(Ch1*4.20)-(Ch3*0.91)-(Ch4*1.13)+(Ch5*3.82)-(Ch6*0.58)-(Ch7*0.92)+2.71$	0.96

TABLE 10. Guymon stepwise classification regression equations using (a) only visible/infrared data and (b) scatterometer (40° look angle) and visible/infrared data [Crop Type: 8=sorghum, 4=alfalfa, 0=bare soil].

	<u>R²</u>
(a) Crop Type = (M ² SCh 4*17.350)-(M ² SCh 7*14.76)- (M ² SCh 8*1.30)+2.85	0.59
(b) Crop Type = (P band cross pole*0.26)+(C band cross pole*0.49)+26.147	0.67
Crop Type = (P band cross pole*0.27)-(C band like pole*0.57)+(C band cross pole*0.88)+28.07	0.73
Crop Type = (L band cross pole*0.25)+(L band cross pole *0.23)-(C band like pole*0.76)+(C band cross pole*0.80)+28.22	0.74
Crop Type = (K band like pole*0.30)+(L band cross pole *0.29)+(P band cross pole*0.18)-(C band like pole*0.89)+(C band cross pole*0.74)+27.39	0.75
Crop Type = (M ² S1Ch5*0.27)+(K band like pole*0.32)+(L band cross pole*0.32)+(P band cross pole*0.17)-(C band like pole*0.81)+(C band cross pole*0.60)+24.2	0.76

ORIGINAL PAGE IS
OF POOR QUALITY

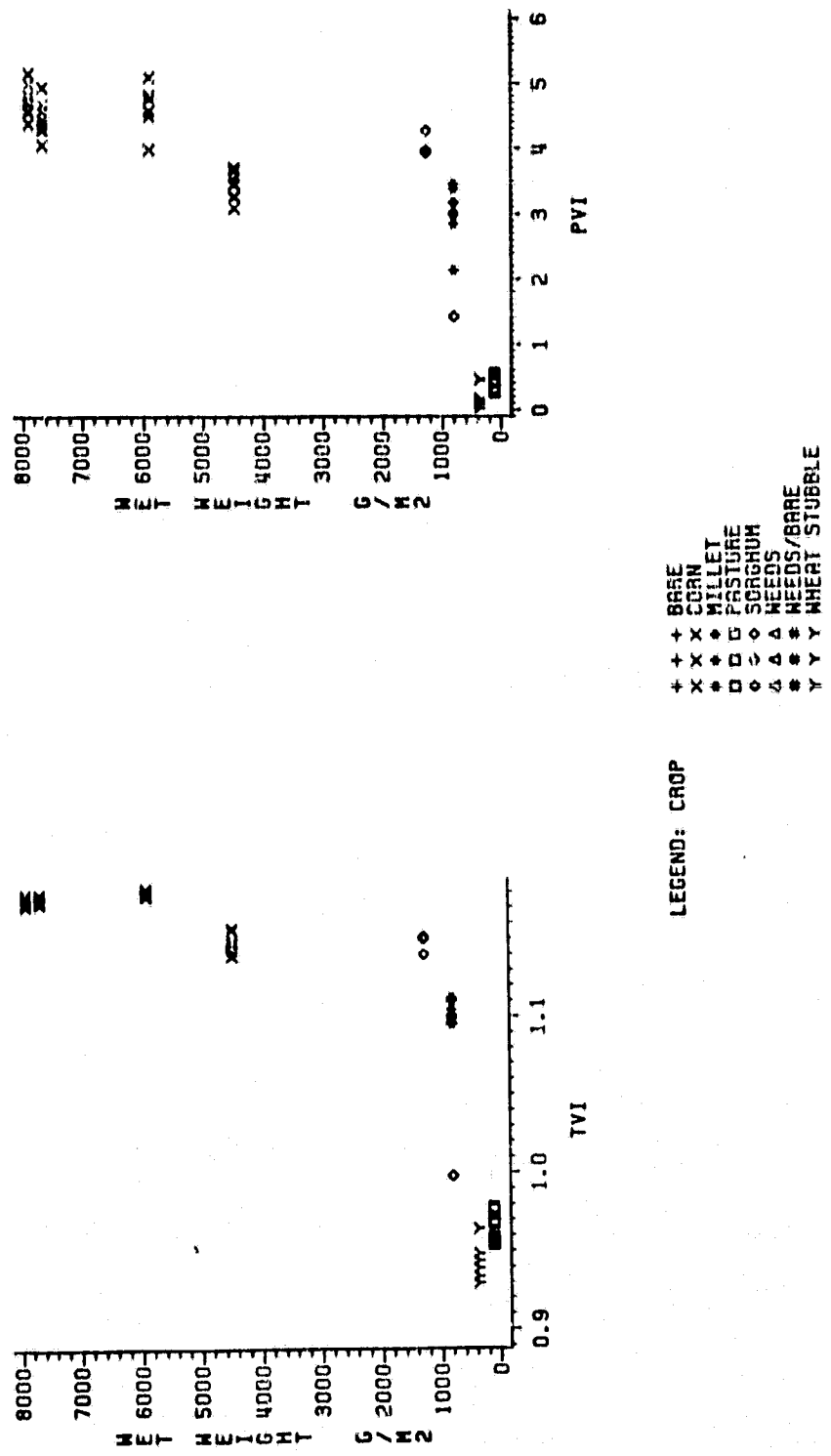


FIG. 26 The relationship between total biomass (g/m²), and TVI and PVI at Dalhart.

other combinations were compared. However, the "saturated" zone of PVI and TVI, where sensitivity decreased for moderate biomass changes, was at biomass levels above 1000 g/m².

The relationship between PVI, TVI and crop yield is less significant than the relationship to biomass due a dependence on crop type (Figure 27). This dependency is expected because the economic or grain yield comprises a different proportion of the biological or vegetative yield for each crop type.

With the additional narrow wavelength bands for the NS001, a study of the intercorrelations between bands was needed to evaluate other potential visible/infrared combinations. Figures 28 through 36 display intercorrelations of each NS001 band to bands 1, 2 and 3. The relationship between band 4 and 6 (1.00-1.30 μm and 1.55-1.75 μm) (Figure 33) was similar to the visible/near infrared relationship, which PVI is based. All of the bare soil and low biomass fields fell along the lower right line; corn and dense sorghum fields fell along the left side of the line. The relationship suggested another possible PVI relationship using a near-infrared band and a water absorption band. The equations used to calculate the new PVI were

$$\text{PVI64} = \sqrt{(\text{RG4} - \text{Z20})^2 + (\text{RG6} - \text{Z35})^2} \quad (19)$$

$$\text{RG4} = -1.919 + 0.365(\text{Z35}) + 0.158(\text{Z20}) \quad (20)$$

$$\text{RG6} = 0.831 + 0.842(\text{Z35}) + 0.365(\text{Z20}) \quad (21)$$

where Z20 is the scene radiance in NS001 band 4 and Z35 is the scene radiance in NS001 band 6. A plot of the new PVI versus total biomass is shown in Figure 37. A definite similarity exists between the conventional PVI and PVI64. A plot of the two combinations revealed

ORIGINAL PAGE IS
OF POOR QUALITY.

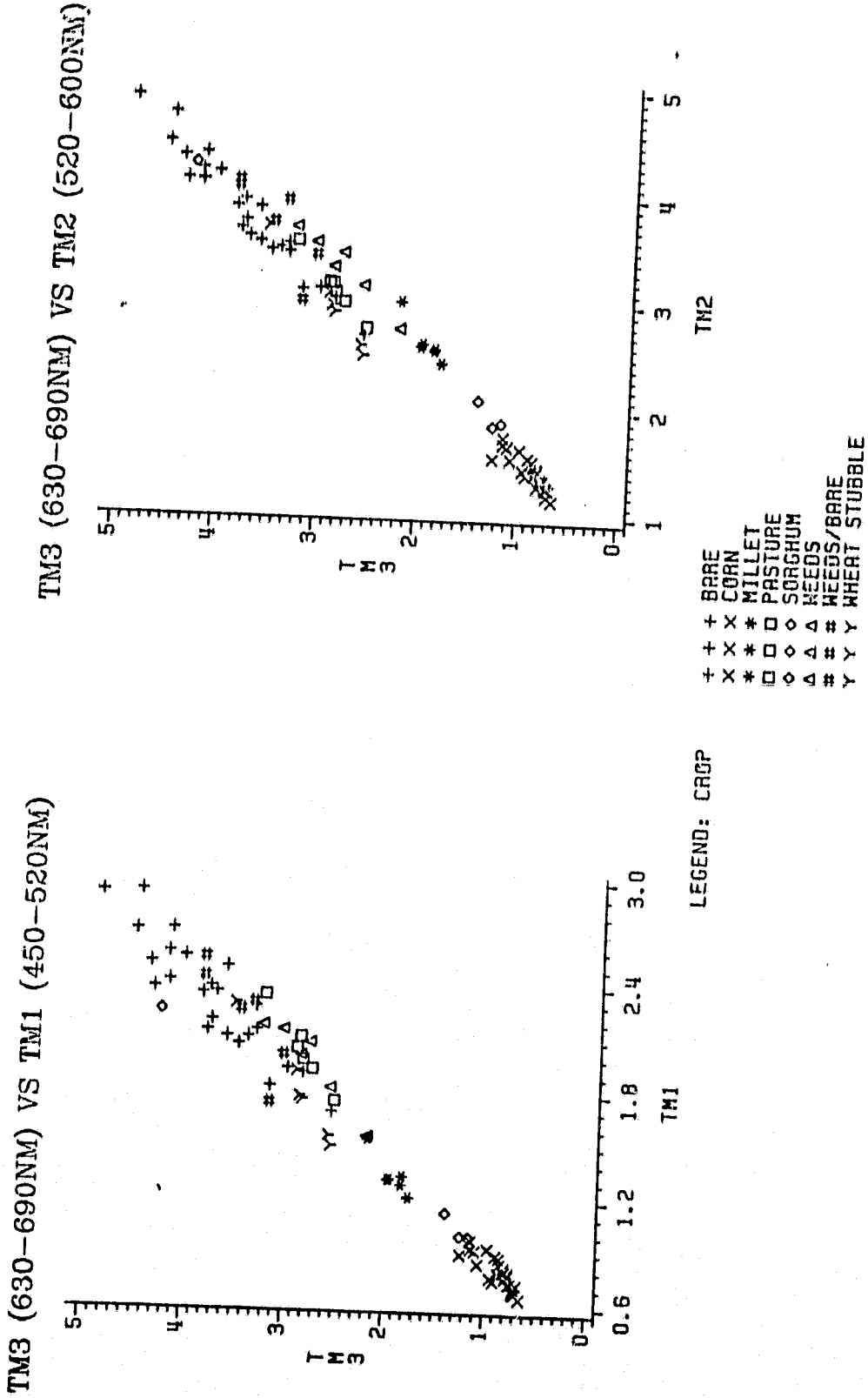
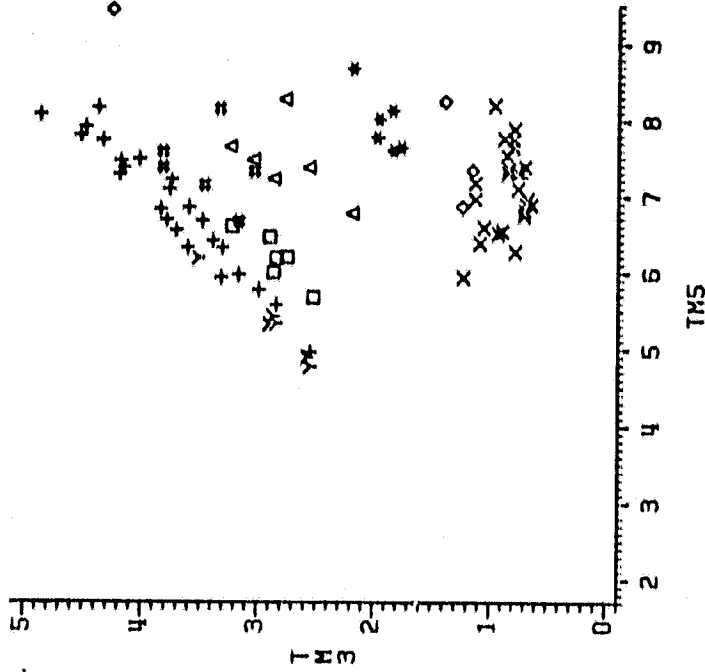


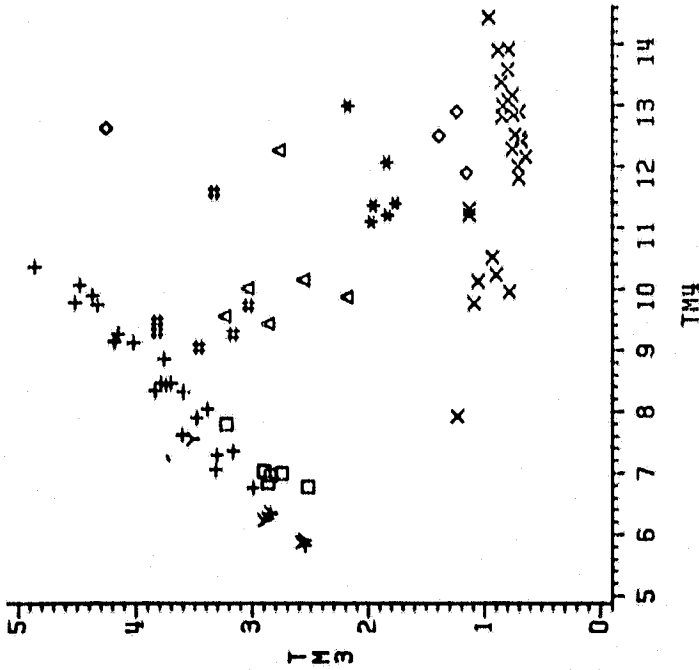
FIG. 28 Field radiance reflectance values of NS001 bands 1 and 2 versus band 3 at Dalhart in 10^{-4} watts $cm^{-2} ster^{-1}$.

ORIGINAL PAGE IS
OF POOR QUALITY

TM3 (630-690NM) VS TM5 (1000-1300NM)



TM3 (630-690NM) VS TM4 (760-900NM)

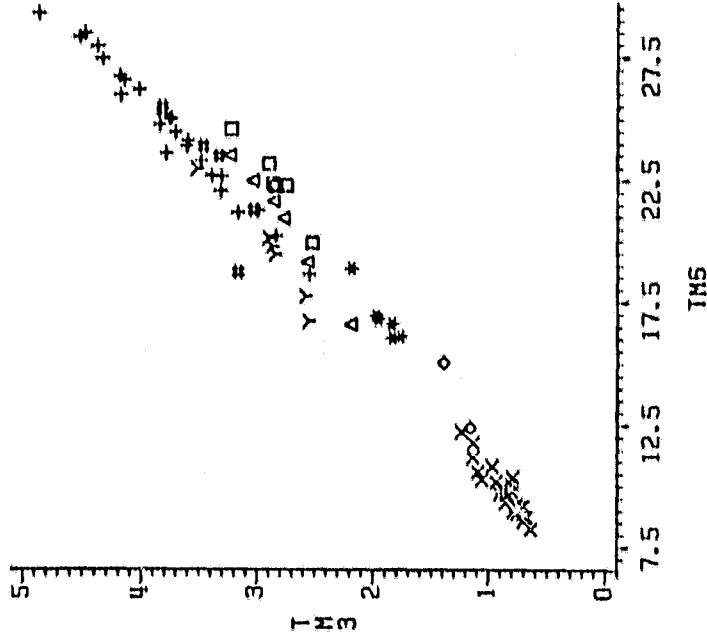


- LEGEND: CROP
- + BARE
 - x CORN
 - * MILLET
 - o PASTURE
 - o SORGHUM
 - # NEEDS/BARE
 - y WHEAT/STUBBLE

LEGEND: CROP

FIG. 29 Field radiance reflectance values of NS001 bands 4 and 5 versus band 3 at Dalhart in 10^{-4} watts cm^{-2} ster^{-1} .

TM3 (630-690NM) VS TM6 (1550-1750NM)



TM3 (630-690NM) VS TM7 (2300-2500NM)

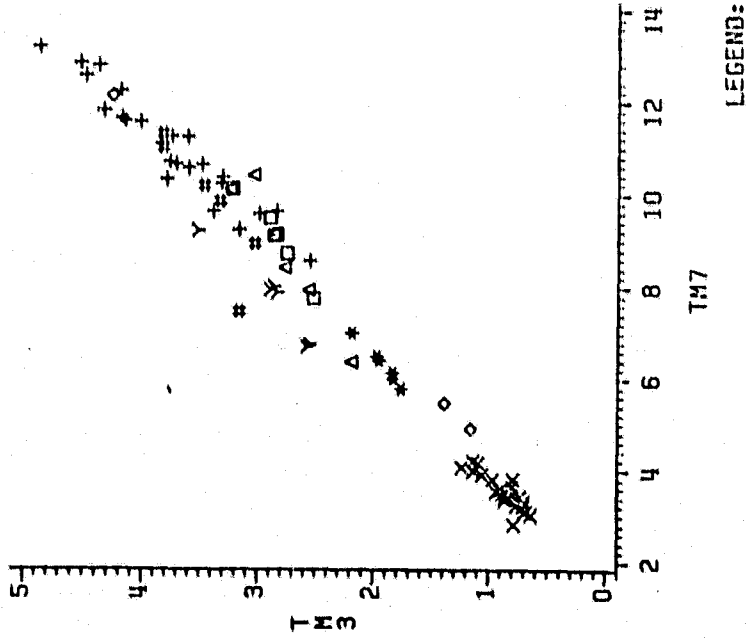
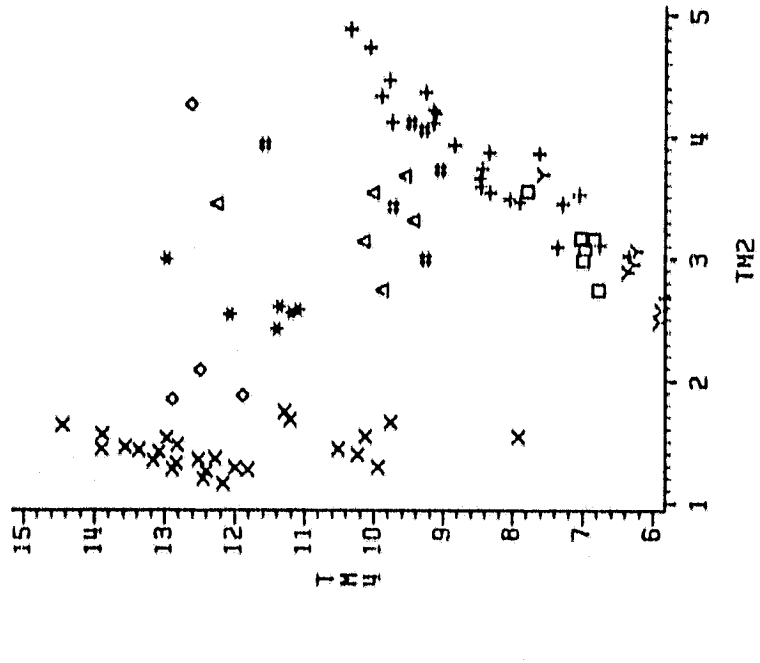
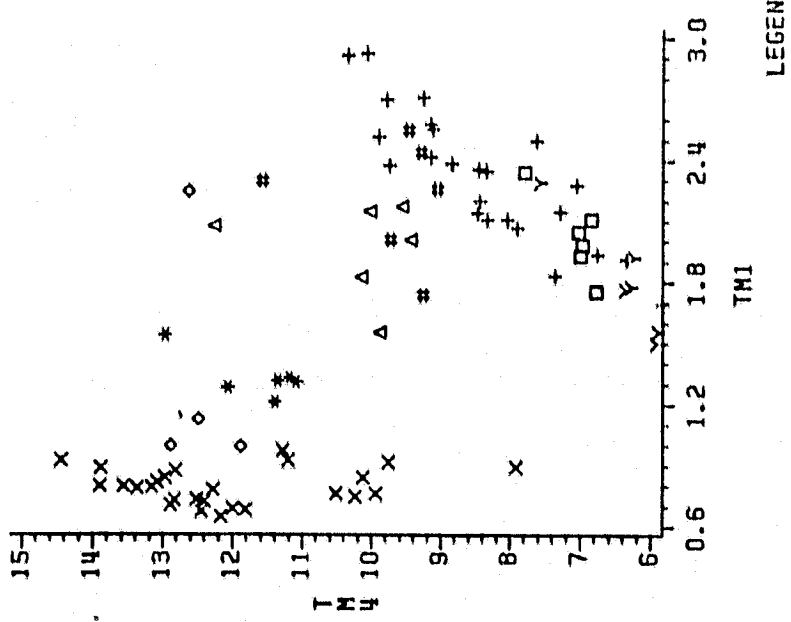


FIG. 30 Field radiance reflectance values of NS001 bands 6 and 7 versus band 3 at Dalhart in 10^{-4} watts $cm^{-2} ster^{-1}$.

TM4 (760-900NM) VS TM2 (520-600NM)



TM4 (760-900NM) VS TM1 (450-520NM)



LEGEND: CROP

- + BARE
- x CORN
- * MILLET
- o PASTURE
- square SORGHUM
- triangle WHEEDS
- # WHEEDS/BARE
- y WHEAT STUBBLE

FIG. 31 Field radiance reflectance values of NS001 bands 1 and 2 versus band 4 at Dalhart in 10^{-4} watts cm^{-2} $ster^{-1}$.

ORIGINAL PAGE IS
OF POOR QUALITY

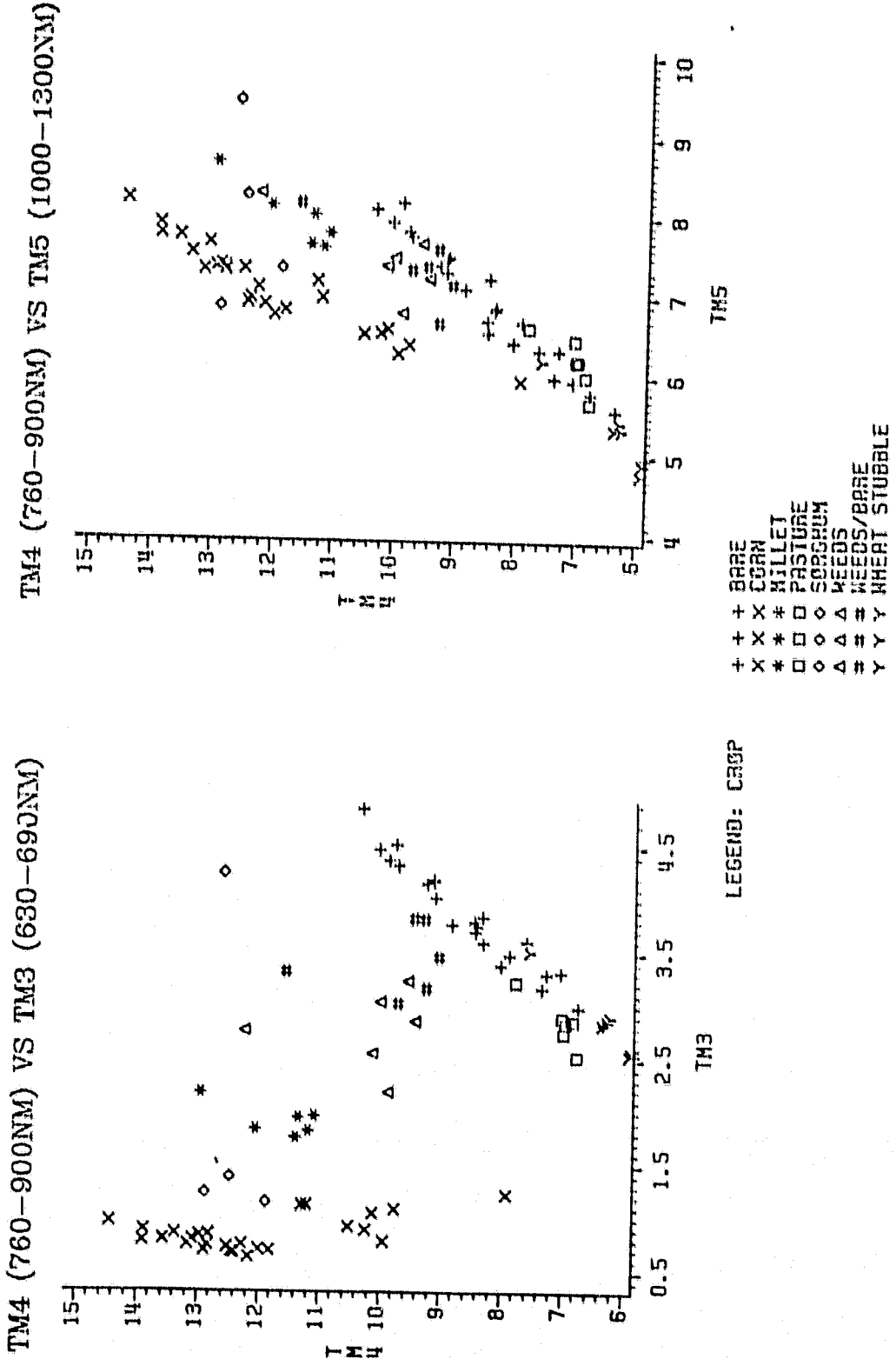
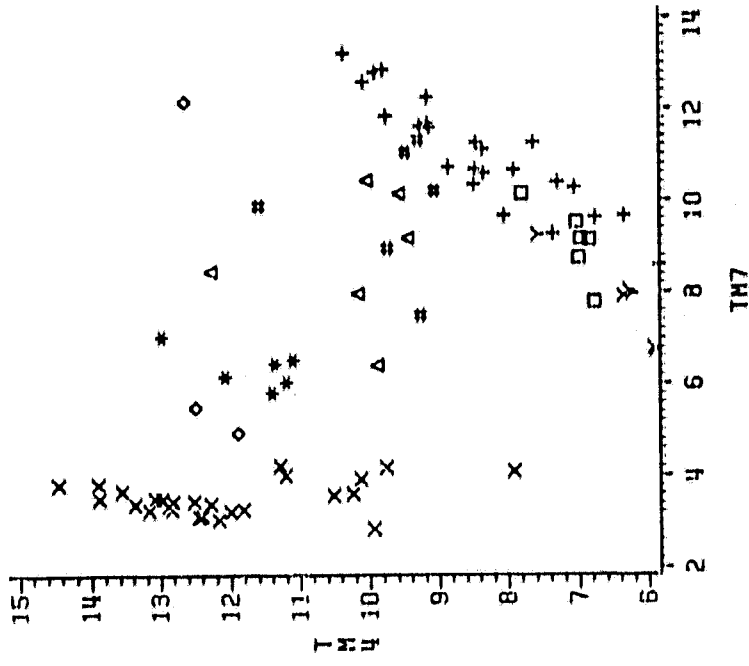
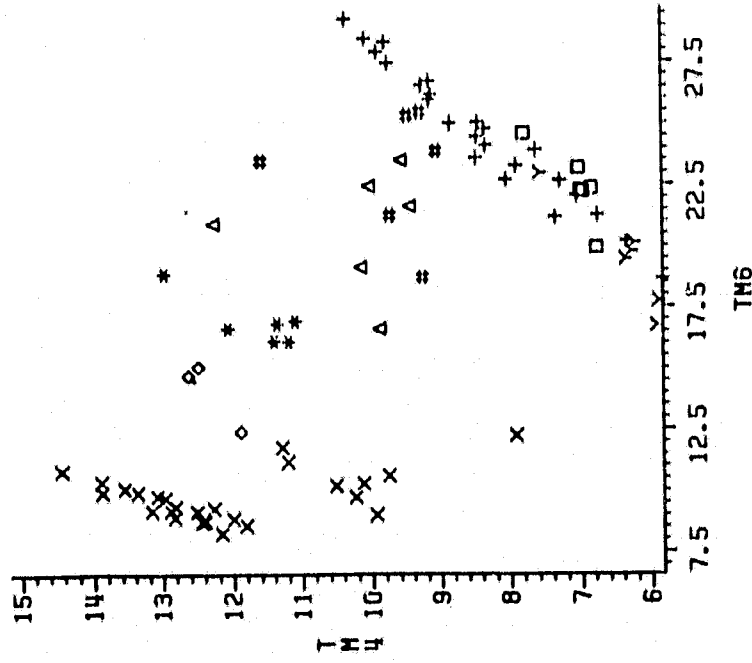


FIG. 32 Field radiance reflectance values of NS001 bands 3 and 5 versus band 4 at Dalhart in 10^{-4} watts cm^{-2} $ster^{-1}$.

TM4 (760-900NM) VS TM7 (2300-2500NM)



TM4 (760-900NM) VS TM6 (1550-1750NM)



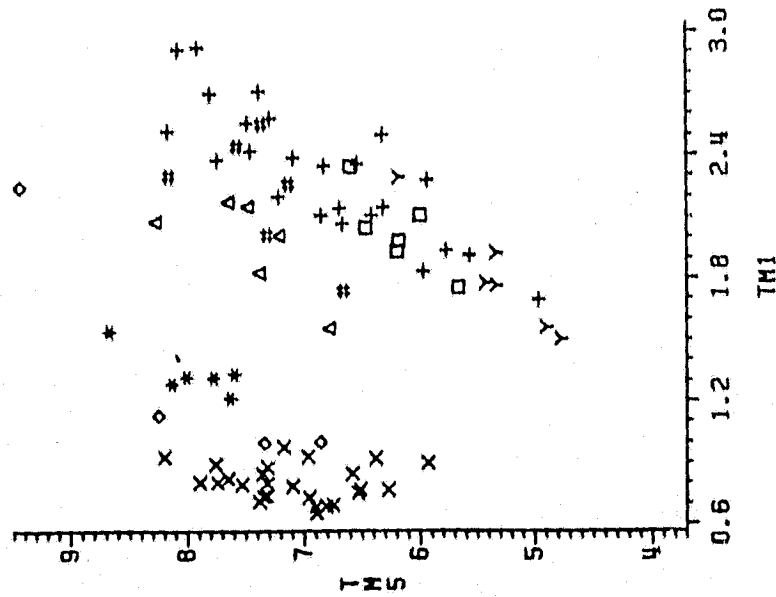
LEGEND: CROP

+	+	+	+	+	+	+	+	+	+
x	x	*	*	*	*	*	*	*	*
o	o	o	o	o	o	o	o	o	o
Δ	Δ	Δ	Δ	Δ	Δ	Δ	Δ	Δ	Δ
#	#	#	#	#	#	#	#	#	#
Y	Y	Y	Y	Y	Y	Y	Y	Y	Y

+ BARE
 x CORN
 * HILLET
 o PASTURE
 Δ SCORCH
 # NEEDS
 Y WHEAT/ROBE
 WHEAT STUBBLE

FIG. 33 Field radiance reflectance values of NS001 bands 6 and 7 versus band 4 at Dalhart in 10^{-4} watts cm^{-2} ster $^{-1}$.

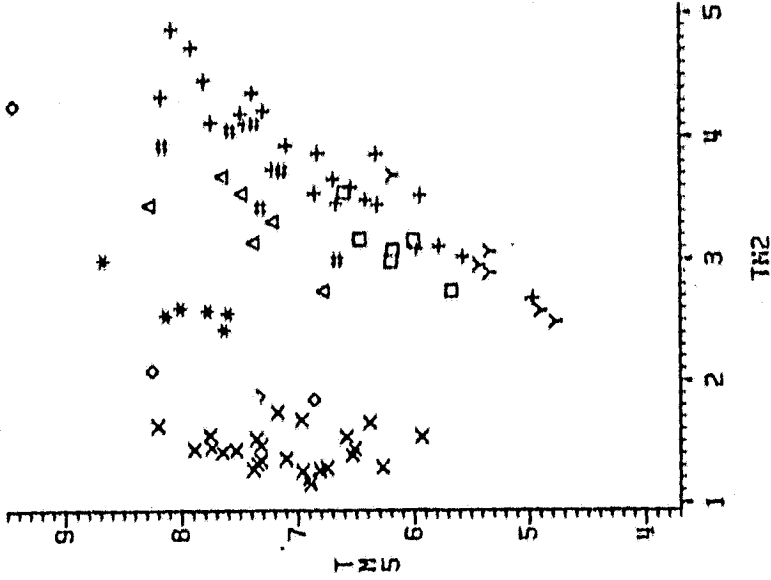
TM5 (1000-1300NM) VS TM1 (450-520NM)



LEGEND: CROP

- + BARE
- x CORN
- * MILLET
- o PASTURE
- Δ SORGHUM
- # NEEDS/BARE
- Y WHEAT STUBBLE

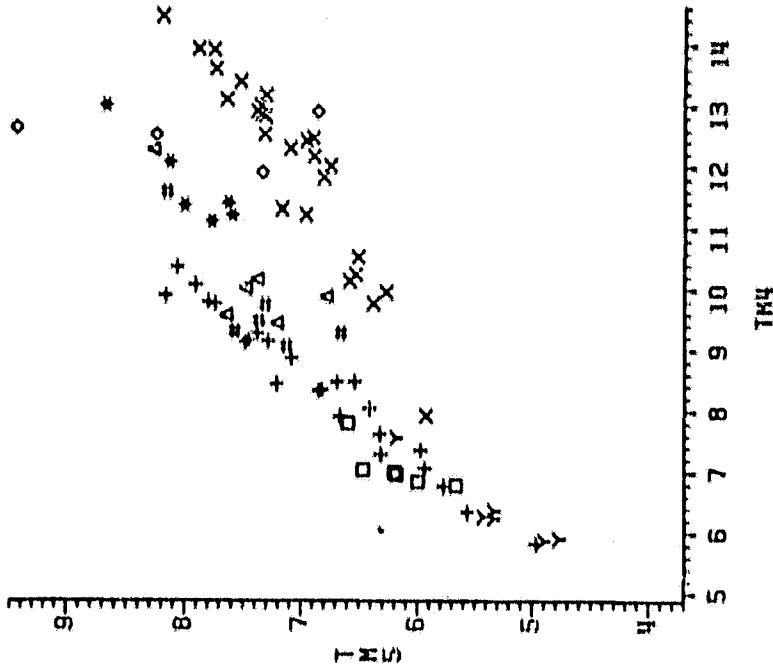
TM5 (1000-1300NM) VS TM2 (520-600NM)



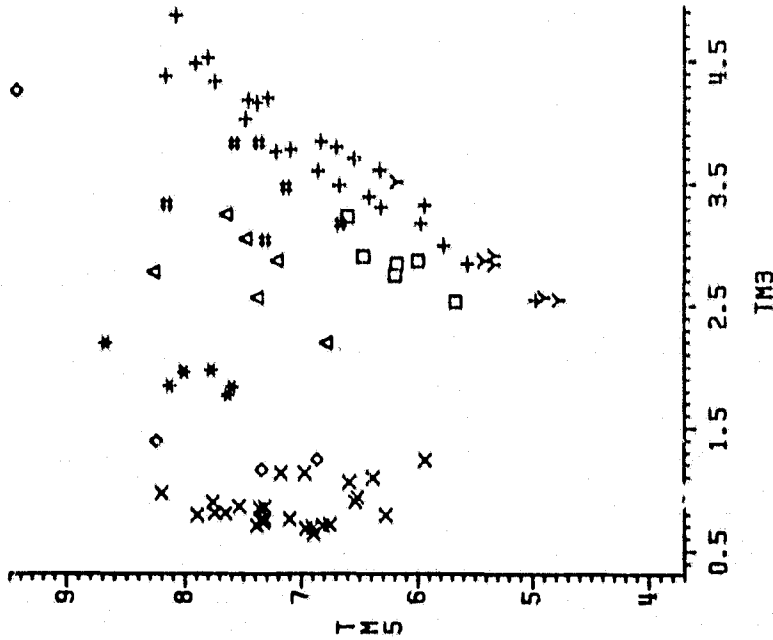
FIELD QUALITY

FIG. 34 Field radiance reflectance values of NS001 bands 1 and 2 versus band 5 at Dalhart in 10^{-4} watts cm^{-2} $ster^{-1}$.

TM5 (1000-1300NM) VS TM4 (760-900NM)



TM5 (1000-1300NM) VS TM3 (630-690NM)

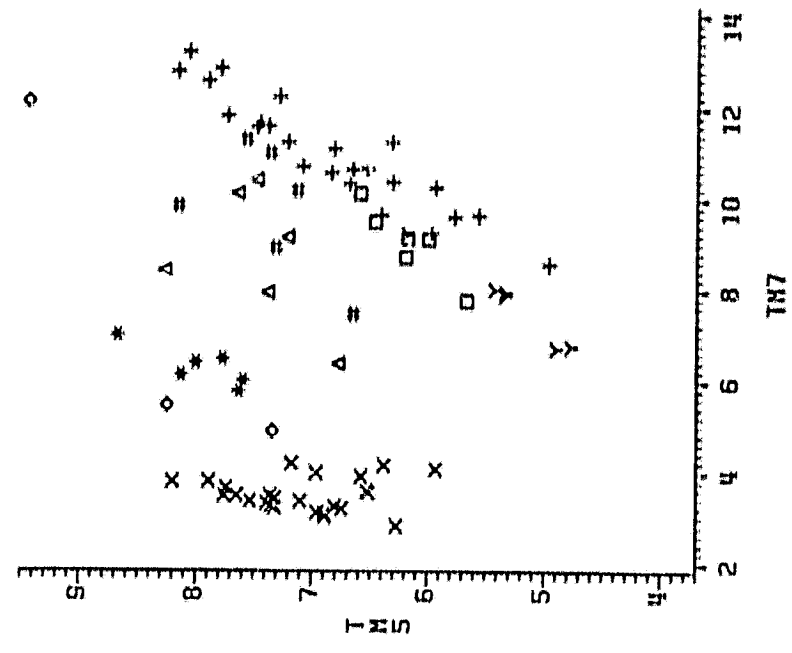


- LEGEND: CROP
- + BARE
 - x x CORN
 - * * MILLET
 - o o PASTURE
 - o o SORGHUM
 - Δ Δ WEEDES
 - # # WEEDES/BARE
 - y y WHEAT STUBBLE

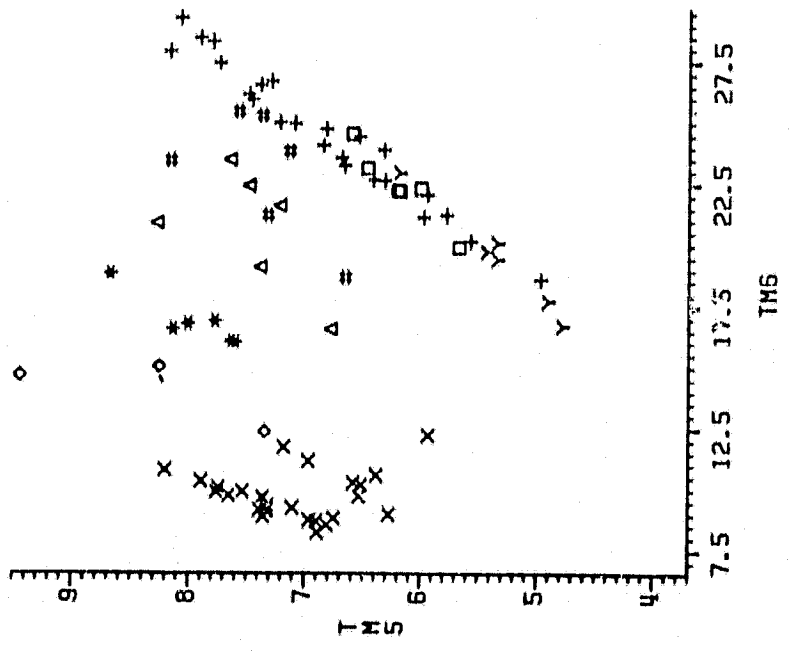
FIG. 35 Field radiance reflectance values of NS001 bands 3 and 4 versus band 3 at Dalhart in 10^{-4} watts cm^{-2} $ster^{-1}$.

ORIGINAL COPY OF POOR QUALITY

TM5 (1000-1300NM) VS TM7 (2300-2500NM)



TM5 (1000-1300NM) VS TM6 (1550-1750NM)



- LEGEND: CROP
- + BARE
 - x CGAN
 - * MILLET
 - o PASTURE
 - Δ SORGHUM
 - ≡ WEEDS/#
 - Y WHEAT STUBBLE

FIG. 36 Field radiance reflectance values of NS001 bands 6 and 7 versus band 5 at Dalhart in 10^{-4} watts cm^{-2} $ster^{-1}$.

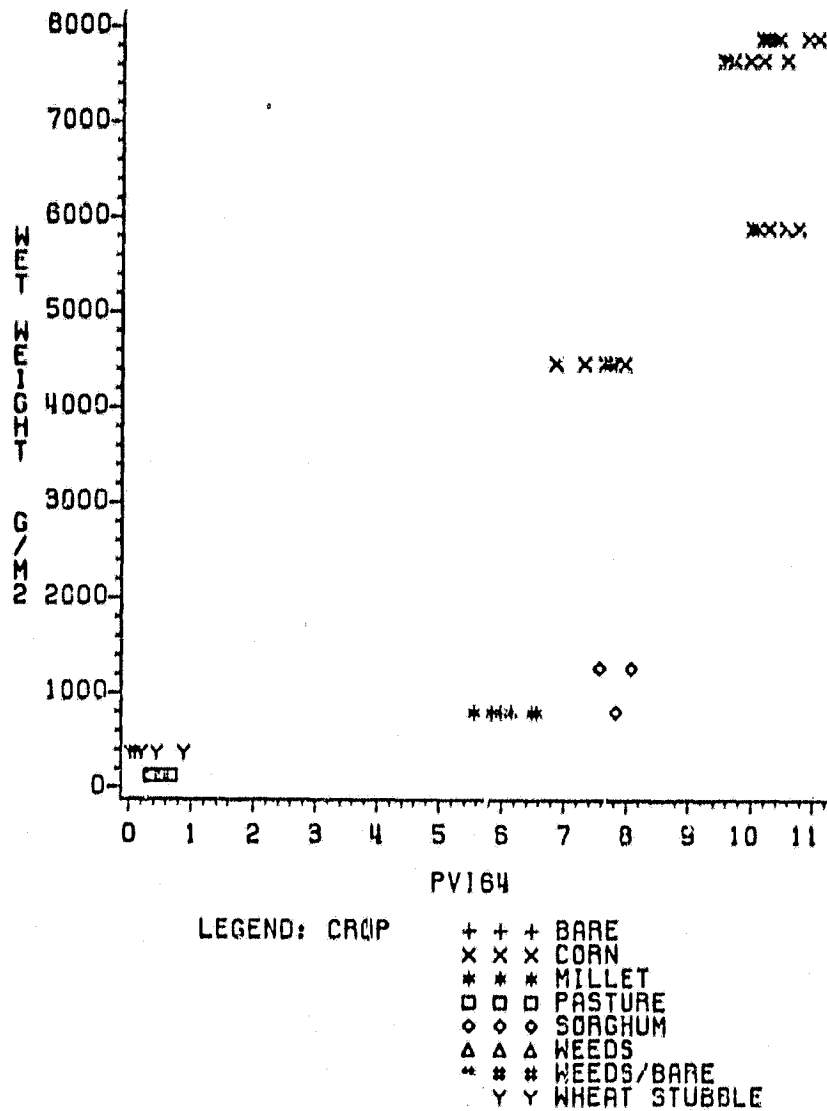


FIG. 37 The relationship between total (wet) biomass (g/m²) and PVI64 at Dalhart.

the new PVI (PVI64) gave more information on corn fields compared to PVI and TVI--corn gave a higher PVI64 compared to PVI and TVI (Figure 38). Not enough ground data were collected to explain this PVI difference.

Figures 39 through 41 demonstrate the variability of PVI64 within corn, alfalfa and sorghum fields at Dalhart. The most striking example was the detection of moisture stressed areas in corn fields 1 and 2. The severely stressed ring-shaped areas within the field are demonstrated by the red color which corresponded to PVI64 values of 4 or less. Dark green areas represent healthy areas within the field with PVI64 values of 6 or greater. Biomass differences are also evident in several alfalfa and sorghum fields.

Summarizing, spectral data from Dalhart suggested the additional proposed thematic mapper wavelength regions provided slightly more information on crop characteristics than present techniques using visible/infrared data.

As mentioned, a normalization technique applied to the active microwave data was needed to help remove roughness and soil moisture effects in the Guymon and Dalhart data sets. Based on the σ^0 response with look angle, as biomass increases, the vegetative response at high look angles should also increase compared to the σ^0 response from the lower look angles. This was especially noted in the line plots (Figures 19 and 20). Figure 42 demonstrates this effect for L band cross pole data from corn (high biomass) and bare soil (low biomass). Biomass differences were strongly evident at the larger look angles, especially greater than 15° off nadir. Figure 43 represents changes in the L band cross pole σ^0 due to soil moisture differences within a

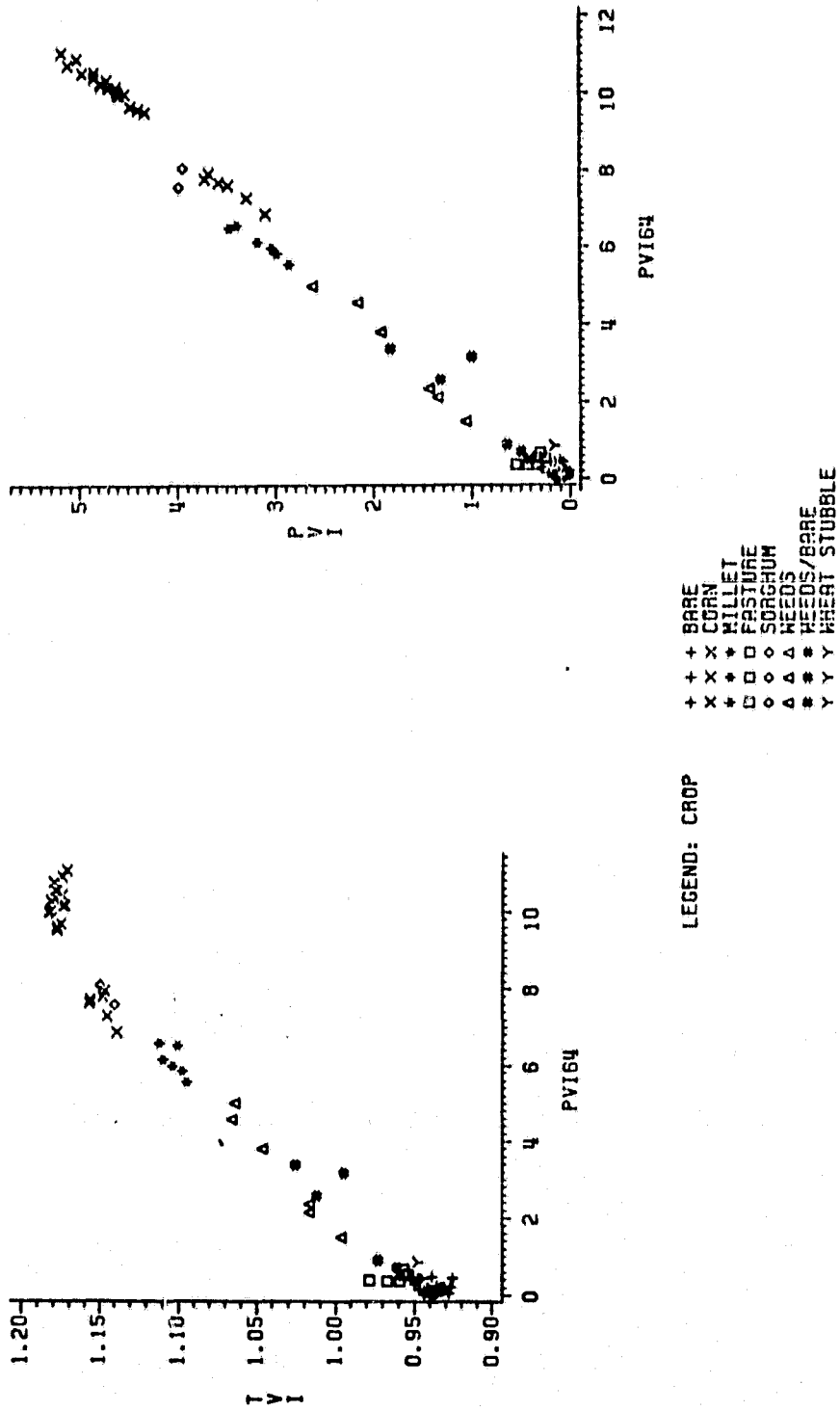


FIG. 38 The relationship between PVI64, and PVI and TVI at Dalhart.

ORIGINAL PAGE
BLACK AND WHITE PHOTOGRAPH

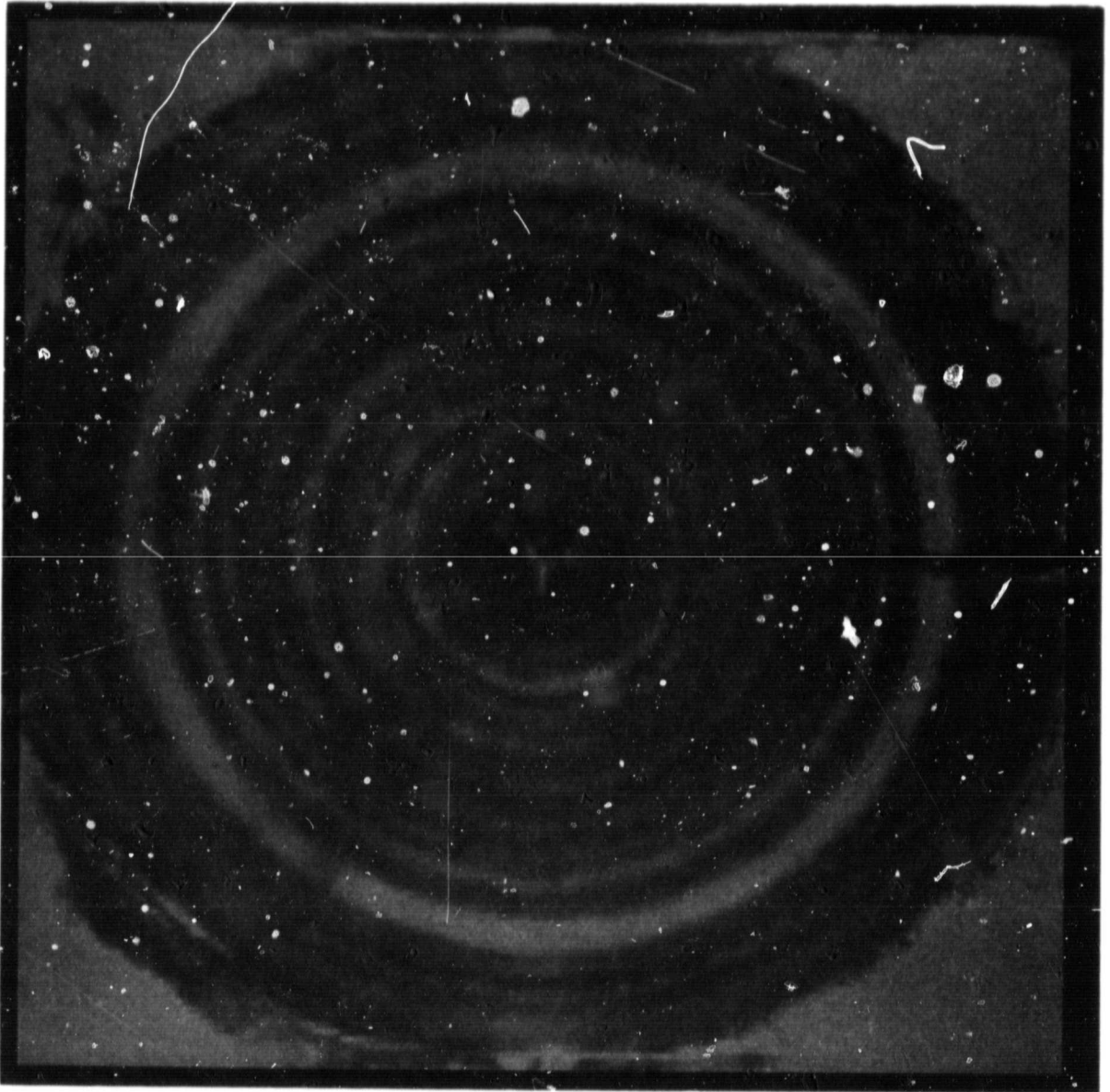


FIG. 39 A photo indicating difference PVI64 levels within a stressed corn field (1 and 2) at Dalhart.

ORIGINAL PAGE
BLACK AND WHITE PHOTOGRAPH

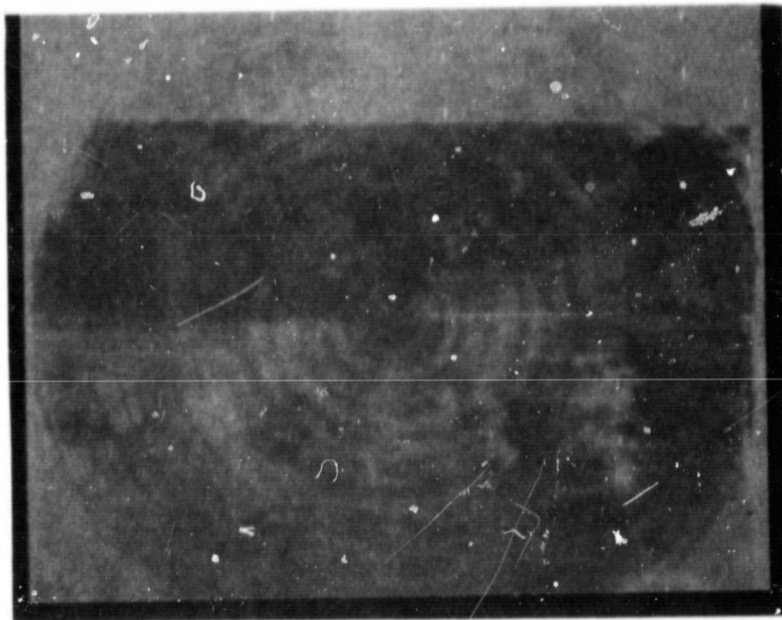


FIG. 40 A photo indicating difference PVI64 levels within a sorghum field (V2) at Dalhart.

ORIGINAL PAGE
BLACK AND WHITE PHOTOGRAPH

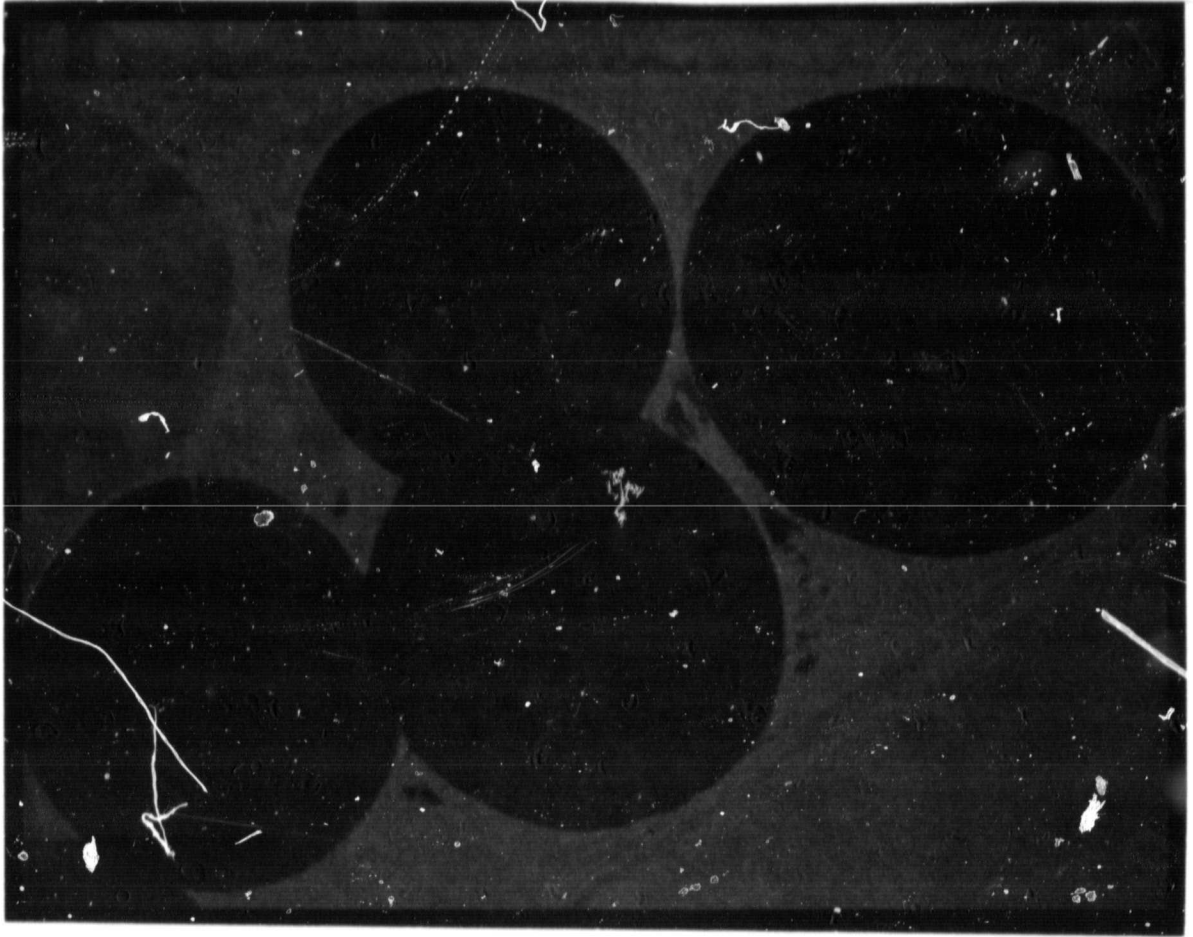


FIG. 41 A photo indicating different PVI64 levels within alfalfa fields (V11, V12, V13) at Dalhart.

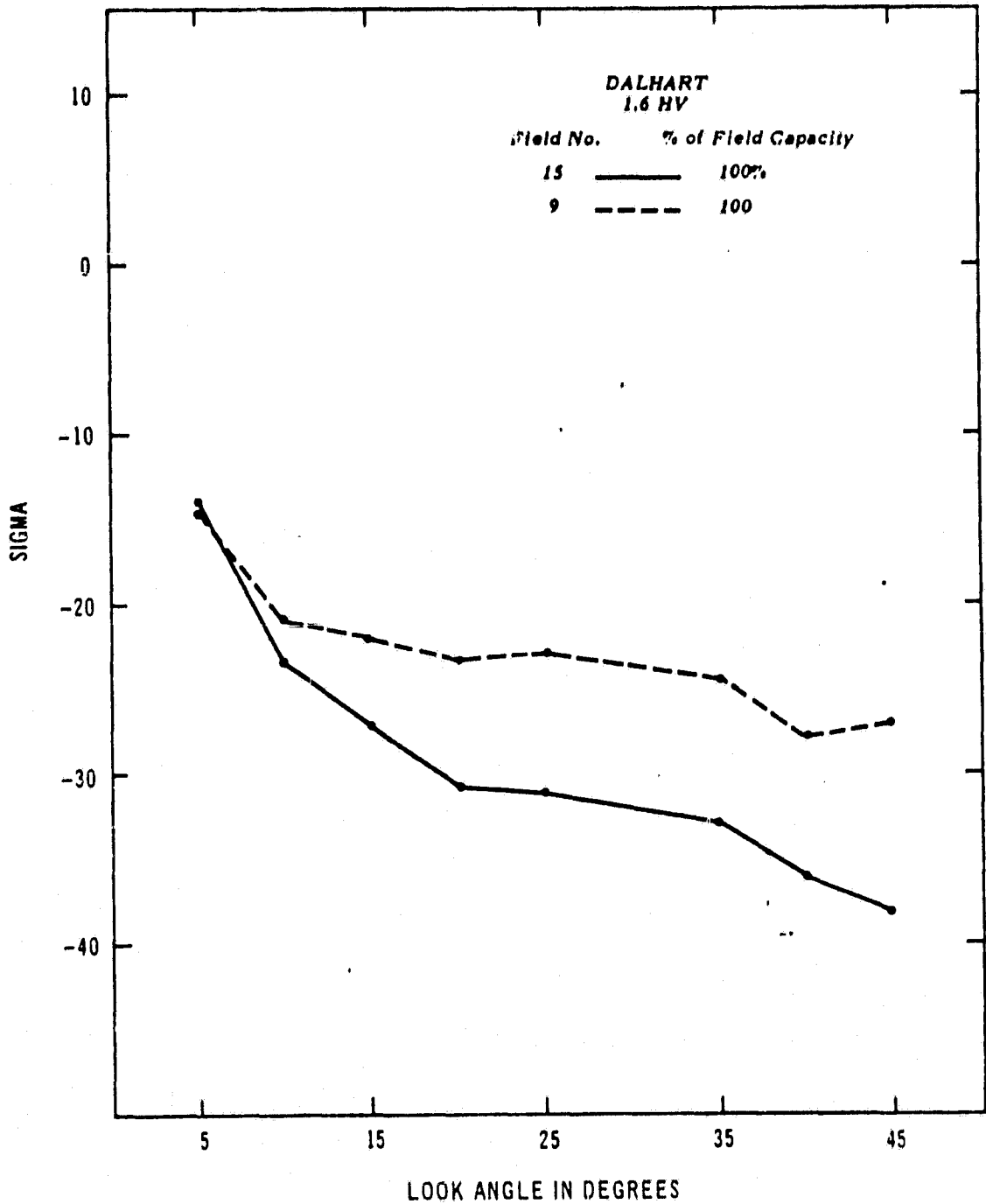


FIG. 42 The relationship between L band cross pole σ^0 and look angle for a corn field (field 9) and bare field (field 15).

ORIGINAL PAGE IS
OF POOR QUALITY

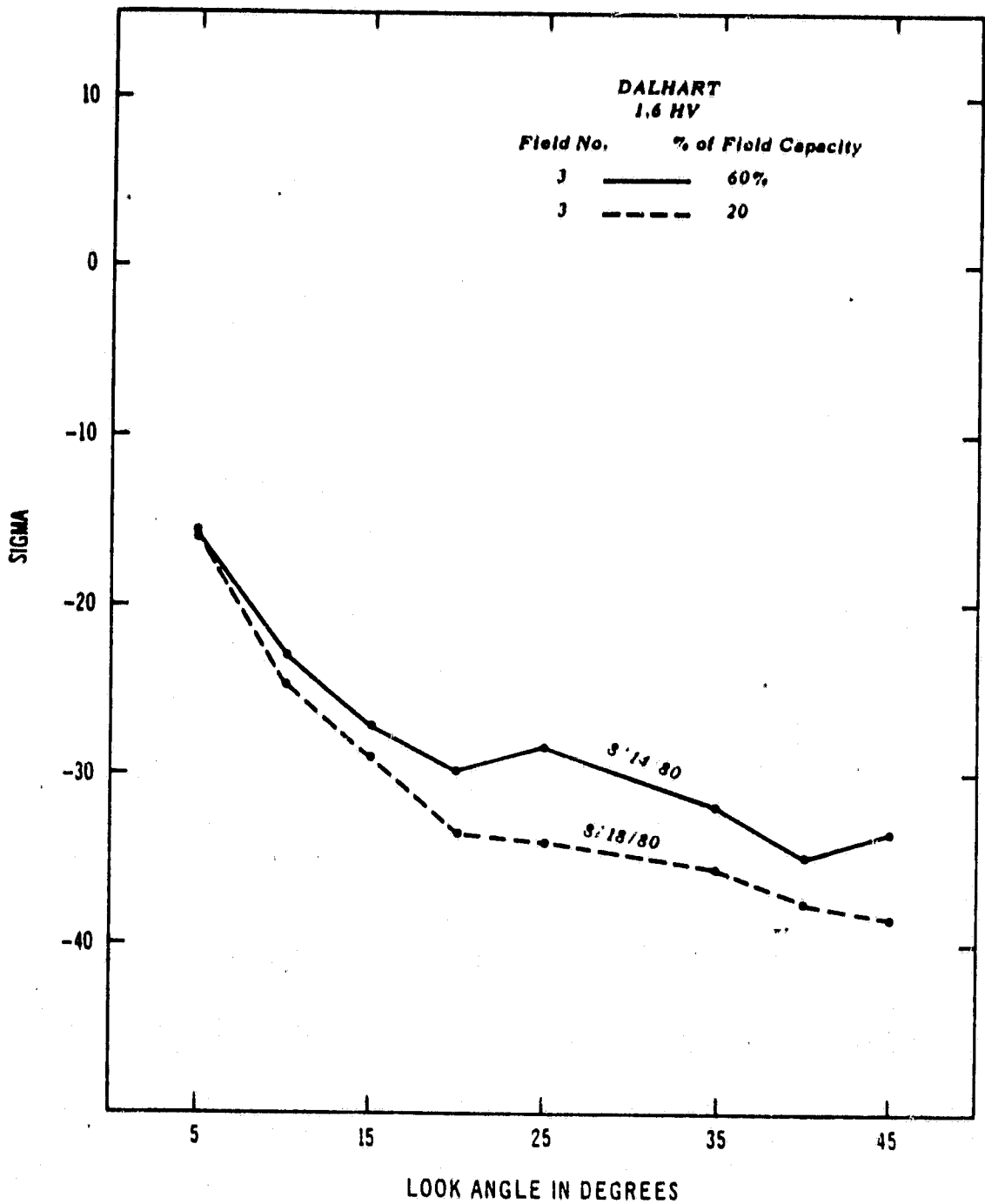


FIG. 43 The relationship of L band cross pole σ^0 and look angle for a millet field (field 3) under different soil moisture conditions.

millet field at Dalhart. Any significant soil moisture increase caused a similar response as the biomass increased. However, by calculating the difference between the response from a large and small look angle, the soil moisture effect was diminished while maintaining a high degree of sensitivity to biomass differences. For example, the difference between the 40° and 10° look angles was roughly the same under different surface (0-2 cm) moisture conditions, 12.5 dB. The last effect, surface roughness was minimized by analyzing cross rather than like polarized data.

Figure 44 demonstrates active microwave returns from the same sorghum field at two different look directions--rows parallel and perpendicular to the flight line. A general shift higher was evident for the σ^0 return from rows parallel to the look direction. The difference between the near and far look angles also remained relatively constant under different surface roughnesses. Consequently, most of the information in the return differences between a near and far look angle in cross-polarized data was related to crop biomass. Since σ^0 is expressed in terms of logarithms, a difference between σ^0 is the same as an arithmetic ratio (a normalization technique). Also, it was anticipated that comparisons of differences in several frequencies and polarizations indicated biomass differences. Comparison of several differences (i.e. 40° L band cross pole σ^0 - 10° L band cross pole σ^0 ; 40° C band cross pole σ^0 - 5° C band cross pole σ^0) indicated the C band cross pole 40° and C band cross pole 5° difference was most independent of roughness and soil moisture and most sensitive to biomass differences.

ORIGINAL PAGE IS
OF POOR QUALITY

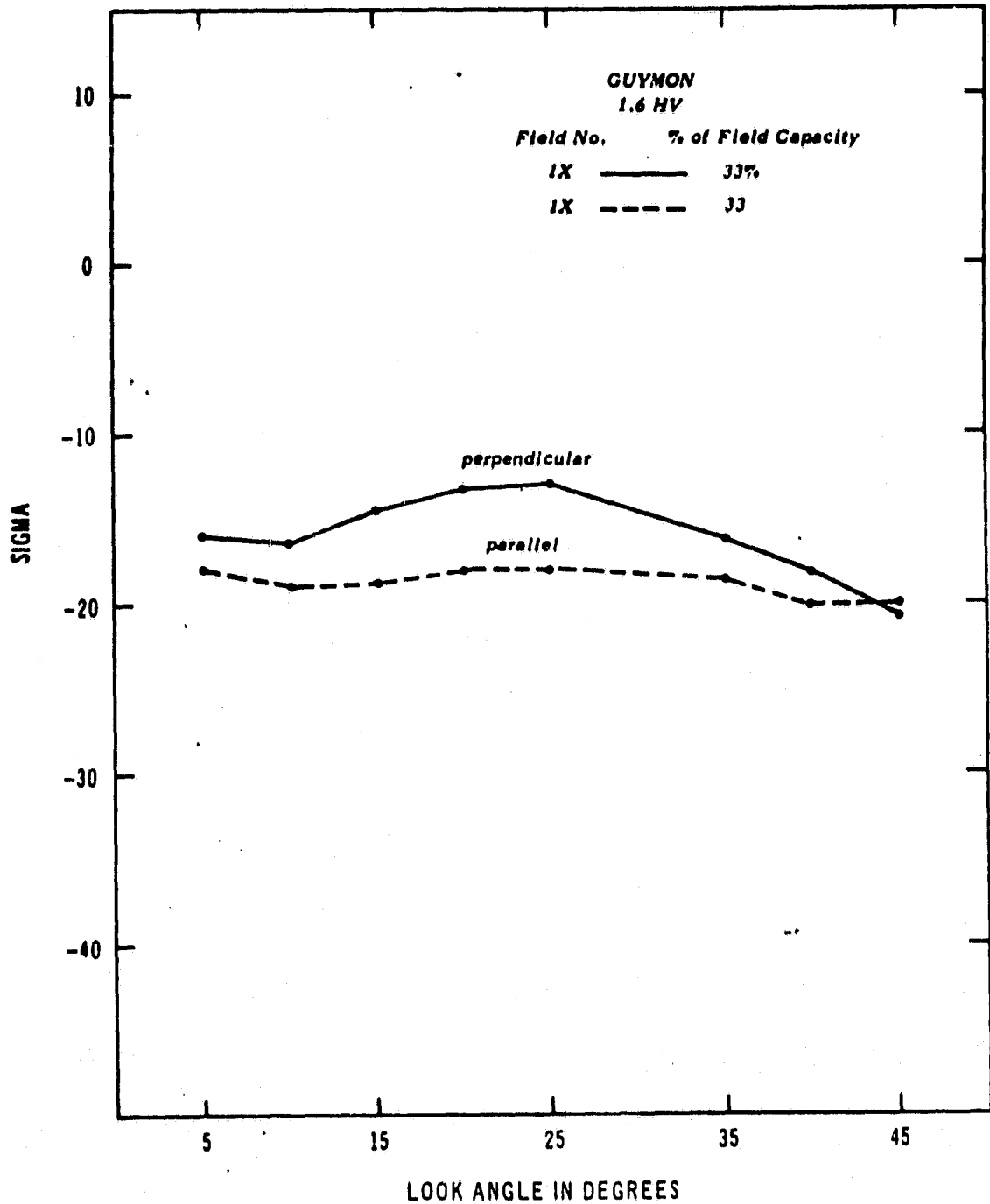


FIG. 44 The L band cross pole σ^0 response as a function of look angle for the same sorghum field (field 1X) from two different directions, the flight line parallel and perpendicular to the tillage direction.

Other differences, such as the L band cross pole difference between the 40° and 10° look angle, were sensitive to surface roughness by penetrating through several alfalfa and sorghum canopies. For example, alfalfa gave the similar index values as bare soil. Consequently, the C band relationship was analyzed and is defined as the scatterometer vegetation index (SVI).

The relationship between SVI and total biomass was similar to the PVI/total biomass relationship (Figure 45). The quadratic relationship between SVI and total biomass ($R^2 = 0.88$) was better than the relationship between PVI and total biomass ($R^2 = 0.74$), or TVI and total biomass ($R^2 = 0.69$). The relationship between PVI, TVI, and SVI was generally linear with bare fields having low SVI and vegetated fields with higher index values (Figures 46 and 47). Alfalfa fields tended to have lower index values compared to the other vegetated fields. The lower value indicated the scatterometer signal was either penetrating through the vegetation and responding to the soil surface, or the signal was responding to the canopy surface only. Changes of SVI within individual fields attributable to soil moisture differences were negligible (Figure 48). At Dalhart, the soil moisture correction factor for bare fields was 2 db/10% change in soil moisture (0% to 100% of field capacity); at Guymon, the factor was 4.5 db/15% change in soil moisture (a change of 80% of field capacity). The effect was also dependent on crop type as SVI values from fields having higher biomass were less dependent on surface soil moisture. Correcting SVI for soil moisture using C band passive microwave brightness temperatures improved the relationship only slightly (Figures 49 and 50). Part of the variance of SVI within each crop type can be explained by

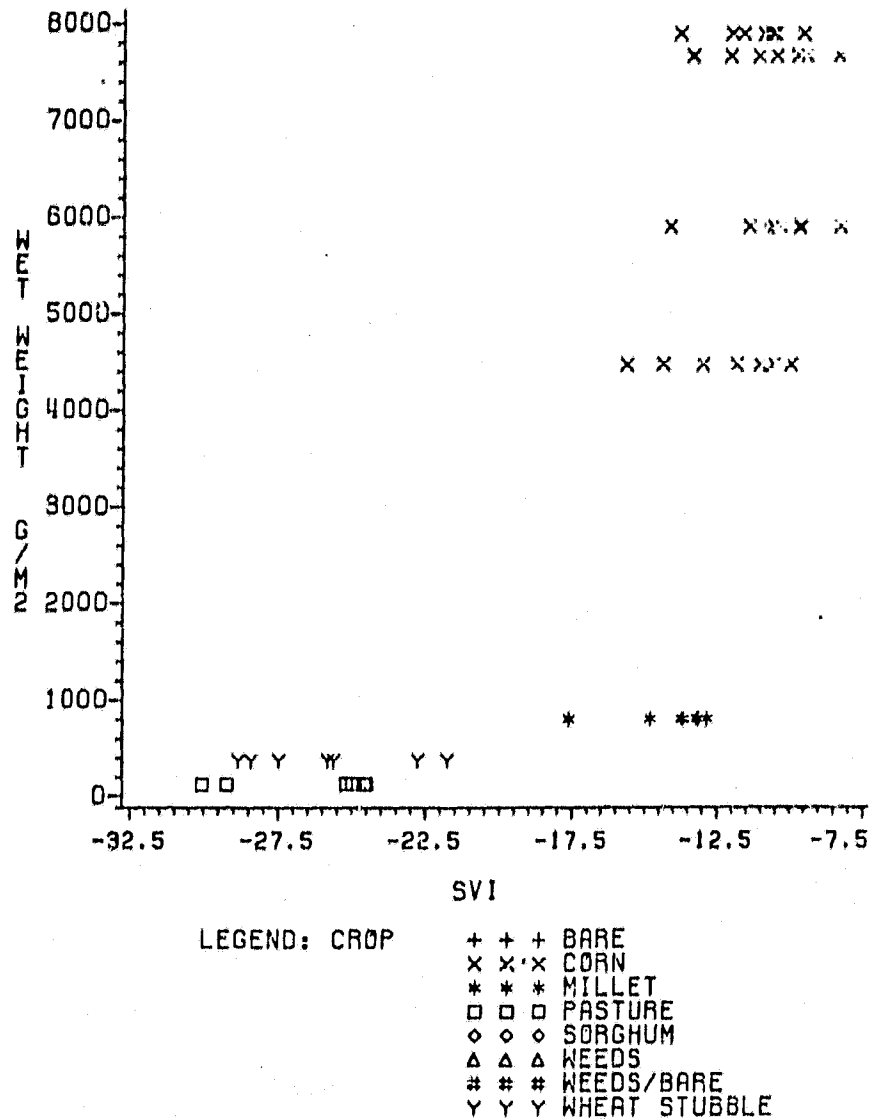


FIG. 45 The relationship between total biomass and the scatterometer vegetation index, SVI. (4.75 HV 40° look angle - 4.75 HV 5° look angle) ($R^2 = 0.88$).

ORIGINAL PAGE IS
OF POOR QUALITY

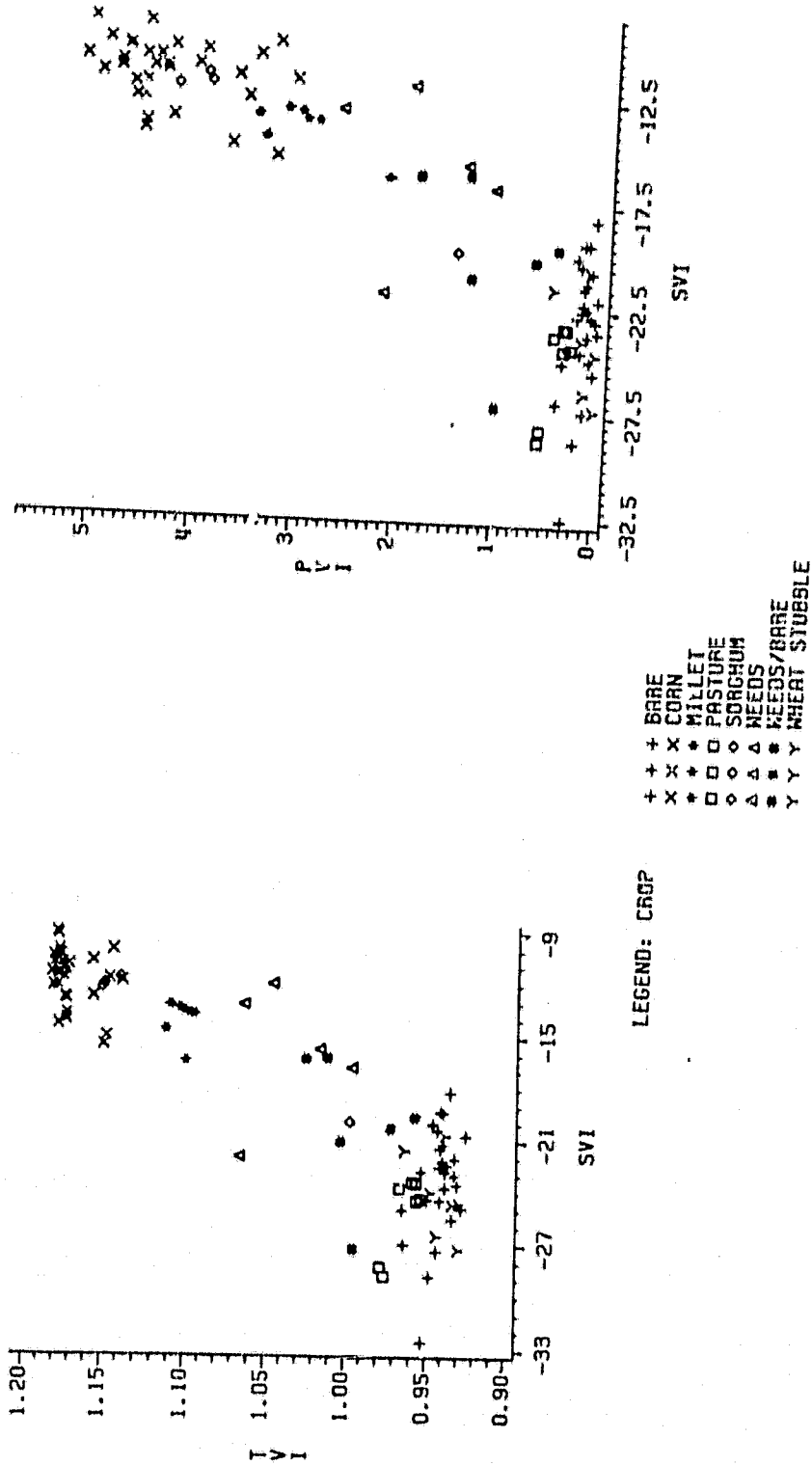


FIG. 46 The relationship between SVI(db), and TVI and PVI at Dalhart.

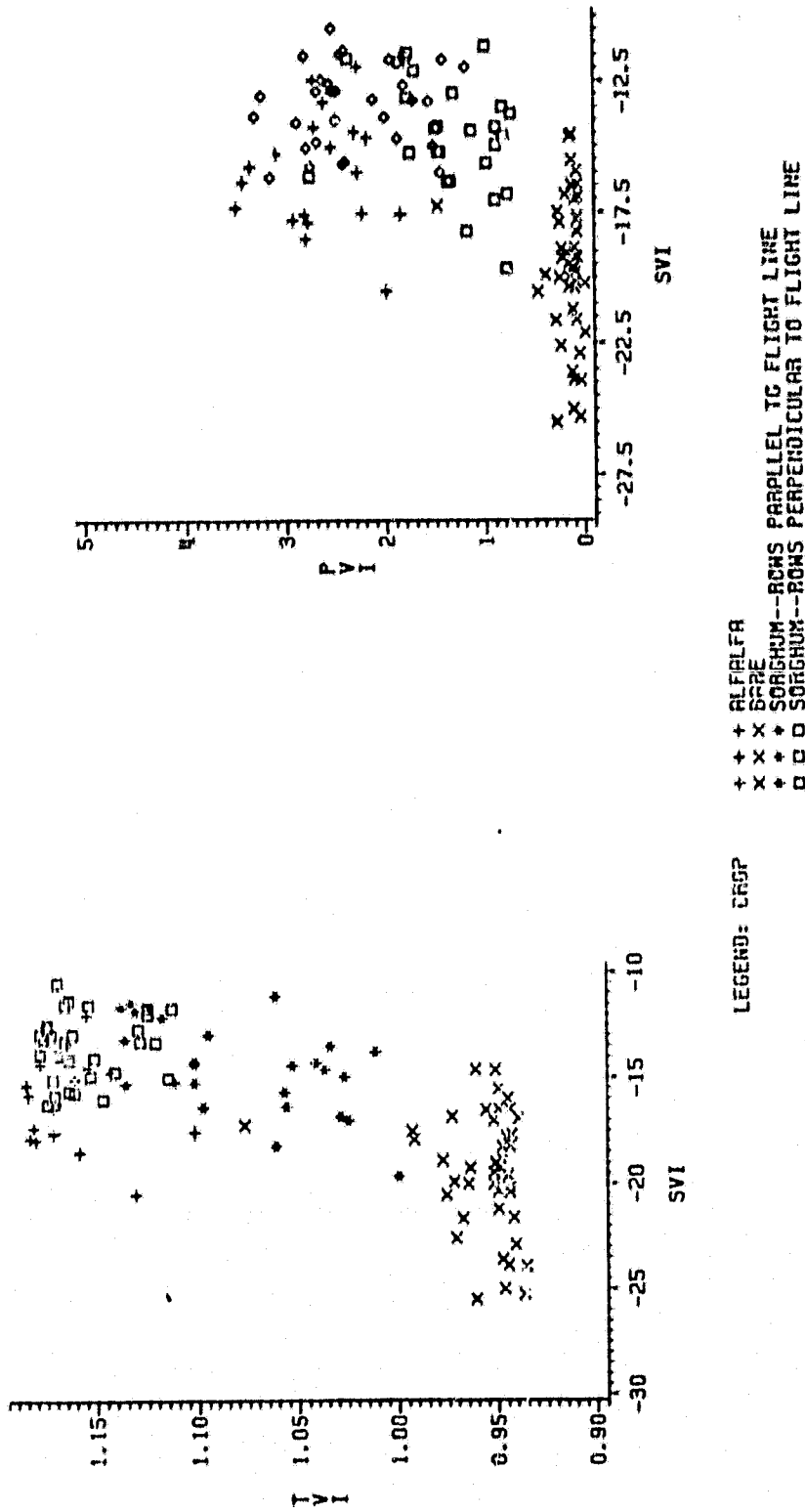


FIG. 47 The relationship between SVI(db), and TVI and PVI at Guymon.

OF YOUR QUALITY

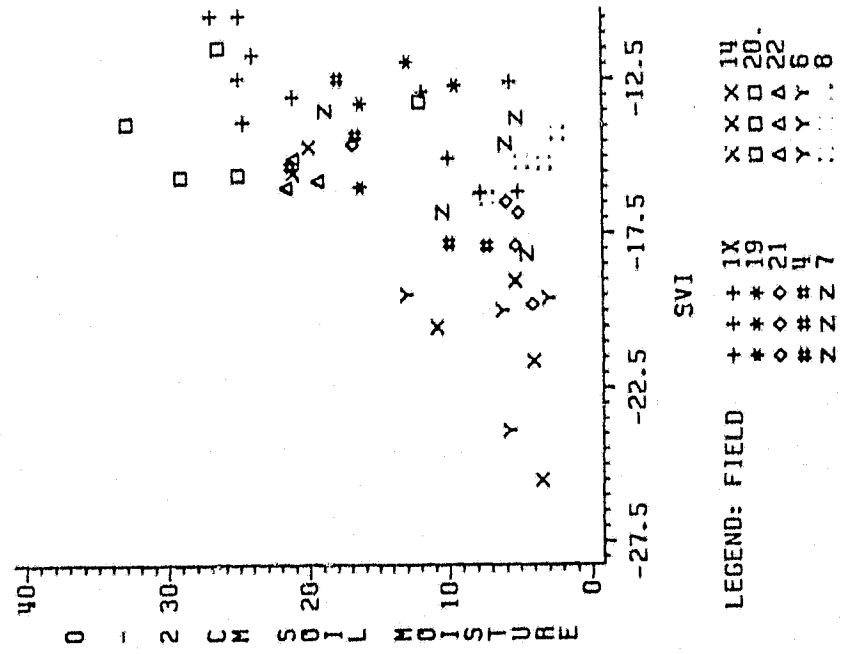
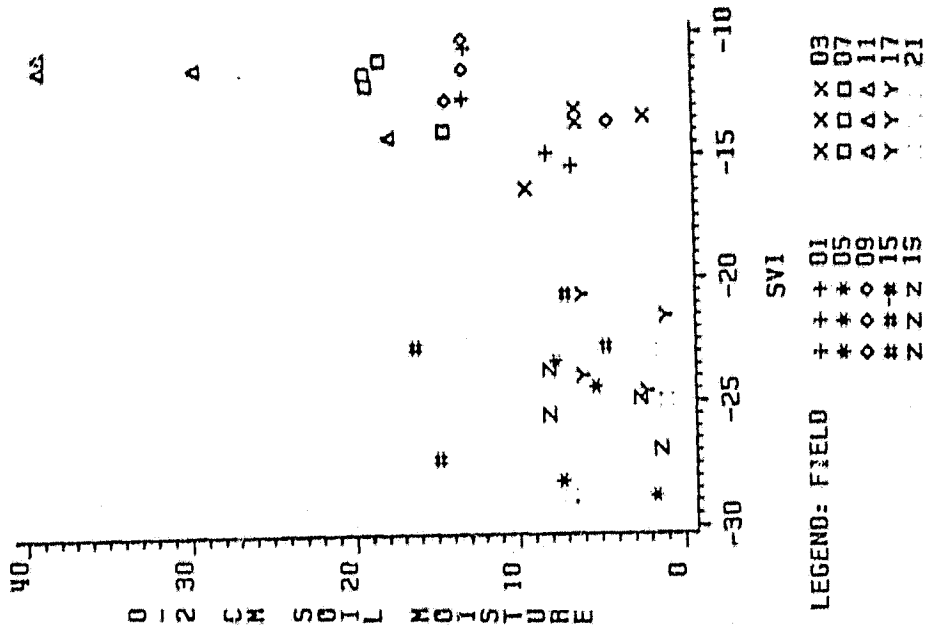


FIG. 48 The relationship between SVI(db), and 0-2 cm soil moisture (%) for selected fields at Guymon and Dalhart.

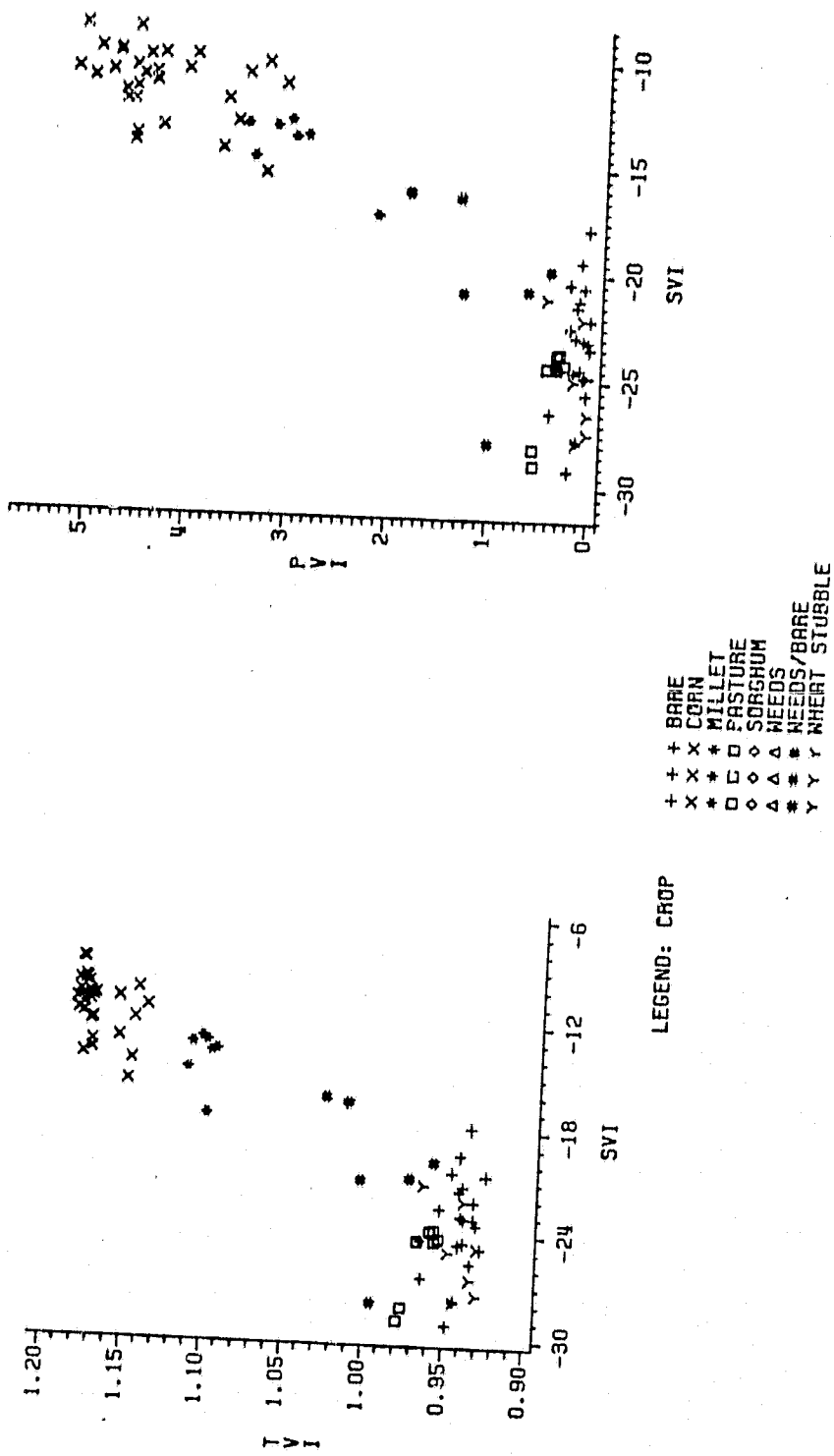


FIG. 49 The relationship between soil moisture corrected SVI(db), and TVI and PVI at Dalhart.

ORIGINAL PAPER
OF POOR QUALITY

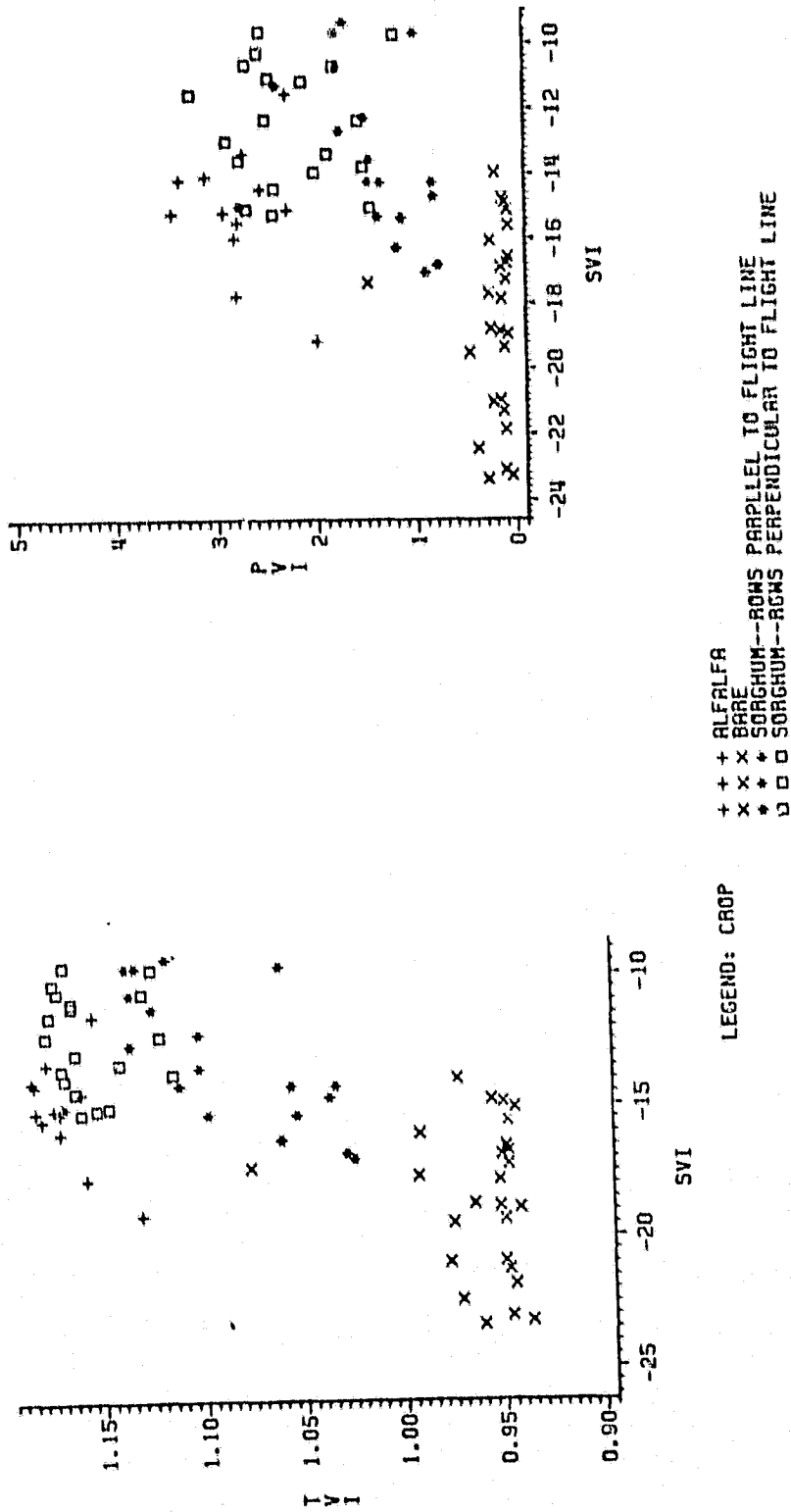


FIG. 50 The relationship between the soil moisture corrected SVI(db), and TVI and PVI at Guymon.

roughness differences. For example, at Guymon, SVI values from fields having rows parallel to the flight line were slightly higher, 2-3 db, than values from fields with rows perpendicular to the flight line. Attempts to remove the roughness effects were fruitless as the vegetation effect was also lost. Analysis of Figures 49 and 50 indicated that SVI was insensitive to low PVI or TVI changes; however, at higher PVI and TVI (PVI greater than 1.5 and TVI greater than 1.06) levels SVI became sensitive to changes in biomass. Indications also show that SVI was slightly more sensitive to biomass changes at high biomass levels than PVI or TVI.

Other attempts to determine combinations that normalized the scatterometer data proved fruitless. Consequently, each data set could only be analyzed separately.

Problem 4

Considering the results from the previous three problems, biomass was a strong indicator of crop type differences within the active microwave region--crops with greater biomass had higher active microwave responses and were classified separately from other low biomass groups. If the tree classification model were applied to an agricultural region which has a crop with different biomass or biophase, misclassification with other crops is likely. For example, the unsupervised classification technique tended to confuse immature sorghum with alfalfa. To fully understand the utility of the tree-classification model under different biophases and adjust the classification model for applications under different biomass levels, visible/infrared and active microwave responses needed to be considered. The sorghum

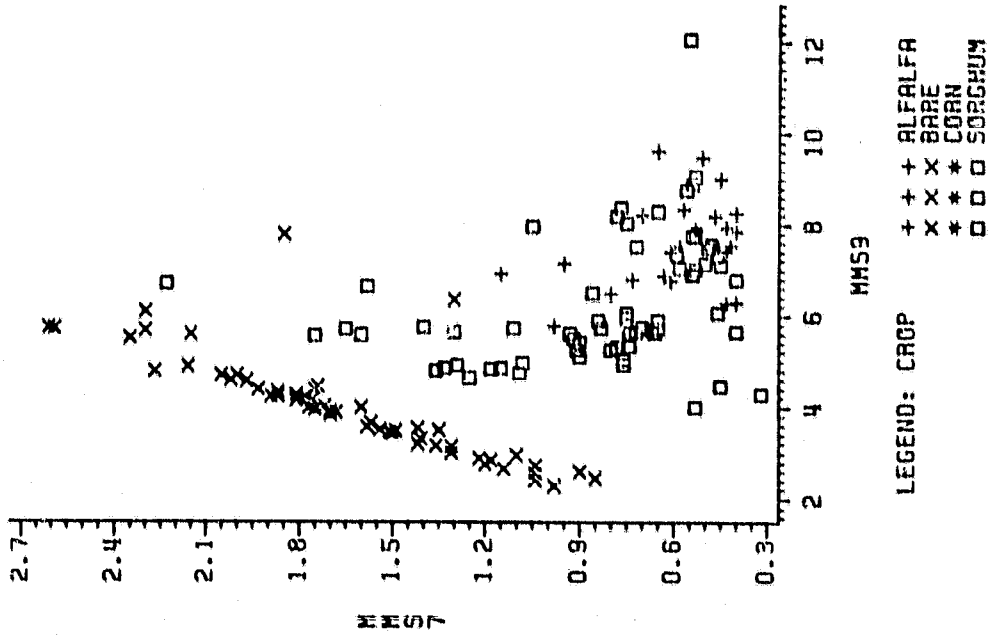
fields at Dalhart and Guymon covered a wide range of biomass and biophases ranging from crops that were just emerging to fully headed. Analysis of the response difference within a given crop type due to biomass differences indicated possible errors of misclassification and gave physical explanation for the tree classification model.

The visible/infrared response showed a definite trend as biomass increased and crops matured. Figure 51 represents the red/near infrared responses at Dalhart and Guymon, respectively. In both cases, data from bare soil and low biomass fields were linearly related. As the crop matured, the distance from the soil line to the data point increased. Data from fields with the highest biomass and at the reproductive biophase had the largest distance from the soil line. The perpendicular distance had been defined as the perpendicular vegetation index (PVI). As the crop matured from heading, leaves began to senesce and PVI decreases. No fields at Guymon or Dalhart were in the last biophase.

The active microwave response from several fields at Dalhart-- 22, V2 and V6, and 12--indicated differences at far look angles which appeared to represent different biomass levels. Field 22 was a bare field at Dalhart; V2 was an irrigated sorghum field at Dalhart that had reached the heading stage; V6 was a dryland immature sorghum field only 60 cm tall at Dalhart; and 2 was a corn field with a high biomass at Dalhart. The K band data indicated no significant differences between the different biomass levels (Figure 52) while the C band cross pole data indicated some differences (Figure 53). The immature sorghum field, V2, had slightly higher returns than the bare field,

ORIGINAL DATA
OF POOR QUALITY

MMS7 (662-701NM) VS MMS9 (770-863NM)



TM3 (630-690NM) VS TM4 (760-900NM)

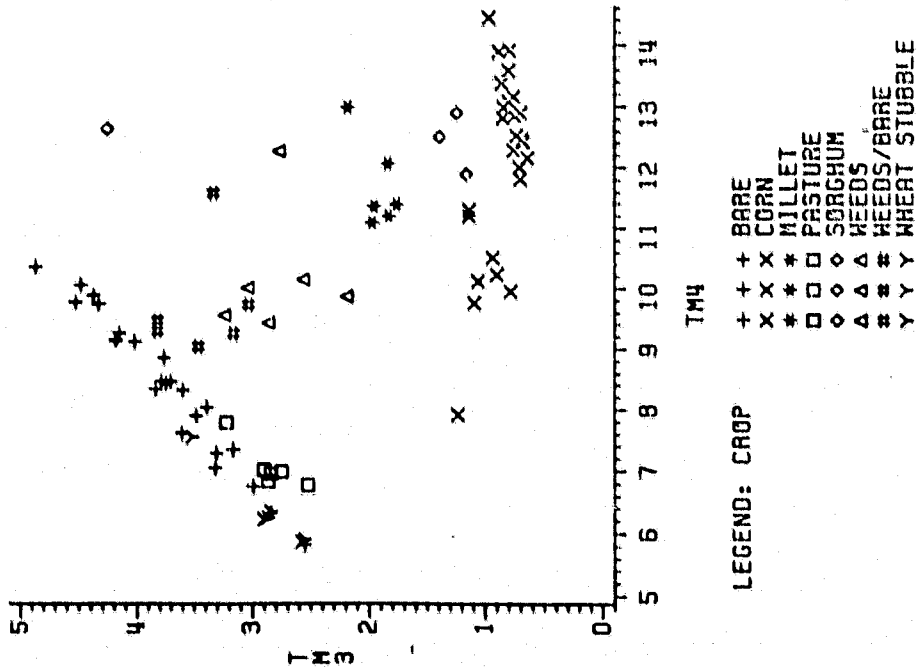


FIG. 51 The red/near-infrared relationship for fields at Gaymon and Dalhart.

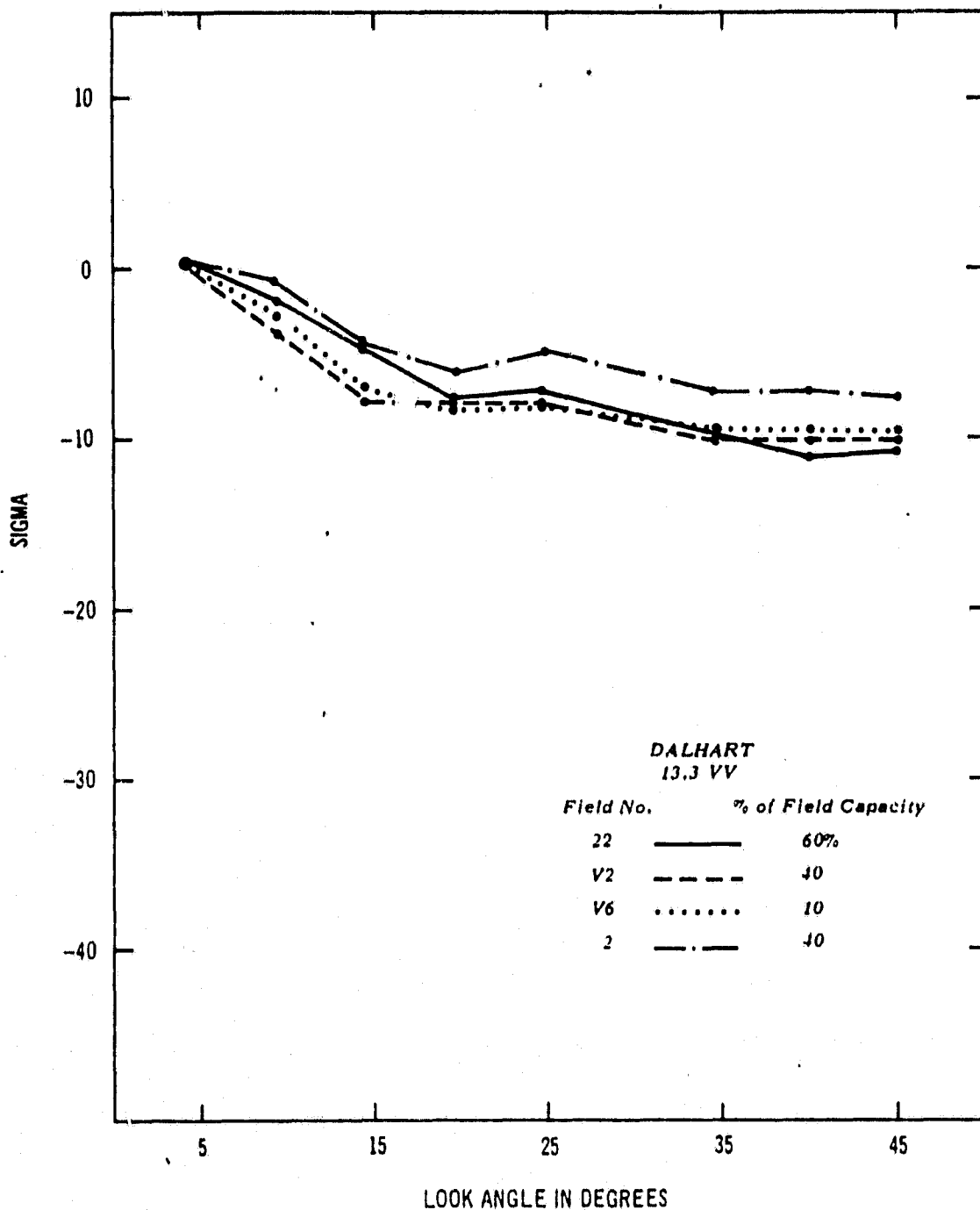


FIG. 52 The K band like pole σ^0 response as a function of look angle for bare soil (field 22), sorghum (field V2 and V6), and corn (field 2) at Dalhart.

ORIGINAL PAGE IS
OF POOR QUALITY

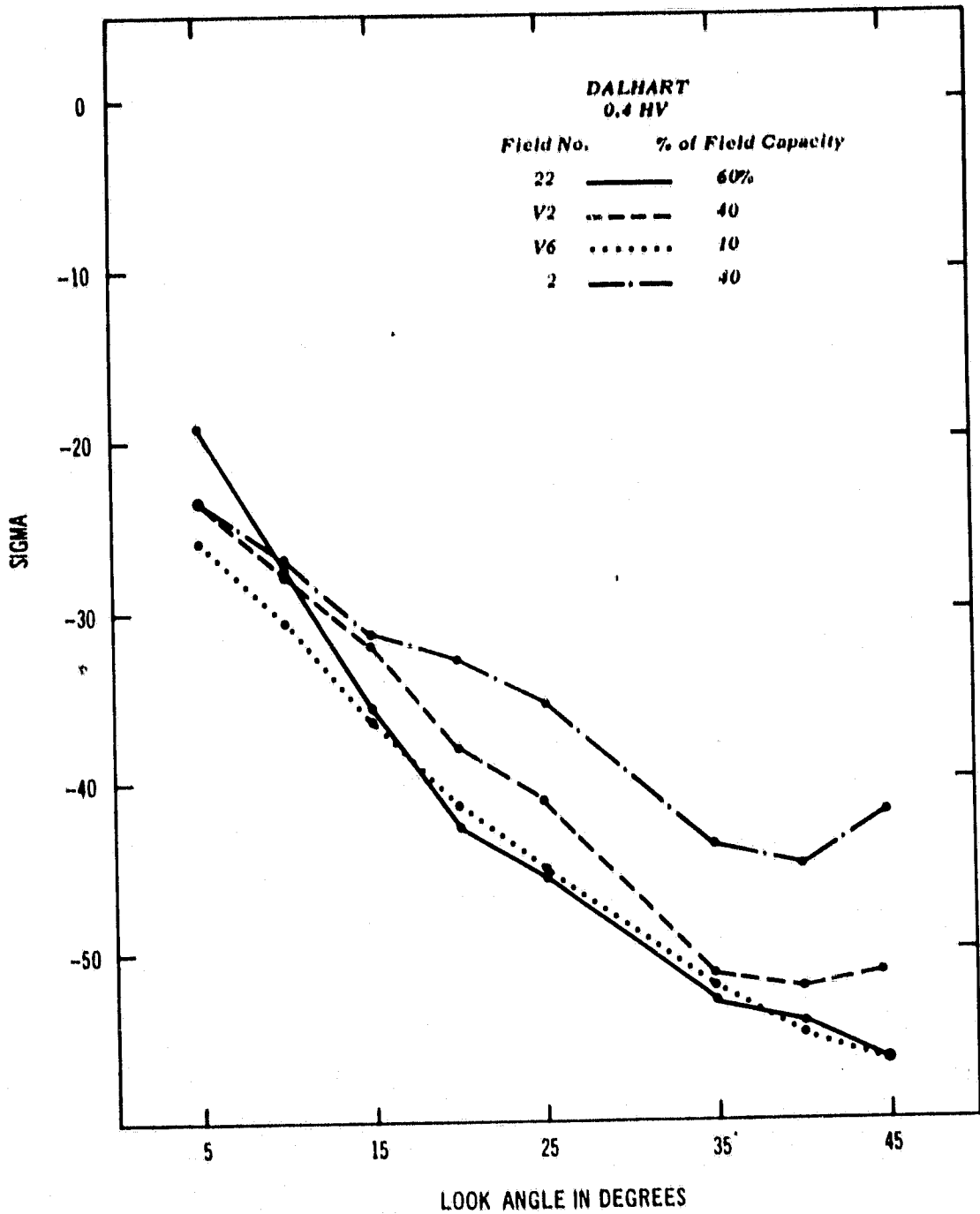


FIG. 53 The C band cross pole response as a function of look angle for bare soil (field 22), sorghum (field V2 and V6), and corn (field 2) at Dalhart.

22. The largest difference was between the vegetation (mature sorghum, corn) and the bare soil--as much as 10 db in the 40° look angle. The L band cross pole data also indicated some differences between different biomass levels. Again, the corn and mature sorghum fields had higher returns at high look angles compared to the bare and low biomass fields--as much as 7 db (Figure 54). However, the responses at the high look angles in the P band cross pole data were sensitive to fields only with high biomass (Figure 55). The analysis therefore implied high frequency active microwave responses "saturated" at relatively low biomass levels while low frequency responses "saturated" at very high biomass levels. C band would then best separate lower biomass crops, L band would separate moderate biomass crops and P band would separate high biomass crops.

The Guymon results also tended to indicate the same situation (Figures 56 through 59). However, roughness from row direction played an important factor also. The best example indicating biomass difference was L band cross pole from field 1X--headed, dense sorghum, 15--emerging sorghum, 4--alfalfa, and 14--bare soil (Figure 58). Again the far look angles were responding to high biomass levels. Data from other look angles indicated that surface roughness influenced the return by masking the vegetative differences. Attempts to eliminate roughness effects proved to be unsuccessful, as removal of roughness also reduced the vegetation effect.

From the analysis of both spectral data sets, a multifrequency active microwave system using a low and high frequency could improve classification and biomass estimation accuracy. Given the scatterometer vegetation index (SVI), which was strongly related to biomass

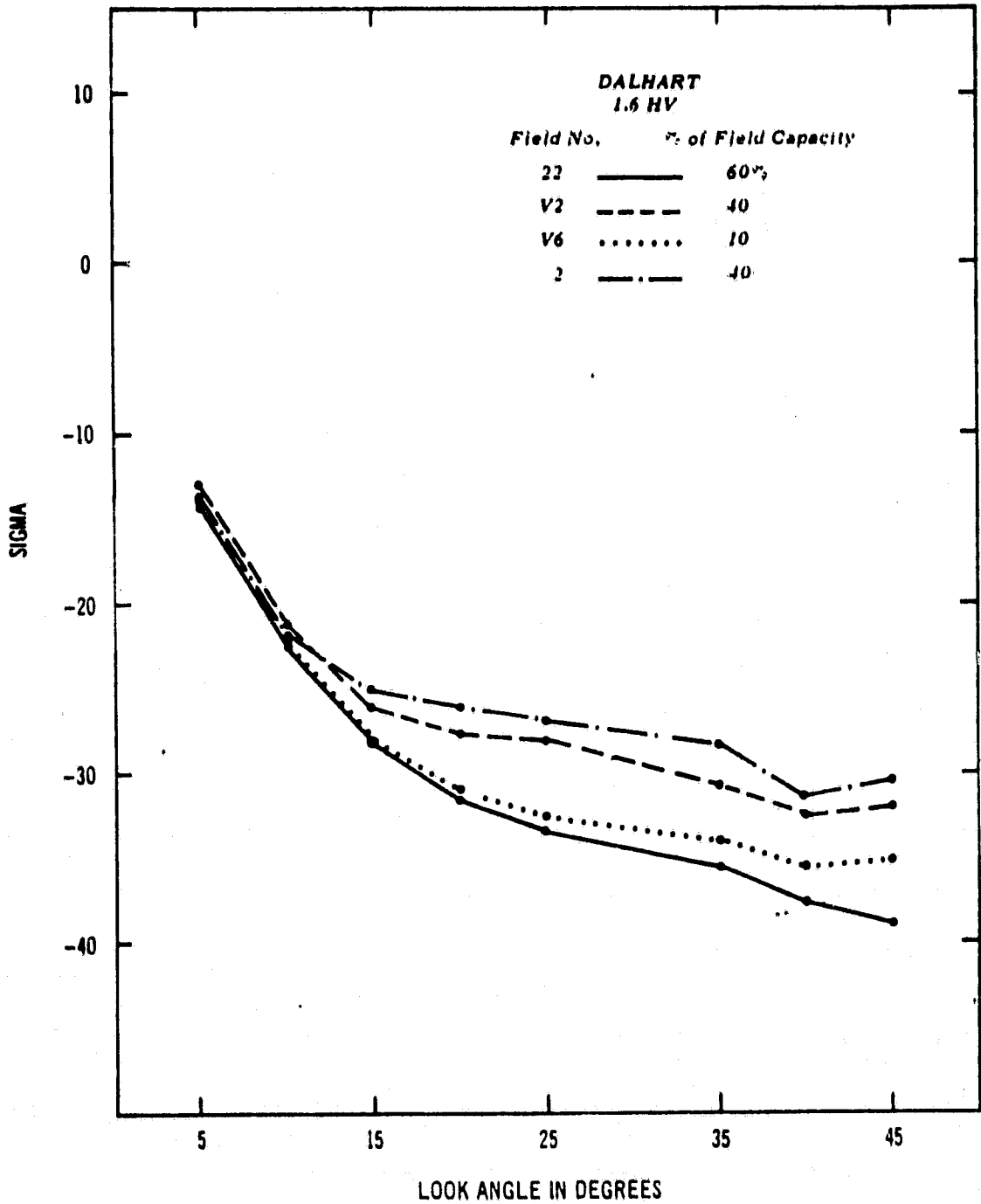


FIG. 54 The L band cross pole σ^0 response as a function of look angle for bare soil (field 22), sorghum (field V2 and V6), and corn (field 2) at Dalhart.

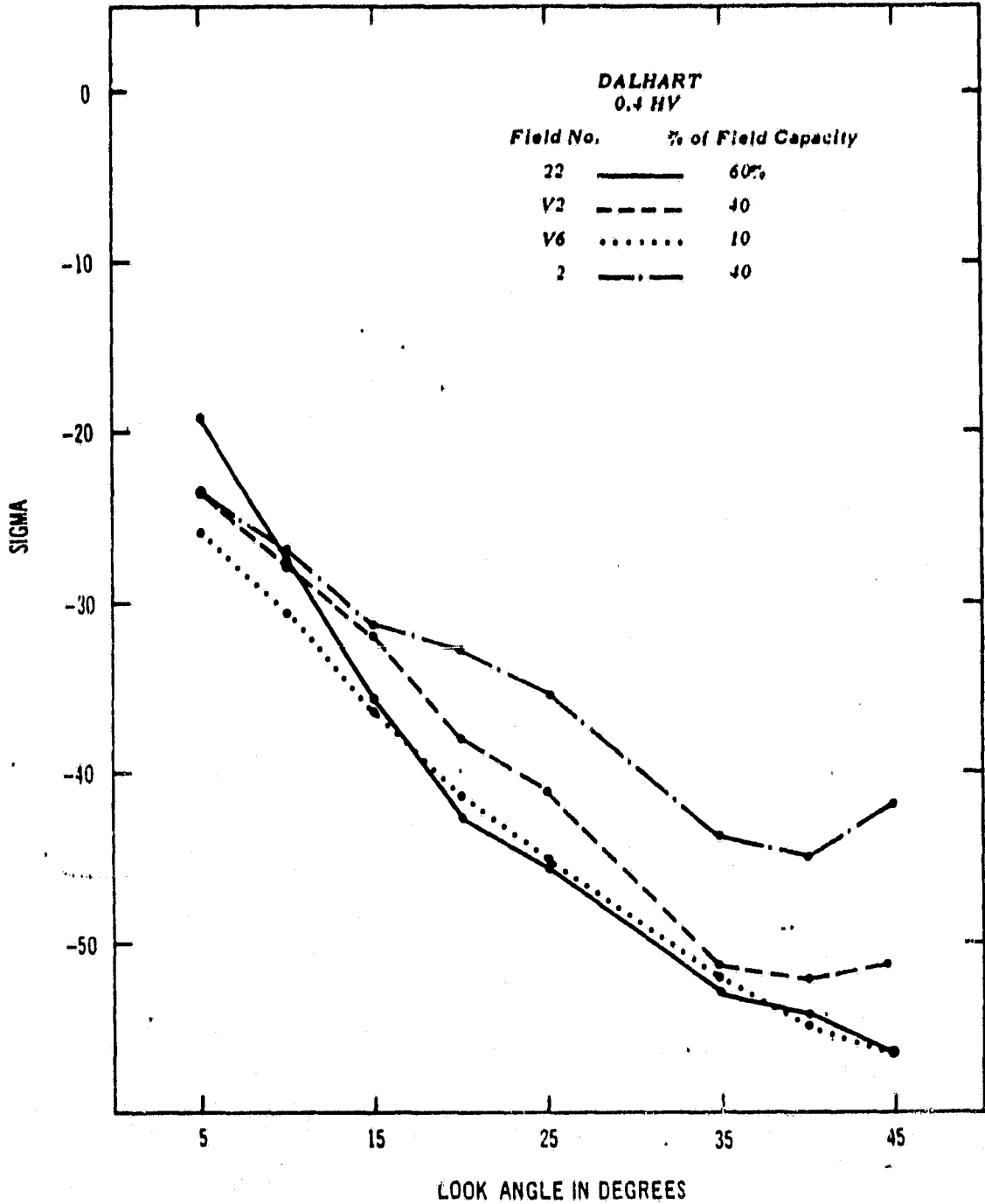


FIG. 55 The P band cross pole σ^0 response as a function of look angle for bare soil (field 22), sorghum (field V2 and V6), and corn (field 2) at Dalhart.

ORIGINAL PAGE IS
OF POOR QUALITY

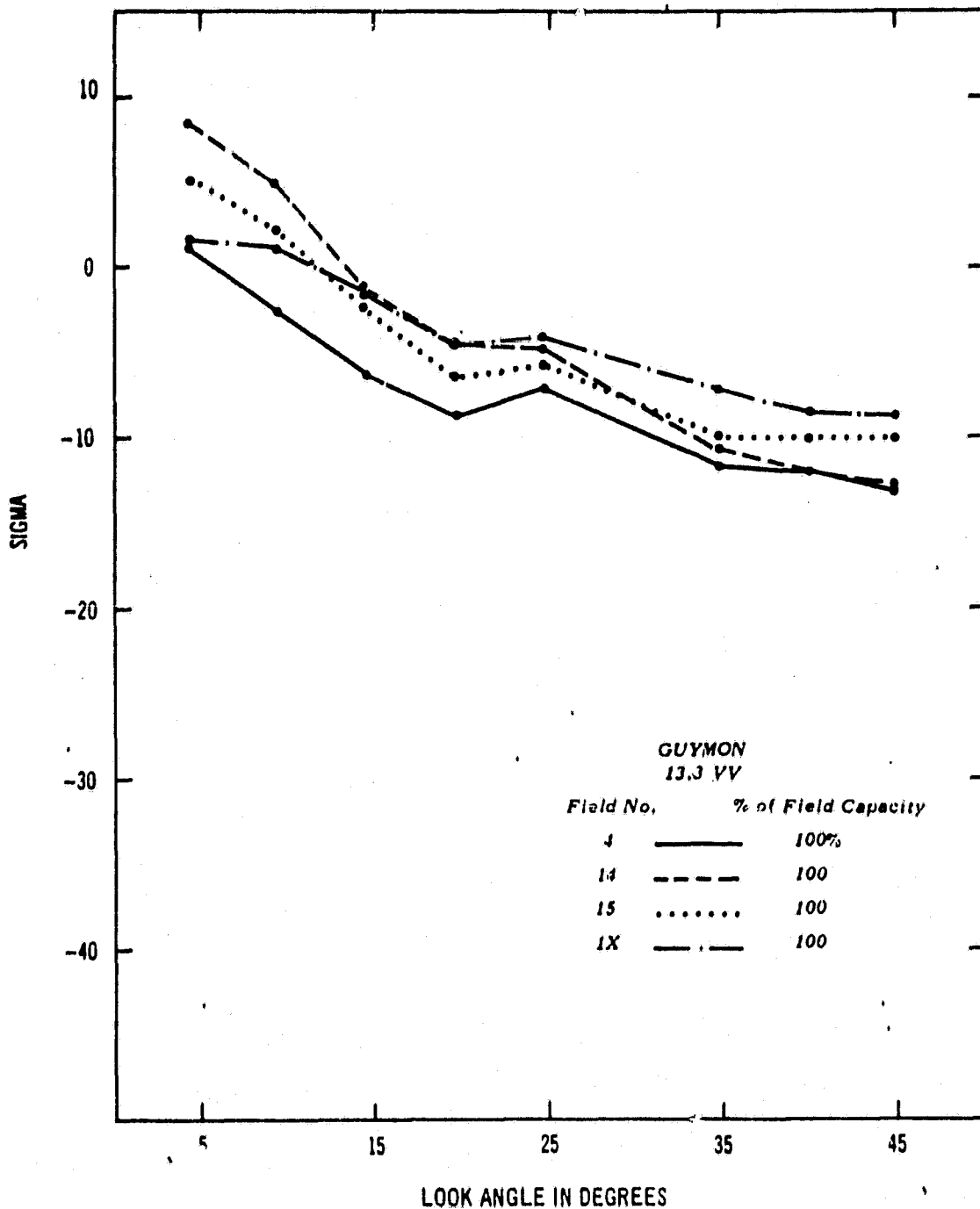


FIG. 56 The K band like pole σ^0 response as a function of look angle for bare soil (field 14), alfalfa (field 4), emerging sorghum (field 15) and headed sorghum (field 1X).

ORIGINAL PAGE IS
OF POOR QUALITY,

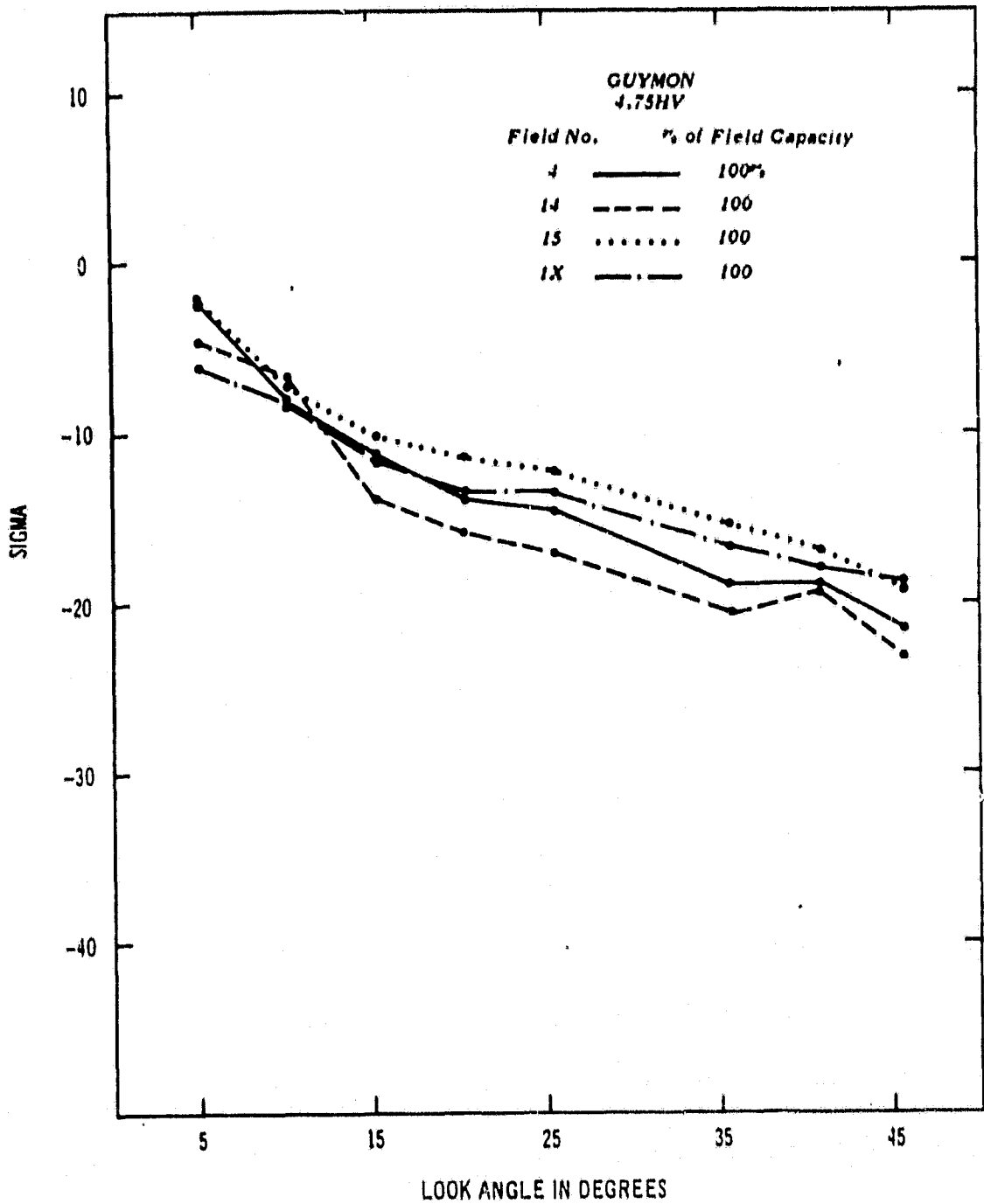


FIG. 57 The C band cross pole σ^0 response as a function of look angle for bare soil (field 14), alfalfa (field 4), emerging sorghum (field 15) and headed sorghum (field 1X).

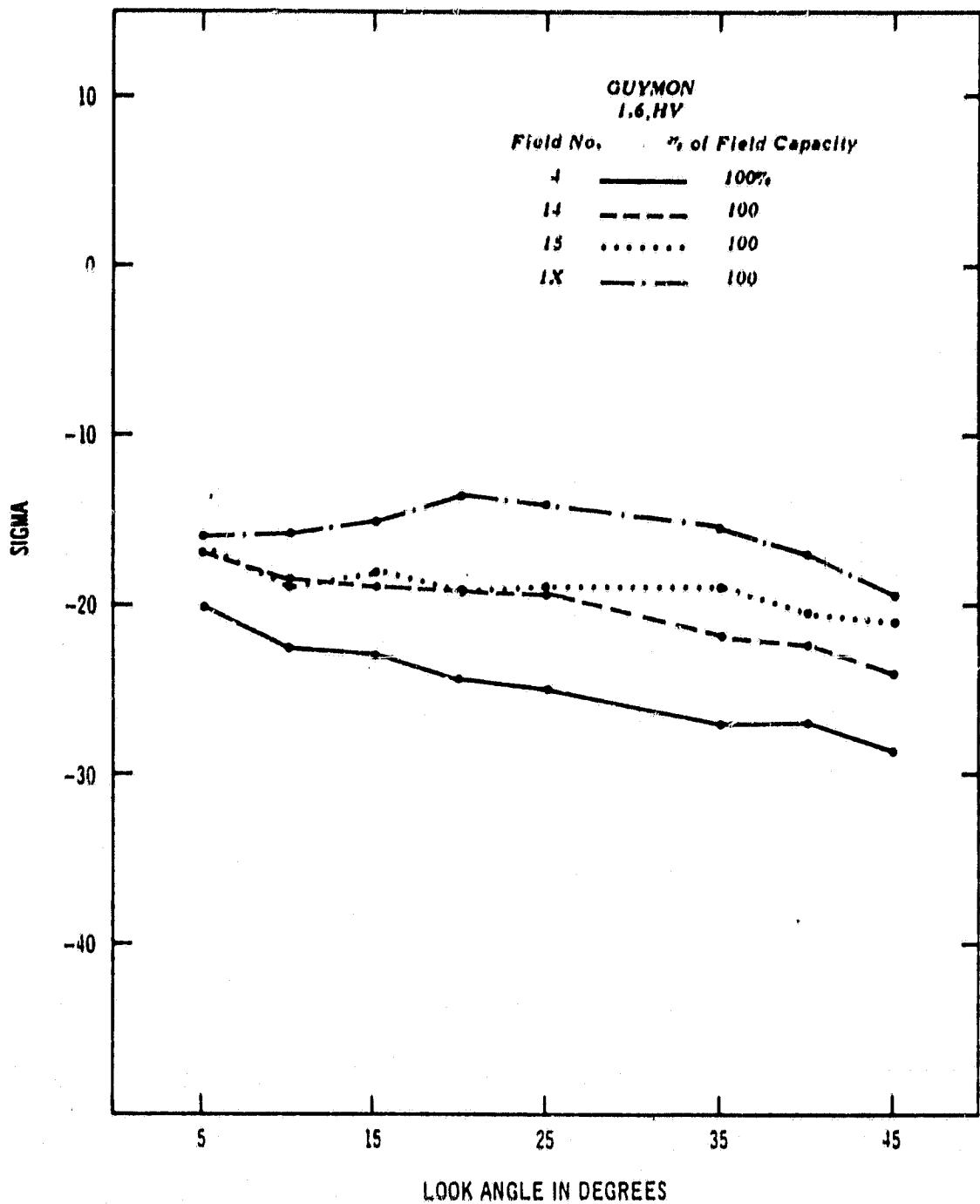


FIG. 58 The L band cross pole σ^0 response as a function of look angle for bare soil (field 14), alfalfa (field 4), emerging sorghum (field 15) and headed sorghum (field 1X).

ORIGINAL PAGE IS
OF POOR QUALITY

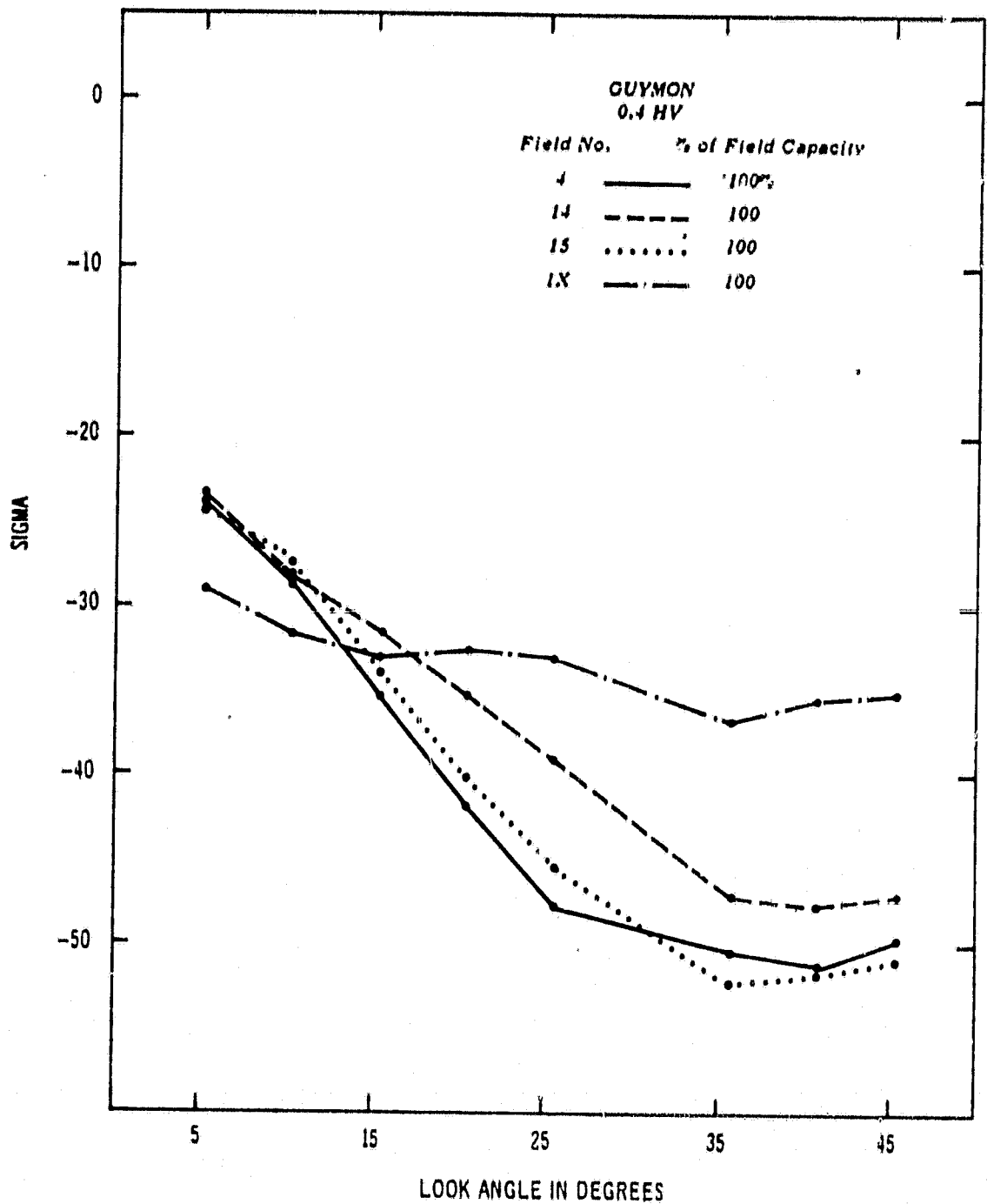


FIG. 59 The P band cross pole σ^0 response as a function of look angle for bare soil (field 14), alfalfa (field 4), emerging sorghum (field 15) and headed sorghum (field 1X).

and PVI, a similar combination using 40° P band cross pole σ^0 - P band cross pole σ^0 was included with SVI. The resulting modified index (SVIM) is defined as

$$\begin{aligned} \text{SVIM} = & (40^\circ \text{ C band cross pole} - 5^\circ \text{ C band cross pole}) \\ & + (40^\circ \text{ P band cross pole} - 5^\circ \text{ P band cross pole}) \quad (22) \end{aligned}$$

The modified SVI was also strongly related to total biomass at Dalhart ($R^2 = 0.73$) (Figure 60). In comparison, the relationship of SVIM to biomass at Dalhart was not as strongly related to PVI or TVI at Guymon (Figure 61). Again, alfalfa did not have high SVI values indicating active microwave penetration through the canopy for P band data. Higher frequency scatterometer data may indicate the presence of dense alfalfa fields. The SVIM responses from sorghum fields were, however, greater than low biomass or bare fields.

With the sensitivity of the P band cross pole data to differences in high biomass, the only change needed in the classification model was to use P band cross pole differences as a first step to separate the high biomass fields from fields with medium and low biomass. Higher frequency L or C band cross pole data were then used as criteria to separate fields with medium and low biomass levels. Using these criteria, the corn and dense sorghum fields at Guymon were separated--anything having a return of -47 db or higher would be classified as corn at Dalhart and -36 db or higher at Guymon. Using these criteria, the accuracy of the tree classifier improved slightly at Dalhart and Guymon--81% at Dalhart and 76% at Guymon.

ORIGINAL, IN PART
OF POOR QUALITY

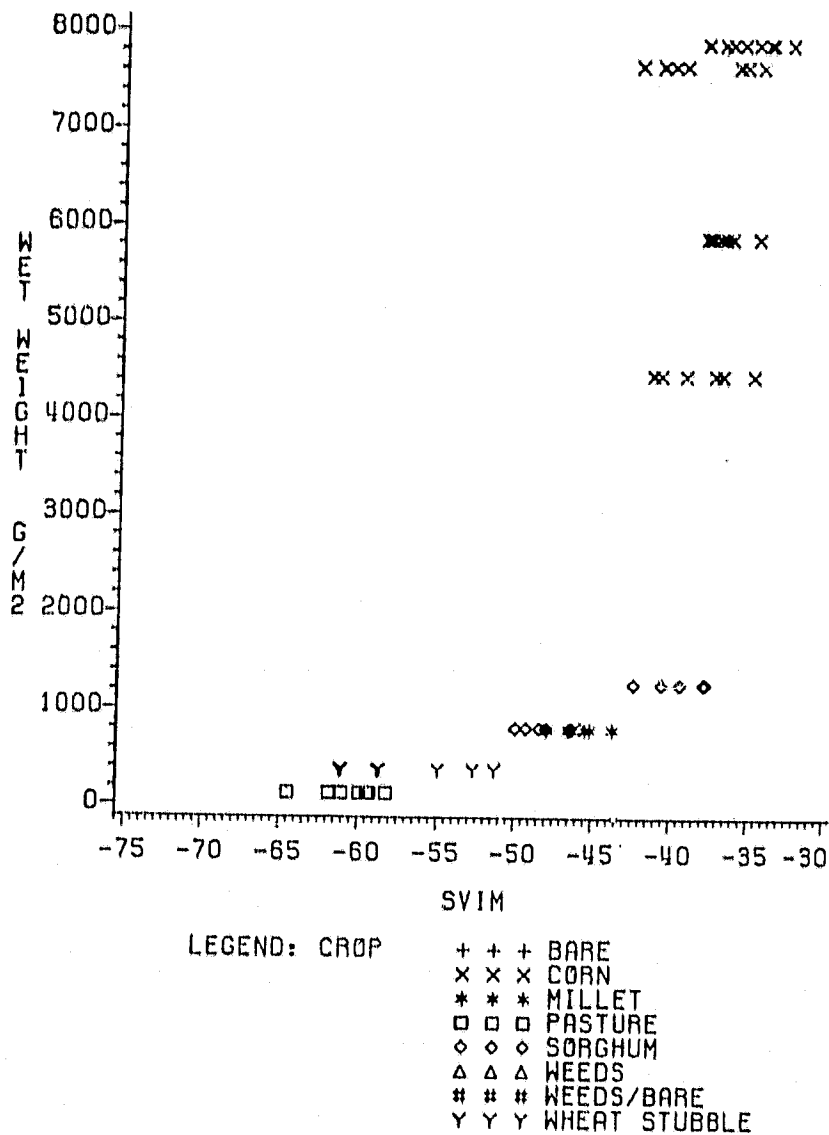


FIG. 60 The relationship between total biomass and the modified scatterometer vegetation index, SVIM [(C band cross pole 40° - C band cross pole 5°) + (P band cross pole 40° - P band cross pole 5°)].

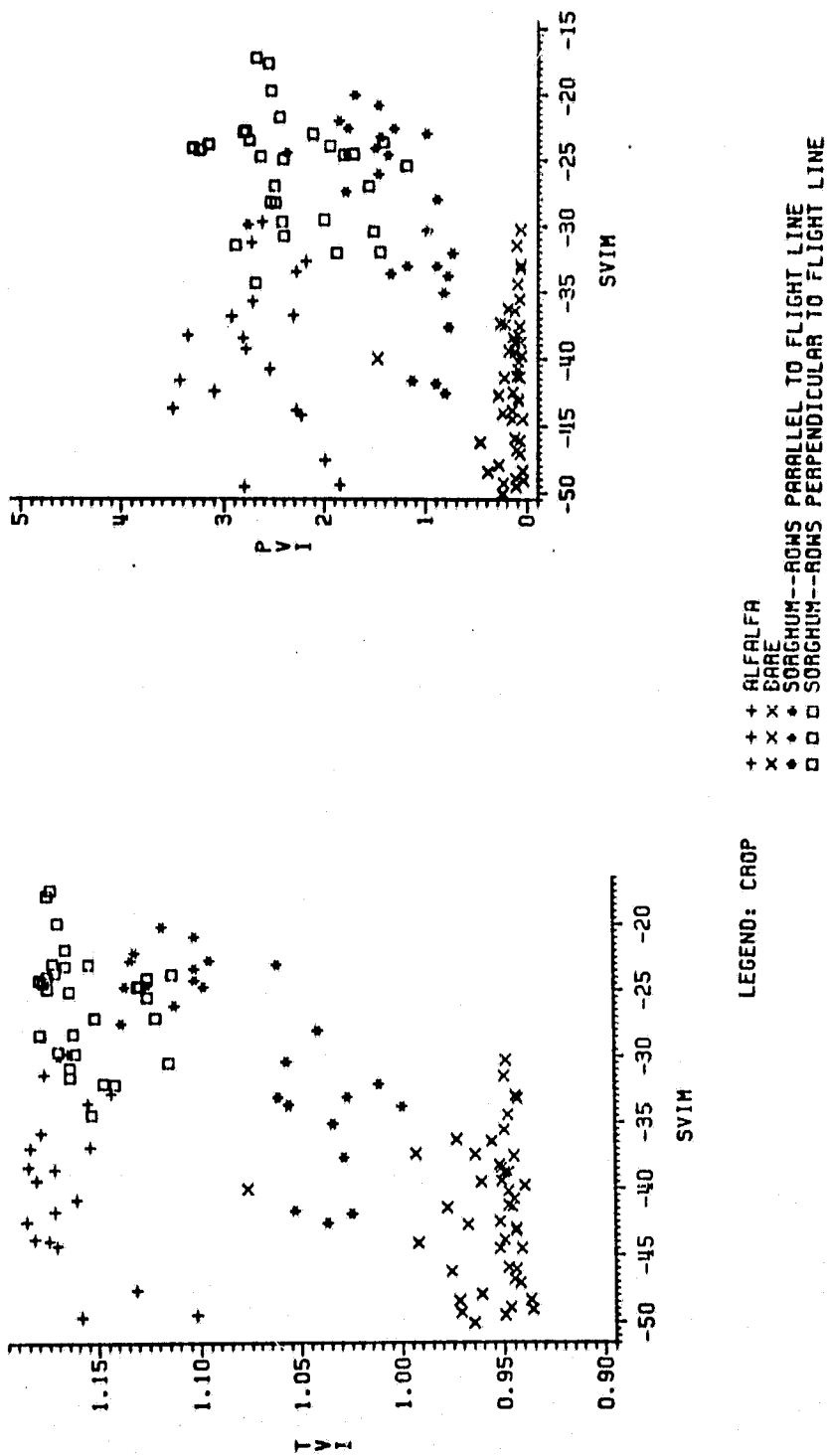


FIG. 61 The relationship between the modified SVI (SVIM) and TVI and PVI at Guymon.

SUMMARY AND CONCLUSIONS

Since the study was divided into four problems, results from each will be discussed in detail. Also, an overview summarizing the study and its implications will follow the discussions of the results.

Problem 1

The first problem determined spectral bands which were sensitive to crop type differences. Results implied that several active microwave frequencies were sensitive to crop type differences, especially at look angles greater than 35° off nadir. The response differences due to vegetation dominated the effects of roughness and soil moisture. The most sensitive frequencies and polarizations included C band cross pole, L band like and cross pole and P band like and cross pole. Depending on the crop type, responses from certain frequencies discriminated crops. For example, L and P band discriminated between sorghum and corn, and C band was able to discriminate between alfalfa and bare soil. Other active microwave sensors were primarily sensitive to roughness or soil moisture. The visible/infrared sensors were not as sensitive while the passive microwave data were sensitive to soil moisture differences. The biomass differences were detected especially well in the visible/infrared bands. Also, stressed areas were noted using NS001 band 6 data (water absorption band). The visible and infrared data were sensitive to the presence or absence of vegetation, but not necessarily certain crop type pairs.

Problem 2

The second problem determined the most accurate crop classifying dendrogram for the Guymon and Dalhart spectral data. In this problem, a relatively accurate dendrogram using active microwave, visible, and infrared data was developed for both Guymon and Dalhart spectral data sets. The dendrogram was based first on separating "rough" from "smooth" fields using active microwave data, and second, on separating each class between the bare and low biomass fields from heavily vegetated fields. The preferred active microwave frequencies and polarization were L and C band cross pole which were most sensitive to biomass differences between crop types. Response differences in both frequencies classified different scales of roughness. Classification accuracies using the similar dendrograms were 77% for Dalhart and 70% for Guymon. Data from other individual bands did not improve the accuracy. The implication was that one model requiring data from four bands (visible through active microwave) could discriminate different crop types with reasonable accuracy. More data sets are needed, however, to thoroughly test the tree classification model.

Problem 3

Problem three determined the utility of estimating biomass and discriminating crops using visible/infrared/microwave data compared to visible/infrared data. The primary result in problem 3 was the indication that microwave data improved or maintained classification and biomass estimation accuracy in comparison to conventional

classification. The conventional classification technique used only visible/infrared data to classify and estimate biomass. Various statistical techniques such as discriminant analysis and step-wise regression indicated the inclusion of active microwave aided in classifying agricultural crops. With higher accuracy, less frequent visible/infrared/microwave satellite or aircraft passes would be required for an adequate estimate of crop acreage or biomass.

In addition, the proposed thematic mapper wavelength bands provided more information on vegetation than the Landsat visible/infrared combinations. For example, a combination similar to the perpendicular vegetation index (PVI), but using input data from the near infrared (0.76 - 0.90 μm) and water absorption band (1.55-17.5 μm) provided additional information on corn compared to the results from broad band MSS red and near infrared wavelengths. Not enough ground data were collected to determine what physiological parameter within field differences of the the new combination was detecting. The new combination, PVI64, was slightly more related to biomass than the original combination of red and near-infrared data that had been used to calculate PVI. Further studies using these bands are needed.

Finally, an active microwave vegetation index (SVI) was developed using C band cross pole data from the 5° and 40° look angles. The combination, which was developed to normalize the two data sets, was highly correlated to PVI. The major implication was that use of this combination would allow a classification and biomass estimation that would be possible regardless of cloud conditions. It is fully recognized that the sensor combination required to collect 5° and 40°

imagery over the same areas with active microwave is highly impractical and most likely not economically feasible. The result is, however, significant from an academic standpoint and may help in understanding the scattering phenomena that take place in vegetative cover. It is significant to note that L band differences between 5° and 40° did not respond to vegetation other than corn and sorghum since the L band energy was penetrating through the canopy more than C band. However, further tests of the model are needed in agricultural regions having different management practices.

In spite of the success in discriminating crops and estimating biomass within each data set--Guymon and Dalhart--the sets could not be combined due to the absence of active microwave calibration. Various attempts to normalize the data sets using combinations, such as the SVI, were unsuccessful. Consequently, both data sets were analyzed separately. Any further experiment requiring collection of active microwave data must include some means of calibrating the microwave sensors.

Problem 4

The fourth problem determined the effect of biomass differences on the crop classifying dendrogram developed in problem 2. Results from problem 4 indicated that the tree-classification model was significantly dependent upon biomass. Implications are that crops which have similar responses at the same time of year, such as wheat and barley may be indiscriminant. However, at certain biophases physiological differences, such as plant water content may be detectable. Consequently, multi-temporal data are still needed to

accurately separate two "confusion" crops. To make the model even more sensitive, multifrequency microwave data are needed to separate even higher biomass levels. Results proved that the P band cross pole scatterometer returns are sensitive at high biomass levels at Dalhart. Inclusion of the P band cross pole data improved crop classification accuracy over the use of L band and C band data.

Overview

Having answered the questions posed by each problem, the hypothesis--can microwave data help improve classification and biomass estimation compared to present techniques using only visible and infrared data--can be validated. Given the results from Guymon, Oklahoma, and Dalhart, Texas, active microwave data do aid in improving classification and biomass estimation. Results indicated that multifrequency active microwave data would be needed to classify multiple-cropped agricultural areas accurately. L and P band data can discriminate between sorghum and corn; C band can discriminate between bare soil and alfalfa but not between corn and sorghum. In addition, NS001 data indicated combinations of the water absorption band (1.55-1.75 μm) and the near-infrared band (1.0-1.3 μm) gave more crop information than the red/near infrared combinations. Accurate multispectral classification and biomass estimation models were developed from both data sets.

However, two major factors pose problems in using active microwave data--soil moisture and surface roughness. With many of the vegetated crops being irrigated and the non-vegetated field remaining fallow, a bias entered into this analysis due to soil moisture differ-

ences. The most accurate technique to remove the soil moisture effect would be to develop a correction factor using passive microwave data which is primarily sensitive to soil moisture changes, as inputs to the model (Schmugge, 1979). The best method to minimize surface roughness is to use cross-polarized active microwave data, which theoretically isolates the volumetric (dielectric) effects while minimizing the scattering (surface roughness) effects. Other combinations that were developed were unable to remove the effects of roughness alone. Attempts to remove the roughness effect also diminished the vegetation effect.

A second problem dealt with spatial resolution. If large areas of the world are to be covered in a short time period, satellite systems will be required. The question arises as to what should the spatial resolution be and should the resolution be similar for each frequency. Visible/infrared data often have high spatial resolution; passive microwave data have low resolution while active microwave resolution can be controlled by system design and processing. Many fields around the world are too small to be seen even by Landsat. Consequently, by increasing spatial resolution to allow analysis of individual fields implies extremely large amounts of both visible/infrared microwave and active microwave data processing. With lower spatial resolution, knowledge of composite (fields of different crop types, soil moisture, and surface roughness) returns within the cell size is required. For example, what effect would the return from a 32-hectare field have on the composite return of a 10 km resolution cell, and can classification and biomass information be extracted from

the larger size cells? Consequently, future studies are needed to find the proper resolution size for reasonably accurate estimates of vegetation using visible/infrared/microwave data.

Advantages of using microwave systems are obvious: independence of weather and sunlight and the opportunity for fewer passes with the visible/infrared systems due to higher classification accuracy. Both reasons are advantageous over present visible/infrared systems developed during the LACIE period. Some foreign agricultural areas that we have previously been unable to monitor from a satellite due to cloud cover could be monitored in the future. The final results would be two-fold: (1) an improved world-wide agricultural production system which would prevent another event such as the U. S./Soviet Union wheat crisis which occurred in 1974, and (2) domestic food supply planning would be more efficient as better production estimates would induce better domestic storage and production, and stabilize commodity prices.

Consequently, active microwave sensors need to be seriously considered as additional sensing tools in evaluating agricultural areas. With the additional data, potential world food disasters may be averted.

REFERENCES

- 1 Allen, W. A., H. W. Gausman, and A. J. Richardson. 1970. Mean effective optical constants of cotton leaves. *J. Opt. Soc. Am.* 60:542-547.
- 2 Bauer, M. E. 1975. The role of remote sensing in determining the distribution and yield of crops. *Adv. Agron.* 27:271-304.
- 3 Bauer, M. E., L. P. Silva, R. M. Hoffer and M. F. Baumgardner. 1977. Agricultural scene understanding. Final Report. LARS Contract Report 112677.
- 4 Beckman, P. 1966. Scattering by composite rough surfaces. *IEEE Trans. on Antennas and Prop.* AP-13:1012-1015.
- 5 Billingsley, F. C., M. R. Helton, and V. M. O'Brien, eds. 1976, LANDSAT follow-on: a report by the applications survey groups. Vol. 1--Executive Summary. NASA JPL Tech. Memo. 33-803.
- 6 Blanchard, A. J. and S. W. Theis. 1981. Volumetric effects in cross-polarized airborne radar data. *Intern. Geosci. and Remote Sensing Symposium, IEEE Washington, D. C. Vol 1.* pp. 629-630.
- 7 Blanchard, B. J., J. L. Nieber, and A. J. Blanchard. 1979. Continuation of measurements of hydrologic soil cover complex with airborne scatterometers. Remote Sensing Center Final Report 3496. NSG-5156, Texas A&M University. 43 pp.
- 8 Brakke, T. W., E. T. Kanemasu, J. L. Steiner, F. T. Ulaby, and E. Wilson. 1981. Microwave radar response to canopy moisture, leaf area index and dry weight of wheat, corn, and sorghum. *Remote Sensing of Environ.* 11:207-220.
- 9 Chance, J. E. and E. W. LeMaster. 1977. Suit's reflectance models for wheat and cotton: theoretical and experimental tests. *Appl. Optics* 16:407-412.
- 10 Choudhury, B. H., T. J. Schmugge, R. W. Newton and A. Chang. 1979. Effect of surface roughness on the microwave emission from soils. *J. Geophys. Res.* 84:5699-5706.
- 11 Clark, B. V. and R. W. Newton. 1979. JSME scatterometer data processing. Remote Sensing Center Final Report 3337. NAS9-14875. Texas A&M University. 110 pp.
- 12 Claassen, J. P., R. O. Stroud, B. V. Clark, B. R. Jean and R. W. Newton. 1979. The system and hardware design of real-time fan beam scatterometer data processors. Remote Sensing Center Final Report 3556. Texas A&M University. 275 pp.
- 13 Cooley, W. W. and P. R. Lohnes. 1971. *Multivariate data analysis.* John Wiley and Sons. New York. 364 pp.

- 14 Davis, B. R., E. B. Lipscomb, and S. J. Knight. 1965. Terrain analysis by electromagnetic means: laboratory investigations in the 0.76- to 5- micron spectral region. U. S. Army Tech. Report 3-693. Vicksburg, Miss. 165 pp.
- 15 Deering, D. W., J. W. Rouse, Jr., R. H. Haas and J. A. Schell. 1975. Measuring "forage production" of grazing units from Landsat MSS data. Tenth Int. Symp. on Remote Sensing of Environment Vol II. pp. 1169-1178.
- 16 DeLoor, G. P., A. A. Jurriens, and H. Gravesteijn. 1974. The radar backscatter from selected agricultural crops. IEEE Geosci. Elect. GE-12:70-77.
- 17 Donald, C. M. 1963. Competition among crop and pasture plants. Adv. Agron. 15:1-118.
- 18 Ellermeier, R. D., D. S. Simonett, and L. E. Dellwig. 1969. The use of multi-parameter radar imagery for the discrimination of terrain characteristics. Center for Res. in Eng. Sci. Report 61-69. Univ. of Kansas. p 127-135.
- 19 Fenner, R. G., G. F. Pels, and S. C. Reid. 1981. A parametric study of tillage effects on radar backscatter. Intern. Geosci. and Remote Sensing Symposium. IEEE. Washington, D. C. Vol II. pp. 1294-1308.
- 20 Gates, D. M. 1980. Biophysical Ecology. Springer-Verlag. New York. 611 pp.
- 21 Hartigan, J. A. 1974. Clustering algorithms. Wiley and Sons. New York. 351 pp.
- 22 Heydorn, R. P., R. M. Bizzell, J. A. Quirein, F. M. Ahottee, and C. A. Sumner. 1979a. Classification and mensuration of LACIE segments. LACIE Proceedings of Tech. Sessions. Vol. I. NASA/JSC p. 73-86.
- 23 Heydorn, R. P., M. C. Trichel, and J. D. Erickson. 1979b. Methods for segment wheat area estimation. LACIE Proceedings of Tech. Sessions. Vol II. NASA/JSC. p. 621-632.
- 24 Holliday, R. 1960a. Plant population and crop yield: part I (Review Article). Field Crop Abstr. 13:159-167.
- 25 Holliday, R. 1960b. Plant population and crop yield: part II (Review Article). Field Crop Abstr. 13:247-254.
- 26 Jackson, T. J., T. J. Schmutge, and J. R. Wang. 1981. Effects of vegetation on passive microwave estimates of soil moisture. Intern. Geosci. and Remote Sensing Symposium. IEEE. Washington, D. C. Vol I. p. 375-387.

- 27 Janza, F. J. 1975. Interaction mechanisms. In Manual of Remote Sensing, Vol I. Chapter 4. p. 75-179.
- 28 Johnson, S. 1967. Hierarchical clustering schemes. Psychometrika 32:241-254.
- 29 Kauth, R. J. and G. S. Thomas. 1976. The tasseled cap--a graphic description of the spectral-temporal development of agricultural crops as seen by Landsat. Proc. Symp. Machine Proc. of Remotely Sensed Data. LARS. IEEE. Cat No. 76.
- 30 Kirdyashev, K. P., A. A. Chukhlantsev, and A. M. Shutko. 1979. Microwave radiation of the earth's surface in the presence of a vegetative cover. Radio Eng. and Electronic Physics. 24:37-44.
- 31 Kubelka, P. and F. Munk. 1931. Ein Beitrag zur Optik der Farbanstriche. Z. Tech. Physik 12:593-601.
- 32 Lundien, J. R. 1971. Terrain analysis by electromagnetic means. Tech. Report 3-693. Report 5. U. S. Army Waterways Expt. Sta. Vicksburg, Miss. 85 pp.
- 33 MacDonald, R. B. 1979. Experiment design. Proceedings of Tech. Sessions: LACIE Symposium. Vol I. NASA/JSC p. 1-2.
- 34 McFarland, M. J. 1976. The correlation of Skylab L-band brightness temperatures with antecedent precipitation. Preprints Conf. on Hydrometeorology. Amer. Met. Soc. Ft Worth. p. 60-65.
- 35 Morain, S. A. and D. S. Simonett. 1967. K-band radar in vegetation mapping. Photogrammetry Eng. 33:730-740.
- 36 National Academy of Sciences. 1977. The world food and nutrition study: the potential contributions of research. National Research Council. Washington, D.C.
- 37 National Research Council. 1977. Microwave remote sensing from space for earth resource surveys. National Academy of Sciences. Washington, D. C., 139 pp.
- 38 Newton, R. W. 1977. Microwave sensing and its application to soil moisture detection. Remote Sensing Center Tech. Report RSC-81. Texas A&M University. 500 pp.
- 39 O'Neill, p. 1981. Personal Communication.
- 41 Orloci, L. 1978. Multivariate analysis in vegetation research. The Hague. Amsterdam. 451 pp.
- 42 Park, J. V. and D. W. Deering. 1981. Relationships between diffuse reflectance and vegetation canopy variables based on the radiative transfer theory. NASA Tech. Memo. 82067. 19 pp.

- 42 Peake, W. H., R. L. Riegler, and C. H. Schultz. 1966. The mutual interpretation of active and passive microwave sensor outputs. Proc. of Fourth Symp. on Remote Sensing of Environment. Ann Arbor, Mich. p.771-777.
- 43 Potter, J. F., E. M. Hsu, A. G. Houston, and D. E. Pitts. 1979. Accuracy and performance of LACIE area estimates. Proceedings of Tech. Sessions: LACIE Symposium. Vol. I. NASA/JSC. p. 527-574.
- 44 Richardson, A. J., C. L. Wiegand, H. W. Gausman, J. A. Cuellar, and A. H. Gerberman. 1975. Plant, soil and shadow reflectance components of row crops. Photogram. Eng. and Remote Sensing 41:1401-1407.
- 45 Richardson, A. J. and C. L. Wiegand. 1977. Distinguishing vegetation from soil background information. Photogram. Eng. and Remote Sensing 43:1541-1552.
- 46 Rouse, Jr., J. W., R. H. Haas, J. A. Schell, and D. W. Deering. 1973. Monitoring vegetation systems in the great plains with ERTS. Third ERTS Symp. NASA SP-351. Vol. I p. 309-317.
- 47 Schmugge, T. 1978. Remote sensing of surface soil moisture. J. Appl. Met. 17:1549-1557.
- 48 Schwarz, D. E. and F. Caspell. 1968. The use of radar in discrimination and identification of agricultural land use. Proc. 5th SRSE.
- 49 Sibley, R. 1973. Microwave emission and scattering from vegetated terrain. Tech. Rpt. RSC-44, Remote Sensing Center, Texas A&M University, College Station, Texas, 148 pp.
- 50 Simonett, D. S., J. E. Eagleman, A. R. Erhart, D. C. Rhodes, and D. E. Schwarz. 1967. The potential of radar as a remote sensor in agriculture. Center for Res. in Eng. Sci. CRES Report 61-21. Univ. of Kansas.
- 51 Swain, P. and B. Davis. 1979. Fundamentals of pattern recognition in remote sensing. In Remote Sensing: the Quantification Approach. Chp. 3 p. 136-187.
- 52 Tucker, C. J., J. H. Elgin, Jr., and J. E. McMurtrey III. 1979. Temporal spectral measurements of corn and soybean crops. Photogram. Eng. and Remote Sensing 45:643-653.
- 53 Ulaby, F. T. and J. E. Bare. 1979. Look direction modulation function of the radar backscattering coefficients of agricultural fields. Photogram. Eng. and Remote Sensing 45:1495-1506.
- 54 Ulaby, F. T., P. P. Battivala and M. C. Dobson. 1978. Microwave backscatter dependence on surface roughness, soil moisture, and soil texture, part I: bare soil. IEEE Trans. Geosci. Elect. GE-16:286-295.

- 55 Ulaby, F. T., P. P. Battivala, and J. E. Bare. 1980. Crop identification with L-band radar. *Photogram. Eng. and Remote Sensing* 46:101-105.
- 56 Ulaby, F. T., T. F. Bush, and P. P. Battivala. 1975. Radar response to vegetation II: 8-18 GHz band. *Trans. IEEE on antennas and Prop.* AP-23: 608-618.
- 57 Ulaby, F. T. and T. F. Bush. 1976a. Monitoring wheat growth with radar. *Photogram. Eng. and Remote Sensing* 42:557-568.
- 58 Ulaby, F. T. and T. F. Bush. 1976b. Corn growth as monitored by radar. *IEEE Trans. on Antennas and Prop.* AP-24:819-828.
- 59 Ulaby, F. T., R. V. Li, and K. S. Shanmugam. 1981. Crop classification by radar. *Intern. Geosci. and Remote Sensing Symp. Vol I.* p. 638-647.
- 60 Waite, W. P. and H. C. MacDonald. 1971. Vegetation penetration with K-band imaging radar. *Trans. IEEE Geosci. Elect.* GE-9:147-155.
- 61 Wang, J. R., R. W. Newton, J. W. Rouse, Jr. 1980. Passive microwave remote sensing of soil moisture: the effect of tilled row structure. *IEEE Trans. on Geosci. and Remote Sensing* GE-18: 296-302.
- 62 Wolfe, W. L. and G. J. Zissis. 1978. *The infrared handbook.* Office of Naval Research-ERIM. 1665 pp.
- 63 Wortman, S. 1976. Food and Agriculture. *Sci. Amer.* 235:31-39.

APPENDIX A
DATA QUALITY, CALIBRATION, AND OMISSIONS

At both Dalhart and Guymon, data were deleted for various reasons--quality and excessive aircraft attitude parameters. This chapter defines the questionable sensor and soil moisture data and the methods used for correcting the data sets. Each sensor system and soil moisture will be discussed in detail.

NS001/M²S

Most of the visible/infrared data were of good quality at both Dalhart and Guymon. One of the exceptions was the excessively noisy water absorption bands (bands 6 and 7) on 8/14/80 at Dalhart. Since no means were possible to correct the data, they were eliminated from further data analysis. Also, at Dalhart band 1 data for fields 6,8, 10,12 and 22 were deleted due to unstable calibration.

With the exception of band 9 (0.77-0.86 μm) M²S data at Guymon, the calibration information proved to be quite stable. Table A1a lists the equations used to convert raw digital counts to radiance values. Note band 9 had three different equations applicable at different periods of the experiment.

All of the working NS001 bands had less stable calibration information at Dalhart. Table A1b lists the equations used to convert digital counts to radiance values. Note that several bands had different calibration values on each flight day.

Calibration of the thermal band proved to be different for Guymon and Dalhart. The calibration, using the PRT-5 data, showed that at Guymon the low temperature calibration black body aboard the plane was

TABLE A1. Equations used to convert raw NS001/M²S digital counts (DC) to radiance values, R, (10⁻⁴ watts cm⁻²ster⁻¹) for Guymon (a) and Dalhart (b)

a.	channel 4	$R = \frac{10.46 \times 10^{-4}}{233} * (DC-12)$
	7	$R = \frac{9.61 \times 10^{-4}}{230} * (DC-13)$
	8	$R = \frac{8.14 \times 10^{-4}}{230} * (DC-14)$
	9	$R = \frac{6.98 \times 10^{-4}}{232} * (DC-12) (8/2, 8/5, \text{ and } 8/8)$
	9	$R = \frac{6.98 \times 10^{-4}}{100} * (DC-10) (8/11)$
	9	$R = \frac{6.98 \times 10^{-4}}{160} * (DC-17) (8/14)$
b.	channel 1	$R = \frac{1.96 \times 10^{-4}}{207} * (DC-1) (8/14 \text{ \& } 8/16 (Flt 1))$
	1	$R = \frac{1.96 \times 10^{-4}}{151} * (DC-1) (8/16 (Flt 2))$
	1	$R = \frac{1.96 \times 10^{-4}}{70} * (DC-1) (8/18)$
	2	$R = \frac{4.63 \times 10^{-4}}{210} * (DC-21) (8/14 - 8/16)$
	2	$R = \frac{4.63 \times 10^{-4}}{140} * (DC-21) (8/18)$
	3	$R = \frac{5.61 \times 10^{-4}}{224} * (DC-29) (8/14-8/16)$
	3	$R = \frac{5.61 \times 10^{-4}}{172} * (DC-29) (8/18)$
	4	$R = \frac{11.42 \times 10^{-4}}{232} * (DC-9) (8/14-8/16 (Flt 1))$
	4	$R = \frac{11.42 \times 10^{-4}}{171} * (DC-9) (8/16 (Flt 2))$

Continued

TABLE A1. (Continued)

4	$R = \frac{11.42 \times 10^{-4}}{107} * (\text{DC-8}) (8/18)$
5	$R = \frac{5.43 \times 10^{-4}}{232} * (\text{DC-8}) (8/14-8/16 (\text{Flt } 1))$
5	$R = \frac{5.43 \times 10^{-4}}{147} * (\text{DC-9}) (8/16 (\text{Flt } 2))$
5	$R = \frac{5.43 \times 10^{-4}}{107} * (\text{DC-9}) (8/18)$
6	$R = \frac{2.8 \times 10^{-3}}{222} * (\text{DC-12}) (8/16)$
6	$R = \frac{2.8 \times 10^{-3}}{166} * (\text{DC-12}) (8/18)$
7	$R = \frac{1.43 \times 10^{-3}}{110} * (\text{DC-16}) (8/16 \text{ \& } 8/18)$

too high while the high temperature calibration black body was measuring the proper temperature. This implied that low surface temperatures were as much as 5°C too high. At Dalhart, the opposite condition occurred. The low temperature calibration black body was reading the proper temperature while the high temperature calibration body was reading 5°C too low, suggesting that high surface temperatures were as much as 5°C too low.

The normalization solar correction factors ($\cos\theta_i$) for Dalhart are as follows: August 14, 5.7; August 16, (flight 1), 2.0; and (flight 2), 1.1; and August 18, 1.0. For Guymon, the normalization solar correction factors are August 2, 1.7; August 5, 1.6; August 8, 5.0; August 11, 1.0; August 14, 1.6 and August 17, 1.6. To normalize the two data sets, the Guymon data set required a multiplication factor of 1.3 to roughly match the radiance values at Dalhart.

Scatterometer

Due to excessive aircraft roll and drift, several look angles had to be eliminated at Dalhart and Guymon due to the uncertainty of the cell being within the field. At Dalhart, all active microwave data from one field had to be eliminated--field 16 on 8/18/80. Also, data at 40° and 45° look angles off nadir from several other fields on 8/18/80 were eliminated due to excessive drift (Table A2). At Guymon, flying conditions were much worse; consequently, data from more fields needed to be deleted. A complete list of omitted look angles are given in Table A3. Data from 8/11, 8/14, and 8/17/78 were most questionable.

TABLE A2. Questionable scatterometer data for Dalhart

Date	Field #	Questionable Analysis
8/14/80	All data is good	
8/16/80	All data is good	
8/18/80	L12 R2 20,8,18 L12 R2 14 L11 R3 16	45° (drift 9°) 40, 45° (drift 11°) All Angles

TABLE A3. Questionable scatterometer data for Guymon

Date	Field #	Questionable Analysis	
8/2/78	L1 R1 2,4,6,7,8,2x,1x	40°,45° (-8° drift, 2° roll)	
	L2 R1 10,13,14,15,2a,2x,1x	45° (-9° drift)	
	L1 R2 2,4,6,7,1a,2x,1x	45° (-9° drift)	
	L2 R2 15,17,2a	45° (-8° drift)	
8/8/78	L2 R1 17, 1x	all angles	
	L2 R2 2A	all angles	
	L4 R1 26	all angles	
	L1 R2 2,6,7	all angles	
8/11/78	L1 R1 6,8,2x	all angles	
	L3 R1 19,22,1x	all angles	
	L2 R1 2x,	all angles	
	L4 R1 24,25,27	all angles	
	L1 R2 4,6,7,1A	all angles	
	L3 R2 22	all angles	
	L2 R2 10,17	45° (-4° drift, 4° roll)	
		2A, 2X	all angles
	L4 R2 24,26,27	all angles	
8/14/78	L1 R2 4	all angles	
	L3 R2 19	40°,45° (-8° drift, 3° roll)	
	L2 R2 13	45° (9° drift)	
		10	40°,45° (9° drift, 3° roll)
	L1 R3 all fields	40°,45° (11° drift)	
	L3 R3 1x	all angles	
	L2 R3 13,14	all angles	
		15	45° (9° drift)
8/17/78	L3 R1 21,22	35°,40°,45° (-12° drift)	
	L4 R1 2x,24,25,26,27	35°,40°,45° (-12° drift)	
	L3 R2 21,22	all angles	
		1x,19,20	40°,45° (-10° drift)
	L4 R2 24,25,2x	45° (-9° drift)	
8/5/78	L1 R1 2	40°,45°	
	L4 R1 2x	40°,45°	
	L2 R2 2x	40°,45°	
	L4 R2 2x	40°,45°	

*delete these same fields for passive data

Signal cross-over between L-band polarizations was quantifiable by Blanchard and Theis (1981). The correction in the cross-polarized data proved to be less than 1 db for the Dalhart and Guymon data sets. There appears to be cross-over in the P band data collected at Guymon and Dalhart. Figure A1 represents like and cross polarized returns with look angle for the same field, 1X, which had rows perpendicular to the flight line. Note the large increase in the like polarized data at 20° look angle. Any rapid increase of σ^0 with increasing look angle can be directly attributed to large scale roughness characteristics. This characteristic is most apparent in like-polarized data; cross-polarized data suppress the roughness effect (Blanchard and Theis, 1981). Consequently, the rapid increase in σ^0 should not appear in the cross-polarized data. Figures A2a and A2b show P band like and cross pole responses from a milo field (25) at Guymon. Note the absence of any large increase in σ^0 at the 15° look angle for the cross pole data compared with the like pole data for the first four flight days. In the later flights the rows were tilled and the row height was increased causing a larger increase in σ^0 at 15° look angle in both like and cross polarizations. This is an example of data with minimum cross-talk. The cross-polarized data should have smaller decreases in σ^0 with higher look angles. Note, however, the P band response for field 1X in figure A1. At the 15° look angle, a large increase in σ^0 occurs in both like and cross pole data. This suggests excessive cross-talk between the like- and cross-polarized data. No attempt has been made to try and correct for the cross-talk in the P band cross polarized data. In addition, note the σ^0 differences in the P band cross polarized data between the

sets. There appears to be cross-over in the P band data collected at Guymon and Dalhart. Figure A1 represents like and cross polarized returns with look angle for the same field, 1X, which had rows perpendicular to the flight line. Note the large increase in the like polarized data at 20° look angle. Any rapid increase of σ^0 with increasing look angle can be directly attributed to large scale roughness characteristics. This characteristic is most apparent in like-polarized data; cross-polarized data suppress the roughness effect (Blanchard and Theis, 1981). Consequently, the rapid increase in σ^0 should not appear in the cross-polarized data. Figures A2a and A2b show P band like and cross pole responses from a milo field (25) at Guymon. Note the absence of any large increase in σ^0 at the 15° look angle for the cross pole data compared with the like pole data for the first four flight days. In the later flights the rows were tilled and the row height was increased causing a larger increase in σ^0 at 15° look angle in both like and cross polarizations. This is an example of data with minimum cross-talk. The cross-polarized data should have smaller decreases in σ^0 with higher look angles. Note, however, the P band response for field 1X in figure A1. At the 15° look angle, a large increase in σ^0 occurs in both like and cross pole data. This suggests excessive cross-talk between the like- and cross-polarized data. No attempt has been made to try and correct for the cross-talk in the P band cross polarized data. In addition, note the σ^0 differences in the P band cross polarized data between the first and fourth--flights as much as 5 db difference. For these reasons we questioned the 0.4 GHz data, especially at Guymon.

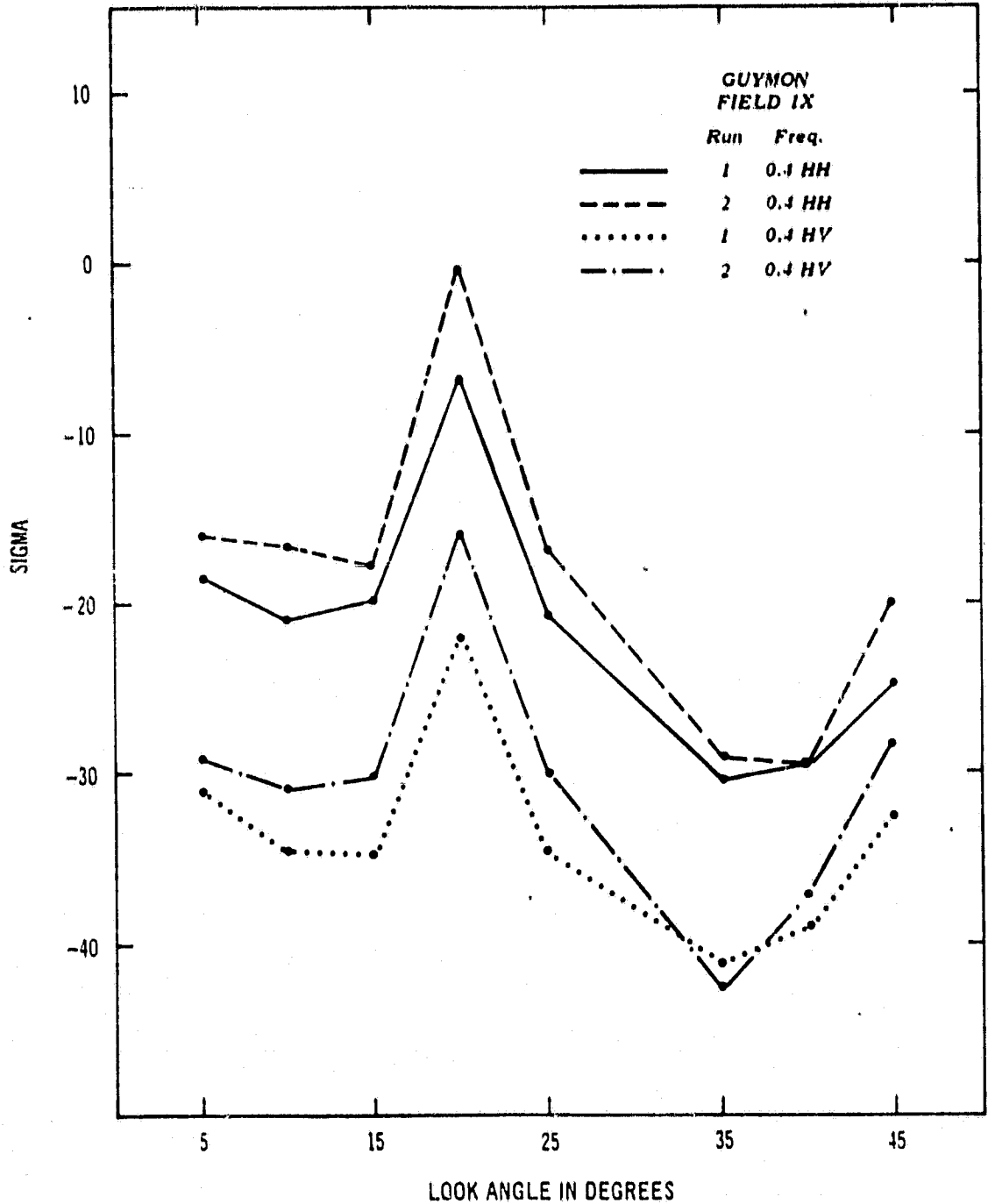


FIG. A1 Field 1X (sorghum) P band like and cross pole response with rows perpendicular to the flight line.

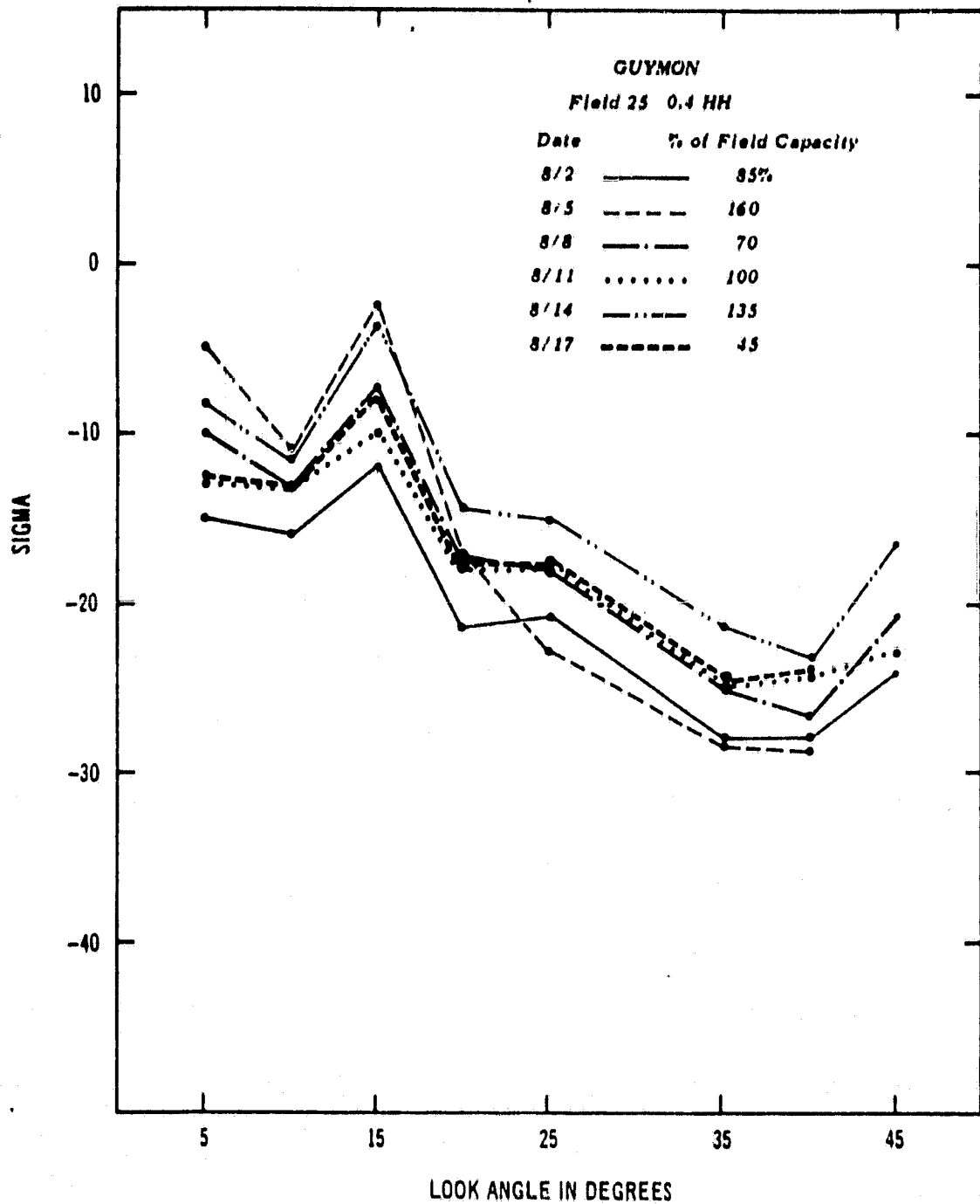


FIG. A2a Scatterometer response from the P band like pole system over field 25 (sorghum) with rows perpendicular to the flight line.

EX-112-103
 1970-1971

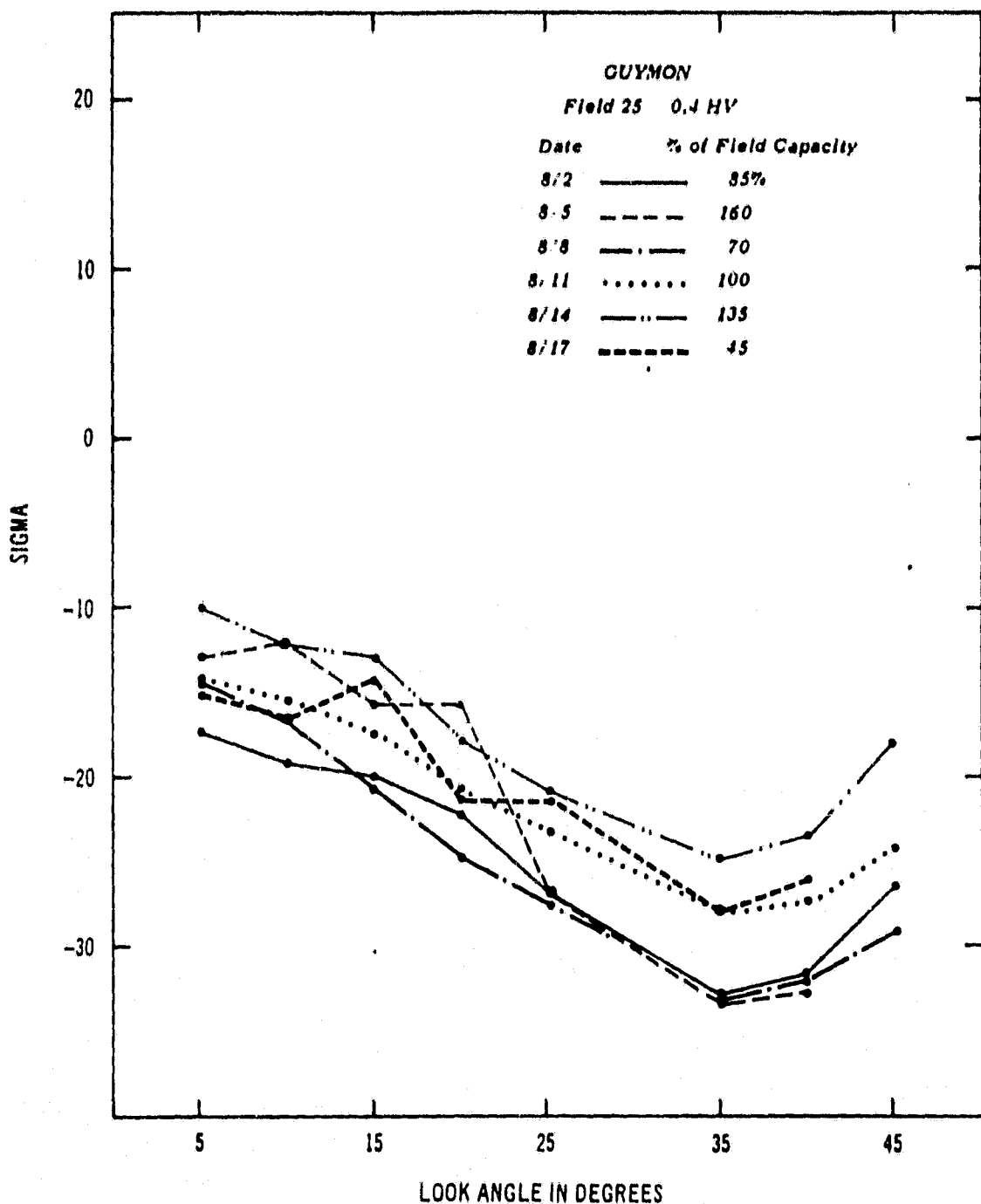


FIG. A2b Scatterometer response from the P band cross pole system over field 25 (sorghum) with rows perpendicular to the flight line.

Figure A3 represents like and cross polarized returns from the C and L band scatterometer for field 25 (sorghum), at Guymon. The field was tilled with rows perpendicular to the flight line and polarization. A slight increase in return at the 20° look angle for the L band like pole and cross pole is evident. The increase suggests again that some cross-talk may exist between the polarizations. Note the absence of cross-talk in the C-band data. A slight increase in the like-polarized data at 10° look angle off nadir is not evident in the cross polarized data. These data suggest that the other frequencies have some degree of cross-talk, but on a much smaller scale than the P band data.

Since scatterometer power was likely different for the Guymon and Dalhart data sets and no means exists for externally calibrating the system, normalizing the two scatterometer data sets proved to be quite difficult. Figures A4 through A7 represent scatterometer responses for each frequency from two bare fields having approximately the same surface soil moisture and roughness at Guymon (field 14) and Dalhart (field 19). Note the extreme difference in shift of L band like polarized data between the different frequencies. As much as a 15 dB difference exists between the two data sets in some instances. In addition, the shift in the like polarization for all frequencies is not constant nor is it even in the same direction. Note that in figures A4 and A6 field 14 is higher than 19 while in Figure A5 it is slightly lower and in Figure A7 they are alike. The far look angles appeared to be the most comparable between data sets. Since the differences

ORIGINAL PAGE IS
OF POOR QUALITY

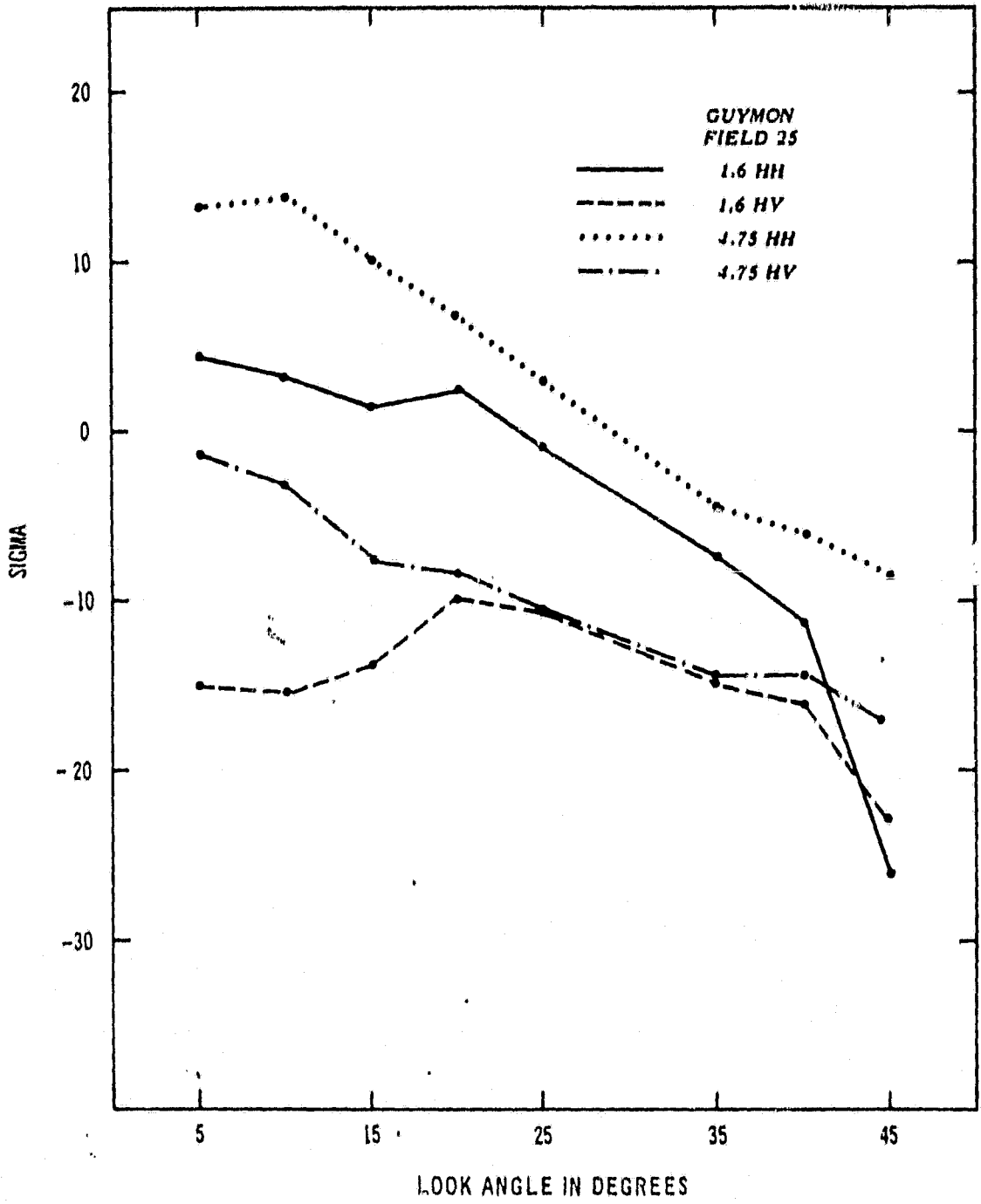


FIG. A3 Scatterometer response (C and L band like and cross pole) from field 25 at Dalhart on 8/16/80.

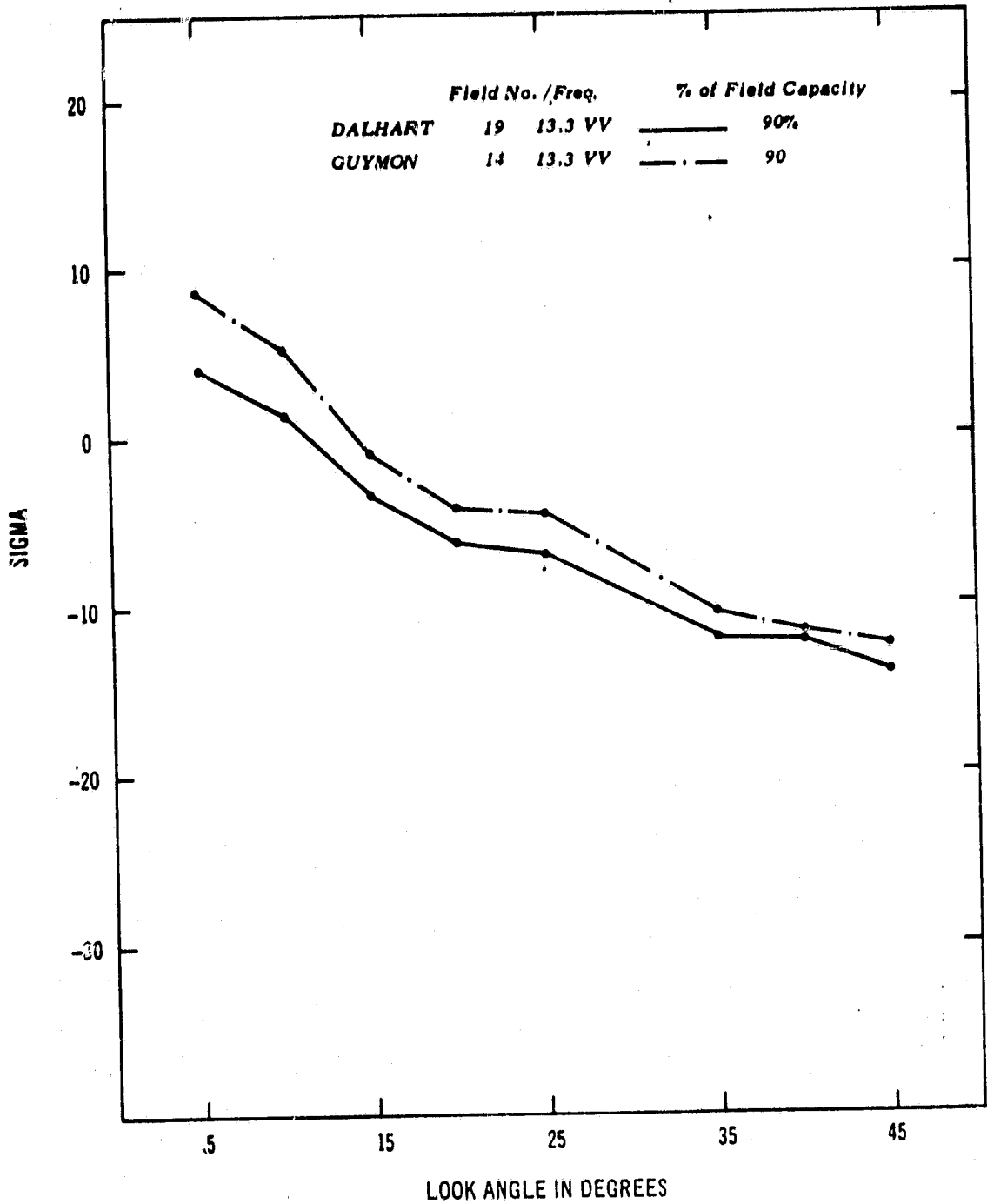


FIG. A4 Scatterometer response (K band like pole) from field 19 at Dalhart on 8/16/80 and field 14 at Guymon on 8/5/78. Soil moisture conditions were approximately 90% of field capacity.

ORIGINAL PAGE IS
OF POOR QUALITY

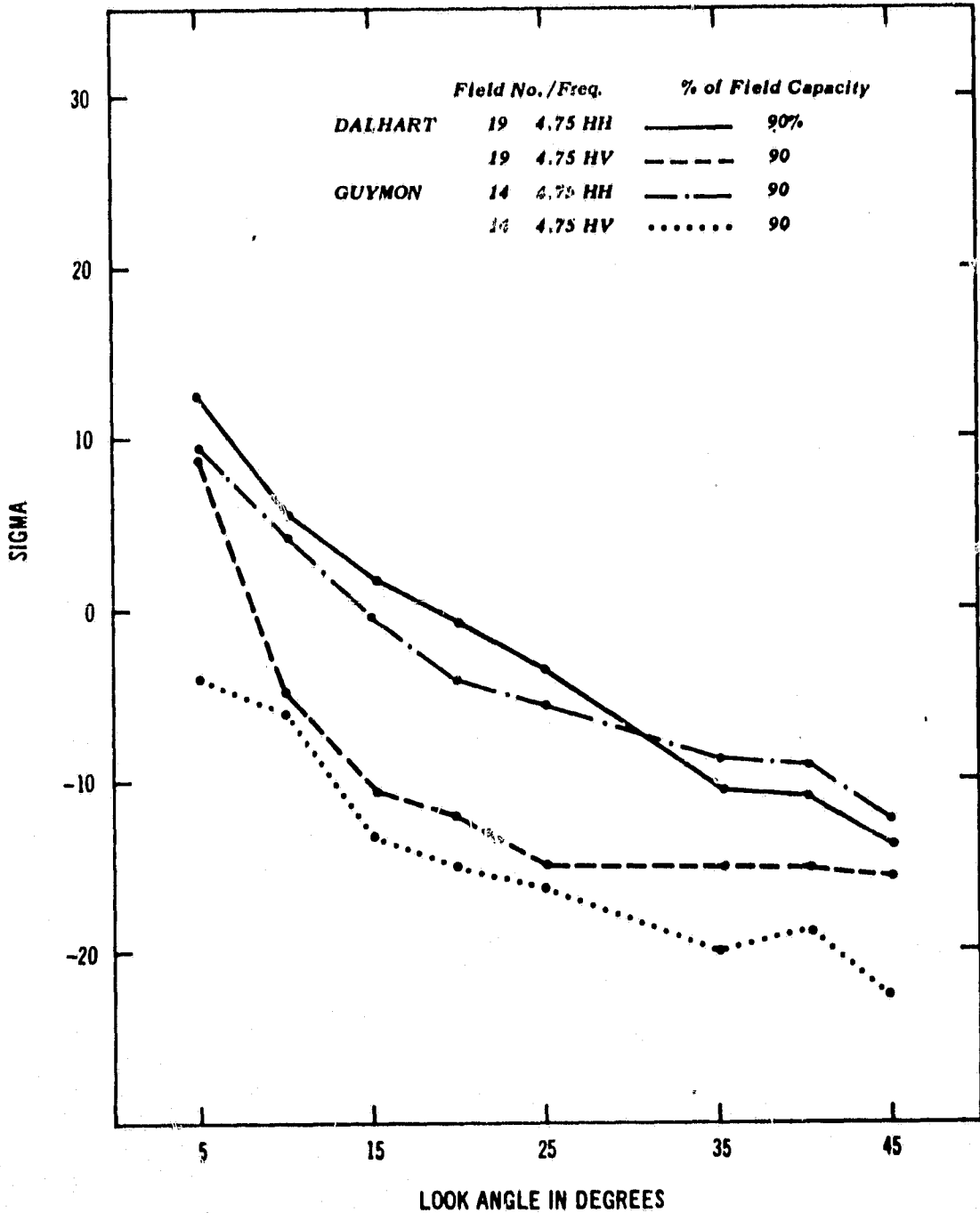


FIG. A5 Scatterometer response (C band like and cross pole) from field 19 at Dalhart on 8/16/80 and field 14 at Guymon on 8/5/78. Soil moisture conditions were approximately 90% of field capacity.

ORIGINAL PAGE IS
OF POOR QUALITY

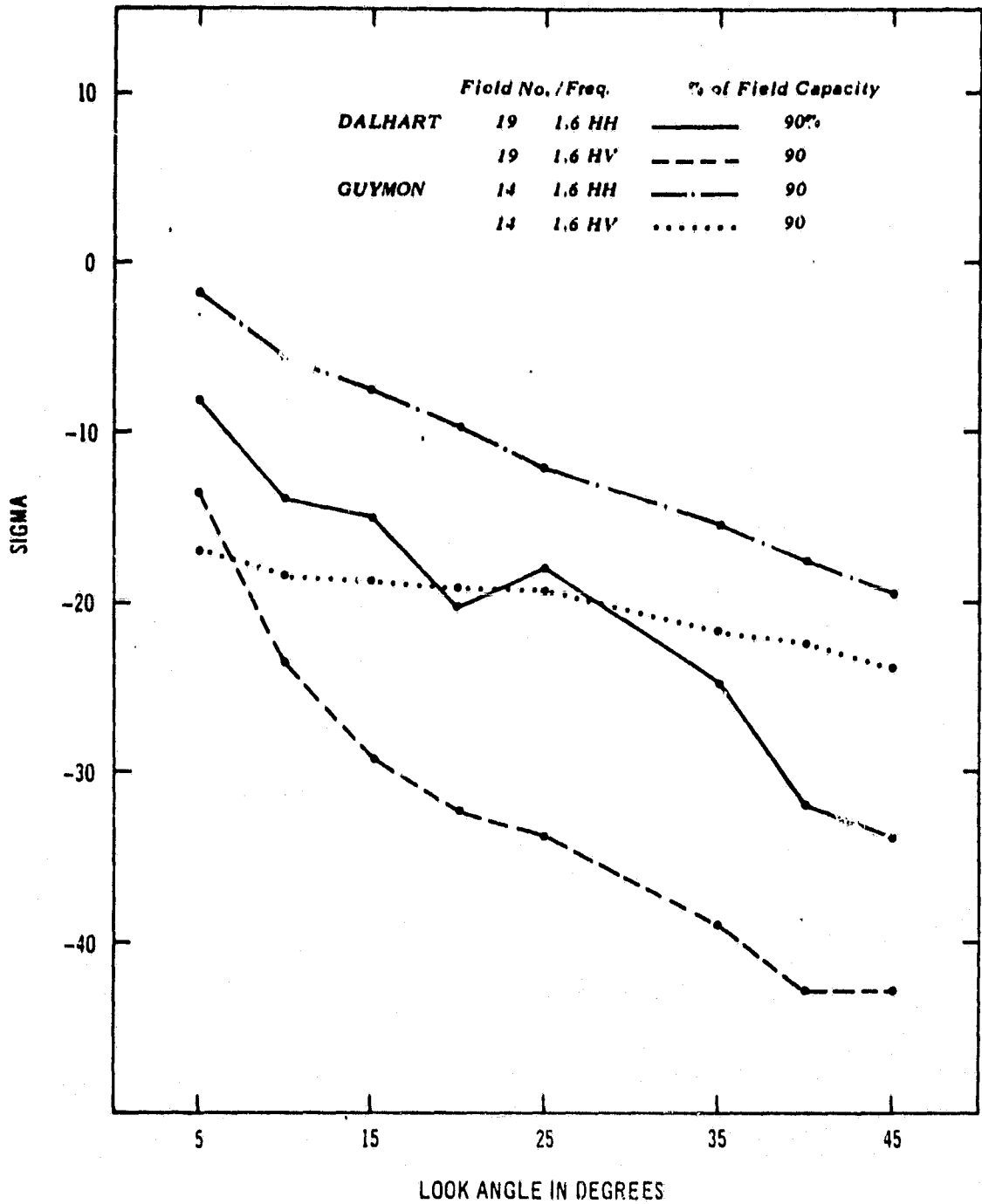


FIG. A6 Scatterometer response (L band like and cross pole) from field 19 at Dalhart on 8/16/80 and field 14 at Guymon on 8/5/78. Soil moisture conditions were approximately 90% of field capacity.

ORIGINAL PAGE IS
OF POOR QUALITY

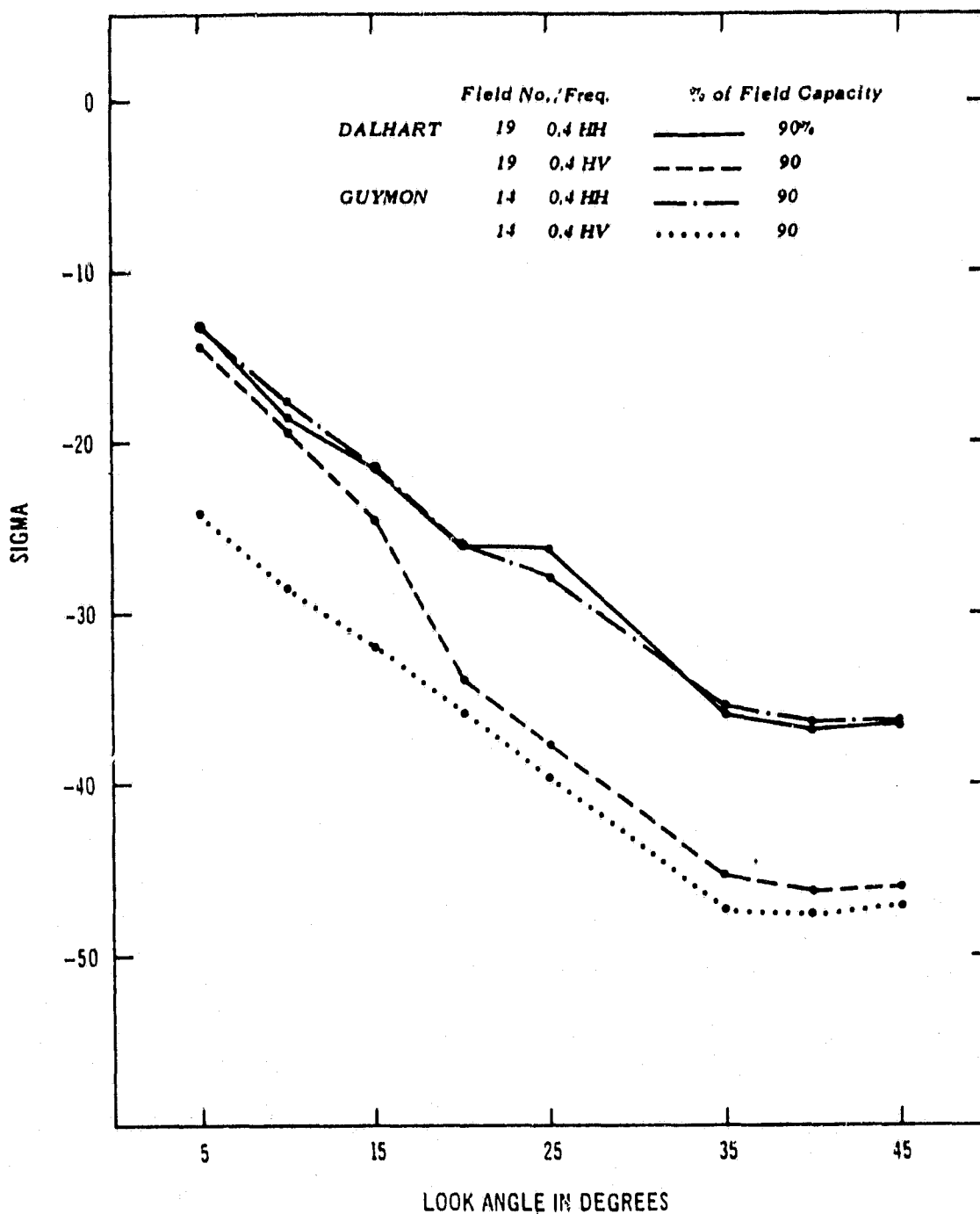


FIG. A7 Scatterometer response (P band like and cross pole) from field 19 at Dalhart on 8/16/80 and field 14 at Guymon on 8/5/78. Soil moisture conditions were approximately 90% of field capacity.

between data sets are not constant with look angle, normalization of the data proved unsuccessful. However, one normalization technique used to compare information within a data set was a data combination using a σ^0 difference between two look angles in the same data set. Since σ^0 is based on the algorithm of σ , a difference implied a ratio between σ --a common normalization technique. It was believed that this technique provided much information on vegetation while minimizing, soil moisture and surface roughness effects, depending on the frequency and polarization.

Passive Microwave (MFMR)

Since the passive microwave radiometer was oriented at a constant angle (3° from nadir), any excessive roll would imply questionable MFMR data. Consequently, any time the airplane had roll greater than 3.5° the field average MFMR data were deleted. Table A4 lists the deleted data. With the exception of data from one flight line at Guymon--L band data on 8/11/77 had highly erratic brightness temperatures on one occasion--brightness temperatures were quite stable. The highly variable brightness temperatures indicated local unmeasured variations in the field. Therefore, the following fields at Guymon were deleted from further analysis: fields 10, 13, 14, 15 and 17.

Soil Moisture

Each sensor has a different cell size. Consequently, to compare data, soil moisture field averages were determined for the area observed by each sensor by averaging only one sample located within the observed area. Unfortunately, in some cases, averaging point locations of soil moisture proved not to be a reliable field average.

TABLE A4. Guymon and Dalhart questionable MFMR data

Date	Field #	% Roll
8/8/78	L2 R1 1X	5.3
8/11/78	L3 R1 1X	4.9
	L1 R2 6	-5.1
	L4 R2 24	4.9
8/14/78	L2 R1 10,17,2a	5.4,-8,-5.6 respectively
	L4 R1 27	4.9
	L3 R3 1X	-4.8
8/17/78	L3 R2 22	5.0
8/18/78	L1 R1 16	6.3

These fields were deleted from the MFMR plots due to excessive roll; drift was not a factor.

For instance, several rows were irrigated and seen by the sensors but not sampled within the field. Also rainfall events occurred at Guymon between sampling periods--on 8/2 and 8/8/78. An attempt was made to correct the soil moisture by adding the amount of rainfall or irrigation, assuming complete infiltration. In some cases, this correction did a good job. But in the end the questionable soil moisture data were deleted from the data set. The fields at Guymon with deleted soil moisture data were for 8/2: 22, 27, 20, 25, 19, 24, 8/8: 1x, 2x, 2, 10 and 8/17: 1x, (line 2).

With the deletions, calibrations, and normalizations the Guymon and Dalhart data sets were complete as possible. Data for the significant channels are presented in Appendix B and C.

APPENDIX B

DALHART DATA SET

DALHART DATASET

C05=L BAND CROSS POLE 5 DEGREE LOOK ANGLE (DB)
 C40=L BAND CROSS POLE 40 DEGREE LOOK ANGLE (DB)
 P05=P BAND CROSS POLE 5 DEGREE LOOK ANGLE (DB)
 P40=P BAND CROSS POLE 40 DEGREE LOOK ANGLE (DB)
 Z15, Z20, Z35=NS001 BANDS 3, 4, AND 6 (10**(4) WATTS CM**(-2) ST**(-1))
 PVI=PERPENDICULAR VEGETATION INDEX (DIMENSIONLESS)
 TVI=TRANSFORMED VEGETATION INDEX (DIMENSIONLESS)
 SM01=0-2 CM VOLUMETRIC SOIL MOISTURE (X)
 PERIODS REPRESENT MISSING VALUES

FIELD	MONTH	DAY	C05	C40	P05	P40	Z15	Z20	Z35	PVI	TVI	SM01
17	AUG	14	1.14	-20.37	-22.99	-52.78	3.23	8.09	.	0.457	0.964	1.1
17	AUG	16	8.95	-14.98	-17.35	-52.16	2.85	5.91	16.71	0.168	0.948	6.1
17	AUG	16	9.75	-10.93	-17.33	-51.61	2.84	6.36	19.44	0.089	0.939	6.1
17	AUG	18	9.73	-14.87	-15.82	-52.38	3.52	7.57	22.97	0.023	0.930	2.2
18	AUG	14	.	.	-20.09	-52.92	3.39	8.47	.	0.477	0.964	1.1
18	AUG	16	9.66	-16.78	-18.51	-50.69	2.57	5.88	17.74	0.130	0.944	10.1
18	AUG	16	9.37	-15.25	-18.49	-46.54	2.87	6.27	19.76	0.027	0.934	10.1
18	AUG	18	2.55	-24.26	-17.41	-51.18	2.90	6.23	20.11	0.023	0.930	2.6

ORIGINAL PAGE IS
OF POOR QUALITY

DALHART DATASET
 C05=L BAND CROSS POLE 5 DEGREE LOOK ANGLE (DB)
 C40=L BAND CROSS POLE 40 DEGREE LOOK ANGLE (DB)
 P05=P BAND CROSS POLE 5 DEGREE LOOK ANGLE (DB)
 P40=P BAND CROSS POLE 40 DEGREE LOOK ANGLE (DB)
 Z15, Z20, Z35=NS001 BANDS 3, 4, AND 6 (10**(-4) WATTS CM**(-2) ST**(-1))
 PVI=PERPENDICULAR VEGETATION INDEX (DIMENSIONLESS)
 TVI=TRANSFORMED VEGETATION INDEX (DIMENSIONLESS)
 SK01=0-2 CM VOLUMETRIC SOIL MOISTURE (X)
 PERIODS REPRESENT MISSING VALUES

FIELD	MONTH	DAY	C05	C40	P05	P40	Z15	Z20	Z35	PVI	TVI	SK01
13	AUG	14	0.54	-20.13	-22.42	-54.18	3.47	10.56	.	1.279	1.003	3.8
13	AUG	16	18.29	-8.91	-3.79	-46.97	3.17	9.27	18.71	1.007	0.995	11.2
13	AUG	16	9.79	-6.33	-16.14	-50.37	3.03	9.74	21.25	1.330	1.012	8.9
13	AUG	18	7.52	-8.69	-15.76	-47.01	3.33	11.58	23.46	1.831	1.026	3.5
14	AUG	14	.	.	-19.16	-53.83	3.37	8.62	.	0.557	0.969	1.7
14	AUG	16	11.36	-8.87	-16.59	-51.32	3.47	9.05	23.88	0.646	0.973	9.5
14	AUG	16	11.04	-8.58	-16.42	-51.54	3.82	9.29	25.46	0.428	0.958	9.5
14	AUG	18	7.02	.	-14.56	.	3.82	9.47	25.33	0.497	0.961	4.2

DALHART DATASET
 C05=L BAND CROSS POLE 5 DEGREE LOOK ANGLE (DB)
 C40=L BAND CROSS POLE 40 DEGREE LOOK ANGLE (DB)
 P05=P BAND CROSS POLE 5 DEGREE LOOK ANGLE (DB)
 P40=P BAND CROSS POLE 40 DEGREE LOOK ANGLE (DB)
 Z15, Z20, Z35=NS001 BANDS 3, 4, AND 6 (16**(-4) WATTS CM**(-2) ST**(-1))
 PVI=PERPENDICULAR VEGETATION INDEX (DIMENSIONLESS)
 TVI=TRANSFORMED VEGETATION INDEX (DIMENSIONLESS)
 SM01=0-2 CM VOLUMETRIC SOIL MOISTURE (%)
 PERIODS REPRESENT MISSING VALUES

***** CROP=WEEDS *****												
FIELD	MONTH	DAY	C05	C40	P05	P40	Z15	Z20	Z35	PVI	TVI	SM01
3W	AUG	14	1.96	-17.17
3W	AUG	16	15.72	-5.17	-4.51	-48.55	2.19	9.88	16.58	2.153	1.066	13.2
3W	AUG	16	9.94	-1.94	.	.	2.56	10.16	19.14	1.931	1.047	8.9
3W	AUG	18	7.89	-5.18	.	.	2.77	12.26	20.95	2.623	1.064	4.7
4W	AUG	14
4W	AUG	16	8.82	-6.82	.	.	2.87	9.44	21.65	1.356	1.017	9.7
4W	AUG	16	11.22	-5.50	.	.	3.24	9.56	23.53	1.067	0.997	9.7
4W	AUG	18	7.54	.	.	.	3.04	10.02	22.45	1.439	1.017	3.5

DALHART DATASET

C05=L BAND CROSS POLE 5 DEGREE LOOK ANGLE (DB)
 C40=L BAND CROSS POLE 40 DEGREE LOOK ANGLE (DB)
 P05=P BAND CROSS POLE 5 DEGREE LOOK ANGLE (DB)
 P40=P BAND CROSS POLE 40 DEGREE LOOK ANGLE (DB)

Z15, Z20, Z35=NS001 BANDS 3, 4, AND 6 (10**(-4) WATTS CM**(-2) ST**(-1))
 PVI=PERPENDICULAR VEGETATION INDEX (DIMENSIONLESS)
 TVI=TRANSFORMED VEGETATION INDEX (DIMENSIONLESS)
 SM01=0-2 CM VOLUMETRIC SOIL MOISTURE (%)
 PERIODS REPRESENT MISSING VALUES

----- CROP=SORGHUM -----

FIELD	MONTH	DAY	C05	C40	P05	P40	Z15	Z20	Z35	PVI	TVI	SM01
V2	AUG	14	0.85	-11.3	-23.6	-52.0	1.24	12.89	.	4.276	1.151	.
V2	AUG	16	5.85	-2.1	-19.2	-45.1	1.16	11.89	12.38	3.936	1.150	.
V2	AUG	16	10.75	-0.8	-21.8	-49.6	1.39	12.49	15.05	3.978	1.140	.
V2	AUG	18	8.25	-4.5	-17.3	-46.8
V2	AUG	14	.	.	-26.0	-48.3	1.24	12.89	.	4.276	1.151	.
V2	AUG	16	1.16	11.89	12.38	3.936	1.150	.
V2	AUG	16	11.45	-0.1	-20.7	-46.9	1.39	12.49	15.05	3.978	1.140	.
V2	AUG	18
V6	AUG	14	2.65	-17.6	-25.7	-54.7
V6	AUG	16	4.26	12.63	14.70	1.432	0.998	.
V6	AUG	16	10.75	-7.4	-22.1	-51.9
V6	AUG	18	5.05	-9.2	-21.8	-53.5
V6	AUG	14	-0.05	-18.0	-25.8	-54.2
V6	AUG	16	11.15	-8.7	-21.4	-50.8	4.26	12.63	14.70	1.432	0.998	.
V6	AUG	16	10.05	-7.3	-23.0	-51.4
V6	AUG	18	2.65	-14.1	-20.8	-52.4

DALHART DATASET
 C05=L BAND CROSS POLE 5 DEGREE LOOK ANGLE (DB)
 C40=L BAND CROSS POLE 40 DEGREE LOOK ANGLE (DB)
 P05=P BAND CROSS POLE 5 DEGREE LOOK ANGLE (DB)
 P40=P BAND CROSS POLE 40 DEGREE LOOK ANGLE (DB)
 Z15, Z20, Z35=NS01 BANDS 3, 4, AND 6 (10**(-4) WATTS CM**(-2) ST**(-1))
 PVI=PERPENDICULAR VEGETATION INDEX (DIMENSIONLESS)
 TVI=TRANSFORMED VEGETATION INDEX (DIMENSIONLESS)
 SM01=0-2 CM VOLUMETRIC SOIL MOISTURE (%)
 PERIODS REPRESENT MISSING VALUES

CROP=PASTURE

FIELD	MONTH	DAY	C05	C40	P05	P40	Z15	Z20	Z35	PVI	TVI	SM01
05	AUG	14	3.49	-25.28	-24.70	-55.82	2.74	7.27	.	0.558	0.976	1.7
05	AUG	16	14.94	-13.28	-15.31	-43.91	2.53	6.78	19.92	0.548	0.978	7.3
05	AUG	16	11.81	-11.53	-15.48	-51.52	2.84	6.97	22.22	0.341	0.959	7.7
05	AUG	18	9.70	-14.72	-17.05	-53.63	3.22	7.79	24.58	0.339	0.956	5.3
06	AUG	14	.	.	-22.76	-55.63	2.87	7.36	.	0.485	0.969	1.3
06	AUG	16	11.16	-12.59	-18.30	-52.72	2.75	6.99	22.27	0.434	0.967	6.8
06	AUG	16	11.81	-11.60	-17.12	-52.99	2.90	7.03	23.18	0.314	0.957	6.8
06	AUG	18	5.92	-18.41	-14.27	-54.37	2.87	6.84	22.36	0.265	0.954	2.7

DALHART DATASET
 C05=L BAND CROSS POLE 5 DEGREE LOOK ANGLE (DB)
 C40=L BAND CROSS POLE 40 DEGREE LOOK ANGLE (DB)
 P05=P BAND CROSS POLE 5 DEGREE LOOK ANGLE (DB)
 P40=P BAND CROSS POLE 40 DEGREE LOOK ANGLE (DB)
 Z15, Z20, Z35=NS001 BANDS 3, 4, AND 6 (10**(=-4) MATTS CM**(=-2) ST**(=-1))
 PVI=PERPENDICULAR VEGETATION INDEX (DIMENSIONLESS)
 TVI=TRANSFORMED VEGETATION INDEX (DIMENSIONLESS)
 SM01=0-2 CM VOLUMETRIC SOIL MOISTURE (X)
 PERIODS REPRESENT MISSING VALUES

FIELD	MONTH	DAY	C05	C40	P05	P40	Z15	Z20	Z35	PVI	TVI	SM01
03	AUG	14	-2.35	-18.70	-19.80	-51.30	1.37	8.09	.	2.149	1.100	9.4
03	AUG	16	8.15	-4.96	-19.55	-52.68	1.76	11.40	16.10	3.177	1.110	6.3
03	AUG	16	9.71	-3.96	-20.21	-52.00	1.97	11.10	16.90	2.063	1.095	6.3
03	AUG	18	7.85	-5.59	-21.22	-54.13	2.18	12.98	18.89	3.458	1.101	2.2
04	AUG	14	.	.	-21.58	-53.96	2.16	12.29	.	3.192	1.096	2.9
04	AUG	16	10.05	-4.28	-21.90	-51.07	1.84	12.07	16.61	3.390	1.112	5.6
04	AUG	16	9.88	-3.75	-22.22	-53.69	1.96	11.36	16.79	2.986	1.098	5.8
04	AUG	18	2.56	-10.30	-18.91	-52.15	1.83	11.20	16.05	3.031	1.104	1.7

CROP=MILLET

DALHART DATASET

C05=L BAND CROSS POLE 5 DEGREE LOOK ANGLE (DB)
C40=L BAND CROSS POLE 40 DEGREE LOOK ANGLE (DB)
P05=P BAND CROSS POLE 5 DEGREE LOOK ANGLE (DB)
P40=P BAND CROSS POLE 40 DEGREE LOOK ANGLE (DB)

Z15, Z20, Z35=NS001 BANDS 3, 4, AND 6 (10**(-4) WATTS CM**(-2) ST**(-1))

PVI=PERPENDICULAR VEGETATION INDEX (DIMENSIONLESS)
TVI=TRANSFORMED VEGETATION INDEX (DIMENSIONLESS)

SM01=0-2 CM VOLUMETRIC SOIL MOISTURE (X)
PERIODS REPRESENT MISSING VALUES

----- CROP=CORIN -----

FIELD	MONTH	DAY	COE	C40	P05	P40	Z15	Z20	Z35	PVI	TVI	SM01
09	AUG	16	10.91	-0.54	-8.90	-38.45	0.71	12.00	8.83	4.385	1.178	13.2
09	AUG	16	10.52	0.27	-17.15	-42.98	0.70	11.81	8.55	4.317	1.178	13.2
09	AUG	18	8.99	-3.74	-13.37	-43.01	0.84	12.98	9.68	4.879	1.174	14.3
10	AUG	14	11.39	0.28	-20.84	-44.29	0.71	11.25	.	4.076	1.175	4.9
10	AUG	16	8.98	-1.02	-18.09	-44.20	0.80	13.57	10.10	4.961	1.178	14.4
10	AUG	16	9.72	0.59	-17.86	-44.38	0.73	12.51	9.12	4.579	1.179	14.4
10	AUG	18	4.39	-6.46	-16.23	-45.71	0.76	12.27	9.24	4.459	1.176	9.0
11	AUG	14	3.76	-10.51	-20.10	-43.54	0.72	12.55	.	4.587	1.178	17.8
11	AUG	16	8.42	-2.32	-11.40	-38.43	0.69	12.45	8.70	4.595	1.181	39.0
11	AUG	16	11.02	-0.27	-15.57	-40.70	0.64	12.16	8.23	4.516	1.183	39.0
11	AUG	18	9.59	-1.74	-16.41	-41.46	0.76	13.16	9.17	4.830	1.179	29.6
12	AUG	14	10.66	0.28	-17.57	-41.79	0.64	10.93	.	3.999	1.178	22.9
12	AUG	16	8.55	-0.46	-14.97	-42.75	0.79	13.91	10.37	5.111	1.180	26.3
12	AUG	16	10.51	0.19	-14.81	-42.49	0.70	12.88	9.20	4.766	1.182	26.3
12	AUG	18	5.29	-6.64	-16.54	-41.72	0.68	12.40	8.75	4.583	1.182	24.3

3

DALHART DATASET

C05=L BAND CROSS POLE 5 DEGREE LOOK ANGLE (DB)
 C40=L BAND CROSS POLE 40 DEGREE LOOK ANGLE (DB)
 P05=P BAND CROSS POLE 5 DEGREE LOOK ANGLE (DB)
 P40=P BAND CROSS POLE 40 DEGREE LOOK ANGLE (DB)

Z15, Z20, Z35=NS001 BANDS 3, 4, AND 6 (10)*(=4) WATTS CM*(=2) ST*(=1)

PVI=PERPENDICULAR VEGETATION INDEX (DIMENSIONLESS)
 TVI=TRANSFORMED VEGETATION INDEX (DIMENSIONLESS)

SM01=0-2 CM VOLUMETRIC SOIL MOISTURE (X)

PERIODS REPRESENT MISSING VALUES

CRDP=CORN

FIELD	MONTH	DAY	C05	C40	P05	P40	Z15	Z20	Z35	PVI	TVI	SM01
01	AUG	14	4.20	-11.25	-21.40	-46.83	0.96	9.89	.	3.272	1.150	6.6
01	AUG	16	10.74	-1.91	-17.54	-41.78	0.93	10.52	10.18	3.565	1.156	13.2
01	AUG	16	10.28	-0.32	-19.61	-53.87	0.90	10.23	9.71	3.472	1.157	13.1
01	AUG	18	9.43	-5.49	-20.10	-44.44	1.13	11.29	11.75	3.709	1.148	8.1
02	AUG	14	.	.	-22.65	-45.19	1.15	10.74	.	3.460	1.143	4.8
02	AUG	16	10.10	-1.52	-18.60	-43.90	1.13	11.21	11.17	3.669	1.147	17.7
02	AUG	16	10.54	0.57	-16.40	-43.78	1.06	10.12	10.28	3.282	1.145	16.6
02	AUG	18	3.72	-8.03	-16.86	-46.51	1.09	9.77	10.58	3.101	1.139	8.6
07	AUG	14	2.86	-11.12	-21.81	-43.62	0.83	12.70	.	4.572	1.173	14.4
07	AUG	16	5.12	-1.94	-14.68	-37.74	0.86	13.37	9.93	4.829	1.175	18.3
07	AUG	16	11.18	-0.90	-17.33	-41.82	0.75	12.84	8.92	4.701	1.179	19.1
07	AUG	18	7.68	-3.94	-15.85	-42.34	0.89	13.88	9.94	5.016	1.175	19.2
08	AUG	14	11.23	-0.03	-20.98	-42.37	0.80	12.23	.	4.397	1.173	15.5
08	AUG	16	9.16	-1.70	-17.28	-41.31	0.97	14.44	10.82	5.176	1.172	19.3
08	AUG	16	5.74	-0.52	-18.13	-41.80	0.80	13.58	9.75	4.754	1.177	19.3
08	AUG	18	5.36	-7.43	-17.77	-42.02	0.85	12.82	9.35	4.602	1.173	12.7
09	AUG	14	3.39	-10.25	-20.15	-46.00	0.79	11.98	.	4.307	1.173	4.4

DATE: 11/21/83
 OF POOR QUALITY

ORIGINAL COVERED
OF POOR QUALITY

DALHART DATASET
 C05=L BAND CROSS POLE 5 DEGREE LOOK ANGLE (DB)
 C40=L BAND CROSS POLE 40 DEGREE LOOK ANGLE (DB)
 P05=P BAND CROSS POLE 5 DEGREE LOOK ANGLE (DB)
 P40=P BAND CROSS POLE 40 DEGREE LOOK ANGLE (DB)
 Z15, Z20, Z35=N5901 BANDS 3, 4, AND 6 (10**(-4) WATTS CM**(-2) ST**(-1))
 PVI=PERPENDICULAR VEGETATION INDEX (DIMENSIONLESS)
 TVI=TRANSFORMED VEGETATION INDEX (DIMENSIONLESS)
 SM01=0-2 CM VOLUMETRIC SOIL MOISTURE (%)
 PERIODS REPRESENT MISSING VALUES

CROP=BARE

FIELD	MONTH	DAY	C05	C40	P05	P40	Z15	Z20	Z35	PVI	TVI	SM01
21	AUG	16	17.45	-11.32	-11.17	-47.11	3.17	7.36	21.16	0.207	0.948	6.9
21	AUG	16	11.33	-10.08	-14.98	-50.62	3.48	7.91	23.27	0.152	0.942	7.0
21	AUG	18	9.13	-13.85	-15.41	-52.40	4.19	9.15	26.74	0.029	0.933	2.0
22	AUG	14	.	.	-19.07	-54.21	2.47	6.22	.	0.774	0.965	0.8
22	AUG	16	8.61	-11.38	-13.82	-52.61	3.00	8.33	24.10	0.222	0.947	6.8
22	AUG	16	10.26	-10.94	-13.76	-52.86	3.75	8.44	25.02	0.131	0.940	6.8
22	AUG	18	4.31	-17.72	-15.76	-52.71	3.84	8.35	24.78	0.015	0.933	1.9
38	AUG	14	-0.07	-23.08
38	AUG	16	19.86	-12.65	-3.06	-45.39	3.39	6.05	22.70	0.293	0.952	9.3
38	AUG	16	5.64	-10.72	.	.	3.71	8.46	24.45	0.184	0.944	9.2
38	AUG	18	7.15	-12.20	.	.	4.42	10.06	28.49	0.153	0.940	2.3
48	AUG	14
48	AUG	16	13.50	-10.45	.	.	3.77	8.85	24.98	0.289	0.950	9.3
48	AUG	16	10.86	-11.65	.	.	4.03	9.13	26.17	0.171	0.942	9.3
48	AUG	18	6.52	-15.89	.	.	4.16	9.26	26.55	0.110	0.938	4.6

DALHART DATASET
 C05=L BAND CROSS POLE 5 DEGREE LOOK ANGLE (DB)
 C40=L BAND CROSS POLE 40 DEGREE LOOK ANGLE (DB)
 P05=P BAND CROSS POLE 5 DEGREE LOOK ANGLE (DB)
 P40=P BAND CROSS POLE 40 DEGREE LOOK ANGLE (DB)
 Z15, Z20, Z35=NS001 BANDS 3, 4, AND 5 (10**(-4) WATTS CM**(-2) ST**(-1))
 PVI=PERPENDICULAR VEGETATION INDEX (DIMENSIONLESS)
 TVI=TRANSFORMED VEGETATION INDEX (DIMENSIONLESS)
 SM01=0-2 CM VOLUMETRIC SOIL MOISTURE (Z)
 PERIODS REPRESENT MISSING VALUES

CROP=BARE

FIELD	MONTH	DAY	C05	C40	P05	P40	Z15	Z20	Z35	PVI	TVI	SM01
15	AUG	14	1.42	-21.34	-21.64	-54.05	2.33	5.56	.	0.216	0.954	4.7
15	AUG	16	14.45	-12.87	-11.49	-49.53	2.55	5.83	18.63	0.131	0.944	14.9
15	AUG	16	9.55	-13.23	-16.11	-52.14	2.84	6.34	20.20	0.080	0.939	16.3
15	AUG	18	8.24	-12.44	-17.03	-52.19	3.61	7.63	23.92	0.077	0.926	7.1
16	AUG	14	.	.	-19.42	-52.30	2.14	5.18	.	0.227	0.556	4.7
16	AUG	16	9.14	-10.17	-15.31	-52.01	2.99	6.76	21.24	0.119	0.942	11.3
16	AUG	16	9.45	-8.70	-16.40	-52.00	3.31	7.29	22.65	0.055	0.936	12.1
16	AUG	18	3.32	7.05	22.09	0.056	0.927	3.7
19	AUG	14	2.22	-24.60	-25.25	-53.45	2.80	7.02	.	0.397	0.964	1.4
19	AUG	16	8.71	-14.95	-14.37	-46.30	3.79	8.47	23.61	0.109	0.939	8.1
19	AUG	16	11.71	-13.79	-18.92	-49.20	4.18	9.15	25.98	0.043	0.934	8.1
19	AUG	18	5.13	-15.75	-16.13	-52.45	4.86	10.35	29.28	0.077	0.928	2.6
20	AUG	14	.	.	-20.40	-51.17	3.13	7.90	.	0.466	0.965	0.9
20	AUG	16	7.25	-14.93	-17.03	-48.83	4.33	9.75	27.46	0.156	0.941	7.2
20	AUG	16	9.97	-14.48	-15.95	-48.77	4.37	9.90	27.94	0.179	0.942	7.2
20	AUG	18	2.15	-21.34	-15.42	-49.69	4.53	9.79	28.31	0.012	0.931	2.0
21	AUG	14	3.44	-21.55	-21.53	-53.32	2.38	5.97	.	0.347	0.965	1.1

APPENDIX C
GUYMON DATA SET

GUYMON DATA SET
 C05=L BAND CROSS POLE 5 DEGREE LOCK ANGLE (DB)
 C40=L BAND CROSS POLE 40 DEGREE LOCK ANGLE (DB)
 P05=P BAND CROSS POLE 5 DEGREE LOCK ANGLE (DB)
 P40=P BAND CROSS POLE 40 DEGREE LOCK ANGLE (DB)
 Z10, Z15, Z25=MKS BANDS 4, 7, AND 9 (10*((-4) WATTS CH00(-2) ST00(-1))
 PVI=PERPENDICULAR VEGETATION INDEX (DIMENSIONLESS)
 TVI=TRANSFORMED VEGETATION INDEX (DIMENSIONLESS)
 SM01=0-2 CM VOLUMETRIC SOIL MOISTURE (X)
 PERIODS REPRESENT MISSING VALUES

----- CROP=ALFALFA -----

FIELD	MCNTH	DAY	RUN	C05	C40	P05	P40	Z10	Z15	Z25	PVI	TVI	SM01
4	AUG	2	1	-25.80	.	.	.	0.82	0.46	7.50	2.727	1.177	22.0
4	AUG	2	2	-23.50	-42.30	-4.10	-16.58	.	.	.	2.727	1.177	17.9
4	AUG	5	1	-26.90	-48.30	-4.16	-18.46	0.80	0.43	7.41	2.716	1.179	16.7
4	AUG	5	2	-24.70	-49.00	2.716	1.179	16.7
4	AUG	8	1	-24.20	-51.30	15.90	0.60	0.80	0.40	8.25	3.096	1.186	21.3
4	AUG	8	2	-23.90	-49.70	3.096	1.186	20.5
4	AUG	11	1	-27.24	-46.28	15.40	-2.40	0.70	0.40	7.85	2.928	1.184	9.9
4	AUG	11	2	2.928	1.184	9.9
4	AUG	14	1	-21.14	.	-4.62	.	0.75	0.43	7.94	2.939	1.182	20.5
4	AUG	14	2	2.939	1.182	20.5
4	AUG	17	1	-25.03	-46.40	-6.11	-24.01	0.74	0.42	7.55	2.784	1.181	7.3
4	AUG	17	2	-24.60	-47.40	2.784	1.181	7.3
13	AUG	2	1	-24.19	-43.19	.	.	0.99	0.73	6.80	2.188	1.143	14.2
13	AUG	2	2	-23.57	-41.60	-3.94	-18.41	.	.	.	2.188	1.143	15.9
13	AUG	5	1	-23.77	-45.28	-4.61	-16.58	0.91	0.61	6.77	2.285	1.155	29.8
13	AUG	5	2	-22.70	-44.00	2.285	1.155	29.8
13	AUG	8	1	-20.94	-46.19	-1.99	-18.36	1.10	0.65	9.60	3.435	1.172	23.5

GUYMON DATA SET
 C05=L BAND CROSS POLE 5 DEGREE LOCK ANGLE (DB)
 C40=L BAND CROSS POLE 40 DEGREE LOCK ANGLE (DB)
 P05=P BAND CROSS POLE 5 DEGREE LOCK ANGLE (DB)
 P40=P BAND CROSS POLE 40 DEGREE LOCK ANGLE (DB)
 Z10, Z15, Z25=MMS BANDS 4, 7, AND 9 (10*(+4) WATTS CM**(2) ST**(-1))
 PVI=PERPENDICULAR VEGETATION INDEX (DIMENSIONLESS)
 TVI=TRANSFORMED VEGETATION INDEX (DIMENSIONLESS)
 SM01=0-2 CM VOLUMETRIC SOIL MOISTURE (X)
 PERIODS REPRESENT MISSING VALUES

FIELD	MCNTH	DAY	RUN	C05	C40	P05	P40	Z10	Z15	Z25	PVI	YVI	SM01
13	AUG	8	2	-21.50	-44.79	3.435	1.172	23.5
13	AUG	11	1	-21.00	-38.90	.	.	0.86	0.58	7.52	2.626	1.165	13.4
13	AUG	11	2	-22.40	-38.80	-3.90	-17.22	.	.	.	2.626	1.165	14.1
13	AUG	14	1	0.70	0.43	6.27	2.238	1.171	8.1
13	AUG	14	2	-19.80	-46.50	-2.78	-20.31	.	.	.	2.238	1.171	8.1
13	AUG	17	1	-22.30	-43.20	-3.64	-21.23	0.86	0.53	7.87	2.818	1.172	23.0
13	AUG	17	2	-22.30	-44.30	2.818	1.172	23.0
22	AUG	2	1	-22.00	-46.90	.	.	0.92	0.63	6.88	2.313	1.154	.
22	AUG	2	2	-23.50	-45.80	-4.81	-19.28	.	.	.	2.313	1.154	.
22	AUG	5	1	-21.04	-46.81	-4.45	-19.50	0.96	0.61	7.39	2.545	1.161	21.1
22	AUG	5	2	-18.40	-46.30	2.545	1.161	21.7
22	AUG	8	1	-19.73	-47.60	13.60	-2.40	0.70	0.40	6.30	2.278	1.175	21.6
22	AUG	8	2	-18.89	-48.40	2.278	1.175	22.5
22	AUG	11	1	0.84	0.47	8.18	3.003	1.155	16.6
22	AUG	11	2	3.003	1.180	24.5
22	AUG	14	1	-22.21	-44.72	-3.74	-19.52	0.82	0.45	8.99	3.361	1.185	19.4
22	AUG	14	2	-21.30	-39.70	3.361	1.185	19.4

GUYMON DATA SET
 C05=L BAND CROSS POLE 5 DEGREE LOOK ANGLE (DB)
 C40=L BAND CROSS POLE 40 DEGREE LOOK ANGLE (DB)
 P05=P BAND CROSS POLE 5 DEGREE LOOK ANGLE (DB)
 P40=P BAND CROSS POLE 40 DEGREE LOOK ANGLE (DB)
 Z10, Z15, Z25=MMS BANDS 4, 7, AND 9 (10**(-4) WATTS CM**(-2) ST**(-1))
 PVI=PERPENDICULAR VEGETATION INDEX (DIMENSIONLESS)
 TVI=TRANSFORMED VEGETATION INDEX (DIMENSIONLESS)
 SM01=0-2 CM VOLUMETRIC SOIL MOISTURE (%)
 PERIODS REPRESENT MISSING VALUES

CROP=ALFALFA

FIELD	MONTH	DAY	RUN	C05	C40	P05	P40	Z10	Z15	Z25	PVI	TVI	SM01
22	AUG	17	1	-17.89	.	-3.47	.	1.15	0.98	5.78	1.534	1.100	11.8
22	AUG	17	2	1.534	1.100	11.8
27	AUG	2	1	-25.00	49.50	.	.	1.22	0.95	7.14	2.131	1.125	.
27	AUG	2	2	-23.35	-49.10	2.131	1.125	.
27	AUG	5	1	-21.76	-48.80	-3.51	-24.02	1.10	0.80	6.48	1.991	1.131	11.2
27	AUG	5	2	-17.00	-46.24	1.951	1.131	15.4
27	AUG	8	1	-19.76	-50.80	15.40	-3.10	1.15	0.70	8.20	2.803	1.159	15.6
27	AUG	8	2	-16.30	-49.40	2.803	1.159	15.6
27	AUG	11	1	0.95	0.57	8.34	2.979	1.171	23.2
27	AUG	11	1	2.979	1.171	23.2
27	AUG	14	1	-15.91	-47.50	.	.	0.91	0.51	9.46	3.503	1.182	12.1
27	AUG	14	2	-19.90	-46.30	-3.81	-21.12	.	.	.	3.503	1.182	8.9
27	AUG	17	1	-20.39	.	.	.	1.39	1.15	6.91	1.853	1.102	4.3
27	AUG	17	2	-15.40	-47.30	-4.43	-21.99	.	.	.	1.853	1.102	5.5

GUYMON DATA SET
 C05=L BAND CROSS POLE 5 DEGREE LOOK ANGLE (DB)
 C40=L BAND CROSS POLE 40 DEGREE LOOK ANGLE (DB)
 P05=P BAND CROSS POLE 5 DEGREE LOOK ANGLE (DB)
 P40=P BAND CROSS POLE 40 DEGREE LOOK ANGLE (DB)
 Z10, Z15, Z25=MWS BANDS 4, 7, AND 9 (10**(-4) WATTS CM**(-2) ST**(-1))
 PVI=PERPENDICULAR VEGETATION INDEX (DIMENSIONLESS)
 TVI=TRANSFORMED VEGETATION INDEX (DIMENSIONLESS)
 SK01=0-2 CM VOLUMETRIC SOIL MOISTURE (X)
 PERIODS REPRESENT MISSING VALUES

----- CROP=BARE -----

FIELD	MCNTH	DAY	RUN	C05	C40	P05	P40	Z10	Z15	Z25	PVI	TVI	SK01
2	AUG	2	1	-25.00	.	.	.	1.05	1.22	2.89	0.104	0.952	2.5
2	AUG	2	2	-28.40	-49.60	-6.11	-23.12	.	.	.	0.104	0.952	2.7
2	AUG	5	1	-25.70	.	-4.81	.	1.22	1.42	3.54	0.155	0.963	10.5
2	AUG	5	2	-24.10	-48.10	0.155	0.963	11.6
2	AUG	8	1	-25.57	-48.50	16.20	-2.70	0.95	1.10	2.95	0.238	0.978	.
2	AUG	8	2	0.238	0.978	.
2	AUG	11	1	-24.39	-46.70	12.40	-11.20	1.73	1.97	4.58	0.132	0.948	5.2
2	AUG	11	2	-20.30	-45.60	0.132	0.948	5.2
2	AUG	14	1	-25.21	.	-4.27	.	1.52	1.81	4.16	0.101	0.945	3.6
2	AUG	14	2	-24.10	-46.30	0.101	0.945	3.6
2	AUG	17	1	-23.40	-47.30	-4.15	-29.16	1.63	1.87	4.34	0.122	0.947	3.3
2	AUG	17	2	-22.40	-46.30	0.122	0.947	3.3
6	AUG	2	1	-25.80	.	.	.	1.43	1.70	3.91	0.056	0.945	3.0
6	AUG	2	2	-23.70	-44.90	-5.67	-25.26	.	.	.	0.096	0.945	3.0
6	AUG	5	1	-24.40	-49.40	-4.55	-24.02	1.46	1.78	4.22	0.153	0.952	13.0
6	AUG	5	2	-23.70	-47.20	0.153	0.952	13.0
6	AUG	8	1	-21.70	-51.77	14.90	-5.10	1.50	1.75	4.40	0.256	0.965	6.2

ORIGINAL PAGE IS
OF POOR QUALITY

GUYMON DATA SET

C05=L BAND CROSS POLE 5 DEGREE LOOK ANGLE (DB)
 C40=L BAND CROSS POLE 40 DEGREE LOOK ANGLE (DB)
 P05=P BAND CROSS POLE 5 DEGREE LOOK ANGLE (DB)
 P40=P BAND CROSS POLE 40 DEGREE LOOK ANGLE (DB)
 Z10, Z15, Z25=NMS BANDS 4, 7, AND 9 (10**(-4) WATTS CM**(-2) ST**(-1))
 PVI=PERPENDICULAR VEGETATION INDEX (DIMENSIONLESS)
 TVI=TRANSFORMED VEGETATION INDEX (DIMENSIONLESS)
 SMOI=0-2 CM VOLUMETRIC SOIL MOISTURE (%)
 PERIODS REPRESENT MISSING VALUES

----- CROP=BARE -----

FIELD	MCNTH	DAY	RUN	C05	C40	P05	P40	Z10	Z15	Z25	PVI	TVI	SMO1
6	AUG	8	2	0.256	0.965	6.2
6	AUG	11	1	1.86	2.16	4.90	0.094	0.942	3.9
6	AUG	11	2	0.054	0.942	3.9
6	AUG	14	1	-23.78	.	-1.42	.	1.28	1.57	3.66	0.109	0.943	20.1
6	AUG	14	2	-23.50	-42.70	0.109	0.948	19.2
6	AUG	17	1	-23.70	-46.60	-4.26	-28.15	1.74	2.05	4.70	0.110	0.945	5.7
6	AUG	17	2	-22.70	-47.10	0.110	0.945	6.0
10	AUG	2	1	-25.00	-47.80	.	.	1.67	1.89	4.25	0.066	0.940	2.2
10	AUG	2	2	-23.70	-46.60	-5.79	-22.71	.	.	.	0.066	0.940	2.2
10	AUG	5	1	-24.70	-48.20	-3.94	-24.30	1.73	2.00	4.70	0.155	0.950	10.2
10	AUG	5	2	-24.60	-45.00	0.155	0.950	10.2
10	AUG	8	1	-21.50	-50.00	-3.64	-23.54	1.85	2.15	5.60	0.356	0.972	.
10	AUG	8	2	-22.10	-50.30	0.356	0.972	.
10	AUG	11	1	-22.80	-44.30	.	.	2.36	2.61	5.75	0.042	0.936	5.7
10	AUG	11	2	-20.40	-45.50	-5.50	-29.44	.	.	.	0.042	0.936	5.7
10	AUG	14	1	-20.70	-46.30	.	.	2.00	2.27	4.80	0.049	0.926	3.9
10	AUG	14	2	-21.30	.	-3.35	0.049	0.926	3.9

ORIGINAL PAGE IS
OF POOR QUALITY

GUYMON DATA SET
 C05=L BAND CROSS POLE 5 DEGREE LOOK ANGLE (DB)
 C40=L BAND CROSS POLE 40 DEGREE LOOK ANGLE (DB)
 P05=P BAND CROSS POLE 5 DEGREE LOOK ANGLE (DB)
 P40=P BAND CROSS POLE 40 DEGREE LOOK ANGLE (DB)
 Z10, Z15, Z25=WVS BANDS 4, 7, AND 9 (100*(-4) WATTS CM**(-2) ST**(-1))
 PVI=PERPENDICULAR VEGETATION INDEX (DIMENSIONLESS)
 TVI=TRANSFORMED VEGETATION INDEX (DIMENSIONLESS)
 SM01=0-2 CM VOLUMETRIC SOIL MOISTURE (%)
 PERIODS REPRESENT MISSING VALUES

FIELD	MCNTH	DAY	RUN	C05	C40	P05	P40	Z10	Z15	Z25	PVI	TVI	SM01
10	AUG	17	1	-22.90	-46.00	-4.06	-29.35	2.34	2.59	5.73	0.052	0.937	3.6
10	AUG	17	2	-23.80	-47.80	0.052	0.937	3.4
14	AUG	2	1	-26.10	-46.58	.	.	1.43	1.72	4.03	0.128	0.950	22.3
14	AUG	2	2	-23.80	-47.10	-3.71	-19.23	.	.	.	0.128	0.950	21.1
14	AUG	5	1	-24.00	-47.80	-4.10	-18.75	1.52	1.81	4.27	0.147	0.951	20.0
14	AUG	5	2	-25.70	-46.50	0.147	0.951	20.4
14	AUG	8	1	-24.80	-50.50	-6.01	-26.15	2.00	2.30	6.10	0.470	0.976	10.8
14	AUG	8	2	-24.00	-52.10	0.470	0.976	10.8
14	AUG	11	1	-24.50	-48.60	.	.	2.07	2.35	5.53	0.165	0.951	5.4
14	AUG	11	2	-23.80	-44.20	-6.62	-25.15	.	.	.	0.165	0.951	5.3
14	AUG	14	1	1.54	1.74	4.45	0.286	0.968	4.0
14	AUG	14	2	-24.30	-45.40	-4.91	-26.14	.	.	.	0.286	0.968	4.0
14	AUG	17	1	-26.10	-48.50	-2.20	-27.70	2.03	2.30	5.68	0.254	0.961	3.5
14	AUG	17	2	-27.10	-50.10	0.254	0.961	3.5
17	AUG	2	1	-27.10	-50.41	.	.	1.70	2.02	4.61	0.099	0.944	3.7
17	AUG	2	2	-26.20	-48.60	-5.21	-25.12	.	.	.	0.099	0.944	4.2
17	AUG	5	1	-28.00	-50.50	-4.98	-24.17	1.49	1.76	4.16	0.146	0.952	5.8

ORIGINAL
OF POOR QUALITY.

GUYMON DATA SET

C05=L BAND CROSS POLE 5 DEGREE LOCK ANGLE (DB)
 C40=L BAND CROSS POLE 40 DEGREE LOCK ANGLE (DB)
 P05=P BAND CROSS POLE 5 DEGREE LOCK ANGLE (DB)
 P40=P BAND CROSS POLE 40 DEGREE LOCK ANGLE (DB)
 Z10, Z15, Z25=HRS BANDS 4, 7, AND 9 (1000(-4) WATTS CH00(-2) ST00(-1))
 PVI=PERPENDICULAR VEGETATION INDEX (DIMENSIONLESS)
 TVI=TRANSFORMED VEGETATION INDEX (DIMENSIONLESS)
 SW01=0-2 CM VOLUMETRIC SOIL MOISTURE (I)
 PERIODS REPRESENT MISSING VALUES

----- CROP=BARE -----

FIELD	MCNTH	DAY	RUN	C05	C40	P05	P40	Z10	Z15	Z25	PVI	TVI	SW01
17	AUG	5	2	-26.50	-49.80	0.146	0.952	5.5
17	AUG	8	1	1.60	1.85	7.80	1.591	1.057	4.3
17	AUG	8	2	-26.70	-52.40	1.551	1.057	4.3
17	AUG	11	1	-26.60	-49.20	.	.	1.66	1.93	4.40	0.053	0.944	4.5
17	AUG	11	2	-25.50	-48.50	-4.68	-24.84	.	.	.	0.053	0.944	4.1
17	AUG	14	1	-26.78	-50.06	.	.	1.22	1.42	3.20	0.053	0.941	3.9
17	AUG	14	2	-26.20	-47.80	-3.69	-26.58	.	.	.	0.053	0.941	3.9
17	AUG	17	1	-26.60	-51.83	-4.65	-26.26	1.60	1.87	4.24	0.080	0.942	2.9
17	AUG	17	2	-25.40	-50.40	0.080	0.942	3.5
2X	AUG	2	1	-31.50	.	.	.	1.36	1.51	3.45	0.076	0.944	4.4
2X	AUG	2	2	-26.36	-42.90	-6.69	-23.17	.	.	.	0.076	0.944	4.4
2X	AUG	5	1	-31.50	-46.50	-6.76	-23.24	1.28	1.41	3.31	0.168	0.950	5.1
2X	AUG	5	2	-30.70	-47.30	0.168	0.950	5.1
2X	AUG	8	1	-28.47	-48.36	16.60	-0.90	0.85	0.90	2.60	0.273	0.993	.
2X	AUG	8	2	-26.80	-46.40	0.273	0.993	.
2X	AUG	11	1	1.62	1.77	4.00	0.070	0.942	4.9
2X	AUG	11	2	-26.90	-41.70	0.070	0.942	4.9

GUYMON DATA SET
 C05=L BAND CROSS POLE 5 DEGREE LOOK ANGLE (DB)
 C40=L BAND CROSS POLE 40 DEGREE LOOK ANGLE (DB)
 P05=P BAND CROSS POLE 5 DEGREE LOCK ANGLE (DB)
 P40=P BAND CROSS POLE 40 DEGREE LOCK ANGLE (DB)
 Z10, Z15, Z25=NMS BANDS 4, 7, AND 9 (10**(-4) WATTS CM**(-2) ST0**(-1))
 PVI=PERPENDICULAR VEGETATION INDEX (DIMENSIONLESS)
 TVI=TRANSFORMED VEGETATION INDEX (DIMENSIONLESS)
 SK01=0-2 CM VOLUMETRIC SOIL MOISTURE (Z)
 PERIODS REPRESENT MISSING VALUES

----- CROP=BARE -----

FIELD	MONTH	DAY	RUN	C05	C40	P05	P40	Z10	Z15	Z25	PVI	TVI	SK01
2X	AUG	14	1	-27.10	.	-5.04	.	1.39	1.58	3.58	0.667	0.942	3.9
2X	AUG	14	2	-27.10	-42.60	0.067	0.942	3.9
2X	AUG	17	1	-29.60	-40.70	-5.60	"24.80	0.86	0.98	2.29	0.070	0.949	4.9
2X	AUG	17	2	-28.70	-42.00	0.070	0.949	4.9
2X	AUG	2	1	-28.30	-44.50	.	.	1.55	1.70	3.86	0.075	0.943	5.2
2X	AUG	2	2	-28.20	-43.70	-6.31	"23.99	.	.	.	0.075	0.943	5.2
2X	AUG	5	1	-29.70	-45.30	-5.29	"24.13	1.38	1.49	3.47	0.102	0.948	6.0
2X	AUG	5	2	-28.50	0.102	0.948	6.0
2X	AUG	8	1	-26.10	-48.88	-1.91	"19.16	1.20	1.30	6.35	1.482	1.077	.
2X	AUG	8	2	-24.90	-48.30	1.482	1.077	.
2X	AUG	11	1	1.61	1.75	3.95	0.068	0.941	5.4
2X	AUG	11	2	0.068	0.941	5.3
2X	AUG	14	1	-26.57	-43.43	.	.	1.44	1.60	4.00	0.225	0.964	4.6
2X	AUG	14	2	-23.60	-41.80	-4.48	"23.73	.	.	.	0.225	0.964	4.6
2X	AUG	17	1	-27.07	-47.62	-4.58	"22.82	0.93	1.04	2.42	0.071	0.948	5.3
2X	AUG	17	2	-30.50	-43.60	0.071	0.948	5.3
2X	AUG	2	1	-27.50	-49.40	0.000	0.000	4.7

GUYMON DATA SET

C05=L BAND CROSS POLE 5 DEGREE LOCK ANGLE (DB)
 C40=L BAND CROSS POLE 40 DEGREE LOCK ANGLE (DB)
 P05=P BAND CROSS POLE 5 DEGREE LOCK ANGLE (DB)
 P40=P BAND CROSS POLE 40 DEGREE LOCK ANGLE (DB)
 Z10, Z15, Z25=MNS BANDS 4, 7, AND 9 (10*(1-4) BATTIS CM*(1-2) ST*(1-1))
 P43=PERPENDICULAR VEGETATION INDEX (DIMENSIONLESS)
 P71=TRANSFORMED VEGETATION INDEX (DIMENSIONLESS)
 SM01=0-2 CM VOLUMETRIC SOIL MOISTURE (X)
 PERIOS REPRESENT MISSING VALUES

***** CROP=BARE *****

FIELD	MCNTH	DAY	RUN	C05	C40	P05	P40	710	Z15	Z25	PVI	TVI	SM01
2X	AUG	2	2	-24.90	-46.80	0.000	0.000	4.7
2X	AUG	5	1	-25.12	0.000	0.000	5.8
2X	AUG	5	2	-25.90	0.000	0.000	5.5
2X	AUG	8	1	-26.10	-50.80	15.30	-4.90	.	.	.	0.000	0.000	.
2X	AUG	8	2	-27.50	-51.80	0.000	0.000	.
2X	AUG	11	1	-24.40	-46.20	11.60	-10.50	.	.	.	0.000	0.000	5.1
2X	AUG	11	2	-24.80	-45.30	0.000	0.000	5.1
2X	AUG	14	1	-24.60	-45.50	.	.	1.52	1.68	3.90	0.110	0.948	4.2
2X	AUG	14	2	-24.40	-46.10	-4.94	-24.51	.	.	.	0.110	0.948	4.2
2X	AUG	17	1	-25.00	.	.	.	1.01	1.14	2.67	0.085	0.950	5.0
2X	AUG	17	2	-25.10	-41.50	-3.15	-22.33	.	.	.	0.085	0.950	5.0
21	AUG	2	1	-26.20	-48.60	.	.	0.88	1.04	2.57	0.123	0.961	15.5
21	AUG	2	2	-24.80	-49.70	-5.43	-20.01	.	.	.	0.133	0.961	16.9
21	AUG	5	1	-30.30	-50.20	-6.05	-22.56	1.04	1.18	2.85	0.124	0.956	5.9
21	AUG	5	2	-28.50	-47.80	0.124	0.956	5.9
21	AUG	8	1	-24.40	-50.60	12.40	-5.50	0.75	0.85	2.45	0.256	0.992	5.3
21	AUG	8	2	-26.24	-51.92	0.256	0.992	6.0

GUYMON DATA SET
 C05=L BAND CROSS POLE 5 DEGREE LOCK ANGLE (DB)
 C40=L BAND CROSS POLE 40 DEGREE LOCK ANGLE (DB)
 P05=P BAND CROSS POLE 5 DEGREE LOCK ANGLE (DB)
 P40=P BAND CROSS POLE 40 DEGREE LOCK ANGLE (DB)
 Z10, Z15, Z25=MS BANDS 4, 7, AND 9 (10*(+4) WATTS CM**(-2) ST**(-1))
 PVI=PERPENDICULAR VEGETATION INDEX (DIMENSIONLESS)
 TVI=TRANSFORMED VEGETATION INDEX (DIMENSIONLESS)
 SM01=0-2 CM VOLUMETRIC SOIL MOISTURE (X)
 PERIODS REPRESENT MISSING VALUES

----- CROP=BARE -----

FIELD	MONTH	DAY	RUN	C05	C40	P05	P40	Z10	Z15	Z25	PVI	TVI	SM01
21	AUG	11	1	-24.20	-44.60	11.90	-7.90	1.20	1.36	3.16	0.090	0.948	4.1
21	AUG	11	2	-22.50	-44.00	.	"	.	.	.	0.090	0.948	4.0
21	AUG	14	1	-26.27	-45.70	-5.90	-22.74	0.91	1.04	2.72	0.156	0.973	5.1
21	AUG	14	2	-24.70	-45.00	.	"	.	.	.	0.156	0.973	5.1
21	AUG	17	1	-23.37	.	-4.07	"	1.04	1.20	2.77	0.072	0.946	4.2
21	AUG	17	2	.	.	.	"	.	.	.	0.072	0.946	4.2
26	AUG	2	1	-30.30	-49.40	.	"	1.10	1.31	3.14	0.127	0.955	14.9
26	AUG	2	2	-26.80	-49.50	.	"	.	.	.	0.127	0.955	14.9
26	AUG	5	1	-25.60	-53.90	-2.91	-24.12	1.31	1.49	3.50	0.115	0.950	7.2
26	AUG	5	2	-28.60	-50.20	.	"	.	.	.	0.115	0.950	6.7
26	AUG	8	1	.	.	.	"	1.20	1.35	3.50	0.242	0.971	6.7
26	AUG	8	2	-25.10	-51.80	17.70	-4.90	.	.	.	0.242	0.971	6.7
26	AUG	11	1	-23.50	-51.37	11.30	-6.90	1.34	1.54	3.52	0.078	0.944	4.8
26	AUG	11	2	0.078	0.944	4.8
26	AUG	14	1	-25.30	-46.30	.	.	1.12	1.31	3.02	0.077	0.946	4.5
26	AUG	14	2	-23.00	-46.50	-4.16	-21.99	.	.	.	0.077	0.946	4.5
26	AUG	17	1	-24.70	.	.	.	1.30	1.50	3.44	0.081	0.945	4.6

GUYMON DATA SET

COS=L BAND CROSS POLE 5 DEGREE LOOK ANGLE (DB)
 C40=L BAND CROSS POLE 40 DEGREE LOOK ANGLE (DB)
 P05=P BAND CROSS POLE 5 DEGREE LOOK ANGLE (DB)
 PA0=P BAND CROSS POLE 40 DEGREE LGCK ANGLE (DB)
 Z10, Z15, Z25=RMS BANDS 4, 7, AND 9 (10*(1-4) WATTS CM**(-2) ST**(-1))
 PVI=PERPENDICULAR VEGETATION INDEX (DIMENSIONLESS)
 TVI=TRANSFORMED VEGETATION INDEX (DIMENSIONLESS)
 SM01=0-2 CM VOLUMETRIC SOIL MOISTURE (X)
 PERIODS REPRESENT MISSING VALUES

FIELD	MONTH	DAY	RUN	C05	C40	P05	PA0	Z10	Z15	Z25	PVI	TVI	SM01
26	AUG	17	2	-25.2	-46.3	-5.41	-21.37	.	.	.	0.081	0.945	4.5

GUYMON DATA SET
 C05=L BAND CROSS POLE 5 DEGREE LOCK ANGLE (DB)
 C40=L BAND CROSS POLE 40 DEGREE LOCK ANGLE (DB)
 P05=P BAND CROSS POLE 5 DEGREE LOCK ANGLE (DB)
 P40=P BAND CROSS POLE 40 DEGREE LOCK ANGLE (DB)
 Z10, Z15, Z25=MS BANDS 4, 7, AND 9 (10*(+4) WATTS CH*(+2) ST*(-1))
 PVI=PERPENDICULAR VEGETATION INDEX (DIMENSIONLESS)
 TVI=TRANSFORMED VEGETATION INDEX (DIMENSIONLESS)
 SM01=0-2 CM VOLUMETRIC SOIL MOISTURE (X)
 PERIODS REPRESENT MISSING VALUES

FIELD	MONTH	DAY	RUN	C05	C40	P05	P40	Z10	Z15	Z25	PVI	TVI	SM01
C1	AUG	5	1	-12.6	-34.0	7.8	-3.8
C1	AUG	5	2	0	0	.
C2	AUG	5	1	-20.8	-33.0	8.6	-1.3	.	.	.	0	0	.
C2	AUG	5	2
C3	AUG	5	1	-10.6	-36.3	9.5	-2.8
C3	AUG	5	2
C4	AUG	5	1	-19.4	-34.9	8.0	-3.2
C4	AUG	5	2

ORIGINAL PAGE IS
OF POOR QUALITY

GUYMON DATA SET

C05=L BAND CROSS POLE 5 DEGREE LOCK ANGLE (DB)
 C40=L BAND CROSS POLE 40 DEGREE LOCK ANGLE (DB)
 P05=P BAND CROSS POLE 5 DEGREE LOCK ANGLE (DB)
 P40=P BAND CROSS POLE 40 DEGREE LOCK ANGLE (DB)
 Z10, Z15, Z25=MMS BANDS 4, 7, AND 9 (10*(=-4) WATTS CM**(-2) ST**(-1))
 PVI=PERPENDICULAR VEGETATION INDEX (DIMENSIONLESS)
 TVI=TRANSFORMED VEGETATION INDEX (DIMENSIONLESS)
 SM01=0-2 CM VOLUMETRIC SOIL MOISTURE (X)
 PERIODS REPRESENT MISSING VALUES

----- CRCP=SORGHUM (PARALLEL ROWS TO FLIGHT LINE) -----

FIELD	MCNTH	DAY	RUN	C05	C40	P05	P40	Z10	Z15	Z25	PVI	TVI	SM01
7	AUG	2	1	-26.30	.	.	.	1.72	1.75	5.56	0.742	1.011	5.2
7	AUG	2	2	-26.50	-44.80	-6.80	-20.54	.	.	.	0.742	1.011	5.2
7	AUG	5	1	-28.00	-48.80	-5.41	-22.23	1.34	1.36	4.80	0.778	1.029	10.4
7	AUG	5	2	-27.50	-51.20	0.778	1.029	10.0
7	AUG	8	1	-23.50	-51.50	13.70	-0.90	1.30	1.25	4.65	0.815	1.037	6.0
7	AUG	8	2	0.815	1.037	6.0
7	AUG	11	1	-22.60	-44.20	12.60	-0.90	1.38	1.33	4.85	0.826	1.034	18.8
7	AUG	11	2	0.826	1.034	18.8
7	AUG	14	1	-24.30	.	-4.05	.	1.26	1.18	4.83	0.554	1.052	7.7
7	AUG	14	2	-25.80	-42.00	0.954	1.052	7.6
7	AUG	17	1	-25.00	-39.90	-4.19	-22.39	1.39	1.30	5.65	1.189	1.061	4.5
7	AUG	17	2	-24.80	-39.60	1.189	1.061	4.5
8	AUG	2	1	-28.50	.	.	.	1.04	0.92	5.51	1.475	1.102	2.3
8	AUG	2	2	-28.80	-35.40	-4.82	-19.66	.	.	.	1.475	1.102	2.3
8	AUG	5	1	-28.40	-36.70	-4.74	-21.11	1.01	0.91	5.26	1.379	1.098	7.2
8	AUG	5	2	-28.50	-36.00	1.379	1.098	8.1
8	AUG	8	1	-27.30	-29.20	14.90	-0.30	0.90	0.80	5.25	1.475	1.112	4.8

ORIGINAL PAGE NO
OF POOR QUALITY.

GUYMON DATA SET

C05=L BAND CROSS POLE 5 DEGREE LOCK ANGLE (DB)
 C40=L BAND CROSS POLE 40 DEGREE LOCK ANGLE (DB)
 P05=P BAND CROSS POLE 5 DEGREE LOCK ANGLE (DB)
 P40=P BAND CROSS POLE 40 DEGREE LOCK ANGLE (DB)
 Z10, Z15, Z25=MMS BANDS 4, 7, AND 9 (100*(-4) WATTS CM**(-2) ST**(-1))
 PVI=PERPENDICULAR VEGETATION INDEX (DIMENSIONLESS)
 TVI=TRANSFORMED VEGETATION INDEX (DIMENSIONLESS)
 SM01=0-2 CM VOLUMETRIC SOIL MOISTURE (%)
 PERIODS REPRESENT MISSING VALUES

----- CRCP=SORGHUM (PARALLEL ROWS TO FLIGHT LINE) -----

FIELD	MONTH	CAY	RUN	C05	C40	P05	P40	Z10	Z15	Z25	PVI	TVI	SM01
8	AUG	8	2	-28.80	-38.30	1.475	1.112	5.0
8	AUG	11	1	1.20	1.11	5.73	1.355	1.084	8.5
8	AUG	11	2	-27.90	-33.30	1.395	1.084	8.5
8	AUG	14	1	-29.42	.	-3.42	0.000	0.000	4.9
8	AUG	14	2	-26.50	-35.20	0.000	0.000	4.9
8	AUG	17	1	-26.00	-34.10	-3.72	-16.93	1.01	0.90	5.42	1.455	1.102	3.2
8	AUG	17	2	-25.50	-32.40	1.455	1.102	3.2
1A	AUG	2	1	-29.60	-38.70	.	.	0.93	0.75	6.07	1.864	1.131	6.1
1A	AUG	2	2	-26.90	-37.20	-6.24	-18.01	.	.	.	1.864	1.131	6.1
1A	AUG	5	1	-29.20	-40.90	-5.38	-16.80	0.91	0.70	5.76	1.780	1.133	5.8
1A	AUG	5	2	-26.70	-39.10	1.780	1.133	5.8
1A	AUG	8	1	-26.90	-42.75	13.60	2.00	0.80	0.65	5.70	1.800	1.138	5.9
1A	AUG	8	2	-25.50	-40.00	1.800	1.138	5.5
1A	AUG	11	1	-28.00	-36.00	11.30	-0.80	1.01	0.84	5.90	1.711	1.118	4.9
1A	AUG	11	2	1.711	1.118	4.9
1A	AUG	14	1	-26.60	.	-2.47	-17.72	0.83	0.66	5.62	1.757	1.136	5.1
1A	AUG	14	2	-26.60	-37.90	1.757	1.136	5.1

GUYMON DATA SET
 C05=L BAND CROSS POLE 5 DEGREE LOCK ANGLE (DB)
 C40=L BAND CROSS POLE 40 DEGREE LOCK ANGLE (DB)
 P05=P BAND CROSS POLE 5 DEGREE LOCK ANGLE (DB)
 P40=P BAND CROSS POLE 40 DEGREE LOCK ANGLE (DB)
 Z10, Z15, Z25=HVS BANDS 4, 7, AND 9 (1000(-4) WATTS CM**(-2) ST**(-1))
 PVI=PERPENDICULAR VEGETATION INDEX (DIMENSIONLESS)
 TVI=TRANSFORMED VEGETATION INDEX (DIMENSIONLESS)
 SMO1=0-2 CM VOLUMETRIC SOIL MOISTURE (X)
 PERIODS REPRESENT MISSING VALUES

FIELD	MCNTH	CAY	RUN	C05	C40	P05	P40	Z10	Z15	Z25	PVI	TVI	SMO1
1A	AUG	17	1	-26.00	-37.50	-4.75	-17.51	0.85	0.67	5.70	1.782	1.136	4.5
1A	AUG	17	2	-25.00	-36.40	1.782	1.136	4.5
1X	AUG	2	1	-24.40	-34.10	0.000	0.000	24.9
1X	AUG	2	2	-29.00	-34.10	-4.22	-14.66	.	.	.	0.000	0.000	24.9
1X	AUG	5	1	-29.40	-35.70	-5.70	-17.40	.	.	.	0.000	0.000	24.0
1X	AUG	5	2	-30.50	-35.00	0.000	0.000	24.0
1X	AUG	8	1	-28.30	-35.40	12.40	0.30	.	.	.	0.000	0.000	.
1X	AUG	8	2	-28.50	-37.00	0.000	0.000	.
1X	AUG	11	1	0.000	0.000	11.0
1X	AUG	11	2	-27.30	-31.50	0.000	0.000	11.0
1X	AUG	14	1	0.51	0.32	4.30	1.512	1.167	7.3
1X	AUG	14	2	-27.90	-33.00	1.512	1.167	7.3
1X	AUG	17	1	-21.90	-35.70	-1.88	-18.04	0.86	0.54	7.76	2.763	1.170	5.1
1X	AUG	17	2	-26.70	2.763	1.170	6.9
15	AUG	2	1	-26.80	-50.99	.	.	2.23	2.23	6.70	0.785	1.000	7.1
15	AUG	2	2	-26.70	-40.80	-4.09	-23.75	.	.	.	0.785	1.000	7.1
15	AUG	5	1	-26.50	-51.32	-4.64	-21.67	1.66	1.65	5.71	0.896	1.025	11.4

GUYMON DATA SET
 C05=L BAND CROSS POLE 5 DEGREE LOOK ANGLE (DB)
 C40=L BAND CROSS POLE 40 DEGREE LOOK ANGLE (DB)
 P05=P BAND CROSS POLE 5 DEGREE LOOK ANGLE (DB)
 P40=P BAND CROSS POLE 40 DEGREE LOOK ANGLE (DB)
 Z10, Z15, Z25=HRS BANDS 4, 7, AND 9 (10**(-4)) WATTS CM**(-2) ST**(-11)
 PVI=PERPENDICULAR VEGETATION INDEX (DIMENSIONLESS)
 TVI=TRANSFORMED VEGETATION INDEX (DIMENSIONLESS)
 SMOI=0-2 CM VOLUMETRIC SOIL MOISTURE (%)
 PERIODS REPRESENT MISSING VALUES

CRCP=SORGHUM (PARALLEL ROWS TO FLIGHT LINE)

FIELD	MONTH	DAY	RUN	C05	C40	P05	P40	Z10	Z15	Z25	PVI	TVI	SMOI
15	AUG	5	2	-25.70	-50.37	0.896	1.025	11.4
15	AUG	8	1	-24.54	-51.79	-1.61	-16.22	1.45	1.40	5.75	1.140	1.053	21.1
15	AUG	8	2	-24.10	-50.33	1.140	1.053	21.8
15	AUG	11	1	-26.06	-40.31	.	"	1.67	1.60	5.58	0.887	1.027	17.5
15	AUG	11	2	-22.00	-40.10	-2.93	-17.87	.	.	.	0.887	1.027	19.7
15	AUG	14	1	-27.02	-41.30	.	"	1.26	1.15	4.85	0.989	1.057	9.5
15	AUG	14	2	-23.70	-38.40	-3.42	-19.08	.	.	.	0.989	1.057	10.9
15	AUG	17	1	-25.30	-42.60	-5.23	-21.55	1.73	1.58	6.64	1.350	1.056	4.9
15	AUG	17	2	-24.60	-40.80	.	"	.	.	.	1.350	1.056	4.9
2A	AUG	2	1	-25.40	-40.40	.	.	1.27	1.29	4.91	0.888	1.041	4.6
2A	AUG	2	2	-28.40	-42.10	-5.98	-20.25	.	.	.	0.888	1.041	4.6
2A	AUG	5	1	-27.20	-39.10	-5.42	-16.55	1.14	1.09	4.74	0.998	1.061	6.7
2A	AUG	5	2	-26.30	-39.00	0.998	1.061	7.1
2A	AUG	8	1	-26.12	-38.96	-2.15	-13.61	1.15	1.05	7.95	2.380	1.125	15.8
2A	AUG	8	2	2.380	1.125	15.8
2A	AUG	11	1	-25.73	-36.28	.	.	1.16	1.08	4.96	1.099	1.069	14.5
2A	AUG	11	2	1.099	1.069	7.2

GUYMON DATA SET

C05=L BAND CROSS POLE 5 DEGREE LOOK ANGLE (DB)
 C40=L BAND CROSS POLE 40 DEGREE LOOK ANGLE (DB)
 P05=P BAND CROSS POLE 5 DEGREE LOOK ANGLE (DB)
 P40=P BAND CROSS POLE 40 DEGREE LOOK ANGLE (DB)
 Z10, Z15, Z25=KVS BANDS 4, 7, AND 9 (10**(-4) WATTS CM**(-2) ST**(-1))
 PVI=PERPENDICULAR VEGETATION INDEX (DIMENSIONLESS)
 TVI=TRANSFORMED VEGETATION INDEX (DIMENSIONLESS)
 SN01=0-2 CM VOLUMETRIC SOIL MOISTURE (X)
 PERIODS REPRESENT MISSING VALUES

----- CRCP=SORGHUM (PARALLEL ROWS TO FLIGHT LINE) -----

FIELD	MONTH	DAY	RUN	C05	C40	P05	P40	Z10	Z15	Z25	PVI	TVI	SN01
2A	AUG	14	1	-26.33	-34.21	.	.	1.01	0.90	5.1	1.321	1.095	6.1
2A	AUG	14	2	-26.00	-35.70	-4.14	-17.10	.	.	.	1.321	1.095	7.5
2A	AUG	17	1	-25.50	-35.30	-4.68	-18.99	1.07	0.93	5.6	1.504	1.102	5.4
2A	AUG	17	2	-24.80	-35.90	1.504	1.102	6.0
M1	AUG	5	1	-12.70	-43.10	7.20	-3.30
M1	AUG	5	2	0.000	0.000	.
M2	AUG	5	1	-20.20	-45.30	7.60	-4.60
M2	AUG	5	2

ORIGINAL DATA
 OF POOR QUALITY.

GUYMON DATA SET
 C05=L BAND CROSS POLE 5 DEGREE LOCK ANGLE (DB)
 C40=L BAND CROSS POLE 40 DEGREE LOCK ANGLE (DB)
 P05=P BAND CROSS POLE 5 DEGREE LOCK ANGLE (DB)
 P40=P BAND CROSS POLE 40 DEGREE LOCK ANGLE (DB)
 Z10, Z15, Z25=WMS BANDS 4, 7, AND 9 (10*((-4) WATTS CM**(-2) ST**(-1)))
 PVI=PERPENDICULAR VEGETATION INDEX (DIMENSIONLESS)
 TVI=TRANSFORMED VEGETATION INDEX (DIMENSIONLESS)
 SM01=0-2 CM VOLUMETRIC SOIL MOISTURE (X)
 PERIODS REPRESENT MISSING VALUES

CRUP=SORGHUM (PERPENDICULAR ROWS TO FLIGHT LINE)

FIELD	MCNTH	DAY	RUN	C05	C40	P05	P40	Z10	Z15	Z25	PVI	TVI	SM01
1X	AUG	2	1	-26.60	.	.	.	0.76	0.46	7.31	2.647	1.175	25.0
1X	AUG	2	2	-26.80	-39.10	-5.16	-17.84	.	.	.	2.647	1.175	25.0
1X	AUG	5	1	-31.50	-40.80	-4.38	-14.83	0.83	0.50	7.14	2.540	1.170	26.9
1X	AUG	5	2	-29.40	-40.40	2.540	1.170	26.9
1X	AUG	8	1	-21.10	-38.48	16.80	3.90	0.70	0.40	6.80	2.488	1.179	.
1X	AUG	8	2	-21.60	-37.00	2.488	1.179	.
1X	AUG	11	1	-27.10	-31.50	11.90	-1.00	0.81	0.49	7.47	2.687	1.173	11.9
1X	AUG	11	2	-23.20	-34.50	2.687	1.173	11.9
1X	AUG	14	1	-28.54	.	-4.42	.	0.75	0.48	7.57	2.738	1.175	6.9
1X	AUG	14	2	-26.40	-37.90	2.738	1.175	6.9
1X	AUG	17	1	-28.90	-34.00	-5.80	-18.40	0.72	0.45	7.10	2.568	1.175	5.6
1X	AUG	17	2	-28.60	-34.70	2.568	1.175	5.6
1X	AUG	2	1	-27.80	-38.30	.	.	0.92	0.53	9.04	3.309	1.179	24.7
1X	AUG	2	2	-27.90	-38.20	-3.65	-17.31	.	.	.	3.309	1.179	24.7
1X	AUG	5	1	-31.20	-42.40	-5.88	-18.94	0.90	0.54	8.90	3.241	1.177	21.1
1X	AUG	5	2	-29.30	-36.53	3.241	1.177	21.1
1X	AUG	8	1	0.90	0.55	12.05	4.853	1.189	.

GUYMON DATA SET
 COS=L BAND CROSS POLE 5 DEGREE LOOK ANGLE (DB)
 C40=L BAND CROSS POLE 40 DEGREE LOOK ANGLE (DB)
 P05=P BAND CROSS POLE 5 DEGREE LOOK ANGLE (DB)
 P40=P BAND CROSS POLE 40 DEGREE LOOK ANGLE (DB)
 Z10, Z15, Z25=M/S BANDS 4, 7, AND 9 (10**(-4) WATTS CM**(-2) ST**(-1))
 PVI=PERPENDICULAR VEGETATION INDEX (DIMENSIONLESS)
 TVI=TRANSFORMED VEGETATION INDEX (DIMENSIONLESS)
 SMOI=0-2 CM VOLUMETRIC SOIL MOISTURE (%)
 PERIODS REPRESENT MISSING VALUES

----- CROP=SORGHUM (PERPENDICULAR ROWS TO FLIGHT LINE) -----

FIELD	MCNTH	DAY	RUN	C05	C40	P05	P40	Z10	Z15	Z25	PVI	TVI	SMOI
1X	AUG	8	2	-25.10	-41.60	4.553	1.189	.
1X	AUG	11	1	-31.16	-38.59	.	.	0.86	0.53	7.82	2.798	1.172	10.0
1X	AUG	11	2	-29.20	-37.00	-4.68	-19.74	.	.	.	2.758	1.172	10.0
1X	AUG	14	1	-29.66	-39.79	.	.	0.86	0.56	8.75	3.160	1.175	7.7
1X	AUG	14	2	-31.20	-38.90	-4.91	-21.10	.	.	.	3.160	1.175	7.7
1X	AUG	17	1	-30.55	-38.31	-3.24	-19.03	0.85	0.53	7.73	2.760	1.171	.
1X	AUG	17	2	-30.30	-40.50	2.760	1.171	.
19	AUG	2	1	-27.28	-42.50	.	.	0.67	0.76	5.05	1.427	1.113	.
19	AUG	2	2	-28.30	-40.30	-4.02	-15.70	.	.	.	1.427	1.113	.
19	AUG	5	1	-28.91	-42.62	-3.56	-16.85	0.90	0.74	5.33	1.563	1.121	16.3
19	AUG	5	2	-32.30	-42.70	1.563	1.121	14.8
19	AUG	8	1	-29.10	-45.13	14.80	-1.20	0.65	0.45	4.45	1.457	1.147	16.3
19	AUG	8	2	-25.40	-42.40	1.457	1.147	17.9
19	AUG	11	1	0.91	0.74	5.63	1.689	1.126	10.1
19	AUG	11	2	-23.90	-36.70	1.689	1.126	10.1
19	AUG	14	1	-24.55	-38.06	-4.20	-16.15	0.67	0.53	4.00	1.156	1.125	12.9
19	AUG	14	2	-22.70	1.196	1.125	12.9

OIL PAINT
OF POOR QUALITY

GUYMON DATA SET

C05=L BAND CROSS POLE 5 DEGREE LOOK ANGLE (DB)
 C40=L BAND CROSS POLE 40 DEGREE LOOK ANGLE (DB)
 P05=P BAND CROSS POLE 5 DEGREE LOOK ANGLE (DB)
 P40=P BAND CROSS POLE 40 DEGREE LOOK ANGLE (DB)
 Z10, Z15, Z25=MWS BANDS 4, 7, AND 9 (10*(1-4) MATIS CM*(-2) ST*(-1))
 PVI=PERPENDICULAR VEGETATION INDEX (DIMENSIONLESS)
 TVI=TRANSFORMED VEGETATION INDEX (DIMENSIONLESS)
 SM01=0-2 CM VOLUMETRIC SOIL MOISTURE (X)
 PERIODS REPRESENT MISSING VALUES

CROP=SORGHUM (PERPENDICULAR ROWS TO FLIGHT LINE)

FIELD	MONTH	DAY	RUN	C05	C40	P05	P40	Z10	Z15	Z25	PVI	TVI	SM01
19	AUG	17	1	-26.23	-38.19	-4.92	-17.61	0.91	0.75	5.95	1.814	1.130	9.5
19	AUG	17	2	-27.76	1.814	1.130	9.5
20	AUG	2	1	-25.29	-39.42	.	.	0.83	0.54	6.92	2.411	1.164	.
20	AUG	2	2	-23.60	-37.30	-2.56	-13.87	.	.	.	2.411	1.164	.
20	AUG	5	1	-26.66	-40.10	-1.04	-16.71	0.86	0.58	7.04	2.425	1.161	29.1
20	AUG	5	2	-22.20	-38.40	2.425	1.161	29.1
20	AUG	8	1	-23.30	-39.00	14.60	0.70	0.65	0.40	5.65	2.006	1.170	33.0
20	AUG	8	2	-22.20	-38.60	2.006	1.170	37.1
20	AUG	11	1	-19.74	-34.95	15.00	-0.60	0.83	0.54	6.90	2.603	1.164	25.1
20	AUG	11	2	-21.50	-33.40	2.603	1.164	20.6
20	AUG	14	1	-24.55	-34.80	-3.98	-17.21	0.67	0.46	6.06	2.123	1.166	12.1
20	AUG	14	2	-24.20	-37.20	2.123	1.166	12.1
20	AUG	17	1	-23.20	-33.60	-2.21	-13.68	0.80	0.53	6.99	2.450	1.166	26.4
20	AUG	17	2	-22.20	-34.80	2.450	1.166	37.9
24	AUG	2	1	-30.00	-43.40	.	.	0.90	0.76	4.93	1.377	1.110	.
24	AUG	2	2	-28.30	-41.70	1.377	1.110	.
24	AUG	5	1	-27.25	-42.67	-3.11	-18.11	0.94	0.78	5.31	1.518	1.115	20.7

GUYMON DATA SET

C05=L BAND CROSS POLE 5 DEGREE LOCK ANGLE (DB)
 C40=L BAND CROSS POLE 40 DEGREE LOCK ANGLE (DB)
 P05=P BAND CROSS POLE 5 DEGREE LOCK ANGLE (DB)
 P40=P BAND CROSS POLE 40 DEGREE LOCK ANGLE (DB)
 Z10, Z15, Z25=MMS BANDS 4, 7, AND 9 (10*(+)) WATTS CM**(-2) SI**(-1))
 PVI=PERPENDICULAR VEGETATION INDEX (DIMENSIONLESS)
 TVI=TRANSFORMED VEGETATION INDEX (DIMENSIONLESS)
 SH01=0-2 CM VOLUMETRIC SOIL MOISTURE (X)
 PERIODS REPRESENT MISSING VALUES

----- CROP=SORGHUM (PERPENDICULAR FIBRS TO FLIGHT LINE) -----

FIELD	MONTH	DAY	RUN	C05	C40	P05	P40	Z10	Z15	Z25	PVI	TVI	SH01
24	AUG	5	2	-27.50	-42.30	1.518	1.115	25.7
24	AUG	8	1	-26.47	-43.83	14.40	-0.30	0.90	0.65	5.90	1.884	1.141	20.5
24	AUG	8	2	-27.60	-42.70	1.824	1.141	22.0
24	AUG	11	1	1.01	0.83	5.73	1.649	1.117	13.9
24	AUG	11	2	1.649	1.117	11.7
24	AUG	14	1	-23.75	-37.84	.	.	0.90	0.72	5.65	1.715	1.129	18.8
24	AUG	14	2	-26.70	-38.00	-3.55	-16.84	.	.	.	1.715	1.129	18.8
24	AUG	17	1	-23.09	.	.	.	1.07	0.86	6.50	1.945	1.125	14.8
24	AUG	17	2	-26.30	-38.60	-4.60	-16.29	.	.	.	1.945	1.125	13.1
25	AUG	2	1	-27.40	-41.50	.	.	1.07	0.78	8.19	2.726	1.152	.
25	AUG	2	2	-24.60	-39.90	2.726	1.152	.
25	AUG	5	1	-22.98	-42.50	0.19	-14.68	1.09	0.75	8.05	2.654	1.153	32.2
25	AUG	5	2	-23.00	-40.30	2.654	1.153	33.5
25	AUG	8	1	-24.40	-41.80	15.50	1.40	1.00	0.65	8.30	2.890	1.164	14.1
25	AUG	8	2	-25.80	-40.90	2.890	1.164	14.1
25	AUG	11	1	1.00	0.72	7.52	2.499	1.151	21.1
25	AUG	11	2	-24.30	-37.30	12.80	-1.20	.	.	.	2.499	1.151	21.1

OF POOR QUALITY

GUYMON DATA SET

C05=L BAND CROSS POLE 5 DEGREE LOCK ANGLE (DB)
 C40=L BAND CROSS POLE 40 DEGREE LOCK ANGLE (DB)
 P05=P BAND CROSS POLE 5 DEGREE LOCK ANGLE (DB)
 P40=P BAND CROSS POLE 40 DEGREE LOCK ANGLE (DB)
 Z10, Z15, Z25=MMS BANDS 4, 7, AND 9 (10*(+4) LATTIS CM*(+2) ST*(+1))
 PVI=PERPENDICULAR VEGETATION INDEX (DIMENSIONLESS)
 TVI=TRANSFORMED VEGETATION INDEX (DIMENSIONLESS)
 SM01=0-2 CM VOLUMETRIC SOIL MOISTURE (X)
 PERIODS REPRESENT MISSING VALUES

----- CROP=SORGHUM (PERPENDICULAR RUNS TO FLIGHT LINE) -----

FIELD	MONTH	DAY	RUN	C05	C40	P05	P40	Z10	Z15	Z25	PVI	TVI	SM01
25	AUG	14	1	-20.1	-33.5	.	.	0.69	0.59	7.34	2.542	1.162	27.4
25	AUG	14	2	-20.0	-35.3	-1.49	-14.39	.	.	.	2.542	1.162	27.4
25	AUG	17	1	-25.2	.	.	.	1.07	0.77	8.37	2.810	1.154	9.7
25	AUG	17	2	-24.9	-36.3	-3.81	-13.35	.	.	.	2.810	1.154	10.6